



UNIVERSITÀ
DEGLI STUDI
DI PADOVA



UNIVERSITÀ DEGLI STUDI DI PADOVA

DIPARTIMENTO DI INGEGNERIA INDUSTRIALE
CORSO DI LAUREA MAGISTRALE IN INGEGNERIA DELL' ENERGIA ELETTRICA

UNIVERSIDAD DE SEVILLA

ESCUELA TÉCNICA SUPERIOR DE INGENIERÍA

TESI DI LAUREA MAGISTRALE IN
INGEGNERIA DELL' ENERGIA ELETTRICA

Current Sensing in LV Distribution Panels through the use of Magnetic Field Sensors

RELATORE: Prof. ROBERTO TURRI

CORRELATORI: Prof. JUAN CARLOS DEL PINO LÓPEZ
Prof. PEDRO LUIS CRUZ ROMERO

Laureando: ENRICO LEORATO

Matricola: 1087096

ANNO ACCADEMICO 2015/2016

A mi familia

A mi novia

A mis maestros

ACKNOWLEDGEMENTS

Por primero querría agradecer mis tutores, el profesor Turri y en particular el profesor Pino López que me ha permitido emprender este proyecto, ayudándome con el uso de los softwares y siendo siempre presente y disponible por cada uno de los infinitos problemas que hemos tenido que afrontar durante el desarrollo del proyecto.

Me complace particularmente el hecho que con el uso de Comsol empecé desde un nivel igual a cero, hasta llegar en estos meses a un buen nivel de conocimiento del programa, aunque si no ha sido fácil y he pasado muchas noches donde me hubiera gustado quemar el ordenador.

Por el soporte moral tengo que agradecer mi novia, que la amo con todo mi corazón, que siempre ha sido presente y me ha consolado cuando nada funcionaba o tenía problemas y también mi familia que siempre está a mi lado.

Mi satisfacción mas grande será verlos felices el día de la graduación porque la felicidad suya es la mi felicidad.

Un agradecimiento especial también a Sevilla que tiene un color especial. Para mí será siempre la ciudad más hermosa del mundo y la experiencia Erasmus que he emprendido aquí cambiará para siempre mi idea del mundo, de las otras culturas y de todo lo que está afuera de la nuestra “comfort zone”. Sin hablar, además, de la satisfacción personal que se tiene cuando se habla otro idioma, lo que bonito es encontrar gente de todo el mundo e intercambiar experiencias, comida, música, costumbres y distintos puntos de vista. Sin olvidar también los momentos intensos que he vivido, que me han hecho sentir vivo. Espero que estas cosas sean un ejemplo en mi vida para vivir siempre a lo máximo.

Gracias a todos los mis amigos y mis compañeros de todos los pisos que he tenido en todo el mundo, porque han pintado mi vida y han aligerado el peso del estudio y los miles fallos.

Gracias, al final, a mi templanza, que me permitió de estudiar y trabajar por más de 6 años sin tener que pedir nada a mi familia, que la quiero mucho. Esta es la demostración que en la vida todo se puede.

“Nacimos para un propósito mucho más grande que ir a trabajar, pagar cuentas y morir”

ABSTRACT

In power systems currents usually flow through flat copper or aluminium conductors called bus bars. Therefore, there is a practical demand for bus bars to be employed in current measurement applications.

The present investigation, taking into account this practical demand, has as its objective the development of a cheap and automatic current monitoring system applicable to electrical bus bars.

The requirement to develop a low cost system is the first step in order to obtain a possible future industrial production of this system and this requirement affected the choice of the hardware tools used in this project.

The bus bars taken into consideration in this project are employed in an electrical LV distribution panel intended to use in the industrial sector.

The panel is employed for the supply of four different 3-phase circuits that provide energy to distinct groups of electrical loads.

This automatic system of monitoring has the purpose of measure the current flowing through every bar with the future goal to check, at any time, electrical information of the electrical system, such as the load curve that denotes every circuit.

The application developed in this investigation assumes that the magnetic field around a bus bar, at a certain distance, is proportional to the applied current at all times. Thus, it is possible to find out the electrical information of a bus bar by measuring and analysing the emanated Magnetic field.

In order to analyse the Magnetic field, it has been taken into consideration, principally for the cost-effectiveness, the implementation of a number of magnetoresistive sensors installed into the panel and supported by an Arduino® board, specially programmed for the case under study.

The main develop of the project was realized using a 3D model of the distribution panel, designed with the support of the Solidworks® software and subsequently implemented in the COMSOL Multiphysics® simulation software for FEM analysis.

The use of the FEM simulation software has been fundamental in order to find out the correct position and configuration of the sensors. The main goal obtained with the FEM simulations was the elimination of the stray MFs influence in the sensor measures. This has been achieved using different configurations for the MF sensors.

At the end of the work it has been reached an advanced level of the project, with the correct functioning of the simulated measurement system and the implementation of an Arduino® algorithm to control the board supporting the sensors.

The correct functioning of the simulation system was figure out with a graphical study of the measured current trends, developed in a Matlab® environment.

TABLE OF CONTENTS

Acknowledgements	vii
Abstract	ix
Table of Contents	xi
List of tables	xiii
List of figures	xv
List of symbols and abbreviations	xvii
Riassunto	19
1 Introduction	21
1.1 Magnetoresistive sensors	22
1.1.1 AMR effect	22
1.1.2 The 3-axis Magnetoresistive sensors: HMC5883L	23
1.2 Theoretical considerations for the MF measurement	24
1.2.1 FEM approach to simulate a Magnetoresistive sensor	26
2 Theoretical framework	29
2.1 Ampere Law	29
2.1.1 Integral form	29
2.1.2 Differential form	30
2.2 Principal laws used for the computation	30
3 Electrical panel presentation	31
3.1 Electrical panel features	31
3.2 Development of the geometry in Solidworks®	33
3.3 Geometry implementation in Comsol Multiphysics®	38
4 Material	39
4.1 Materials hypothesis for the FEM simulation.	39
5 Implementation of the physic study	41
5.1 Setting of a current	41
5.1.1 Boundary conditions	42
5.2 Modelling of a basic electrical conductor in Comsol Multiphysics	43
6 Mesh implementation	45
6.1 Mesh characteristics	47
7 First approach of study: consideration of a 2D cut-plane	49
7.1 The choose of the cut-planes for the 2D study	49
8 Positioning of the measurement points in the simulation software	53
8.1 First possible disposition of measurement sensors	53
8.1.1 Disposition of the R-S sensors in the z cut-plane	54
8.1.2 Disposition of the T sensors in the y cut-plane	61
8.1.3 Final position of the sensors in the 3D model	65
8.2 Second possible disposition of the measurement sensors	67
8.3 Final position of the sensors in the 3D model	71
9 Derivation of the current values	73
9.1 Implementation of the matrix $[K]$	73

9.2	How to figure out the current values	76
9.2.1	Implementation with Matlab	76
10	Study of the error - 2D case	79
10.1	First disposition of measurement sensors	79
10.1.1	K matrix	79
10.1.2	Arrays $[B(t)]$	81
10.1.3	Graphical results	84
10.2	Corrective coefficients for the measured current	108
10.2.1	Test of the invariance of the matrix	109
10.2.2	Results with the corrective coefficient	110
10.3	A particular case: unbalanced electrical system	114
10.3.1	Graphical results	116
10.3.2	Results with the implementation of a corrective coefficient	119
10.4	Second disposition of measurement sensors	121
10.4.1	K matrix	121
10.4.2	Array $[B(t)]$	122
10.4.3	Graphical results	123
10.4.4	Implementation of a corrective coefficient	127
11	Study of the error - 3D case	133
11.1	First disposition of measurement sensors	133
11.1.1	K matrix	133
11.2	Second disposition of measurement sensors	134
11.2.1	K matrix	134
12	Monitoring of magnetoresistive sensors with the implementation of an Arduino board	135
12.1	Arduino advantages	135
12.2	Arduino model: MEGA 2560	135
12.2.1	Technical specs	136
12.3	Connection system between the sensors and the MEGA 2560 Arduino board.	137
12.4	Limitations encountered with the implementation of the MCU	138
12.5	Exceedance of the technical limitations	138
12.6	Development of the programming code	139
12.7	Total approximate cost for the hardware parts used in the project	140
13	Final considerations and future works	141
	Appendix	143
	Bibliography	151

LIST OF TABLES

Table 3.1	Size of domain blocks.	38
Table 4.1	Properties of air.	40
Table 4.2	Properties of aluminium.	40
Table 6.1	Tetrahedral mesh n°1	47
Table 6.2	Tetrahedral mesh n°2	47
Table 6.3	Tetrahedral mesh n°3	47
Table 8.1	Values of different vector components of MF for different points.	54
Table 8.2	Values of \mathbf{B}_y referred to the points in the Fig. 8.3	56
Table 8.3	Values of MF referred to the points in the Fig. 8.13	62
Table 8.4	Values of \mathbf{B}_y referred to the points in the fig. 8.22	68

LIST OF FIGURES

Fig. 1.1	Resistance of a thin Permalloy film as a function of an applied external field angle.	23
Fig. 1.2	Honeywell HMC5883L magnetoresistive sensor.	23
Fig. 1.3	Distribution of MF around an electrical wire.	24
Fig. 1.4	Disposition of sensors for an electrical wire.	25
Fig. 1.5	Detection of MF by the sensors. Case with two electrical wires.	25
Fig. 1.6	Detection of MF by the sensors. Case with two bus bars.	26
Fig. 3.1	Photo of the electrical distribution panel.	31
Fig. 3.2	Input bars of the electrical panel (N, R, S, T bars).	32
Fig. 3.3	Output terminals for the connection of different 3-phase circuits.	32
Fig. 3.4	Holders for the fuses.	32
Fig. 3.5	3D CAD model of the electrical panel.	33
Fig. 3.6	3D CAD model of the electrical panel.	34
Fig. 3.7	3D CAD model of the electrical panel.	34
Fig. 3.8	Axonometric drawing of the original model.	35
Fig. 3.9	Axonometric drawing of the model with prolonged bars.	36
Fig. 3.10	Axonometric drawing of the model with prolonged bars.	37
Fig. 3.11	Block 1.	38
Fig. 5.1	Model of an electrical wire with FEM.	42
Fig. 5.2	Model of a conductor. Return of current through the external domain.	43
Fig. 5.3	Model of the electrical panel with the respective first domain.	44
Fig. 6.1	3D elements types.	45
Fig. 6.2	Tetrahedral mesh n° 1.	46
Fig. 6.3	Tetrahedral mesh n°2 .	46
Fig. 7.1	Cut-plane for the R-S bars sensors of the first disposition, 3D and 2D views.	50
Fig. 7.2	Cut-plane for the T-bars sensors of the first disposition, 3D view.	50
Fig. 7.3	Cut-plane for the T-bars sensors of the first disposition, 3D view.	51
Fig. 7.4	Cut-plane for the second disposition, 3D view.	51
Fig. 7.5	Cut-plane for the second disposition, 2D view.	52
Fig. 8.1	Points of measure in the 2D cut-plane.	54
Fig. 8.2	Points of measure referred to the table 8.1	55
Fig. 8.3	Points of measure referred to the Table 8.2	56
Fig. 8.4	Magnetic flux density considering only the y component of the MF. Input current: 10 A.	57
Fig. 8.5	Direction of the Magnetic flux density considering the x and y components of the MF.	57
Fig. 8.6	Magnetic flux density of the phases R1, S1, R2 considering only the y component of the MF.	58
Fig. 8.7	Magnetic flux density considering only the x component of the MF.	58

Fig. 8.8 Magnetic flux density of the phases R1, S1, R2 considering only the x component of the MF.	59
Fig. 8.9 Magnetic flux density of the neutral bar considering only the y component of the MF.	59
Fig. 8.10 Magnetic flux density of the neutral bar considering only the x component of the MF.	60
Fig. 8.11 Direction of the Magnetic flux density of the neutral bar considering the x and y components of MF.	60
Fig. 8.12 Points of measure in the 2D cut-plane.	61
Fig. 8.13 Points of measure referred to the table 8.3	61
Fig. 8.14 Magnetic flux density of the phases T considering only the x component of the MF.	63
Fig. 8.15 Magnetic flux density of the phases T considering only the y component of the MF.	64
Fig. 8.16 Position of the sensors for the cut-plane z.	65
Fig. 8.17 Position of the sensors for the cut-plane z.	65
Fig. 8.18 Settings of the sensors adopted in order to delete the stray MFs contribution.	65
Fig. 8.19 Position of the sensors for the cut-plane y.	66
Fig. 8.20 Settings of the sensors adopted in order to delete the stray MFs contribution.	66
Fig. 8.21 Points of measure in the 2D cut-plane.	67
Fig. 8.22 Points of measure referred to the table 8.4	68
Fig. 8.23 Magnetic flux density considering only the x component of the MF.	69
Fig. 8.24 Magnetic flux density considering only the y component of the MF.	70
Fig. 8.25 Position of the sensor installed for the phase R.	71
Fig. 8.26 Position of the sensor installed for the phases R and S.	71
Fig. 8.27 Position of the sensor installed for the phases R and S.	72
Fig. 8.28 Settings of the sensors adopted in order to delete the stray MFs contribution.	72
Fig. 10.1 Trends of currents and errors, case with corrective coefficient. Phase R ₁	113
Fig. 12.1 Arduino Mega (version for USA) and Genuino Mega (version not for USA).	136
Fig. 12.2 MCU MEGA 2560.	137

LIST OF SYMBOLS AND ABBREVIATIONS

AMR	Anisotropic Magnetoresistance	
MF	Magnetic Field	
I	Current	A
ω	Angular frequency	rad/s
J	Current density	A/m ²
D	Electric displacement	C/m ²
E	Electric field	V/m
σ	Electrical conductivity	S/m
j, i	Imaginary unit	-
H	Magnetic field	A/m
B	Magnetic flux density	T
A	Magnetic potential vector	Wb/m
B_x	Magnetic flux density, vector component x	T
B_y	Magnetic flux density, vector component y	T
B_z	Magnetic flux density, vector component z	T
[B]	Magnetic flux density matrix	μ T
[I]	Matrix of currents	A
[B(t)]	Time dependent magnetic flux density matrix	μ T
[I(t)]	Time dependent matrix of currents	A
[K]	Matrix of constant elements	-
[K]_{corr}	Matrix of corrective coefficients	-
MCU	Microcontroller unit	
ADC	Analog-to-Digital converter	
OA	Operational Amplifier	

Lo scopo del presente progetto di tesi è quello di sviluppare un sistema di monitoraggio della corrente, applicabile a barre conduttrici, installabile in un quadro elettrico di distribuzione operante in bassa tensione.

I principali obiettivi tenuti in conto nella progettazione del sistema di misurazione sono quelli di costruire un sistema economico e che realizzi la misurazione della corrente in modo completamente automatizzato.

La principale innovazione presente nel sistema di misurazione è infatti l'utilizzo di sensori di campo magnetico al posto di altri sistemi di misurazione della corrente attualmente diffusi. Tali sensori infatti presenteranno un notevole vantaggio, dal punto di vista economico, nel sistema finale e saranno comandati tramite una piattaforma hardware Arduino® la quale a sua volta ha il vantaggio di essere economica.

Il quadro elettrico in questione è destinato all'uso industriale per l'alimentazione di quattro circuiti trifase che andranno a sua volta ad alimentare diversi gruppi di carichi elettrici. Data la sua applicazione nel suddetto quadro, il sistema di monitoraggio avrà il fine di monitorare correnti e tensioni di ogni circuito per ricavare importanti informazioni elettriche sul funzionamento di ogni circuito, come ad esempio le varie potenze, il fattore di potenza e la curva di carico.

I sensori di campo magnetico presi in considerazione sono i sensori Honeywell HMC5883L di tipo magnetoresistivo. La disposizione di tali sensori è stata abbastanza ostacolante nella realizzazione del progetto a causa dell'influenza, nella misurazione del campo magnetico emanato da ciascuna barra, di campi magnetici dispersi da altre barre.

Per la risoluzione del problema è stata adottata una configurazione in cui venivano installati due sensori ai lati di ciascuna barra disposti con direzione di misurazione opposta, con lo scopo di eliminare nella misurazione gli effetti dei campi dispersi.

La realizzazione del progetto è sostanzialmente divisa in due fasi principali.

La prima è una fase prettamente simulativa del problema, sviluppata tramite simulazioni FEM con l'utilizzo del software COMSOL Multiphysics® supportato da Matlab®. La seconda è una fase indirizzata al controllo dei sensori tramite la programmazione del microcontroller ATmega2560 della scheda Arduino Mega utilizzata.

Nella prima fase, che è la più sostanziosa del progetto, è stato modellizzato il quadro elettrico tramite il software CAD Solidworks® per poi essere trasferito nella piattaforma COMSOL Multiphysics®. In quest'ultima è stato analizzato il sistema tramite simulazioni dei campi magnetici prodotti da ciascuna barra, conseguenti all'alimentazione del quadro con opportune correnti elettriche di input.

Tali analisi simulate hanno avuto come principali obiettivi i seguenti:

- Trovare la miglior configurazione per l'installazione dei sensori con lo scopo di ridurre al minimo l'influenza nel monitoraggio di eventuali campi magnetici dispersi dalle varie barre;
- Trovare la relazione che legasse il campo magnetico rilevato dai sensori per ogni barra alla corrispondente corrente presente nella barra;
- Implementare tale relazione con lo scopo di realizzare un sistema di monitoraggio affidabile.

La principale relazione ottenuta per la rilevazione della corrente tramite i valori di campo \mathbf{B} è stata la seguente:

$$[I(t)] = \left[[K]^{-1} \cdot [B(t)]^T \right]^T$$

dove, per capire il significato di ciascuna matrice, rimando al capitolo [9].

Tale relazione, implementata con una matrice di coefficienti correttivi, permetterà di ricavare i valori di corrente per ciascuna barra con la sola misura del campo magnetico da parte dei sensori.

Tramite le varie simulazioni si è potuto studiare il comportamento del sistema, appurandone il corretto funzionamento dal punto di vista simulativo. Uno degli scopi futuri sarà appunto l'implementazione di tali relazioni nella programmazione della scheda Arduino® per il funzionamento reale del sistema di misurazione.

Per quanto riguarda la seconda fase del progetto è stato implementato un codice di programmazione che ha lo scopo di controllare il microprocessore della scheda Arduino Mega. Questo per realizzare l'acquisizione dei valori rilevati dai sensori, digitalizzarli ed elaborarli per ottenere le varie informazioni elettriche dei circuiti discussi precedentemente.

Le principali limitazioni incontrate sono state dovute a vari ritardi riscontrati nel passaggio dalla lettura di un canale ad un altro che portava ad avere un errore nella misurazione della differenza di fase tra tensione e corrente.

Tali limitazioni sono state superate con l'utilizzo di varie strategie di programmazione del microprocessore che hanno ridotto considerevolmente l'errore.

Con il presente studio si è conclusa una prima parte del progetto complessivo che porterà al funzionamento pratico del sistema di monitoraggio. Gli sviluppi futuri da realizzare saranno i seguenti:

- Cablaggio del circuito comprendente i sensori, la scheda Arduino® ed eventuali Amplificatori Operazionali;
- Installazione dei sensori (24 sensori per le fasi e 2 per il neutro);
- Implementazione, delle relazioni teoriche ottenute, nel codice di programma di Arduino®;
- Verifica della compatibilità elettromagnetica;
- Collaudo del sistema.

1 INTRODUCTION

“Measurement is the first step that leads to control and eventually to improvement.

If you can't measure something, you can't understand it.

If you can't understand it, you can't control it.

If you can't control it, you can't improve it.”

-H. James Harrington-

The application developed in this investigation assumes that the magnetic field around a bus bar, at a certain distance, is proportional to the applied current at all times. Thus, it's possible to find out the electrical information of a bus bar by measuring and analysing the emanated magnetic field.

This type of current measurement application was implemented, in this study, in order to develop an automatic and low cost system for the monitoring of the currents that flow through a group of bus bars.

This automatic system of measurement is destined to a L.V. electrical panel, employed in the industrial sector. The panel supplies four different circuits of the electrical installation providing energy to distinct groups of electrical loads. The circuits into consideration are 3-phase circuits, thus every circuit is composed by three different bus bars referred to the phases R, S, T and also the neutral bar.

The purpose of the study is to monitor, at any time, the current flowing through every bar in order to know the load curve and the main electrical information that denotes every circuit without the use of classical and manual measurement methods.

The main difficulty, encountered in the development of the project, was the implementation of a system able to achieve the immunity from stray magnetic fields, which can significantly disturb the measurement accuracy.

To fulfil this objective two magnetoresistive sensors, installed with different configurations, have been implemented for every bus bar, as explained in the next paragraph.

Considering the difficulty to develop the present investigation with practical methods was used a theoretical approach based on a modelling of the problem with a Finite Element Method (FEM).

The modelling with a FEM allows to make various studies of the problem and to simulate the behaviour of various electrical parameters depending on the settings. In this particular case, the big advantages in the use of a FEM have been principally the possibility to set infinite values for the input current (useful for the implementation of the various tests) and the possibility to supply, or not, every singular bar of every circuit.

The FEM software used in this investigation is COMSOL Multiphysics®, used with the support of Solidworks® for the geometrical part and with the support of Matlab® for the graphical results part.

Regarding the practice development of the study, which aims to monitor the currents in the real panel, it was programmed an Arduino® board in order to collect the values of MF from the sensors and to elaborate these data so as to find other electrical information.

1.1 Magnetoresistive sensors

Magnetoresistance (MR) is defined as the property of a material to change the value of its electrical resistance when an external magnetic field is applied to it.

The first magnetoresistive effect was discovered by William Thomson (better known as Lord Kelvin) in 1851.

With his experiments he discovered that in a piece of iron the resistance increases when the current is in the same direction as the magnetic force and decreases when the current is at 90° to the magnetic force. Making, subsequently, the same experiment with nickel he finds that the piece of iron was affected in the same way but the magnitude of the effect was greater. This effect is referred to as anisotropic magnetoresistance (AMR).

On a theoretical level, depending on the magnetic field conditions, the material has a minimum and maximum resistance, R_{min} and R_{max} respectively, where R_{min} is taken as the reference resistance value and its variation can be expressed by the ratio:

$$(1.1) \quad MR = \frac{(R_{max} - R_{min})}{R_{min}} \times 100$$

being MR the percentage of the magnetoresistive effect in the material or device. [1,2]

The main different magnetoresistive mechanisms are: anisotropic magnetoresistance (AMR), giant magnetoresistance (GMR) and tunnel magnetoresistance (TMR).

1.1.1 AMR effect

Thomson's experiments are an example of AMR, property of a material in which a dependence of electrical resistance on the angle between the direction of electric current and direction of magnetization is observed.

The maximum resistance is obtained when the magnetic field direction is parallel to the current flow, while the minimum value occurs when the magnetic field and the electric current have perpendicular directions. This effect is a characteristic of ferromagnetic alloys, such as Fe and Ni compounds, and arises from spin orbit interactions among the 3d shells electrons. It is related with the scattering of the conduction electrons in d orbitals (spin-orbit coupling), being the scattering probability higher when these orbitals are parallel to the current direction, resulting in different scattering cross sections for perpendicular and parallel configurations.

The orientation of d orbitals is set by the magnetic field orientation. The largest AMR effect at room temperature was observed for Ni_{1-x}Cox presenting a value of 6%.

AMR of new materials is being investigated and magnitudes up to 50% have been observed in some ferromagnetic uranium compounds.

Actually the AMR effect is used in a wide array of sensors for the measurement of Earth's magnetic field (electronic compass), for electric current measuring (by measuring the magnetic field created around the conductor), for traffic detection and for linear position and angle sensing. The biggest AMR sensor manufacturers are Honeywell, NXP Semiconductors, and Sensitec GmbH. [3]

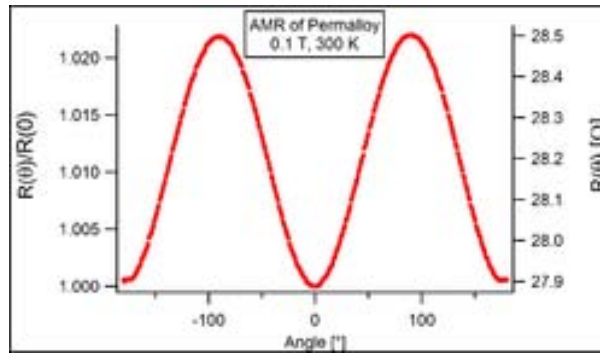


Fig. 1.1 Resistance of a thin Permalloy film as a function of an applied external field angle.

1.1.2 The 3-axis Magnetoresistive sensors: HMC5883L

The MR sensors used in this project are three-axis sensors named HMC5883L and produced by the Honeywell company (USA).

The Honeywell HMC5883L is a surface-mount, multi-chip module designed for low-field magnetic sensing with a digital interface for applications such as low-cost compassing and magnetometry.

The device uses the Anisotropic Magnetoresistive technology (AMR), mentioned in the previous paragraph, and includes high-resolution HMC118X series magneto-resistive sensors plus an ASIC (Application Specific Integrated Circuit) containing amplification and a 12-bit ADC with high accuracy.

The HMC5883L is a 3.0x3.0x0.9mm surface mount 16-pin and for its size it finds also varied applications in Mobile Phones, Netbooks, Consumer Electronics, Auto Navigation Systems and Personal Navigation Devices.

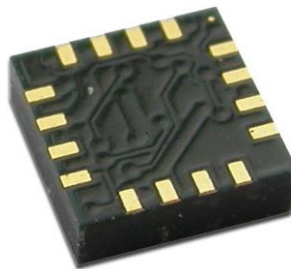


Fig. 1.2 Honeywell HMC5883L magnetoresistive sensor

The main characteristics and assets of the sensor are:

- Small size, that permits a highly integration in the electrical panel;
- Low cost and good cost-effectiveness;
- Low-Cost functionality test after assembly in production;
- Low voltage operations (2.16 to 3.6V) and low power consumption (100 μ A), also compatible with batteries;
- High resolution;
- High speed: 160 Hz maximum output rate;
- Operating temperature range: -30 \div 85 $^{\circ}$ C.

Where the main important characteristics that lead to choose this sensor for the implementation in the present project are: the low cost advantage, the small size and the big operating temperature range that allows to bear the heat produced by the bars.

1.2 Theoretical considerations for the MF measurement

Focusing on the goal of the work, the target is to measure the MF generate by an electrical bar of the electrical panel trying to not measure the stray MFs produced by the other bars.

To simplify the problem, an electrical conductive wire in which flows an electric current may be taken into account. As a consequence of this current flow, a magnetic field will arise and surround the electrical wire forming concentric circles around it, as in the following image.

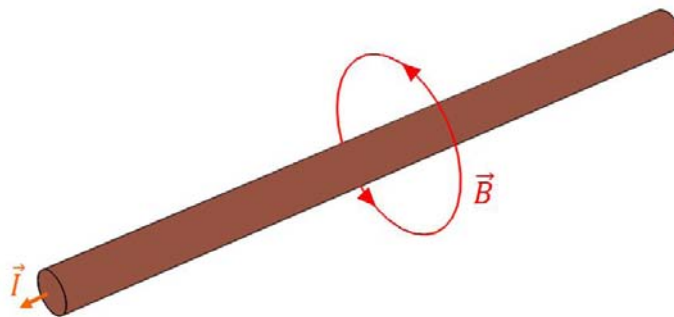


Fig. 1.3 Distribution of MF around an electrical wire.

Now, if is taken into consideration that the MF surrounds the cable in the form of circular lines, to figure out the value of MF it may be sufficient to measure the primary magnetic field in a point into the space close to the cable.

This it can be true if the magnetic field produced by the current is not influenced by other stray MFs produced, for example, by other active conductors or electrical devices present near the cable.

On the other side, if is taken into consideration the presence of another powered electrical wire, there will be some component of MF generated by the second wire that may have influence in the measure of the main MF produced by the first wire.

A solution to this problem can be found with a more practical approach. This happens with the simultaneous use of two magnetoresistive sensors instead of one, by placing these sensors in order to measure the same magnitude of MF.

In fact, the idea is to eliminate the effects produced by other powered conductors with the implementation of two magnetoresistive sensors with different configurations.

To do this we have to install a MF sensor on one side of the conductive wire and to configure it to measure the component of MF, caused by the current, in a certain direction. Then it's necessary to install a second MF sensor, positioned in the other side of the conductor (substantially opposite to the first sensor), configuring it to measure the opposite component of MF respect the previous sensor. In the next image is shown a wire affected by an electric current that causes a MF which components are measured by two MF sensors, arranged as just explained.

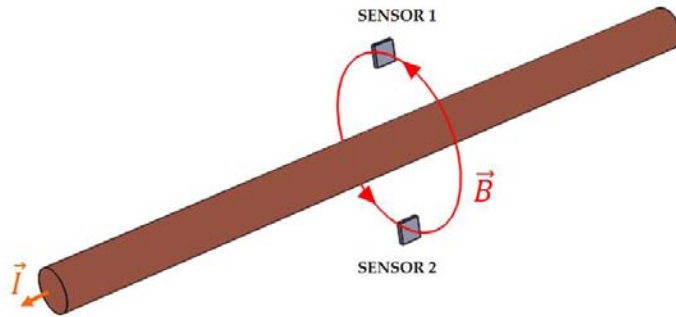


Fig. 1.4 Disposition of sensors for an electrical wire

Referring to the image, we can consider the vertical plane passing through the sensors and that cut the line of MF in a perpendicular way. It's possible to note that the lines of MF can be incoming or outgoing to the considered plane, namely, incoming or outgoing to the two sensors.

In this way there will be measured, for example, for the sensor 1 (incoming MF line) and for the sensor 2 (outgoing MF line) a positive value of MF. This is because the MF sensors are directional and have an opposite direction of measure. This configuration can be realized just installing the couple of sensors with opposite directions to each other.

A consequence is that the sum of the two values it will be the double of the real MF value in that moment (neglecting the probable measurement errors).

Let's move to the case of two powered electrical wires, positioned at a respective distance much bigger than the distance between the two sensors. In this case the lines of MF, produced by the current flowing in the second wire, will be both incoming in the plane into consideration, i.e. incoming in the sensors surface, as can be seen in the next image.

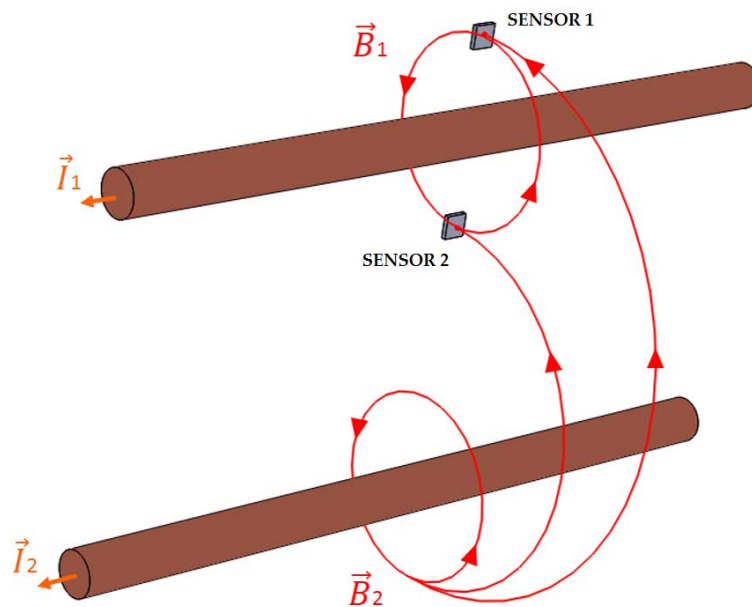


Fig. 1.5 Detection of MF by the sensors. Case with two electrical wires.

Going now to sum the two components of stray MF measured by the sensors, the obtained result will be, thanks to the sensors configurations, the difference of the two measures instead of the sum. This leads to obtain the almost total elimination of stray fields contribute in the measure.

It's important to note that, when multiple alimented conductors are arranged in parallel, the magnetic field gradient decreases with the distance. This means that the cancelation of the effects caused by surrounding conductors will be better if they will be at greater distance.

All these considerations are obviously applicable to the electrical bars under study in this project, creating an automatic system for the monitoring of the MF and consequently for the monitoring of the electric currents that flow into the bars.

The next image represents the idea just explained referring it to the case with the bus bars under study, mounted on the electrical panel.

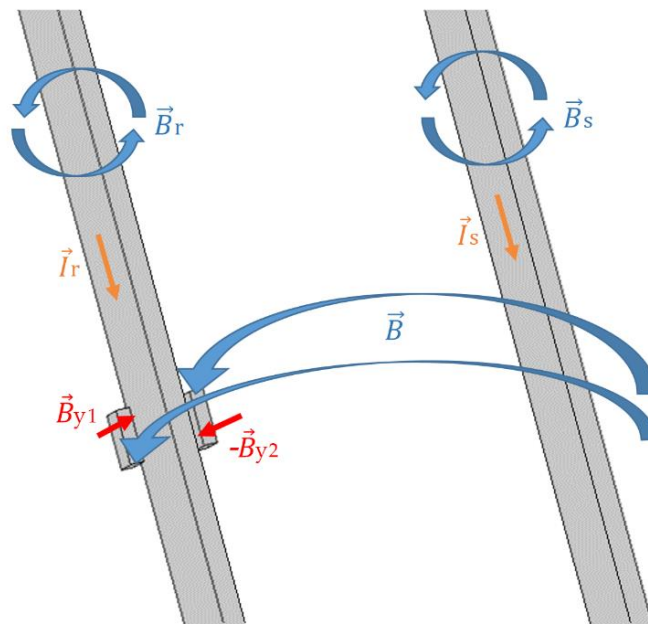


Fig. 1.6 Detection of MF by the sensors. Case with two bus bars.

In the image are represented with the vectors \vec{B}_{y1} and \vec{B}_{y2} the settings adopted in order to use the sensors in opposite configuration mode. As explained before, the two sensors measure a component of the MF (in this case the vector component y) but installing the sensors with opposite directions it brings to eliminate the part of measure influenced by the stray magnetic fields.

The final result will be a double measure of the magnetic field produced by the interest bar, with also another additional term (error) that consider the fact that the sensors are close but not in the same point.

Indeed, considering that the distance from every bar is in the order of some cm and the distance between two sensors will be in the order of 1.5 cm, it's normal to think that the sensors will detect a value of MF a little bit different among themselves, especially for the MF contribution by the nearest bars.

1.2.1 FEM approach to simulate a Magnetoresistive sensor

After the first tests to ascertain the proper functioning of the model it was possible to elaborate the first simulations in order to figure out the veracity of the theoretical hypothesis explained in the previous paragraph.

To obtain this it was necessary, first of all, simulate the presence of these sensors in the FEM model, i.e. simulate a point of measure for the MF in the space around the bars. Secondly it was necessary to determine a good site for the installation of the sensors remembering the real geometry of the electrical panel.

To model the sensors in Comsol has been used a tool in the post processing section named “Domain Point Probe” that allows to evaluate the MF in a fixed point in the space and also to evaluate the three main vector components of the MF: \mathbf{B}_x , \mathbf{B}_y and \mathbf{B}_z .

This last feature has been useful in order to model the future system of measure that will be installed in the panel, this is because also the MF sensors are able to measure a component of magnetic field corresponding to a specific direction.

2 THEORETICAL FRAMEWORK

2.1 Ampere Law

In classical electromagnetism, Ampère's circuital law, discovered by André-Marie Ampère in 1823, relates the integrated magnetic field around a closed loop to the electric current passing through the loop and therefore relates magnetic fields to electric currents that produce them.

In its original form, Ampère's circuital law relates a magnetic field to its electric current source. The law can be written in two forms described below, the "integral form" and the "differential form". [4]

2.1.1 Integral form

In SI units, the "integral form" of the original Ampère's circuital law is a line integral of the magnetic field around some closed curve C (arbitrary but must be closed).

The mathematical statement of the law is a relation between the total amount of magnetic field around some path (line integral) due to the current which passes through that enclosed path (surface integral). It can be written in a number of forms. [5]

In terms of total current, which includes both free and bound current, the line integral of the magnetic B-field (in tesla, T) around closed curve C it's proportional to the total current I_{enc} passing through a surface S (enclosed by C):

$$(2.1) \quad \oint_C \mathbf{B} \cdot d\mathbf{l} = \mu_0 \int_S \mathbf{J} \cdot d\mathbf{S} = \mu_0 I_{enc}$$

where \mathbf{J} is the total current density (in ampere per square metre, Am^{-2}).

Alternatively, in terms of free current, the line integral of the magnetic H-field (in ampere per metre, Am^{-1}) around closed curve C equals the free current $I_{f,enc}$ through a surface S :

$$(2.2) \quad \oint_C \mathbf{H} \cdot d\mathbf{l} = \int_S \mathbf{J}_f \cdot d\mathbf{S} = I_{f,enc}$$

where \mathbf{J}_f is the free current density only.

The \mathbf{B} and \mathbf{H} fields are related by the constitutive equation:

$$(2.3) \quad \mathbf{B} = \mu_0 \cdot \mathbf{H}$$

where μ_0 is the magnetic constant.

2.1.2 Differential form

By the Stokes' theorem, this equation can also be written in a "differential form". Again, this equation only applies in the case where the electric field is constant in time, meaning the currents are steady (time-independent, else the magnetic field would change with time)

In SI units, the equation states for total current:

$$(2.4) \quad \nabla \times \mathbf{B} = \mu_0 \mathbf{J}$$

and for free current

$$(2.5) \quad \nabla \times \mathbf{H} = \mathbf{J}$$

where $\nabla \times$ is the curl operator, \mathbf{J} is the total current density vector (in ampere per square metre, Am⁻²) and where \mathbf{B} and \mathbf{H} are the magnetic field vectors.

2.2 Principal laws used for the computation

In order to calculate the magnetic field generated by the currents the simulation software will use these Maxwell's laws of electromagnetism:

- Ampere Law:

$$(2.6) \quad \nabla \times \mathbf{H} = \mathbf{J}$$

where \mathbf{H} is the magnetic field vector and \mathbf{J} is the current density at a given location in a resistive material;

- Gauss Law for magnetism:

$$(2.7) \quad \mathbf{B} = \nabla \times \mathbf{A}$$

where \mathbf{B} is the magnetic field vector and the vector field \mathbf{A} is called magnetic vector potential;

- Reformulation of Ohm's Law:

$$(2.8) \quad \mathbf{J} = \sigma \mathbf{E}$$

where \mathbf{E} is the electric field and σ is a material-dependent parameter called electrical conductivity (in Siemens per metre, S/m).

3 ELECTRICAL PANEL PRESENTATION

3.1 Electrical panel features

The electrical panel taken into consideration is used in the industrial sector and is installed in a MV/LV substation for the electrical distribution in LV.

The electrical panel is principally composed by:

- External aluminium structure;
- Electrical bus bars made of aluminium;
- Holders for the fuses made of copper;
- Plastic parts to support the bus bars and for the protection against direct contact with live parts;
- 12 fuses.

Electrical features:

- $I_n = 400 \text{ A}$;
- $V_n = 400 \text{ V}$.

The dimensions of the structure are presented in the next paragraph.



Fig. 3.1 Photo of the electrical distribution panel.

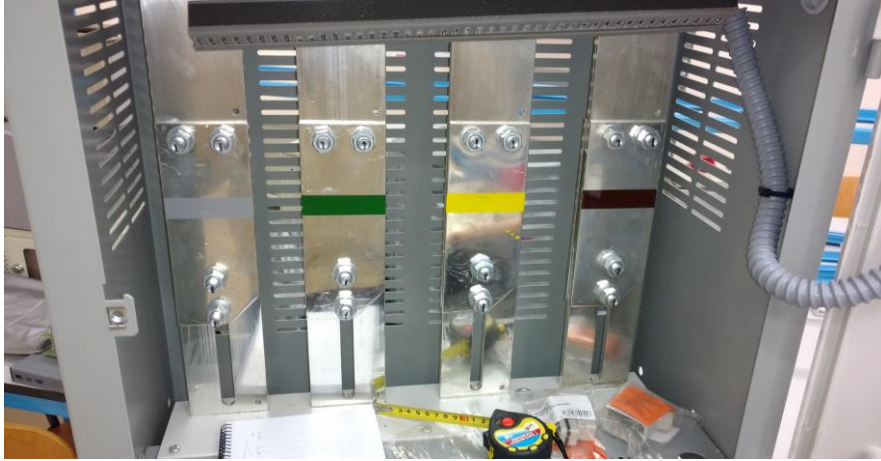


Fig. 3.2 Input bars of the electrical panel (N, R, S, T bars).



Fig. 3.3 Output terminals for the connection of different 3-phase circuits.



Fig. 3.4 Holders for the fuses.

3.2 Development of the geometry in Solidworks®

The CAD software Solidworks® was used in order to realize the 3D geometry of the model, that, was built, at first drawing all the single parts of the electrical panel and then assembling these parts each other.

In the following images is represented the final model, drawn in the CAD software and subsequently imported in the Comsol software for the analysis.

In the *Figure 3.8* is shown the original model and in the *Figure 3.9* is shown the same model but with a prolongation of the final part of the bars with the length of 120 cm. This is because the external domain will be much bigger than the panel size and for this will be necessary the prolongation of the bars in order to connect that bars to the external domain, closing the paths for the currents. This choice will be taken up in the next chapters and explained more deeply.

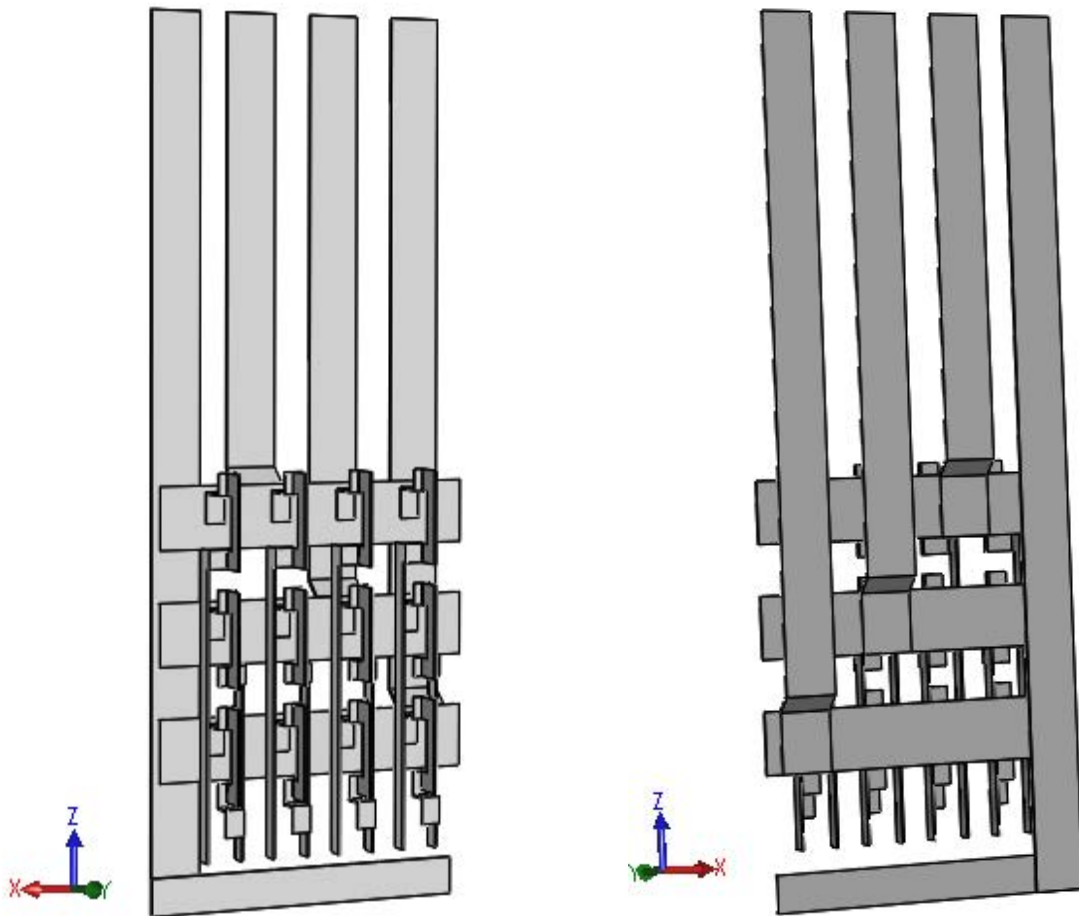


Fig. 3.5 3D CAD model of the electrical panel.

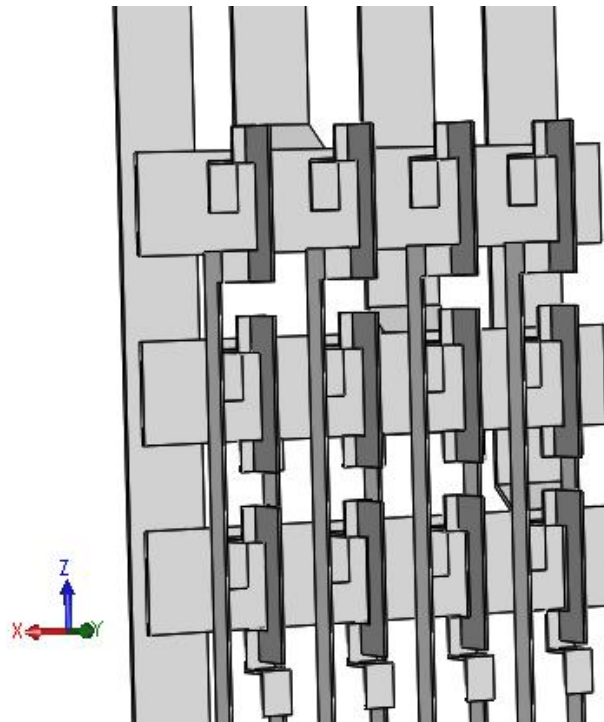


Fig. 3.6 3D CAD model of the electrical panel.

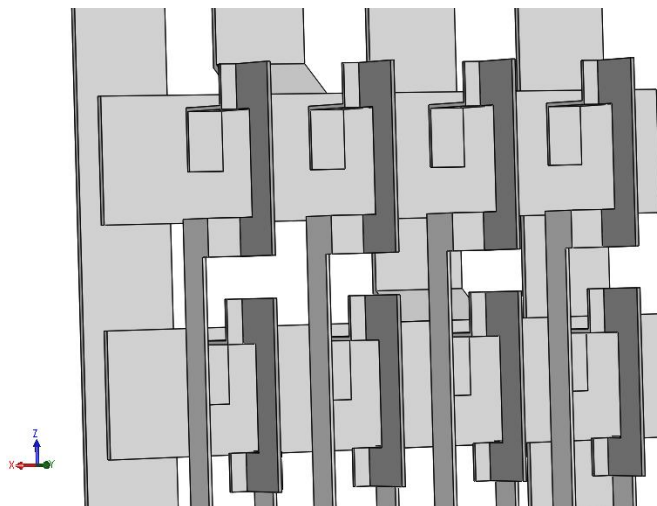


Fig. 3.7 3D CAD model of the electrical panel.

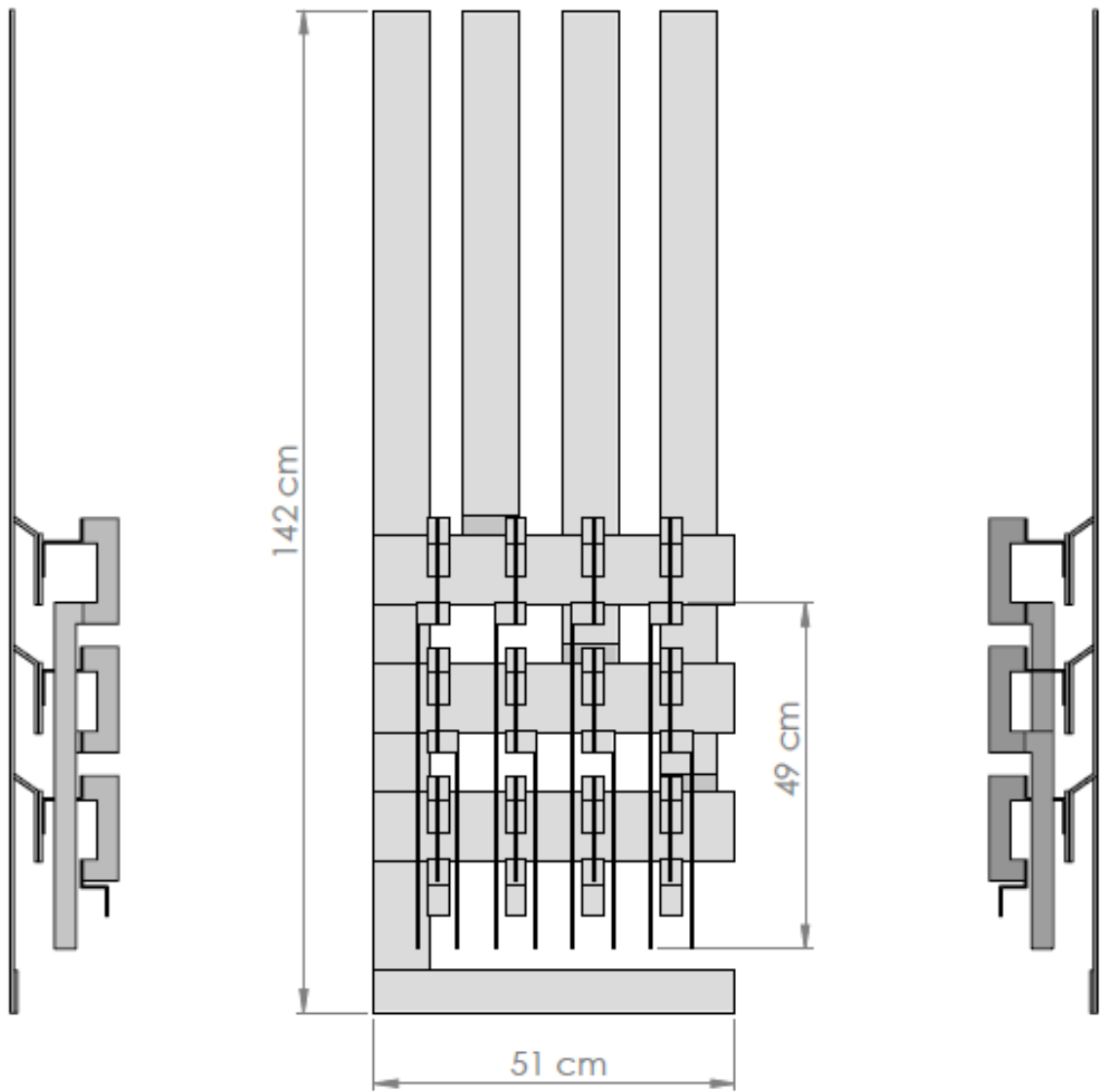


Fig. 3.8 Axonometric drawing of the original model.

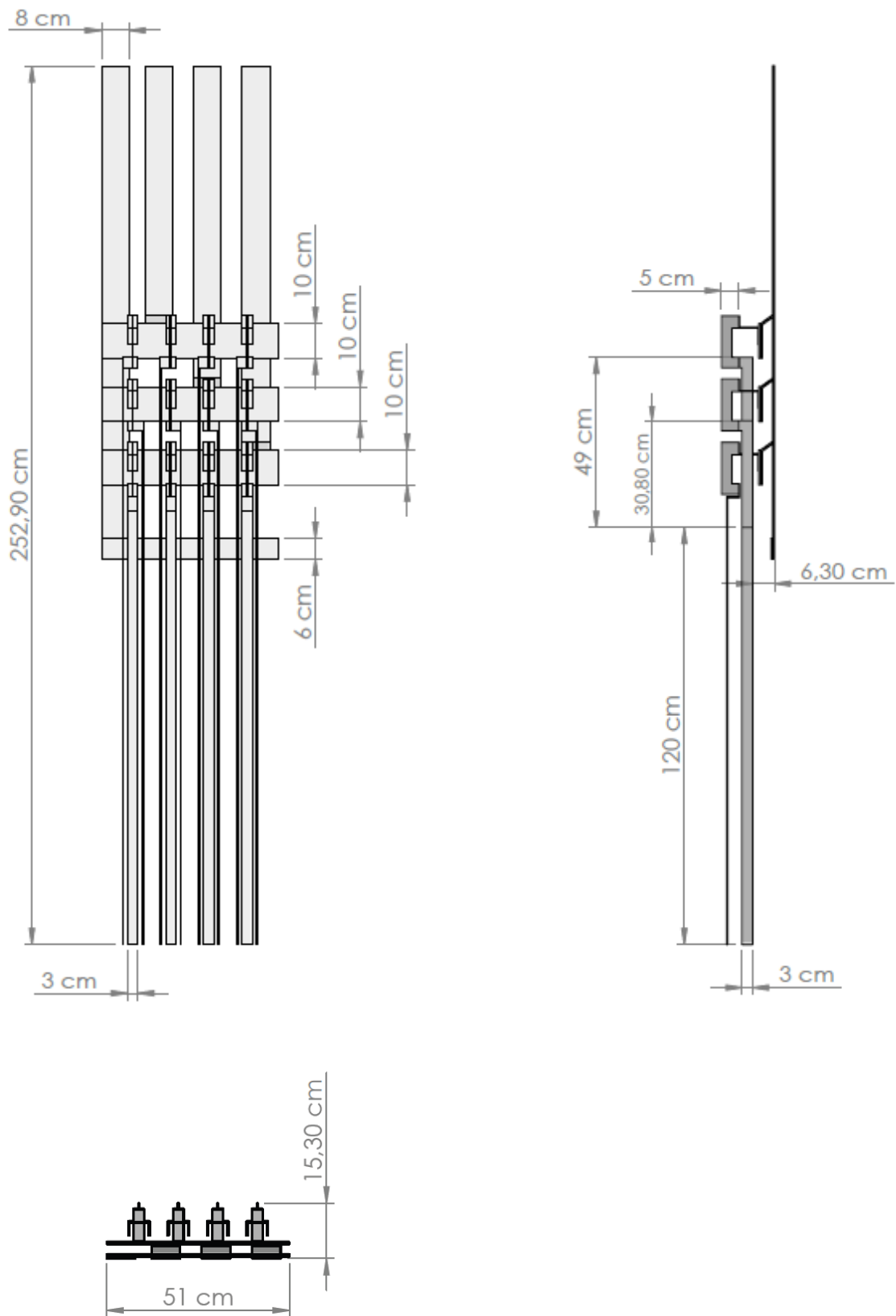


Fig. 3.9 Axonometric drawing of the model with prolonged bars.

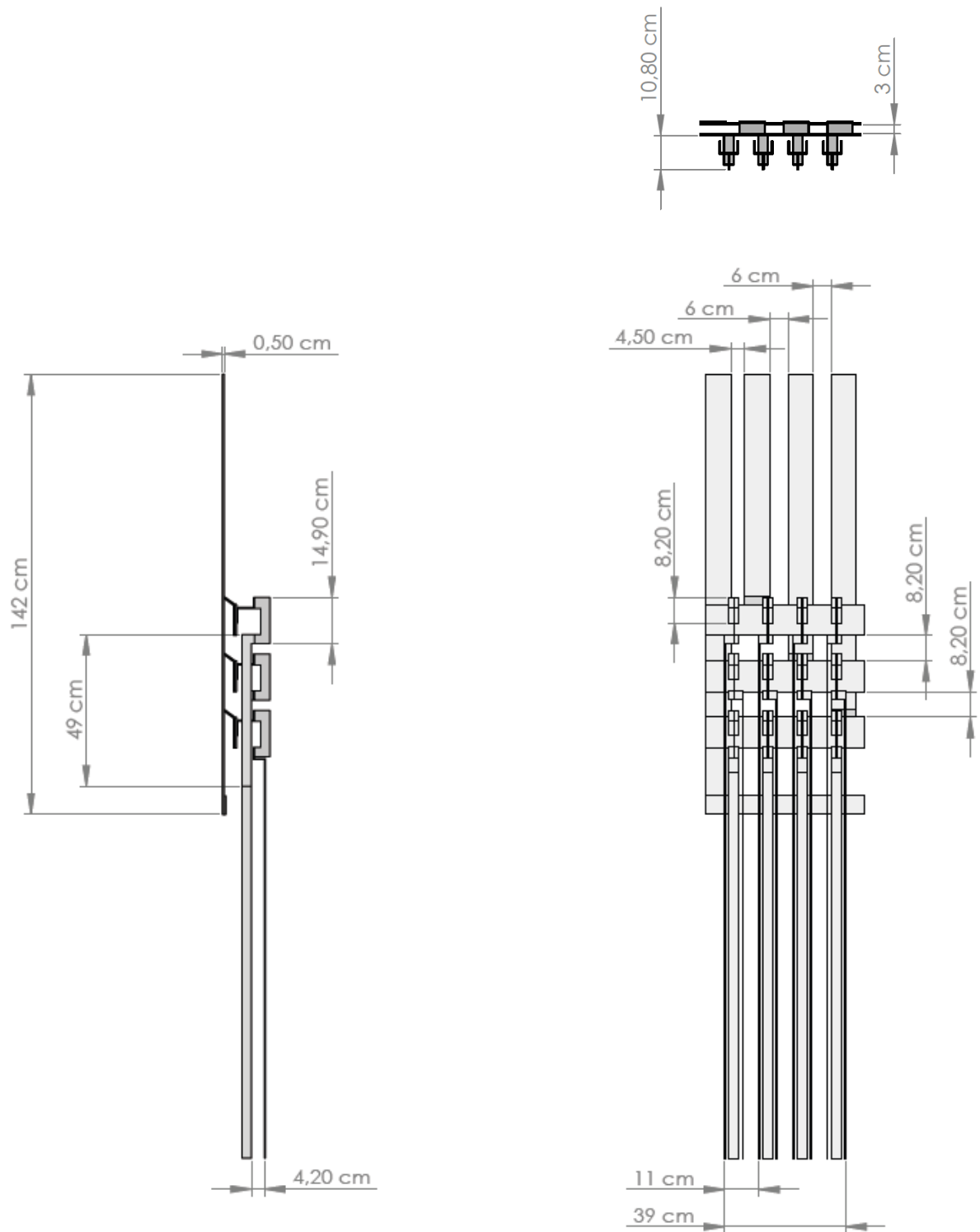


Fig. 3.10 Axonometric drawing of the model with prolonged bars.

3.3 Geometry implementation in Comsol Multiphysics®

For the geometry implementation in Comsol was used the tool that permits to import Solidworks projects in the Comsol GUI ensuring that all the measures were read correctly from the software and all the parts were considered as solid parts.

At this point there were inserted other two blocks, positioned around the panel designed, in order to form the external domain and consequently the way to return for the currents, as it will be explained in the chapter [5].

The two blocks represented in the *Figures 3.11* and *3.12* are characterized by the following measures:

	<i>Width [cm]</i>	<i>Depth [cm]</i>	<i>Height [cm]</i>
<i>Block 1</i>	70	30	252.7
<i>Block 2</i>	300	200	252.7

Table 3.1 Size of domain blocks.

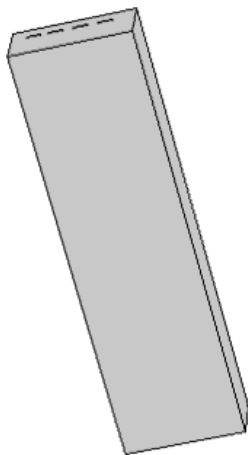


Fig. 3.11 Block 1.

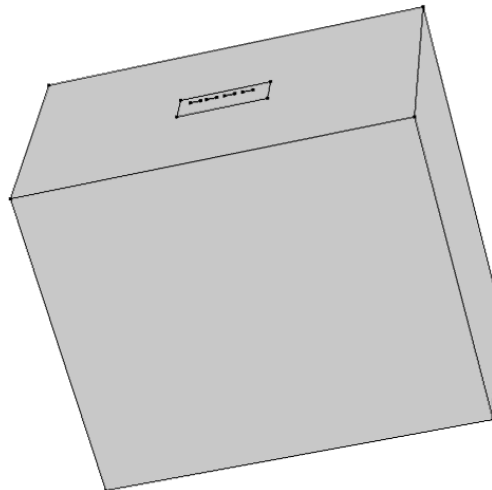


Fig. 3.12 Block 2.

4 MATERIAL

There are a lot of consideration to do regarding the materials with which is made the subject of study because all the results depend on the electrical properties of materials.

In this particular case the electrical panel is principally made of these materials:

- Aluminium, with which are made the bus bars and the external box;
- Plastic, with which are made a lot of parts acting as support for some components of the panel and significantly to protect the user against unintentional direct contacts with live parts;
- Copper, for the holders where will be insert the fuses;
- Steel, of the nuts and bolts used to fix the various parts of the panel.

Most of these materials will be not taken into consideration in the modelled study of the electrical panel, as it's explained in the next paragraph.

4.1 Materials hypothesis for the FEM simulation.

As introduced before, not all the parts that composed the panel have been taken into account in the construction of the Comsol model, this is because not all the parts are interested in the flow of current neither are particularly influent in the expansion of the magnetic field in the air.

Furthermore, as seen before, it would not be possible to make a drawing with all the single parts really present in the panel. Substantially, in the Comsol model have been represented the aluminium bars and the fuses holders, that are the parts of interest, omitting the other parts.

Moreover, the fuses holders have been simplified omitting the copper parts and considering a single piece of aluminium instead of them.

The result of all these considerations brings to use, in the simulation software, all the solid parts (bus bars) made of aluminium and all the other parts made of air.

After these considerations is possible to set, in the Comsol GUI, to every part of the model the respective material through the appropriate tool.

In the subsequent developments of the project will be taken into consideration these two different material approaches:

- A first approach considering the bus bars made of aluminium, as in the real case, in order to study the model including the effects of the mutual inductance;
- A second approach considering the bus bars made of air, in order to study the model neglecting the mutual inductance effects between the bars.

These approaches will be better taken up in the *chapter 10*.

In the next tables are presented the main properties of the materials used in the simulations:

	<i>Value</i>	<i>Unit</i>
<i>Relative permeability</i>	<i>1</i>	-
<i>Relative permittivity</i>	<i>1</i>	-
<i>Electrical conductivity</i>	<i>10</i>	[S/m]

Table 4.1 Properties of air.

	<i>Value</i>	<i>Unit</i>
<i>Relative permeability</i>	<i>1</i>	-
<i>Relative permittivity</i>	<i>1</i>	-
<i>Electrical conductivity</i>	<i>3.77E+07</i>	[S/m]

Table 4.2 Properties of aluminium.

As it can be seen, for the air was used an electrical conductivity of 10 [S/m] so as to speed up the simulations. This change will not affect the calculation of the results.

5 IMPLEMENTATION OF THE PHYSIC STUDY

A fundamental part for the study of a model in Comsol is the setting of the physic, i.e. the setting of the type of study we need to take into consideration.

In the particular model taken into account in this project the type of study chosen is a Magnetic field study. This type of study allows to set a current or a potential difference to the element of interest. The purpose is to calculate the respective Magnetic field produced, its distribution in the space and it's also possible to see the distribution of the current density in the object.

Another fundamental part is the selection of a domain of study. About this, it has been taken into consideration principally the time domain. This for the fact that the current flowing through the panel bars is an alternating current depending on time, the frequency taken into account is the industrial frequency of 50 Hz.

In addition to the time domain it was used a steady-state analysis of the same in order to find out some constant value that will be explained in next paragraphs.

5.1 Setting of a current

For the setting of the currents has been used an easy and practice way consisting in considering the subject of the study like a coil in which is possible to set a closed path for currents.

In order to do this, in the software there are nodes (tools) named "Coil" that are used to simplify the setup of magnetostatic and low-frequency electromagnetic models.

In many such applications, the magnetic field is generated by electric currents flowing in conductive materials (for example: cables, wires, coils, or solenoids) and the coil features can be used to easily model these structures and to translate lumped quantities (currents and voltages) into distributed quantities (current densities and electric fields).

There are two types of coil tools, the Single-Turn Coil and the Multi-Turn Coil which differ by the physical system represented.

The Multi-Turn Coil tool implements a homogenized model of a coil consisting of numerous tightly-wound conducting wires, separated by an electrical insulator.

On the other hand, the Single-Turn Coil tool models a single, solid region of a conducting material (for example metal) in which the current flows and this is the case that most befits our study.

After choosing the Single-Turn Coil as default tool for the study and after the selection of the parts representing the aluminium bars is necessary to set the currents that will flow through the circuits generating the magnetic field.

All these coil can be excited either with current and voltage excitation and the supplied value or expression is translated to a current density or electric field applied to the domain into consideration.

The excitation is applied by means of specialized subnodes:

- Boundary Feed subnode, in which it's possible to set the input current on the interest boundary, thus creating a way in for the current in the turn coil;
- Ground subnode, that enforces the coil potential to be zero on the selected boundaries.

The lumped voltage and current of the coil correspond respectively to the integral of the electric field along the coil length and to the integral of the current density on a cross section. [6]

With these settings can be created a path for the currents that actually is not a closed path, for doing a closed path we have to introduce an important topic for the FEM simulations: the study of the Boundary Conditions.

5.1.1 Boundary conditions

Taking into consideration a current carrying conductor, as a consequence of the current flow, a magnetic field arises and surrounds the wire. This is a vector field, having both a magnitude and direction, and can be computed from Ampère's law. We are interested in learning how to model this magnetic field and how it interacts with other objects.

A reasonable computational model of a current carrying wire may be shown with the following image.

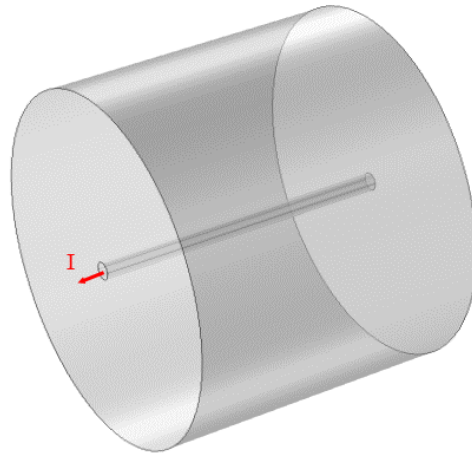


Fig. 5.1 Model of an electrical wire with FEM.

At first, it can be seen that there is a cylinder around the wire. This cylinder represents the air domain and is the computational domain within which we are solving the magnetic field.

This domain is a finite-sized domain that permits to reduce the computational effort. This is because the MF intensity will drop off with the inverse of distance to a wire, so the field magnitude will be quite small far away from it. Although it will never be precisely zero, we can reasonably truncate our modeling domain to a finite-sized space in order to not require a big computational effort in the resolution.

By choosing a finite modelling region around the wire, we are assuming that we are only interested in the fields in this region and this choice introduces an assumption to the boundaries. Indeed, we need to consider some boundary conditions along the boundaries of the cylinder or whatever surrounding domain shape we choose. The main boundary conditions available in Comsol are the Magnetic Insulation and the Perfect Magnetic Conductor conditions.

The Magnetic Insulation condition can be physically interpreted as a boundary to a domain that has infinite electrical conductivity. It implies that our wire is enclosed within a sphere of very high conductivity. Currents can flow and be induced on a magnetic insulation boundary. Mathematically speaking, the magnetic insulation fixes the field variable that is being solved to be zero to the boundary; it's a homogeneous Dirichlet boundary condition.

On the other hand, the Perfect Magnetic Conductor boundary condition is the opposite. In fact, mathematically, it enforces the homogeneous Neumann condition, meaning the derivative of the solution field in the direction normal to the boundary is zero. No current can flow, nor be induced on, a perfect magnetic conductor boundary. [7,8]

Since our wire extends to the boundaries of the modelling domain, concerning in what was explained in the previous paragraph, we need to provide a current return path via the Magnetic Insulation boundary condition to allow the current to flow through this domain.

5.2 Modelling of a basic electrical conductor in Comsol Multiphysics

As seen above, one of the most basic points in modelling an electrical wire is the concept of a closed current path. Also in the case of study there needs to be a closed path of current and the model must satisfy this condition to be valid.

If we want to impose a current that flows through an open circuit conductor, it will be equivalent to impose to the current (electrons) to move instantaneously from one end of the open circuit to the other. This may violate Maxwell's equations.

Moving on the particular case under study, we have a current that flows through the bars and, as a consequence of the computed current flow, magnetic fields that arise and surround the bars. Taking into account a single bus bar, it has been imposed a grounded boundary condition to one side, this means an imposition of an electric potential of zero. Subsequently it has been imposed a higher electric potential on the other side.

At this point it's necessary to set a path for the current in order to obtain a closed circuit for its return. This can be solved considering some boundary conditions along the boundaries of the block representing the external domain, discussed in the previous paragraph. Therefore, in order to set a closed path for the current it was necessary to insert around the model a block representing the external domain and set for it an appropriate boundary condition.

In this project has been considered a boundary condition that represents a perfect electrical conductor for the return of current, namely a Magnetic Insulation boundary condition.

For the physical interpretation of this, it can be assumed that the conductor sits inside of a cylindrical metal container. As a consequence of the boundary condition, the current, which is flowing along the wire from one side to the other, will flow back along the surface of the modelled domain as shown in the image below.

In this way it was possible to apply an electric current to the bars obtaining a perfect simulation of its flow in the conductive material.



Fig. 5.2 Model of a conductor. Return of current through the external domain.

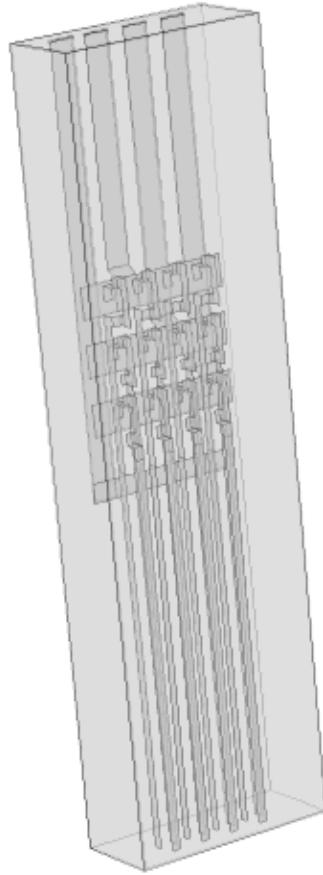


Fig. 5.3 Model of the electrical panel with the respective first domain.

6 MESH IMPLEMENTATION

The finite element method approximates the solution within each element using some elementary shape function that can be constant, linear, or of higher order.

Substantially the finite element mesh serves two purposes. For first subdivides the CAD geometry being modelled into smaller pieces, or elements, over which it is possible to write a set of equations describing the solution to the governing equation. Then the mesh is also used to represent the solution field to the physics being solved.

There are four different 3D element types that are tets, bricks, prisms, and pyramids:

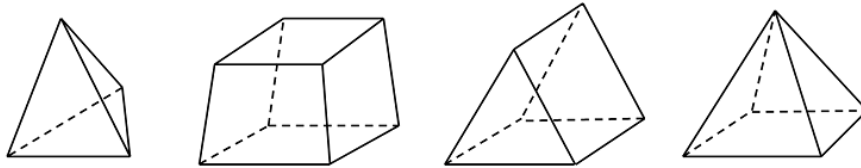


Fig. 6.1 3D elements types

These four elements can be used, in various combinations, to mesh any 3D model (for 2D models, there are available triangular and quadrilateral elements).

Tetrahedral elements are the default element type for most physics within Comsol Multiphysics and any 3D volume, regardless of shape or topology, can be meshed with tets. They are also the only kind of elements that can be used with adaptive mesh refinement.

The other three element types (bricks, prisms, and pyramids) should be used only when it is motivated to do so. It is simple to note that these elements will not always be able to mesh a particular geometry. [9]

For these considerations in our model of study has been chosen a tetrahedral mesh approach for the mesh construction, considering also that is possible, in this way, to custom the properties of the mesh.

In the next figures are shown the graphical representation of the mesh for every part of the model. Are considered three different sizes of mesh, as it can be seen in the tables. For the external domains (block 1 and block 2) have been chosen meshes with larger size elements in order to reduce the computing time.

The mesh was built with a Delaunay triangulation algorithm.

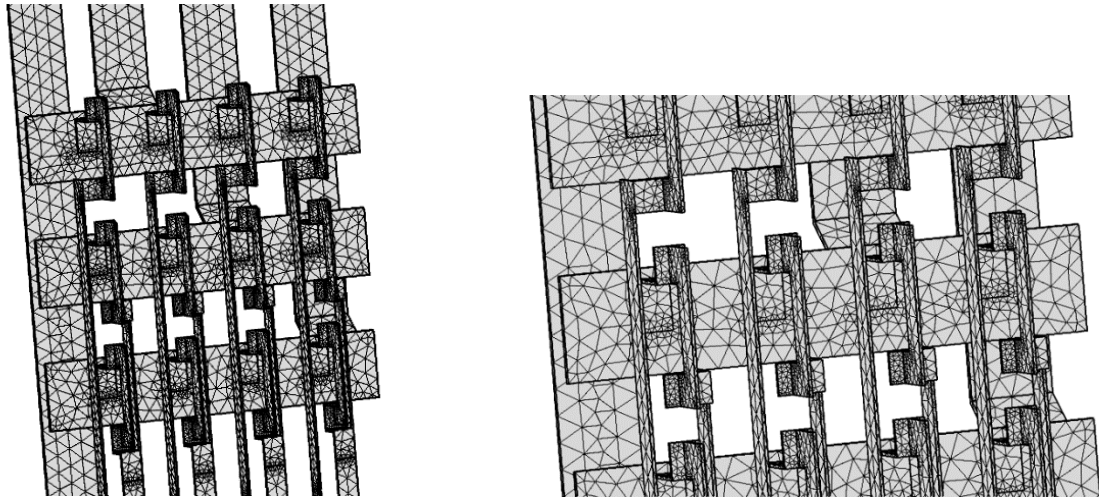


Fig. 6.2 Tetrahedral mesh n° 1

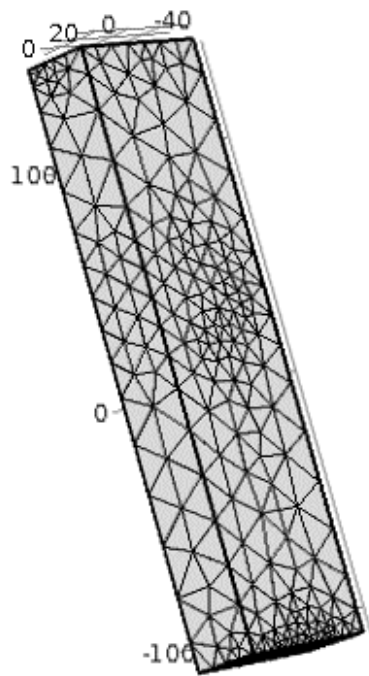


Fig. 6.3 Tetrahedral mesh n°2

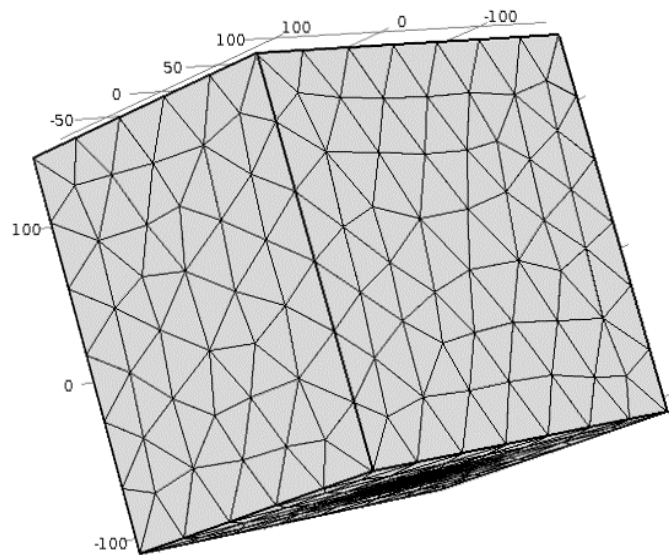


Fig. 6.4 Tetrahedral mesh n°3

6.1 Mesh characteristics

Table 6.1 Tetrahedral mesh n°1

	Value
<i>Maximum element size [cm]</i>	25.3
<i>Minimum element size [cm]</i>	2.3
<i>Minimum element growth rate</i>	1.5
<i>Curvature factor</i>	0.6
<i>Resolution of narrow regions</i>	0.5

Table 6.2 Tetrahedral mesh n°2

	Value
<i>Maximum element size [cm]</i>	25.3
<i>Minimum element size [cm]</i>	2.5
<i>Minimum element growth rate</i>	1.5
<i>Curvature factor</i>	0.6
<i>Resolution of narrow regions</i>	0.5

Table 6.3 Tetrahedral mesh n°3

	Value
<i>Maximum element size [cm]</i>	45
<i>Minimum element size [cm]</i>	8.4
<i>Minimum element growth rate</i>	1.6
<i>Curvature factor</i>	0.7
<i>Resolution of narrow regions</i>	0.4

7 FIRST APPROACH OF STUDY: CONSIDERATION OF A 2D CUT-PLANE

In this section there will be described the main reasons that brought into consideration the possibility to start the simulations with the FEM software in a 2D representation instead of a 3D representation.

This is possible considering a plane obtained “cutting” the 3-dimensional model in a given plane of interest.

This cutting plane will form an area in which it will be possible to find a location for the sensors, namely, in the simulation case, a good location for the measurement points created with the appropriate Comsol tool.

The Comsol tool used is named “point probe” and permits to measure the three vector components of a MF in a determinate point in the space, simulating a MF sensor behaviour.

Obviously every test in 2D will be followed by a 3D test considering the same points of measure, including so also the effects of the MF caused by the bars not considered in the 2D model.

The main criteria that led to the use of a 2D approach were:

- reduction of the geometric complexity;
- reduction of the physic complexities due to the setting of the currents and their repartition in all the circuits;
- focalization in a more reduced area;
- reduction of the heavy computation in order to reduce the computation time.

The last point, in particular, has a great influence in the present case because change the model slightly means re-solving the model study and for computation-heavy models (like the 3D model under study) this it can lead to have a big time-consuming process.

7.1 The choose of the cut-planes for the 2D study

One of the most difficult points in the development of the FEM model was to choose an opportune 2D cut plane to simulate the sensors measurement.

The main difficulties found were caused by the geometry complexity of the electrical panel in the real physic case. This because, as it can be seen in the photos, there are a lot of plastic parts that don't allow to install a sensor wherever we want. Moreover, there are other parts in which is not convenient the installation of a sensor because of the high concentration of different magnetic fields that could influence the measures.

For these reasons were considered, in every case, both the simplified model and the real electrical panel, in order to assure the connection between the theoretical simulation and the real physic realization.

The two planes selected for the study are the follows:

- A plane x-y obtained slicing the model at the height of $z = 35.25$ cm;
- A plane x-z obtained slicing the model at the height of $y = 11.4$ cm;
- A plane y-z obtained slicing the model at the height of $x = 6.9$ cm;

In this way it has been divided the study of the model into the two following possible dispositions of sensors:

- First possible disposition of sensors, composed by the first two cut-planes ($z = 35.25$ cm and $y = 11.4$ cm);
- Second possible disposition of sensors, composed by the third cut-plane ($y = 6.9$ cm).

In the first disposition were considered two different planes because in the first cut plane there are present the electrical bars referred to the phases R and S but there are not present the T-phase bars.

Therefore, the first option contains two different planes of disposition for the sensors: the first cut-plane for the sensors used for the bars referred to the phases R-S and the second cut-planes for the sensors used in the T-phase bars.

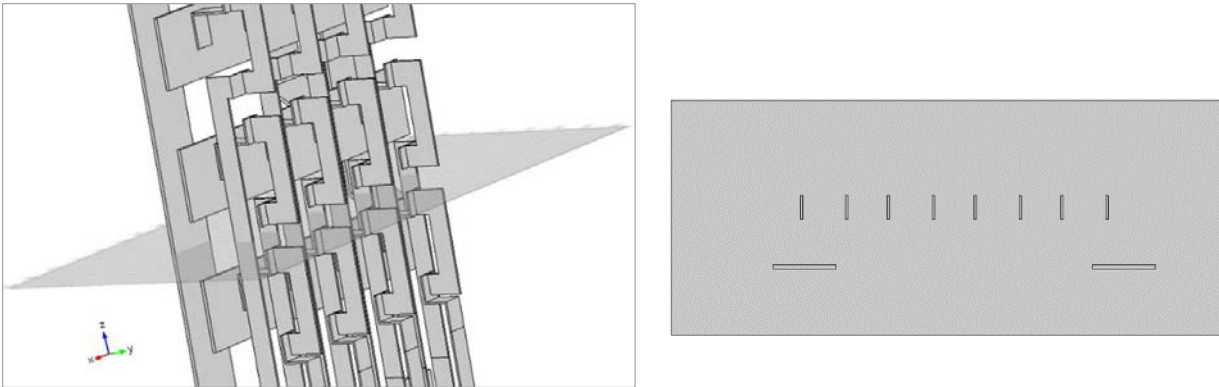


Fig. 7.1 Cut-plane for the R-S bars sensors of the first disposition, 3D and 2D views.

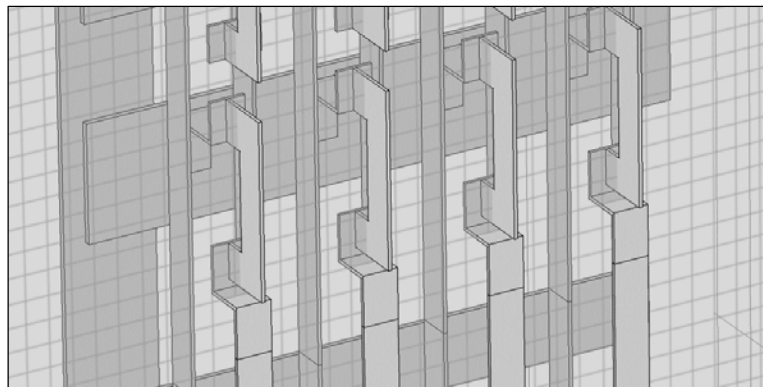


Fig. 7.2 Cut-plane for the T-bars sensors of the first disposition, 3D view.

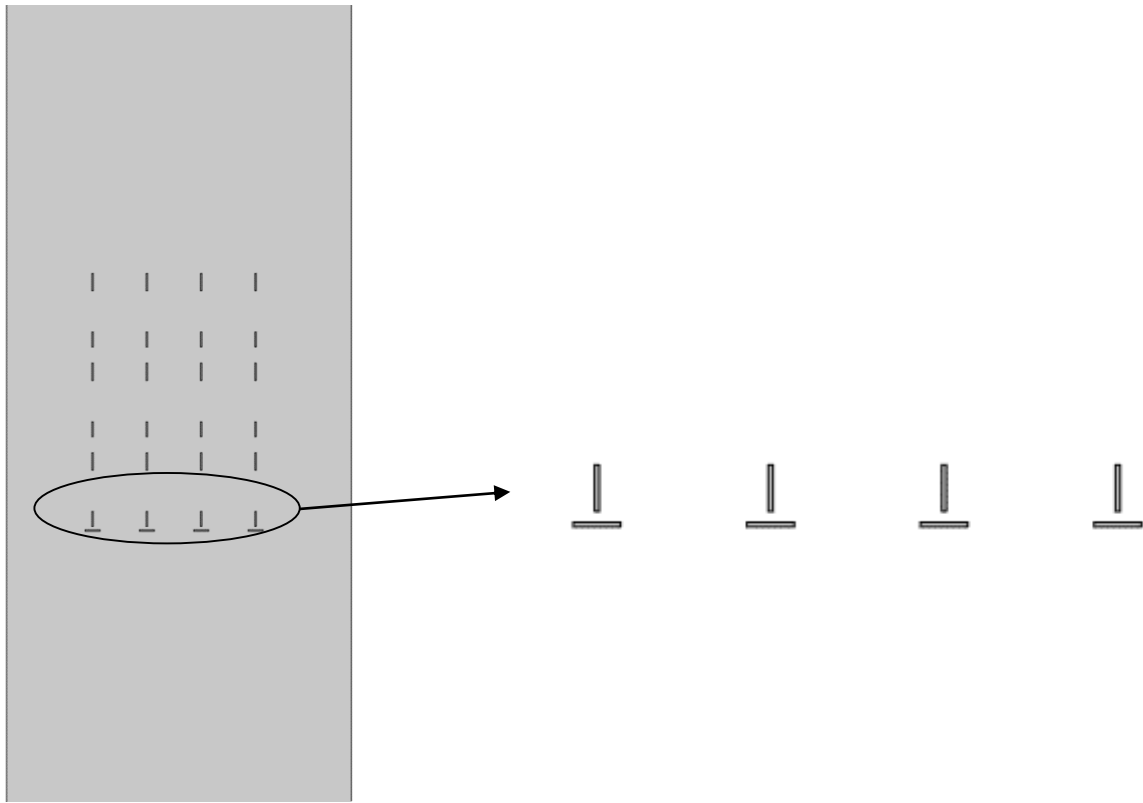


Fig. 7.3 Cut-plane for the T-bars sensors of the first disposition, 3D view.

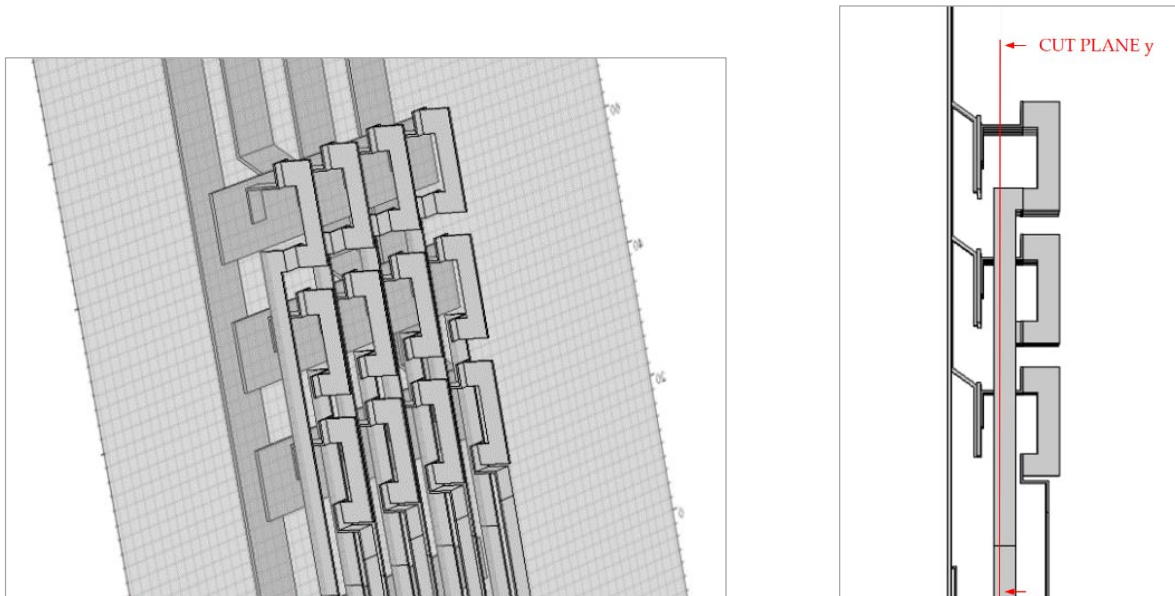


Fig. 7.4 Cut-plane for the second disposition, 3D view.

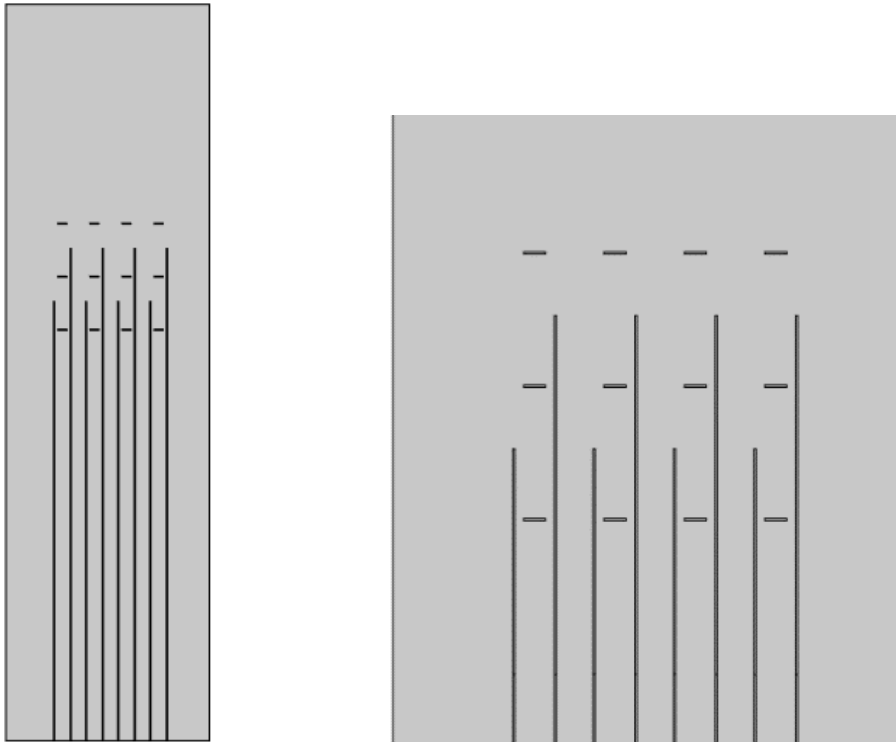


Fig. 7.5 Cut-plane for the second disposition, 2D view.

8 POSITIONING OF THE MEASUREMENT POINTS IN THE SIMULATION SOFTWARE

The presence of the sensors, as explained before, was simulated in the model with the use of a virtual tool that allows to measure the MF and its vector components in a given point.

The main steps for the implementation of the measuring points in the 2D cut-plane have been:

- Consider the position in which it's possible to insert the sensor in the real electrical panel, trying to follow a certain physic symmetry;
- Find sites characterized by a small distance between the sensors;
- Find out the vector component of the MF more adapt for the point taken into consideration in the previous step;
- Make a brief study about the distribution of the MF around the electrical bars. This in order to find out the sites near the bar that present the highest magnitude of the MF for the vector component taken into consideration.

To explain the principal decisions adopted it's better to divide the problem into the two different cut planes taken into account seeing them as separate.

8.1 First possible disposition of measurement sensors

The first alternative of sensors disposition, as seen before, is divided into two different cut-planes, one is the cut plane at the height of $z=35.25$ cm from the point zero and the other one is a cut plane at the high of $y= 11.4$ cm.

For the first cut-plane it has been chosen to insert all the sensors respect to a horizontal line with a view to simplify the future installation making it more easy and fast.

For the second cut-plane was adopted the same criteria of the reference line but for the positioning there weren't a lot of alternatives because of the small length of the T bars. For this fact it was thought to the eventual possibility to cut a small part of plastic, for the insertion of one of the two sensors for every circuit.

8.1.1 Disposition of the R-S sensors in the z cut-plane

In the following image are indicated with black points the points of measure set out in the Comsol Multiphysic simulation, these points represent the positions chosen for the sensors in this plane.

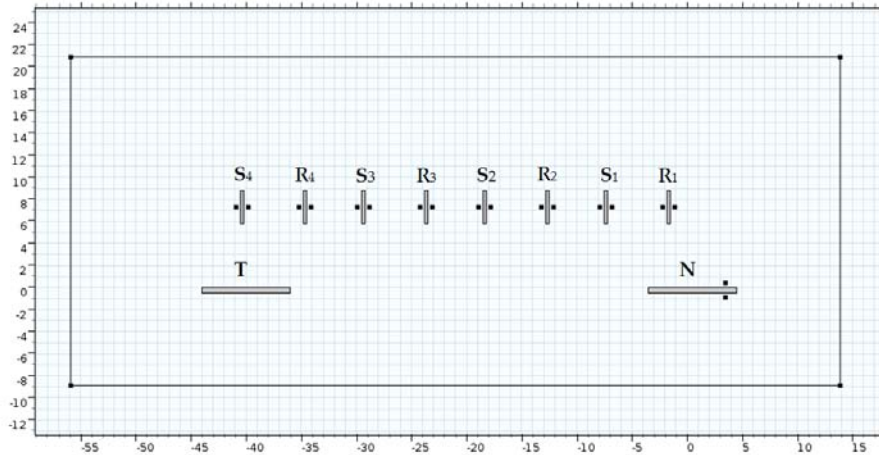


Fig. 8.1 Points of measure in the 2D cut-plane.

For the positioning of the points in this plane have been chosen the right and left side of the bars, because in this way it's possible to minimize the distance between the sensors. For the same reason it was chosen to dispose other two points in the upper and lower part of the neutral bar.

After that it was necessary to discover the component of MF that gave the highest level of it. This in order not to fall in the future risk to have such a low value of MF to induce in making errors caused by the sensibility of the sensors.

To figure out this it was necessary to make some measure, in a couple of point near the bars, confronting the components B_x , B_y and picking out the vector component with the highest value.

In the next table are listed some measures made in different points close to the bars and it's possible to observe that for the points 1 and 2 it's preferable to set the Comsol tool to measure the component B_y of the field.

On the other hand, for the points 4 and 5 close to the neutral bar, it's better to make a measure of the B_x component of the MF.

<i>Point</i>	B_x [μT]	B_y [μT]
1	-24.696	248.43
2	25.066	254.83
3	20.87	210.01
4	-114.81	23.361
5	-93.254	15.795

Table 8.1 Values of different vector components of MF for different points.

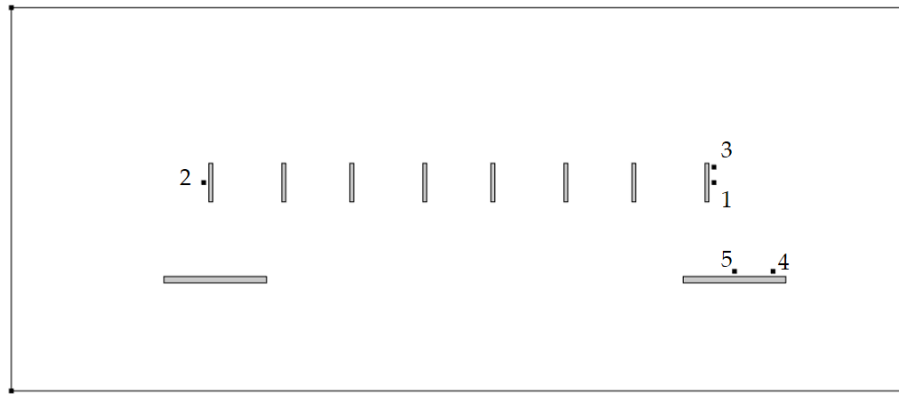


Fig. 8.2 Points of measure referred to the table 8.1

Regarding the points 3 and 5, they represent other probes made in order to establish the best measuring position around the bars. In fact, with the point 3 have been evaluated the changes in magnitude of the MF respect to the point 1, one more time in the interest to find the highest value of MF. The same was done for the points 5 and 4.

In the table above (*Tab.8.1*) it can be seen that it's preferable to set the measure tools in the points 1 and 4 because of the highest MF component.

Other important considerations to do are about the distance of installation between the detectors and the bars. To figure out the best distance it was considered that the sensors can't be installed too close to the bars, because of the heat released by the bars during the normal operation. It was established for this reason a minimum distance of 0,4 cm between all the sensors installed in this project and the bars.

About a possible increase of the distance from 0,4 cm to a higher distance it's important to note that it means an increment of the distance between the two sensors. This it can cause a following increment of measurement errors because the initial hypothesis for the elimination of the stray magnetic field are compromised.

Another concept to take in mind is that moving with the sensors away to the bars implies a decrease of MF magnitude monitored by the detectors. To avoid this, have been made some tests in order to figure out the best configuration of installation. One of the tests was made with the bar of the phase R1 shown in the next image. In this case were considered the points 1 and 2 situated at a distance of 0,4 cm from the bar and the points 3 and 4 at a distance of 1 cm.

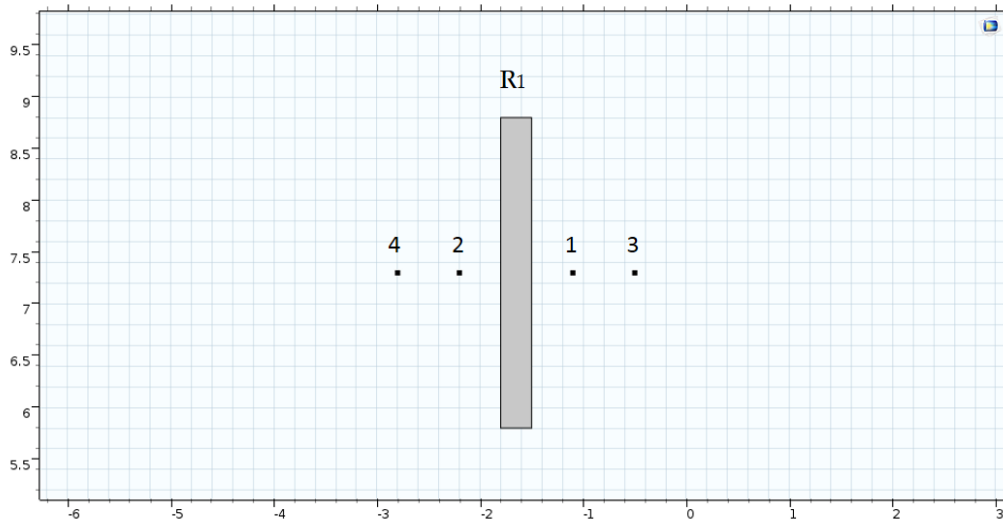


Fig. 8.3 Points of measure referred to the Table 8.2

As it can be seen in the next table, for the point 1 and 2, closer to the bar, it can be detected a higher magnitude of MF and so these points are preferable in order to reduce the possible errors.

<i>Point</i>	<i>B_y [μT]</i>
1	166.93
2	157.09
3	127.25
4	117.58

Table 8.2 Values of B_y referred to the points in the Fig. 8.3

In the next figures are illustrated some graphical solutions, obtained with the simulations in the Comsol model, that confirm the choices just explained.

The simulations have been computed supplying the bars with an input current of 10[A].

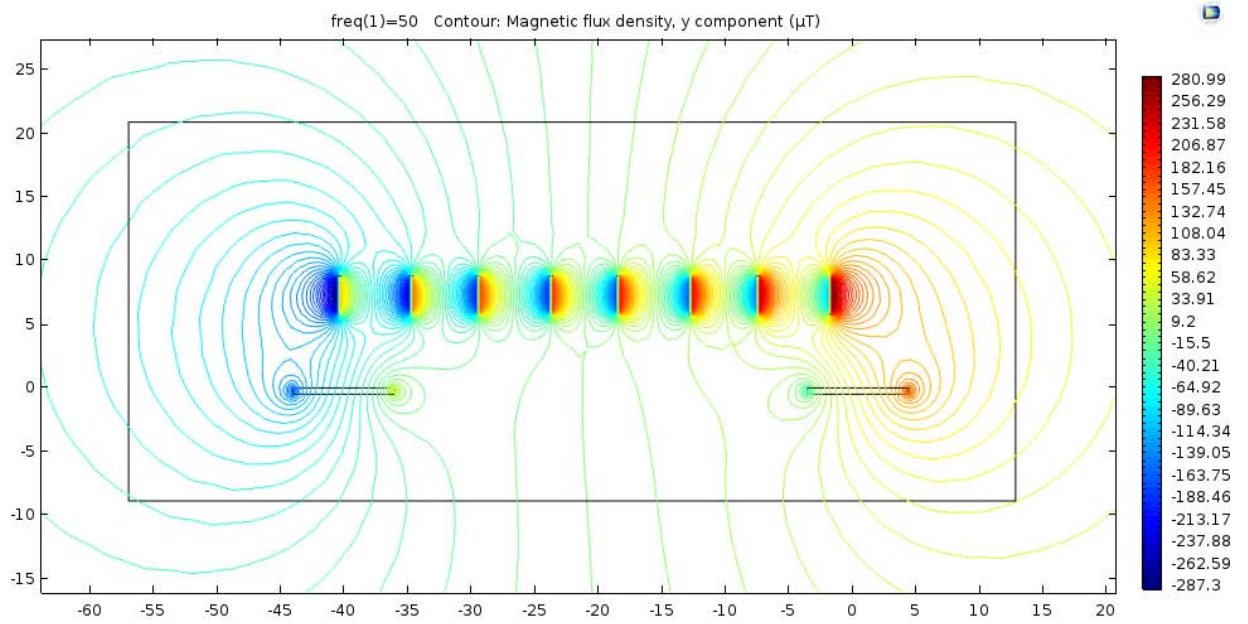


Fig. 8.4 Magnetic flux density considering only the y component of the MF. Input current: 10 A.

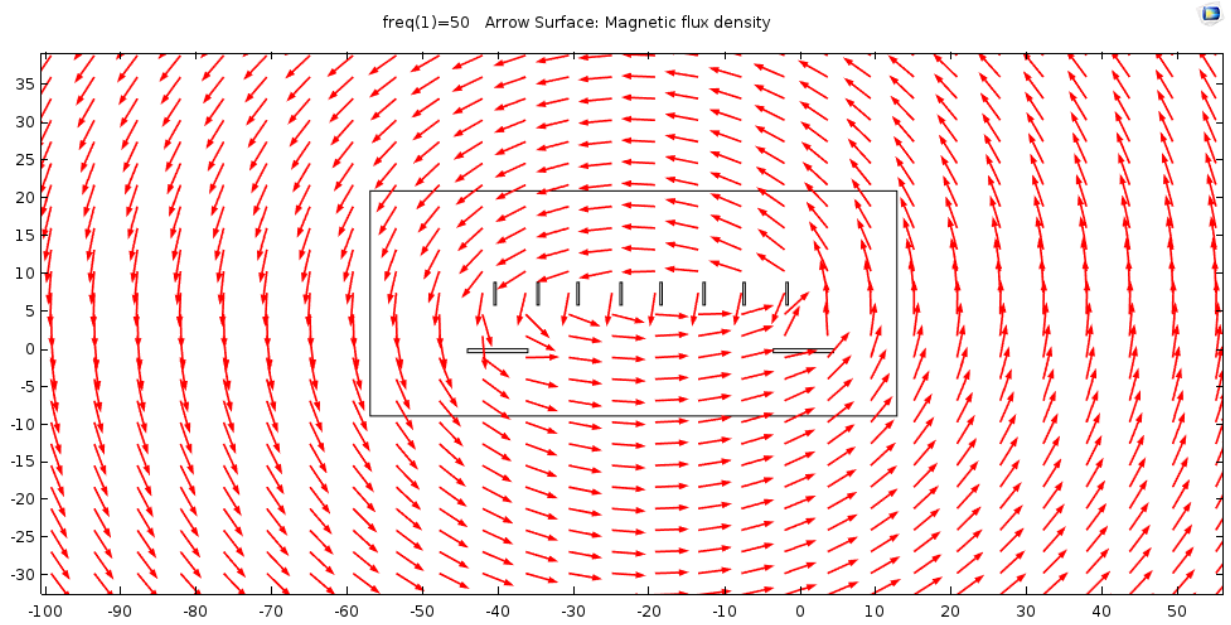


Fig. 8.5 Direction of the Magnetic flux density considering the x and y components of the MF. Input current: 10 A.

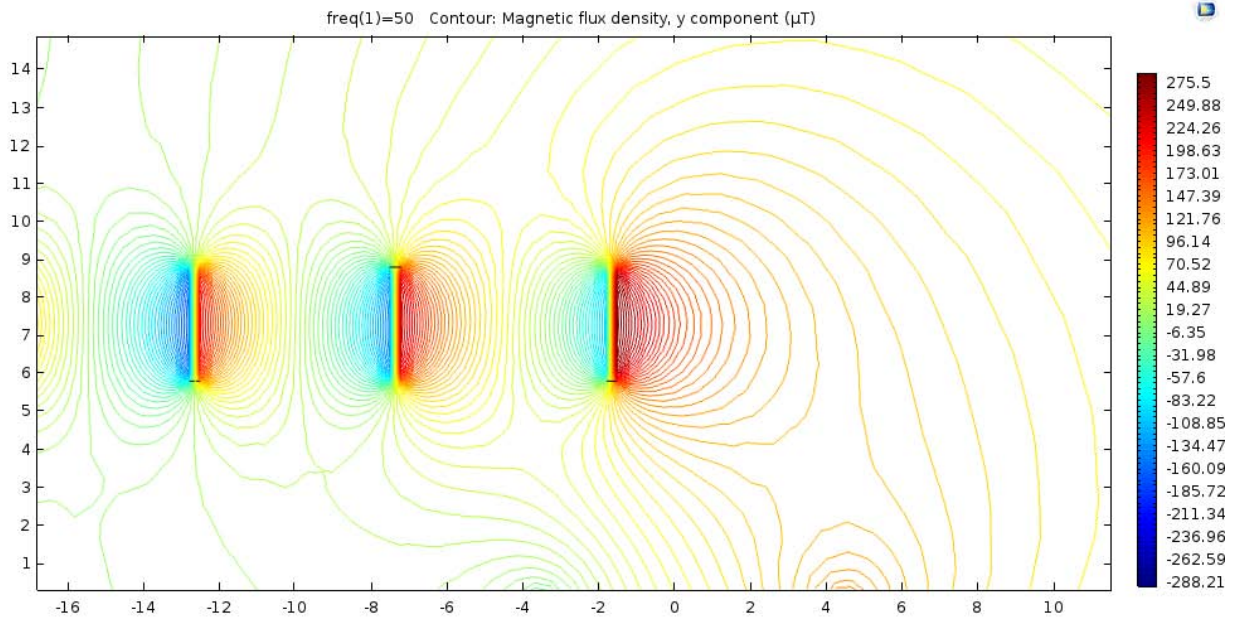


Fig. 8.6 Magnetic flux density of the phases R1, S1, R2 considering only the y component of the MF.

Input current: 10 A.

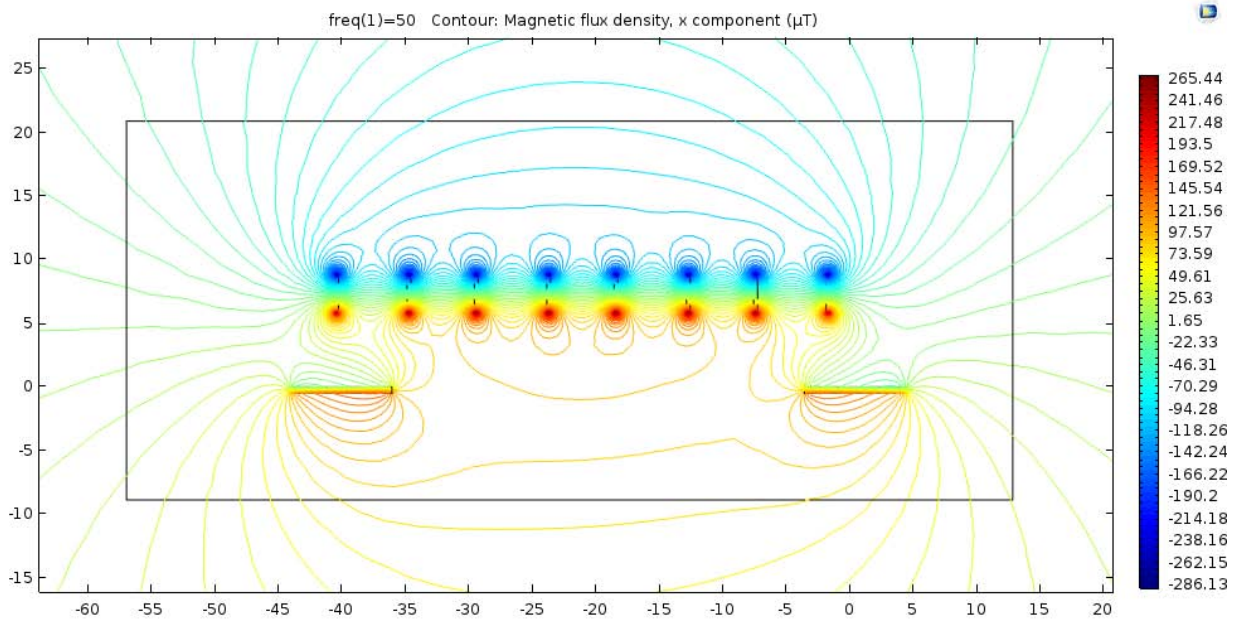


Fig. 8.7 Magnetic flux density considering only the x component of the MF.

Input current: 10 A.

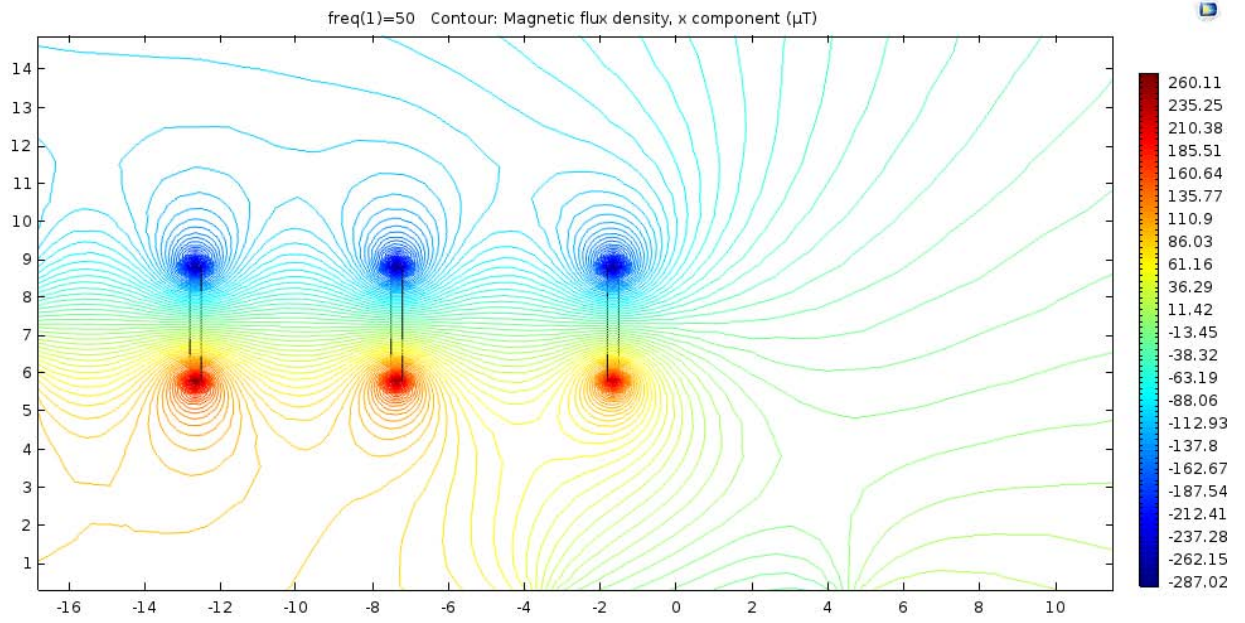


Fig. 8.8 Magnetic flux density of the phases R1, S1, R2 considering only the x component of the MF.

Input current: 10 A.

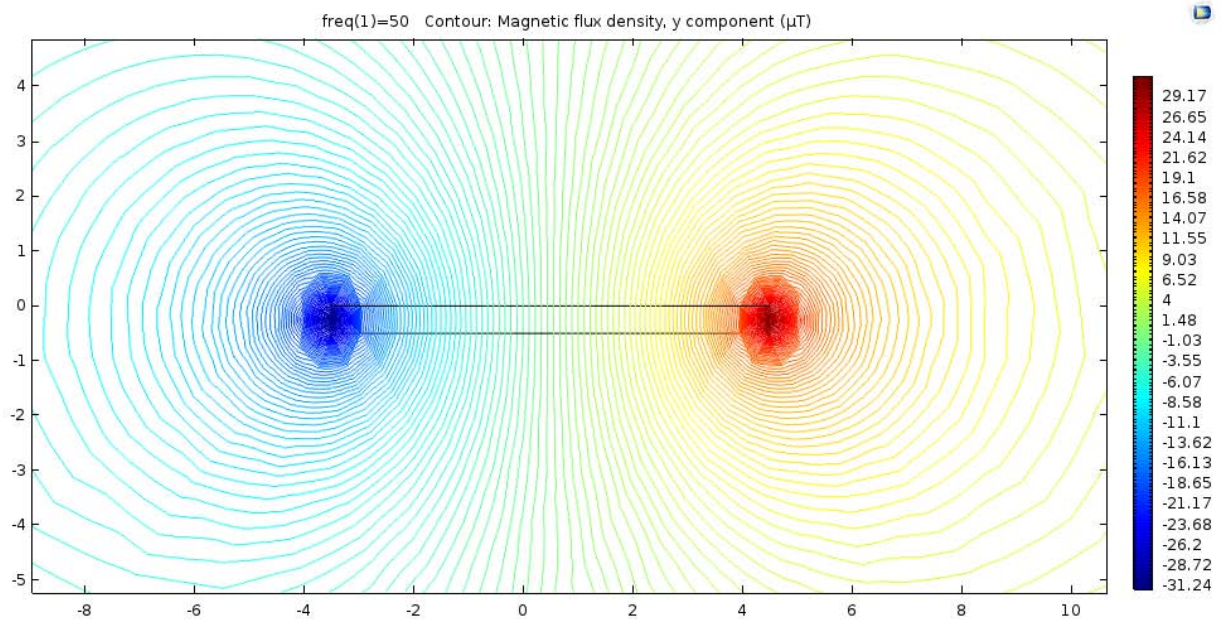


Fig. 8.9 Magnetic flux density of the neutral bar considering only the y component of the MF.

Input current: 10 A.

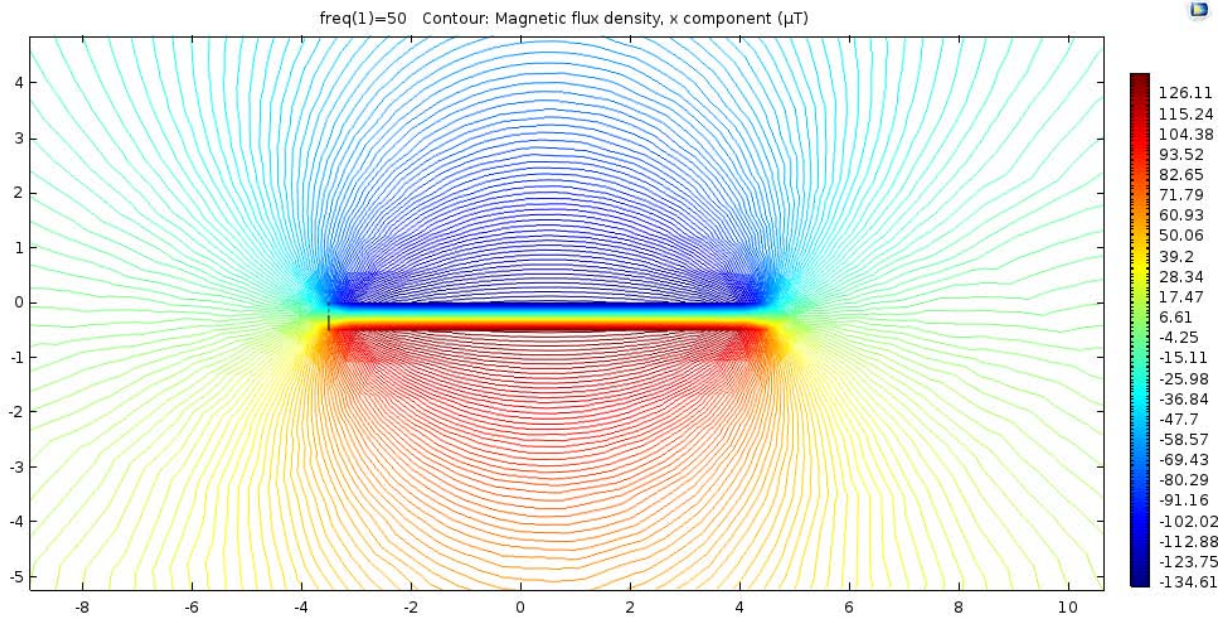


Fig. 8.10 Magnetic flux density of the neutral bar considering only the x component of the MF.

Input current: 10 A.

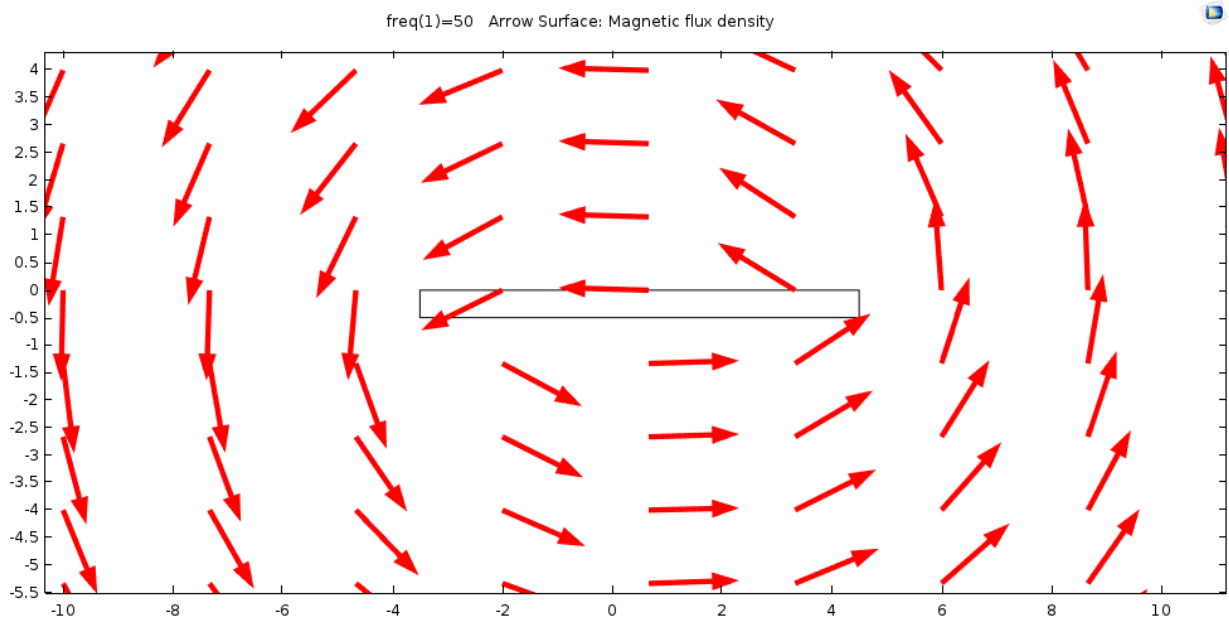


Fig. 8.11 Direction of the Magnetic flux density of the neutral bar considering the x and y components of MF.

Input current: 10 A.

8.1.2 Disposition of the T sensors in the y cut-plane

For the disposition of the T sensors have been done the same steps of the previous case, in order to reach a good measurement accuracy for the points taken into consideration.

In this case the distribution of the sensors in the cut-plane is the following:

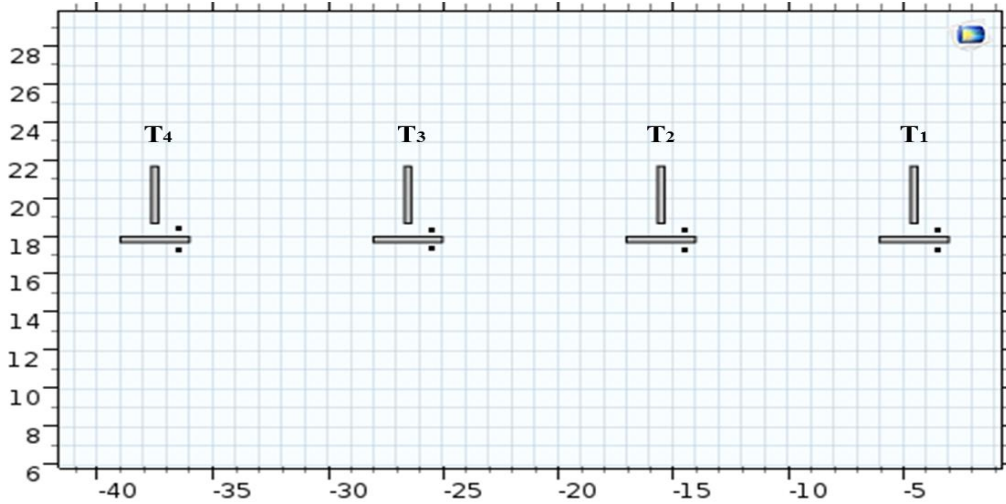


Fig. 8.12 Points of measure in the 2D cut-plane.

The next step was to find out the best vector component of MF to use for the MF monitoring, as it has been made in the previous cut-plane.

In order to do this were considered the points selected in the next image for the bars T1 and T2 and were compared the results for the components B_x and B_y shown in the *Table 8.3*.

The final choice was to consider the x vector component for the measures, this is because it had the highest magnitude of MF as it can be seen in the table.

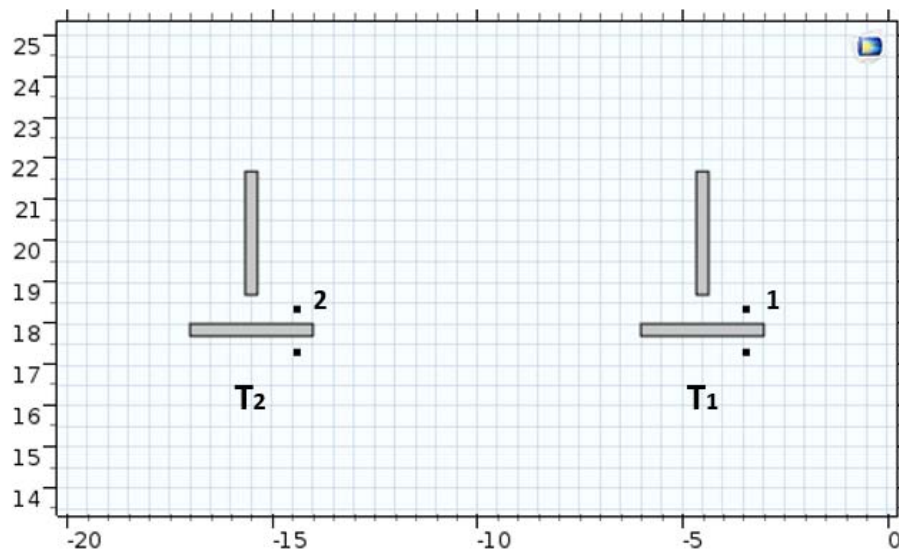


Fig. 8.13 Points of measure referred to the table 8.3

<i>Point</i>	\mathbf{B}_x [μT]	\mathbf{B}_y [μT]
1	218.14	-9.11
2	215.74	-7.54

Table 8.3 Values of MF referred to the points in the Fig. 8.13

In the next figures are illustrated some graphical solutions, obtained with the simulations in the Comsol model, that confirms the reasons just explained.

The simulations have been computed supplying the bars with an input current of 10[A].

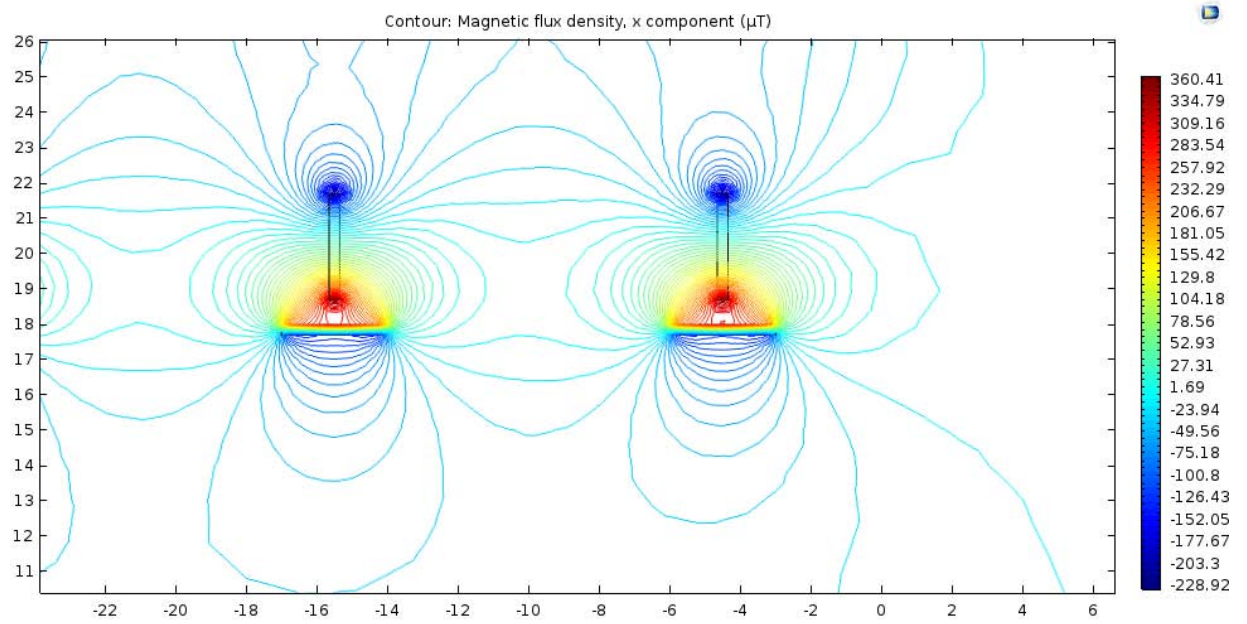
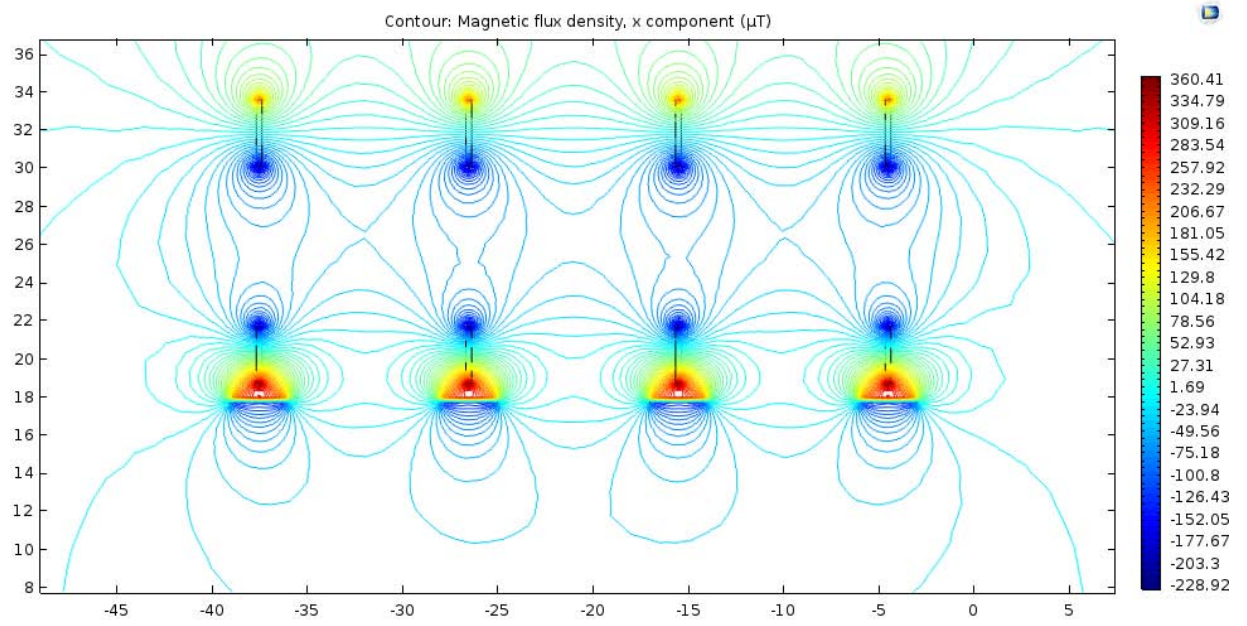


*Fig. 8.14 Magnetic flux density of the phases T considering only the x component of the MF.
Input current: 10 A.*

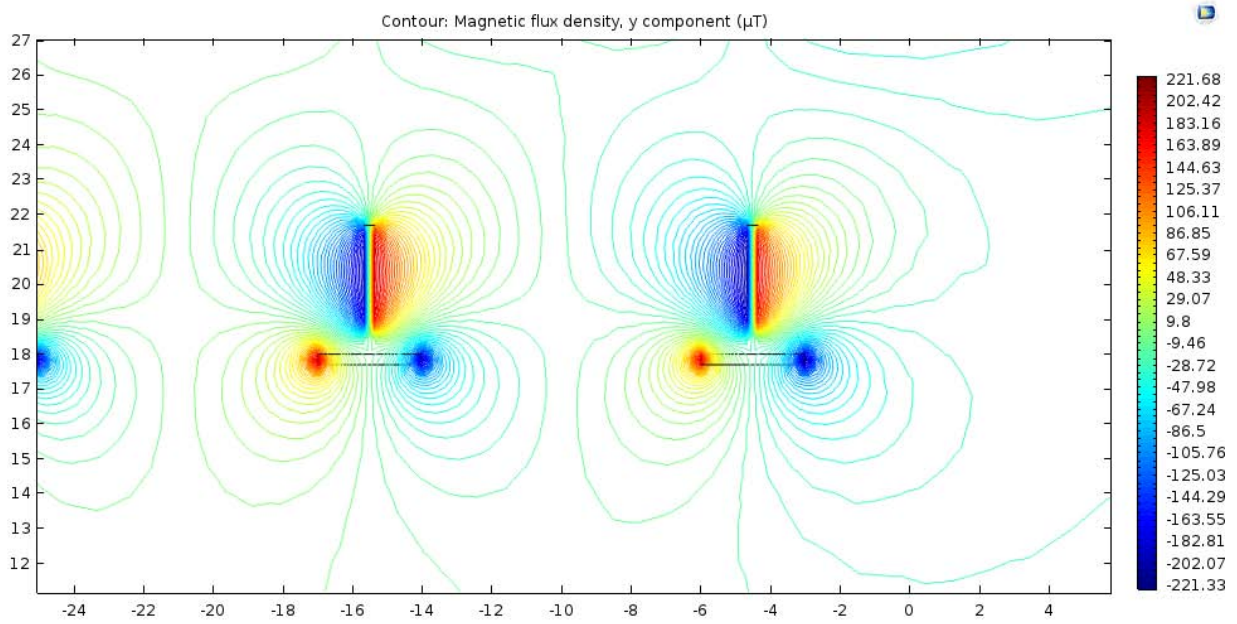
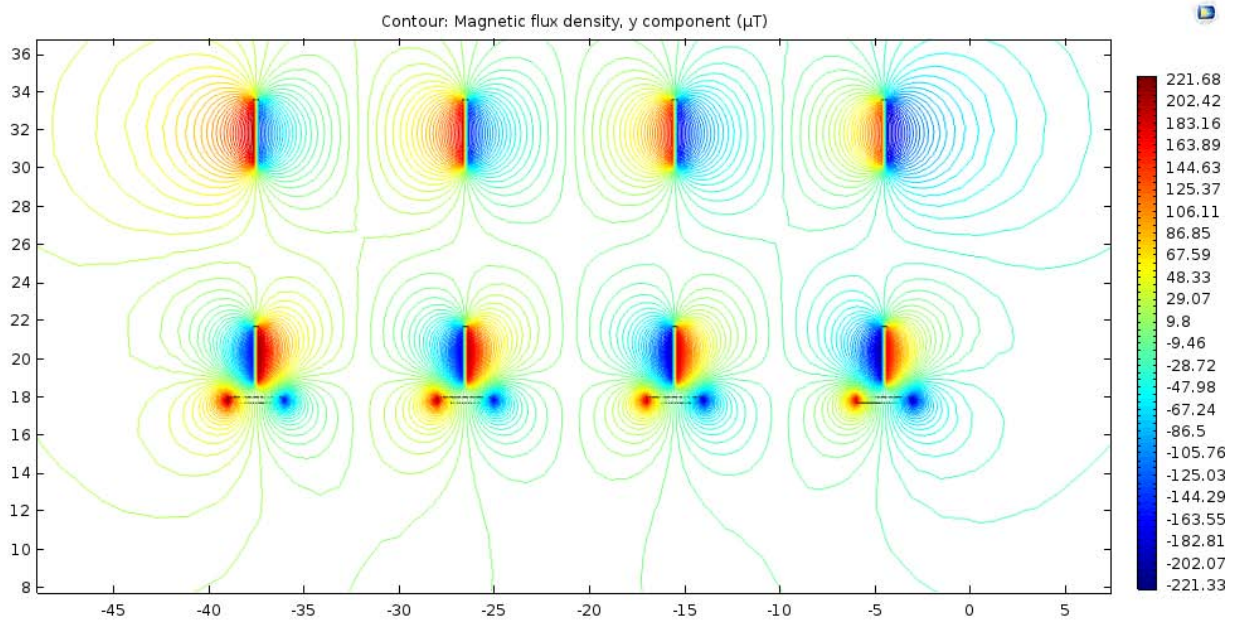


Fig. 8.15 Magnetic flux density of the phases T considering only the y component of the MF, input current: 10 A.

8.1.3 Final position of the sensors in the 3D model

- Cut plane z



Fig. 8.16 Position of the sensors for the cut-plane z.

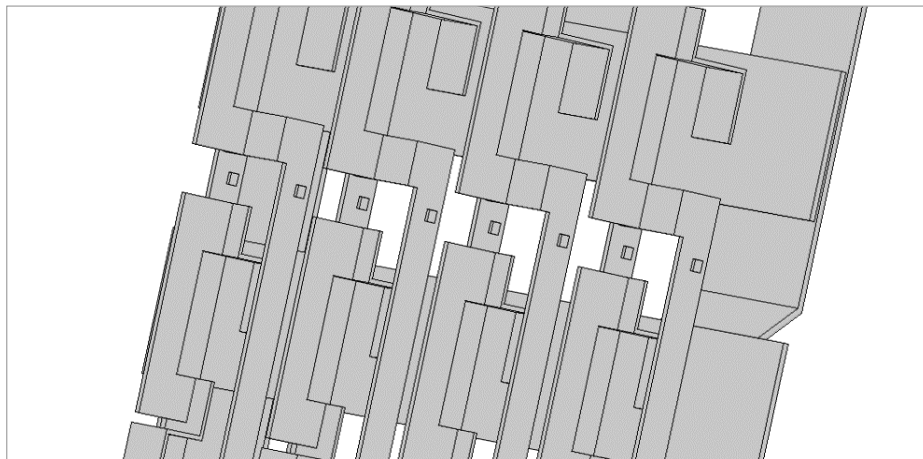


Fig. 8.17 Position of the sensors for the cut-plane z.

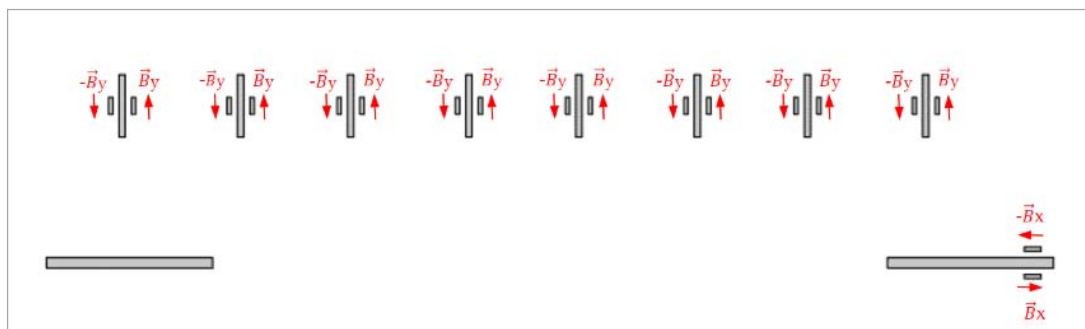


Fig. 8.18 Settings of the sensors adopted in order to delete the stray MFs contribution.

- **Cut-plane y**

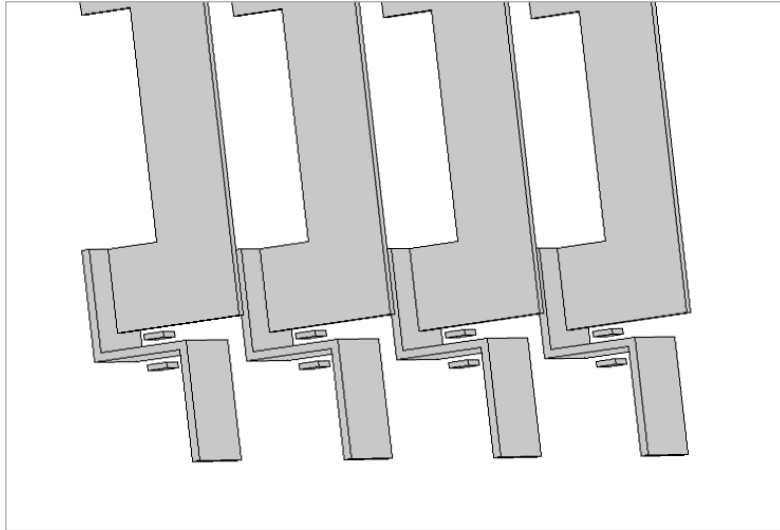


Fig. 8.19 Position of the sensors for the cut-plane y.

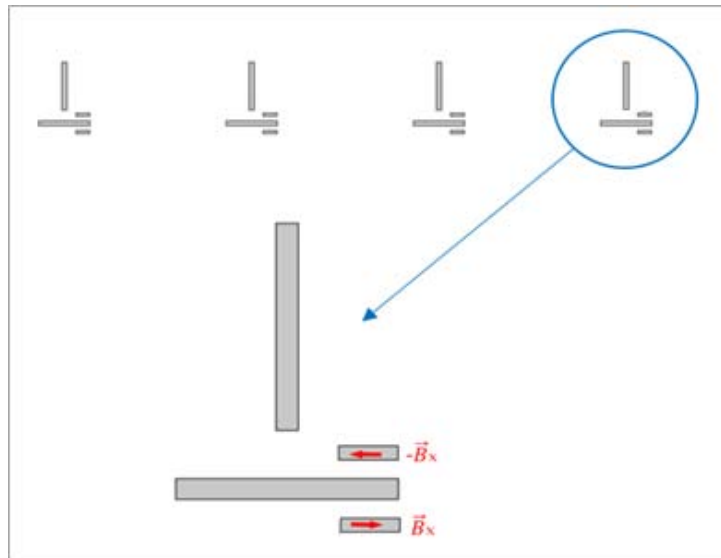


Fig. 8.20 Settings of the sensors adopted in order to delete the stray MFs contribution.

8.2 Second possible disposition of the measurement sensors

The cut plane adopted for the second disposition of sensors is obtained cutting the 3D model with a plane parallel to the y-axis, at the height of $y=6,9$ cm. This cut-plane permits to consider all the phases of all the circuits in this single plane and so presents the advantages to simplify and to focus the 2D study in a single simulation.

In the same way of the first disposition, it has been chosen to insert all the sensors respecting to a horizontal line in order to simplify the future installation. This, despite to the fact that it will be necessary to make certain changes to the electrical panel, cutting some plastic parts for the installation of one of the two sensors for every bar.

In the following image there are indicated the points of measure set out in the Comsol Multiphysic simulation, these points represent the positions of the sensors chosen for this plane.

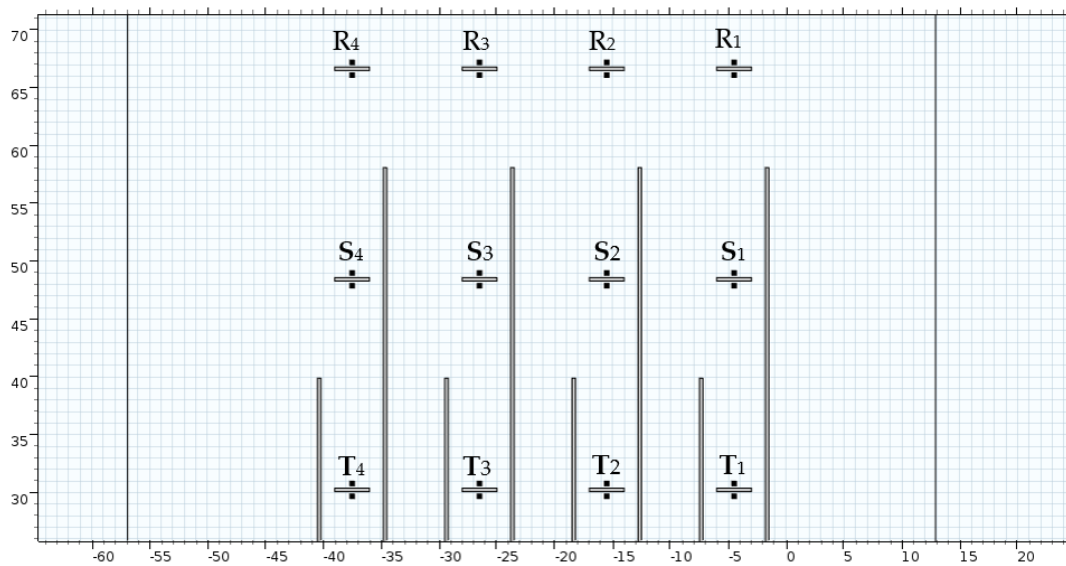


Fig. 8.21 Points of measure in the 2D cut-plane.

To figure out the best configuration for these sensors have been followed the same steps done in the previous cases. In particular, considering that a sensor has a size around to 1.5×1.5 [cm] and the electrical bars have a width of 3 cm there wasn't a lot of space to change the position of the sensors. For this reason, it was preferred to facilitate the installation inserting the sensors in the middle of the bars, taking advantage to the fact that there wasn't a big difference between the measures taken in the central position and in the lateral position.

The next step, as in the previous disposition of sensors, was to find the best vector component of MF to use for the MF monitoring. In order to do this, were considered the points selected in the next image for the bars R2, S2, T2 and were compared the results for the components B_x and B_y shown in the Table 8.4.

The final choice was to consider the x vector component of MF for the measures, this because this component had the highest magnitude of MF.

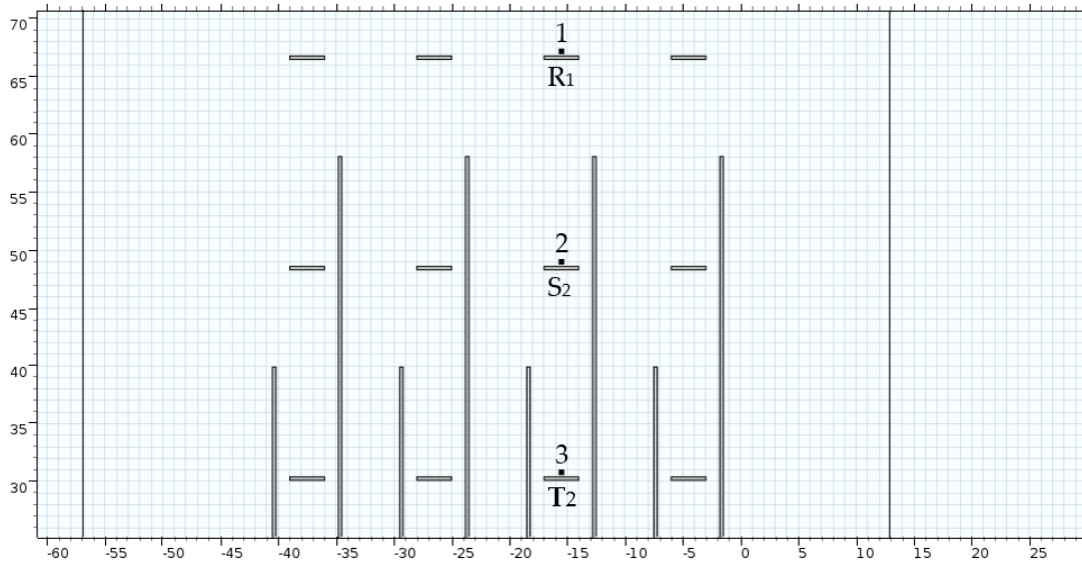


Fig. 8.22 Points of measure referred to the table 8.4

<i>Point</i>	B_x [μT]	B_y [μT]
1	-221.11	16.345
2	-168.72	19.587
3	-117.08	16.863

Table 8.4 Values of \mathbf{B} referred to the points in the fig. 8.22

In the next figures are illustrated some graphical solutions, obtained with the simulations in the Comsol model, that confirms the reasons just explained.

An important consideration to do is that the vertical bars presented in the images, that are the bars R-S presented in the model and cut by the cut-plane, have not been considered in the measures. This because the respective MFs produced by that bars don't influence the vector component x of the MF measured by the sensors. For this reason, they have been considered made of air and so not considered as active in the model simulation.

The following simulations have been computed supplying the bars with an input current of 10[A].

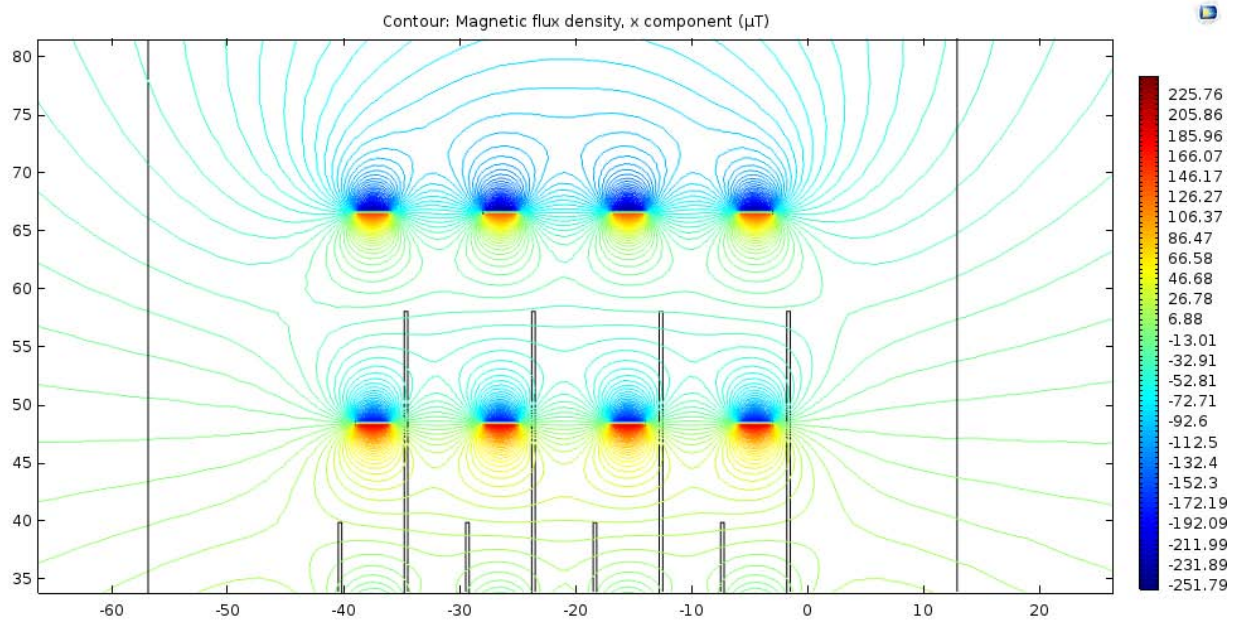
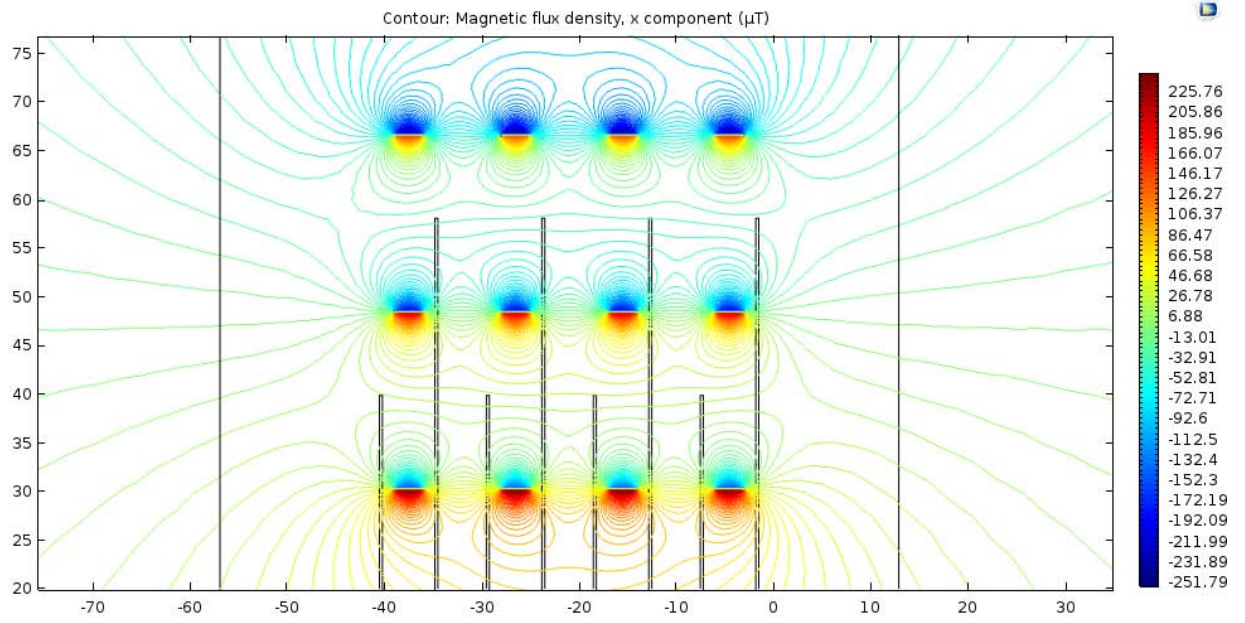


Fig. 8.23 Magnetic flux density considering only the x component of the MF. Input current: 10 A.

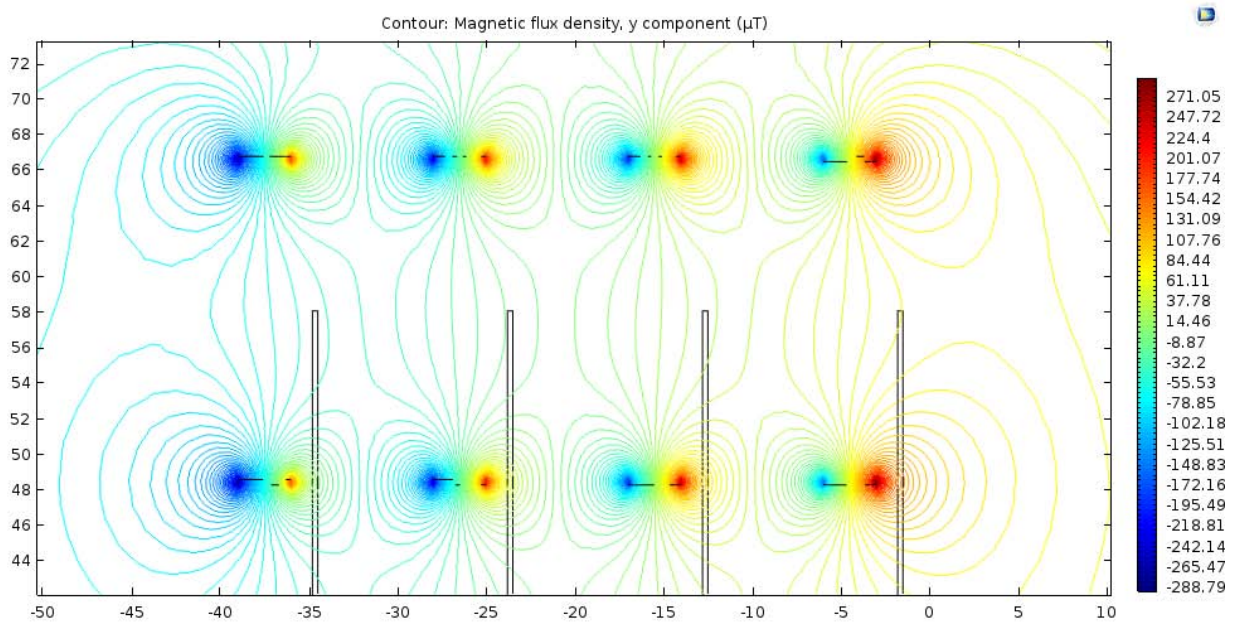
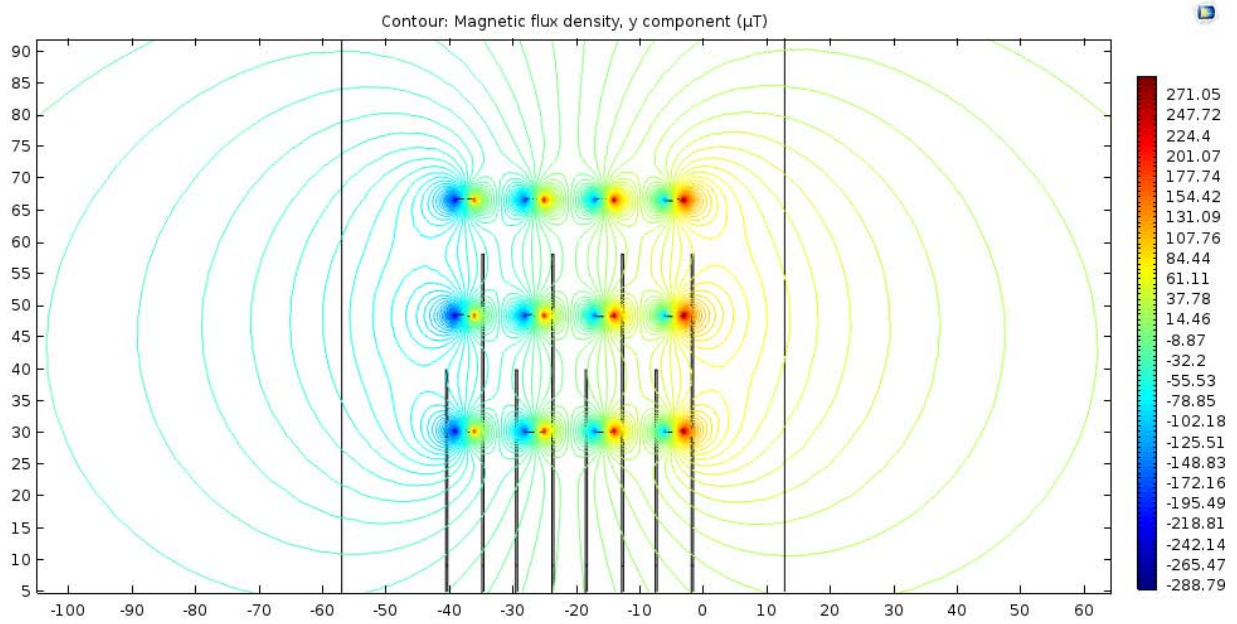


Fig. 8.24 Magnetic flux density considering only the y component of the MF. Input current: 10 A.

8.3 Final position of the sensors in the 3D model

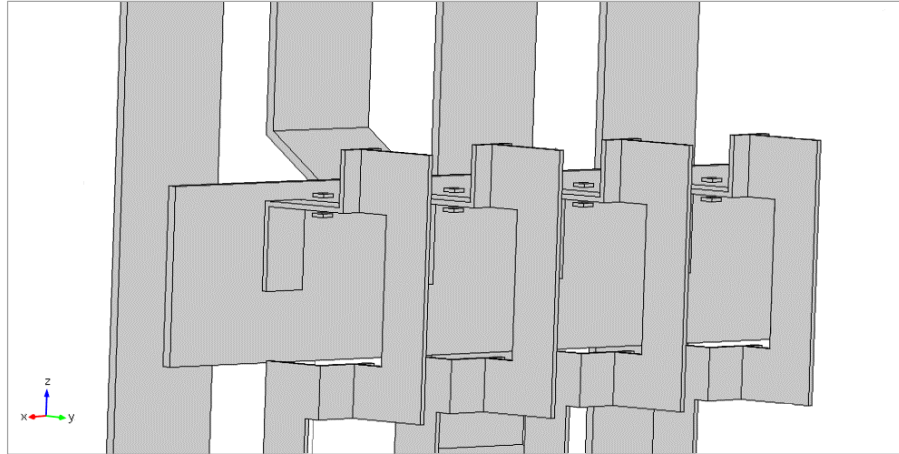


Fig. 8.25 Position of the sensor installed for the phase R.

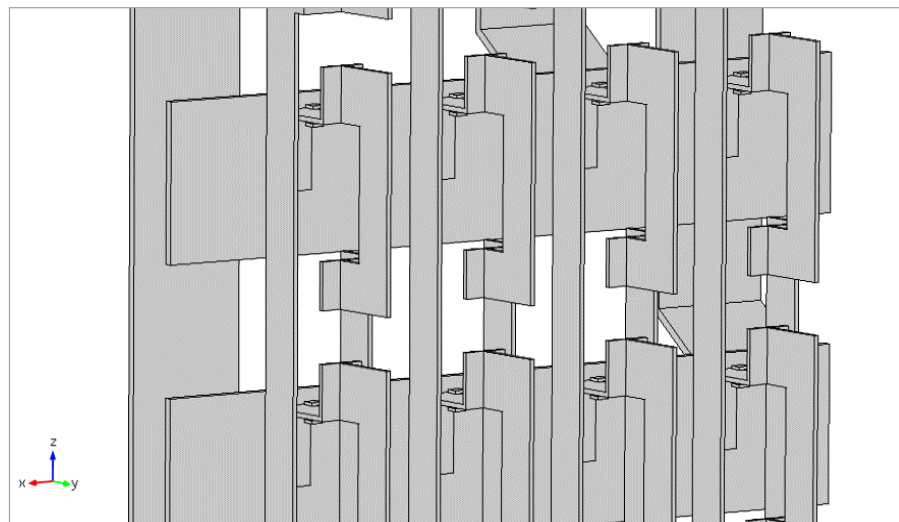


Fig. 8.26 Position of the sensor installed for the phases R and S.

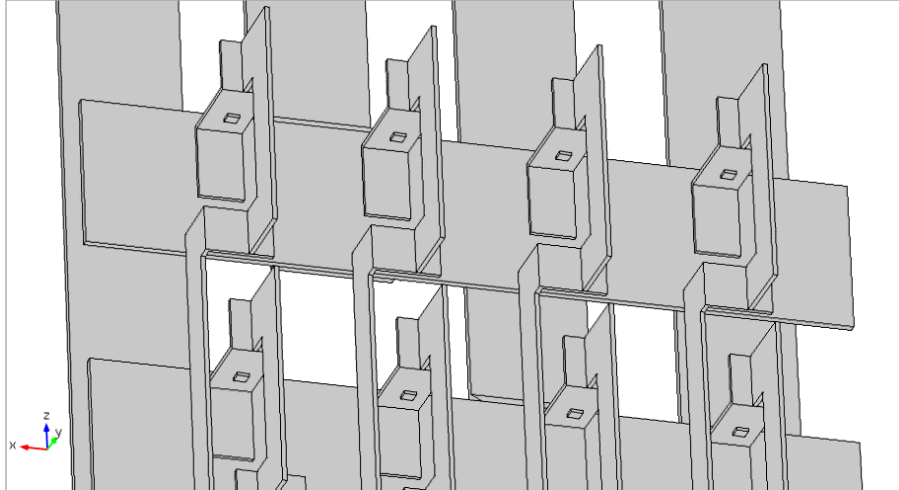


Fig. 8.27 Position of the sensor installed for the phases R and S.

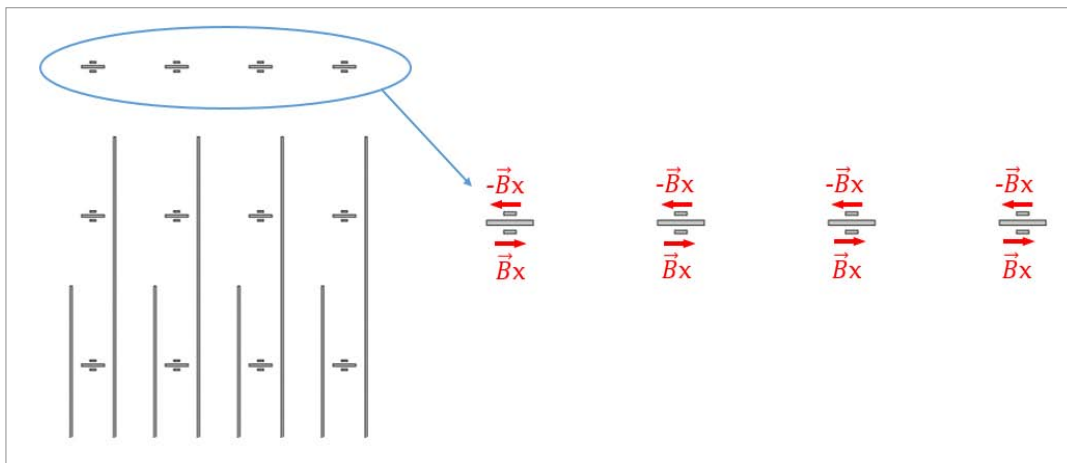


Fig. 8.28 Settings of the sensors adopted in order to delete the stray MFs contribution.

9 DERIVATION OF THE CURRENT VALUES

In this section of the document are explained the principle steps and ideas that led to obtain a functional automatization for the indirect monitoring of current, in every temporal instant, through the use of the MF sensors installed in the electrical panel.

Firstly, it's important to think that the sensors will have to work in the temporal domain, because the electrical panel will be supplied with an alternative current with a frequency of 50 Hz. For this reason, will be used the temporal domain in order to analyse the trends of MF measured in a temporal period.

Stepping back to the simulation model in Comsol it's important to remember that the development of the MF in the space is produced by the flow of a current and that current was set as an input parameter, in order to obtain an estimation of the MF.

On the other point of view, it's important to note that in the real operation of the systems it's necessary to do almost the opposite, i.e. to measure a Magnetic field in order to obtain the value of electric current flowing in every circuit.

At this point it's possible to realize that there is a relationship between the measured MF and the input current. Once this relationship has been found it's easy to obtain the input currents values, having only the MF values and the relationship found.

9.1 Implementation of the matrix $[K]$

To find the relationship between the MF and the input current it was necessary to make a study in the steady-state. This, in order to find a coefficient that could represents the relationship between the two known terms, ensuring also that this relation could be valid and constant in the temporal domain.

The following equation expressed as a function of time represents the relationship between MF and input current:

$$(9.1) \quad \mathbf{B}(t) = k \cdot \mathbf{I}(t)$$

where k is the constant that represent the relationship between the MF measured $\mathbf{B}(t)$ and the input current in the time domain $\mathbf{I}(t)$.

First of all, to simplify the problem, it has been tried to find this constant in the stationary domain by imposing the time equal to zero and obtaining:

$$\mathbf{B}(t) = k \cdot \mathbf{I}(t) \quad t = 0$$

$$\mathbf{B}(0) = k \cdot \mathbf{I}(0)$$

$$(9.2) \quad \mathbf{B} = k \cdot \mathbf{I}$$

Then the only thing to do was to find the value of k taking into consideration that B and I are known terms and also ensuring that the value of k remains valid and constant for different input currents.

Once obtained the constant k it has been possible to use this constant in the cases in which B is a known term and I is unknown.

With the purpose of find the constant k , in the Comsol model has been imposed an input current for every bar of 1[A]. Subsequently was used a sort of superposition principle, in which was considered the effect caused in the measures by the MFs generated from every bar.

To apply the superposition principle, the bars have been supplied with a current one at a time and have been considered the measures detected with the two sensors of every bar. This in order to figure out the values of MF measured by a determinate couple of sensors installed in a bar, for every single bar powered. After that the values detected by a couple of sensor has been added up in order to eliminate the stray MF effects, the result of the sum will be the double of the MF value in the point of measure.

In the end, every single value measured represents the constant term that we are looking for, because the current was set to a value of 1[A].

Considering the fact that we need to monitor the current that flows through every bar of every circuit it's convenient to group every result in a matrix, to simplify the management of the results.

This matrix will be named $[K]$ and will be formed by a number of single elements k .

Every row of the matrix is referred to the sensors considered for the measure and every column is referred to the active bar powered. Therefore, every element k will be defined according to the sensor and the powered phase taken into consideration.

The final matrix equation will be:

$$(9.3) \quad [B] = [K] \cdot [I]$$

A generic representation of the matrix $[K]$ is represented in the next page.

$$\begin{bmatrix}
 B_{R1} \\
 B_{S1} \\
 B_{T1} \\
 B_{R2} \\
 B_{S2} \\
 B_{T2} \\
 B_{R3} \\
 B_{S3} \\
 B_{T3} \\
 B_{R4} \\
 B_{S4} \\
 B_{T4}
 \end{bmatrix}
 =
 \begin{bmatrix}
 K_{R1R1} & K_{R1S1} & K_{R1T1} & K_{R1R2} & K_{R1S2} & K_{R1T2} & K_{R1R3} & K_{R1S3} & K_{R1T3} & K_{R1R4} & K_{R1S4} & K_{R1T4} \\
 K_{S1R1} & K_{S1S1} & K_{S1T1} & K_{S1R2} & K_{S1S2} & K_{S1T2} & K_{S1R3} & K_{S1S3} & K_{S1T3} & K_{S1R4} & K_{S1S4} & K_{S1T4} \\
 K_{T1R1} & K_{T1S1} & K_{T1T1} & K_{T1R2} & K_{T1S2} & K_{T1T2} & K_{T1R3} & K_{T1S3} & K_{T1T3} & K_{T1R4} & K_{T1S4} & K_{T1T4} \\
 K_{R2R1} & K_{R2S1} & K_{R2T1} & K_{R2R2} & K_{R2S2} & K_{R2T2} & K_{R2R3} & K_{R2S3} & K_{R2T3} & K_{R2R4} & K_{R2S4} & K_{R2T4} \\
 K_{S2R1} & K_{S2S1} & K_{S2T1} & K_{S2R2} & K_{S2S2} & K_{S2T2} & K_{S2R3} & K_{S2S3} & K_{S2T3} & K_{S2R4} & K_{S2S4} & K_{S2T4} \\
 K_{T2R1} & K_{T2S1} & K_{T2T1} & K_{T2R2} & K_{T2S2} & K_{T2T2} & K_{T2R3} & K_{T2S3} & K_{T2T3} & K_{T2R4} & K_{T2S4} & K_{T2T4} \\
 K_{R3R1} & K_{R3S1} & K_{R3T1} & K_{R3R2} & K_{R3S2} & K_{R3T2} & K_{R3R3} & K_{R3S3} & K_{R3T3} & K_{R3R4} & K_{R3S4} & K_{R3T4} \\
 K_{S3R1} & K_{S3S1} & K_{S3T1} & K_{S3R2} & K_{S3S2} & K_{S3T2} & K_{S3R3} & K_{S3S3} & K_{S3T3} & K_{S3R4} & K_{S3S4} & K_{S3T4} \\
 K_{T3R1} & K_{T3S1} & K_{T3T1} & K_{T3R2} & K_{T3S2} & K_{T3T2} & K_{T3R3} & K_{T3S3} & K_{T3T3} & K_{T3R4} & K_{T3S4} & K_{T3T4} \\
 K_{R4R1} & K_{R4S1} & K_{R4T1} & K_{R4R2} & K_{R4S2} & K_{R4T2} & K_{R4R3} & K_{R4S3} & K_{R4T3} & K_{R4R4} & K_{R4S4} & K_{R4T4} \\
 K_{S4R1} & K_{S4S1} & K_{S4T1} & K_{S4R2} & K_{S4S2} & K_{S4T2} & K_{S4R3} & K_{S4S3} & K_{S4T3} & K_{S4R4} & K_{S4S4} & K_{S4T4} \\
 K_{T4R1} & K_{T4S1} & K_{T4T1} & K_{T4R2} & K_{T4S2} & K_{T4T2} & K_{T4R3} & K_{T4S3} & K_{T4T3} & K_{T4R4} & K_{T4S4} & K_{T4T4}
 \end{bmatrix}
 \begin{bmatrix}
 I_{R1} \\
 I_{S1} \\
 I_{T1} \\
 I_{R2} \\
 I_{S2} \\
 I_{T2} \\
 I_{R3} \\
 I_{S3} \\
 I_{T3} \\
 I_{R4} \\
 I_{S4} \\
 I_{T4}
 \end{bmatrix}$$

The array \mathbf{B} of the equation contains the values of MF measured by all the sensors installed in the bars from R_1 to T_4 when all the bars of the circuits are powered with a current of 1[A] and the array \mathbf{I} represents the input currents of the bars.

For the arrays \mathbf{B} and \mathbf{I} the first subscript denotes the phase of the bar taken into account and the second denotes the circuit considered (e.g. for B_{R1} , R denote the bar corresponding to the phase R and 1 denotes the first circuit).

For the matrix \mathbf{K} it's the same and also the first couple of subscripts denotes the sensor that takes the measure and the second couple denotes the active phase considered.

9.2 How to figure out the current values

Once obtained the matrix \mathbf{K} is possible to figure out the values of currents, considered as unknown terms, using the values of \mathbf{B} when all, or a part of the circuits, are powered. Then it's possible to measure the currents using only the values of \mathbf{B} detected by the sensors.

To do this, it's necessary to elaborate the following equation in the time domain:

$$(9.4) \quad [B(t)] = [K] \cdot [I(t)]$$

in order to obtain:

$$(9.5) \quad [I(t)] = \left[[K]^{-1} \cdot [B(t)]^T \right]^T$$

Where all the terms, excepted for the elements k , are time-dependents, in particular:

- $[I(t)]$ is the array composed by all the sinusoidal currents, with their proper electric displacement of 120° , that flow through the electrical bars in a determinate instant of time;
- $[B(t)]$ is the array of MF values, computed with the Comsol model simulations in the points selected for the sensor installation, in a determinate instant of time.

The values of time taken into consideration are the values from $t=0$ [s] to $t=0,02$ [s] with intervals of 0,001 [s], namely:

$$t = (0; 0.001; 0.002; \dots ; 0.019; 0.02)$$

9.2.1 Implementation with Matlab®

In order to verify the proper functioning of the system have been made some scripts, using the Matlab software, with the purpose of evaluate the matrix $\mathbf{I}(t)$. These script are also used to evaluate the possible error between the values of current found out with this method and the values of input current set in the Comsol model.

The script reported in the *Appendix A.1* is an example of Matlab algorithm used to test if the matrix \mathbf{K} was correct.

In specific terms, the program, given the array \mathbf{B} and the matrix \mathbf{K} , tries to figure out if the relative array \mathbf{I} , calculated with this method, is equal to the original array of input currents set in the Comsol model.

The array of currents derived with this script will be equal to the input current array only if the matrix \mathbf{K} considered is correct. Then, a correct result has to be an array where all the currents have a value equal to the correspond input current set for this bar.

Another example of script used in this project is the algorithm present in the *Appendix A.2*. This script yields the array of currents with the insertion, in the appropriate program lines, of the array $\mathbf{B}(t)$ and the matrix \mathbf{K} . It also makes a comparison between the original input currents and the currents computed with the matrix method, in order to discover possible differences.

In the script is possible to individuate a matrix named \mathbf{B} . This matrix is composed by the elements representing the measures of MF, made by the measure points, in the different instants of time considered in the previous paragraph.

More specifically, every element of the matrix depends on:

- The sensor that make that measure (9 sensors in this case);
- The instant of time considered (21 instants in this case);

building so a 21×9 dimensions matrix.

It's important to point out that this is only an example of script used in the project and that the array $\mathbf{B}(t)$ can change according to the number of bars taken into consideration, as it will be possible to see in the next paragraphs.

Another element to note, in the Matlab script, is the division of the solutions into two cases:

- A first case, called *Exact calculation*, in which the array of current $[I(t)]$ (called I_m in the script) is calculated with the equation:

$$(9.6) \quad [I(t)]_{exact} = \left[[K]^{-1} \cdot [B(t)]^T \right]^T$$

- A second case, called *Approximate calculation*, in which the same array is calculated with the following equation:

$$(9.7) \quad [I(t)]_{approx.} = [K_d]^{-1} [B(t)]$$

Where the matrix \mathbf{K}_d is the matrix \mathbf{K} where are considered only the diagonal values.

The result is that, with the array $\mathbf{I}(t)_{approx.}$, the current flowing through a bar is calculated not considering the effects of stray MFs produced by the currents flowing through the other bars.

It's possible, furthermore, to calculate the error between the initial input current and the current calculated with the use of the matrix.

To do this there were implemented the following equations:

- For the error between the true input current and the current calculated with the *Exact calculation*:

$$(9.8) \quad e_{exact} = [I(t)]_{exact} - [I(t)]_{input}$$

- For the error between the true input current and the current calculated with the *Approximate calculation*:

$$(9.9) \quad e_{approx.} = [I(t)]_{approx.} - [I(t)]_{input}$$

After the computation of these parameters all the results will graph in order to show the trend of the current wave forms and the errors.

10 STUDY OF THE ERROR - 2D CASE

In this section will be shown the procedure to obtain the correct measure of current focusing on every particular cut-plane considered. In every case it will be shown the respective K matrix utilized and the solutions in graphical form.

It's important to anticipate that for the probes there were considered these two different cases:

- A study of the model neglecting the phenomenon of mutual inductance which may be incurred between the bars;
- A study considering the phenomenon of mutual inductance.

To simulate these two types of study it has been used the same Comsol model in two different configurations: for the first study (mutual inductance neglected) were considered all the bars and circuits made by air instead of aluminium, for the second was considered the normal configuration with aluminium.

10.1 First disposition of measurement sensors

10.1.1 K matrix

In this paragraph there are presented the matrices $[K]$ used for the calculation of the measured current. All the values of the matrix elements are in $[\mu T]$.

a) Case neglecting the mutual inductance effect

		ACTIVE PHASE									
		R1	S1	R2	S2	R3	S3	R4	S4	T	N
K =	RI	32.448	-0.63872	-0.17978	-0.079189	-0.046106	-0.029409	-0.020951	-0.015426	-0.014192	0.26106
	S1	-0.63766	32.441	-0.73116	-0.17971	-0.083036	-0.0461	-0.03025	-0.020949	-0.018561	0.016993
	R2	-0.17971	-0.73139	32.447	-0.63771	-0.17963	-0.07915	-0.04609	-0.029401	-0.024522	-0.045264
	S2	-0.079154	-0.17966	-0.63783	32.444	-0.73108	-0.17969	-0.083028	-0.046095	-0.03387	-0.039465
	R3	-0.046097	-0.083032	-0.17971	-0.7313	32.453	-0.63794	-0.17966	-0.079151	-0.044139	-0.02936
	S3	-0.0294	-0.046089	-0.079147	-0.17961	-0.63741	32.43	-0.73094	-0.17969	-0.033091	-0.021429
	R4	-0.020949	-0.030252	-0.046103	-0.083045	-0.17975	-0.73166	32.46	-0.63797	0.11414	-0.016435
	S4	-0.015421	-0.020943	-0.029397	-0.04608	-0.079129	-0.17957	-0.63729	32.446	0.29887	-0.012736
	T	0.014605	0.018754	0.02434	0.033251	0.045202	0.058239	0.026484	-0.3162	12.451	0.014702
	N	-0.10356	0.054683	0.0536	0.039178	0.028929	0.02147	0.016761	0.013215	0.014712	12.451

This matrix, as explained before, was calculated based on the imposition of a current of 1[A] in every bar of every circuit one at a time, the results was obtained with a steady-state study of the model.

To obtain this matrix have been considered the electrical bars present in the cut-plane z: R-bars, S-bars, neutral-bar and also the bar T because may influence the measures taken by the sensors in the plane.

Regarding the sensors, were taken into account also two sensors near the bar T, that will not be installed in the electrical panel. These sensors have been necessary in this case to complete the matrix, because, considering only the effects of the bar T on the other sensors and not the effects of the other bars on the sensors of the bar T it means have a different number of row and column in the matrix. This translates into have a non-square matrix and so a non-invertible matrix.

A thing to notice is that the highest values of MF are present in the diagonal of the matrix, this because in the diagonal there are all the measures taken by the sensors installed in proximity of the powered bars. These values also represent the true MFs that we have to measure.

All the other elements of the matrix have a very low value and so will affect the measures with a very low contribute. This fact can suggest that the theoretical considerations made about the 2-sensors method are true.

b) Case considering the mutual inductance effect

		ACTIVE PHASE									
		R1	S1	R2	S2	R3	S3	R4	S4	T	N
K =	SENSOR R1	32.448	-0.63872	-0.17978	-0.079189	-0.046106	-0.029409	-0.020951	-0.015426	-0.014192	0.26106
	S1	-0.63766	32.441	-0.73116	-0.17971	-0.083036	-0.0461	-0.03025	-0.020949	-0.018561	0.016993
	R2	-0.17971	-0.73139	32.447	-0.63771	-0.17963	-0.07915	-0.04609	-0.029401	-0.024522	-0.045264
	S2	-0.079154	-0.17966	-0.63783	32.444	-0.73108	-0.17969	-0.083028	-0.046095	-0.03387	-0.039465
	R3	-0.046097	-0.083032	-0.17971	-0.7313	32.453	-0.63794	-0.17966	-0.079151	-0.044139	-0.02936
	S3	-0.0294	-0.046089	-0.079147	-0.17961	-0.63741	32.43	-0.73094	-0.17969	-0.033091	-0.021429
	R4	-0.020949	-0.030252	-0.046103	-0.083045	-0.17975	-0.73166	32.46	-0.63797	0.11414	-0.016435
	S4	-0.015421	-0.020943	-0.029397	-0.04608	-0.079129	-0.17957	-0.63729	32.446	0.29887	-0.012736
	T	0.014605	0.018754	0.02434	0.033251	0.045202	0.058239	0.026484	-0.3162	12.451	0.014702
	N	-0.10356	0.054683	0.0536	0.039178	0.028929	0.02147	0.016761	0.013215	0.014712	12.451

As can be seen, the matrix K in this case is exactly the same as the previous one, even taking into account the mutual inductance effects.

This can be explained with the fact that we are studying the system in a stationary domain condition and the input currents are constant currents. Because of this, as it can be demonstrated in the next equations, the derivative of current respect to the time will be zero and there will not the formation of an electromotive force induced on the other bars.

$$(9.10) \quad E = -M \frac{di}{dt} \quad \text{with} \quad \frac{di}{dt} = 0$$

$$\rightarrow E = 0$$

10.1.2 Arrays $[B(t)]$

To monitor the correct functioning of the measure system have been done some tests with different input currents. This in order to discover the development of the errors between the indirect measurement of currents and the real currents flowing through the panel bars.

For every single case taken into consideration it will be represented the respective matrix $\mathbf{B}(t)$ used for the computation.

The following arrays $[B(t)]$ are derived with the input currents set in this way:

$$\begin{array}{l}
 \dot{i}(t)_{R1} = I_1 \sin(2\pi 50 t) \\
 \dot{i}(t)_{R2} = I_2 \sin(2\pi 50 t) \\
 \dot{i}(t)_{R3} = I_3 \sin(2\pi 50 t) \\
 \dot{i}(t)_{R4} = I_4 \sin(2\pi 50 t) \\
 \dot{i}(t)_{S1} = I_1 \sin(2\pi 50 t + 2\pi / 3) \\
 \dot{i}(t)_{S2} = I_2 \sin(2\pi 50 t + 2\pi / 3) \\
 \dot{i}(t)_{S3} = I_3 \sin(2\pi 50 t + 2\pi / 3) \\
 \dot{i}(t)_{S4} = I_4 \sin(2\pi 50 t + 2\pi / 3) \\
 \dot{i}(t)_T = 4 I_1 \sin(2\pi 50 t + 4\pi / 3)
 \end{array}
 \quad \left| \quad I_1 = I_2 = I_3 = I_4 = 1, 50, 100 [A]$$

Where I_1, I_2, I_3, I_4 are the peak values of the alternative currents considered, the electrical system considered is symmetrical and balanced.

It's important to note that for the phase T the input current set was 4 time the current set for the other bars. This is because the bar T in this case is not a bar of an electrical circuit but it's the principle phase-T bar in which flows a current that will split through the four circuits.

The resulting arrays are shown below according to their respective input currents; all the values are expressed in $[\mu T]$.

a) CASE NEGLECTING THE MUTUAL INDUCTANCE EFFECT

Time [s]	R1	S1	R2	S2	R3	S3	R4	S4	T
0	-0.60782	27.792	-1.269	27.693	-1.238	27.797	-1.4402	27.139	-42.924
0.001	9.4855	21.152	9.0041	21.09	9.0488	21.106	8.5039	20.125	-48.843
0.002	18.639	12.309	18.307	12.276	18.371	12.306	17.84	11.464	-49.572
0.003	25.985	2.2465	25.836	2.2462	25.913	2.2868	25.447	1.667	-45.454
0.004	30.791	-8.0427	30.839	-8.0106	30.921	-7.9631	30.567	-8.3001	-36.88
0.005	32.58	-17.54	32.82	-17.479	32.9	-17.429	32.692	-17.45	-24.699
0.006	31.189	-25.323	31.598	-25.238	31.668	-25.191	31.626	-24.895	-10.112
0.007	26.709	-30.608	27.246	-30.508	27.298	-30.468	27.427	-29.883	5.4944
0.008	19.624	-32.89	20.237	-32.786	20.267	-32.757	20.553	-31.941	20.536
0.009	10.61	-31.936	11.239	-31.837	11.243	-31.822	11.659	-30.855	33.554
0.01	0.57718	-27.885	1.1605	-27.8	1.1392	-27.801	1.6442	-26.777	43.301
0.011	-9.4808	-21.155	-8.9992	-21.094	-9.0439	-21.11	-8.499	-20.128	48.841
0.012	-18.644	-12.273	-18.313	-12.24	-18.377	-12.27	-17.846	-11.429	49.522
0.013	-26.004	-2.174	-25.856	-2.174	-25.933	-2.2146	-25.469	-1.5971	45.37
0.014	-30.786	8.0436	-30.834	8.0115	-30.916	7.964	-30.562	8.3008	36.871
0.015	-32.577	17.529	-32.817	17.468	-32.896	17.418	-32.688	17.44	24.71
0.016	-31.175	25.304	-31.584	25.219	-31.653	25.172	-31.611	24.876	10.12
0.017	-26.715	30.609	-27.253	30.509	-27.305	30.469	-27.434	29.884	-5.485
0.018	-19.645	32.91	-20.259	32.805	-20.289	32.776	-20.575	31.96	-20.532
0.019	-10.647	31.989	-11.277	31.889	-11.281	31.874	-11.697	30.906	-33.578
0.02	-0.62133	27.963	-1.2061	27.878	-1.1849	27.879	-1.6906	26.853	-43.354

	R1	S1	R2	S2	R3	S3	R4	S4	T
$ B(t) _{50[A]} =$									
Time [s] 0	-30.391	1389.6	-63.448	1384.6	-61.901	1389.8	-72.01	1357	-2146.2
0.001	474.29	1057.6	450.21	1054.5	452.45	1055.3	425.2	1006.2	-2442.1
0.002	931.95	615.44	915.37	613.81	918.55	615.3	892	573.2	-2478.6
0.003	1299.2	112.39	1291.7	112.37	1295.6	114.4	1272.3	83.408	-2272.7
0.004	1539.5	-402.09	1541.9	-400.49	1546	-398.11	1528.3	-414.96	-1844
0.005	1629.1	-877.01	1641.1	-873.95	1645	-871.46	1634.7	-872.52	-1235
0.006	1558.9	-1265.8	1579.4	-1261.6	1582.8	-1259.2	1580.7	-1244.4	-505.24
0.007	1336.2	-1530.9	1363.1	-1525.9	1365.7	-1523.9	1372.1	-1494.7	274.24
0.008	982.8	-1646.3	1013.5	-1641.1	1015	-1639.6	1029.3	-1598.8	1027
0.009	532.61	-1600	564.12	-1595	564.34	-1594.3	585.16	-1545.9	1679.4
0.01	29.717	-1396.2	58.92	-1392	57.859	-1392	83.129	-1340.8	2166.8
0.011	-474.92	-1056.9	-450.86	-1053.8	-453.1	-1054.6	-425.86	-1005.5	2442
0.012	-932.69	-614.96	-916.11	-613.33	-919.3	-614.82	-892.74	-572.73	2479
0.013	-1299.7	-110.47	-1292.3	-110.47	-1296.1	-112.5	-1272.8	-81.564	2270.4
0.014	-1539.3	403.64	-1541.8	402.03	-1545.9	399.65	-1528.2	416.44	1841.3
0.015	-1628	876.75	-1640	873.68	-1643.9	871.2	-1633.6	872.25	1233.7
0.016	-1557.4	1265.2	-1577.8	1260.9	-1581.3	1258.6	-1579.2	1243.8	503.85
0.017	-1334.4	1530.3	-1361.3	1525.3	-1363.9	1523.3	-1370.4	1494	-276.09
0.018	-982.96	1645.4	-1013.6	1640.2	-1015.1	1638.7	-1029.4	1597.9	-1025.3
0.019	-533.28	1598.3	-564.74	1593.4	-564.97	1592.6	-585.75	1544.3	-1675.6
0.02	-29.471	1396.2	-58.675	1392	-57.613	1392	-82.887	1340.8	-2167.2

	R1	S1	R2	S2	R3	S3	R4	S4	T
$ B(t) _{100[A]} =$									
Time [s] 0	-60.782	2779.2	-126.9	2769.3	-123.8	2779.7	-144.02	2713.9	-4292.4
0.001	948.16	2113.9	900.04	2107.7	904.51	2109.3	850.05	2011.2	-4881.5
0.002	1863.8	1231.1	1830.6	1227.8	1837	1230.8	1783.8	1146.6	-4957.2
0.003	2597.7	225.94	2582.8	225.91	2590.4	229.97	2543.9	167.95	-4546.1
0.004	3079.9	-804.98	3084.7	-801.77	3092.9	-797.02	3057.5	-830.71	-3688.2
0.005	3258.3	-1754.2	3282.3	-1748.1	3290.3	-1743.1	3269.5	-1745.2	-2470.1
0.006	3117.6	-2531.6	3158.5	-2523.1	3165.4	-2518.4	3161.2	-2488.8	-1010.1
0.007	2671.7	-3061	2725.5	-3051	2730.7	-3047.1	2743.5	-2988.5	548.4
0.008	1965.3	-3292.3	2026.7	-3281.9	2029.7	-3279	2058.4	-3197.3	2054.1
0.009	1065.7	-3200.5	1128.7	-3190.5	1129.1	-3189.1	1170.8	-3092.2	3358.8
0.01	61.465	-2795.2	119.92	-2786.7	117.8	-2786.8	168.36	-2684.3	4334.8
0.011	-948.72	-2116.3	-900.55	-2110.1	-905.02	-2111.7	-850.51	-2013.6	4886.3
0.012	-1866	-1230.2	-1832.8	-1226.9	-1839.2	-1229.9	-1786.1	-1145.7	4959.5
0.013	-2600	-223.08	-2585.1	-223.06	-2592.7	-227.12	-2546.2	-165.16	4545.2
0.014	-3079.5	804.67	-3084.3	801.45	-3092.5	796.7	-3057.1	830.4	3688
0.015	-3257	1753	-3281	1746.8	-3289	1741.9	-3268.2	1744	2470
0.016	-3116.7	2530.4	-3157.6	2522	-3164.5	2517.3	-3160.3	2487.6	1010.6
0.017	-2671.5	3060.5	-2725.3	3050.5	-2730.4	3046.6	-2743.3	2988.1	-547.92
0.018	-1964.2	3290.3	-2025.5	3279.9	-2028.5	3277	-2057.1	3195.4	-2052.8
0.019	-1064.9	3198.3	-1127.9	3188.3	-1128.3	3186.9	-1169.9	3090.1	-3356.5
0.02	-61.111	2793.9	-119.54	2785.4	-117.42	2785.5	-167.96	2683	-4333.2

b) CASE CONSIDERING THE MUTUAL INDUCTANCE EFFECT

	R1	S1	R2	S2	R3	S3	R4	S4	T
$ B(t) _{1[A]} =$									
Time [s] 0	-0.94151	19.699	-1.8639	19.568	-1.8395	19.598	-2.579	18.303	-41.631
0.001	8.7127	21.372	8.4175	21.355	8.456	21.352	7.8569	20.418	-50.742
0.002	17.964	12.798	17.834	12.808	17.89	12.824	17.334	12.028	-49.74
0.003	25.459	2.8306	25.498	2.8657	25.567	2.8975	25.1	2.3156	-44.67
0.004	30.462	-7.4153	30.665	-7.3578	30.74	-7.3141	30.405	-7.621	-35.646
0.005	32.488	-16.936	32.834	-16.862	32.907	-16.81	32.738	-16.81	-23.317
0.006	31.329	-24.798	31.783	-24.714	31.848	-24.66	31.859	-24.352	-8.7766
0.007	27.096	-30.217	27.611	-30.132	27.662	-30.081	27.853	-29.495	6.607
0.008	20.227	-32.691	20.752	-32.614	20.784	-32.57	21.136	-31.764	21.336
0.009	11.391	-31.991	11.871	-31.929	11.881	-31.897	12.359	-30.949	33.983
0.01	1.4268	-28.136	1.8161	-28.096	1.8021	-28.079	2.3603	-27.082	43.282
0.011	-8.6819	-21.525	-8.4234	-21.51	-8.4592	-21.51	-7.8761	-20.562	48.349
0.012	-17.939	-12.801	-17.837	-12.814	-17.891	-12.83	-17.34	-12.022	48.68
0.013	-25.437	-2.8306	-25.504	-2.8694	-25.571	-2.9004	-25.105	-2.3128	44.265
0.014	-30.438	7.4154	-30.667	7.354	-30.74	7.3114	-30.406	7.6213	35.5
0.015	-32.452	16.931	-32.823	16.853	-32.895	16.803	-32.725	16.805	23.272
0.016	-31.298	24.79	-31.774	24.702	-31.838	24.65	-31.849	24.343	8.7668
0.017	-27.085	30.225	-27.621	30.136	-27.671	30.087	-27.861	29.502	-6.6066
0.018	-20.218	32.701	-20.762	32.62	-20.792	32.578	-21.144	31.772	-21.336
0.019	-11.36	31.954	-11.86	31.889	-11.868	31.858	-12.347	30.91	-33.972
0.02	-1.4041	28.118	-1.8116	28.074	-1.7966	28.059	-2.3548	27.061	-43.315

	R1	S1	R2	S2	R3	S3	R4	S4	T
$ B(t) _{30[A]} =$									
Time [s] 0	-47.075	984.94	-93.196	978.41	-91.973	979.89	-128.95	915.15	-2081.6
0.001	435.62	1068.7	420.86	1067.8	422.78	1067.7	392.84	1021	-2537.2
0.002	898.2	639.9	891.68	640.37	894.47	641.18	866.69	601.38	-2487.2
0.003	1273	141.54	1274.9	143.3	1278.4	144.88	1255	115.79	-2233.6
0.004	1523.2	-370.78	1533.3	-367.91	1537.1	-365.72	1520.3	-381.06	-1782.4
0.005	1624.4	-846.85	1641.7	-843.13	1645.4	-840.57	1636.9	-840.57	-1166.2
0.006	1566.1	-1239.6	1588.8	-1235.4	1592.1	-1232.8	1592.7	-1217.4	-438.72
0.007	1354.9	-1511	1380.7	-1506.8	1383.2	-1504.2	1392.8	-1474.9	330.37
0.008	1011.6	-1634.9	1037.8	-1631	1039.4	-1628.8	1057	-1588.5	1066.9
0.009	568.83	-1597.9	592.94	-1594.8	593.4	-1593.2	617.36	-1545.8	1699
0.01	70.962	-1406.1	90.488	-1404.1	89.786	-1403.3	117.71	-1353.4	2165.5
0.011	-434.22	-1075.7	-421.25	-1075	-423.04	-1075	-393.86	-1027.5	2418.8
0.012	-897.09	-640.15	-891.98	-640.77	-894.68	-641.58	-867.13	-601.2	2435.2
0.013	-1271.8	-141.54	-1275.1	-143.47	-1278.5	-145.02	-1255.2	-115.65	2213.3
0.014	-1522.1	370.81	-1533.5	367.75	-1537.2	365.62	-1520.5	381.11	1775.4
0.015	-1621.7	846.15	-1640.2	842.24	-1643.8	839.74	-1635.3	839.82	1163.2
0.016	-1565.5	1239.9	-1589.3	1235.5	-1592.5	1232.9	-1593	1217.5	438.58
0.017	-1354.3	1511.3	-1381.1	1506.9	-1383.6	1504.4	-1393.1	1475.2	-330.39
0.018	-1011.2	1635.5	-1038.4	1631.5	-1039.9	1629.4	-1057.5	1589.1	-1066.9
0.019	-568.57	1598.9	-593.54	1595.7	-593.95	1594.1	-617.86	1546.7	-1699
0.02	-70.335	1406.2	-90.649	1404.1	-89.905	1403.3	-117.8	1353.4	-2164.7

	R1	S1	R2	S2	R3	S3	R4	S4	T
$ B(t) _{100A1} =$	-94.151	1969.9	-186.39	1956.8	-183.95	1959.8	-257.9	1830.3	-4163.1
Time [s] 0	871.24	2137.9	841.75	2136.3	845.6	2136	785.74	2042.7	-5075
0.001	1796.4	1279.8	1783.4	1280.8	1789	1282.4	1733.4	1202.8	-4974.2
0.002	2545.9	283.06	2549.8	286.57	2556.7	289.74	2510	231.56	-4467.2
0.003	3045.9	-741.46	3066.2	-735.71	3073.7	-731.33	3040.2	-762.02	-3564.3
0.004	3249	-1693.7	3283.6	-1686.3	3290.9	-1681.1	3274	-1681.1	-2331.9
0.005	3134.3	-2480.9	3179.7	-2472.5	3186.3	-2467.1	3187.4	-2436.3	-878.23
0.006	2709.9	-3022	2761.4	-3013.5	2766.5	-3008.4	2785.6	-2949.8	660.77
0.007	2022.6	-3268.8	2075.1	-3261.1	2078.2	-3256.8	2113.5	-3176.1	2133.3
0.008	1136.9	-3193.1	1185.1	-3186.9	1186	-3183.8	1233.9	-3088.9	3394.9
0.009	141.69	-2810.9	180.81	-2806.8	179.41	-2805.1	235.34	-2705.3	4332.2
0.01	-868.04	-2150.1	-842.05	-2148.6	-845.63	-2148.6	-787.24	-2053.7	4837.8
0.011	-1794.1	-1280.2	-1783.9	-1281.4	-1789.3	-1283.1	-1734.2	-1202.3	4871.6
0.012	-2543.8	-283.09	-2550.4	-286.95	-2557.1	-290.05	-2510.5	-231.3	4427.4
0.013	-3044.1	741.61	-3066.9	735.48	-3074.3	731.21	-3040.9	762.2	3550.8
0.014	-3242.9	1692	-3279.8	1684.2	-3287	1679.2	-3270	1679.3	2326.1
0.015	-3125	2475.2	-3172.5	2466.4	-3178.9	2461.2	-3180	2430.6	875.89
0.016	-2707.7	3021.6	-2761.2	3012.8	-2766.2	3007.8	-2785.2	2949.3	-660.38
0.017	-2020.6	3268.2	-2074.9	3260.1	-2078	3255.9	-2113.1	3175.4	-2132.6
0.018	-1136.6	3196.7	-1186.6	3190.1	-1187.4	3187.1	-1235.3	3092.2	-3398.7
0.019	-140.25	2810.4	-181.03	2806	-179.54	2804.5	-235.42	2704.7	-4332.2
0.02									

10.1.3 Graphical results

In this section there are gathered all the graphical solutions that will permit to observe the influence of the error in the sensor measures.

The graphs were obtained with Matlab scripts similar to the script reported in the *Appendix A.2*, but adapted to every single case.

In every image will be graph, for every powered bar, the trends of currents and errors with respect to time.

For the trends of currents have been considered the exact and approximate cases explained before (Exact and Approximate measure) and also the true input current that flows through the bars in the simulated model (Real current).

For the trends of currents have been considered the differences between the Real current trends and the trends of the other currents.

With the name “Phase XY” means that it was taken into consideration the trend of current flowing into the bar connected to the X-phase of the panel in the circuit Y.

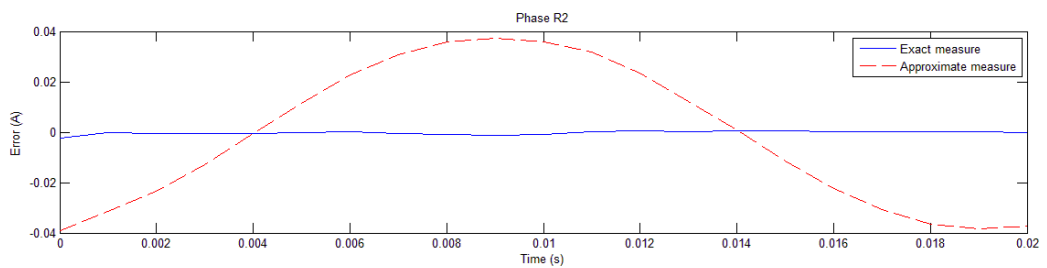
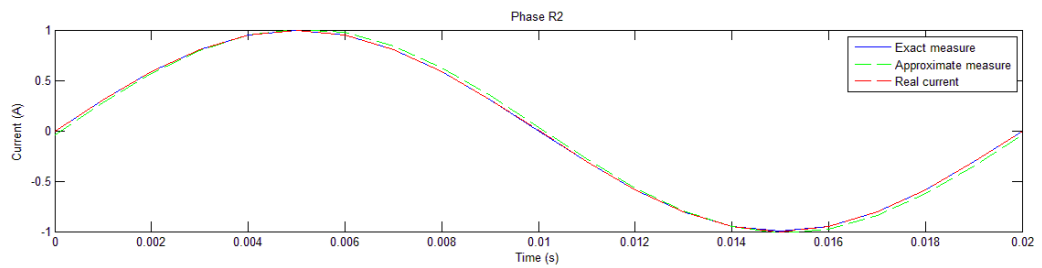
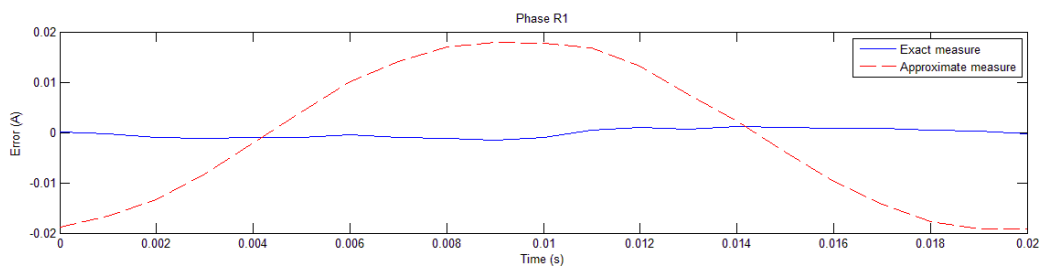
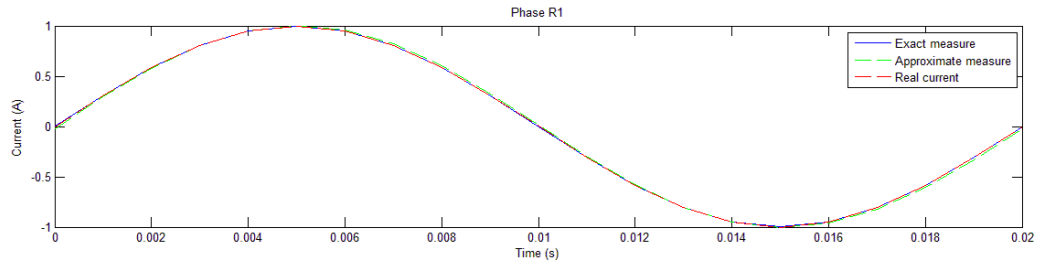
For example, “Phase R1” means that the graph is referred to the trend of current that flows in the bar connected to the R-phase of the panel in the circuit 1.

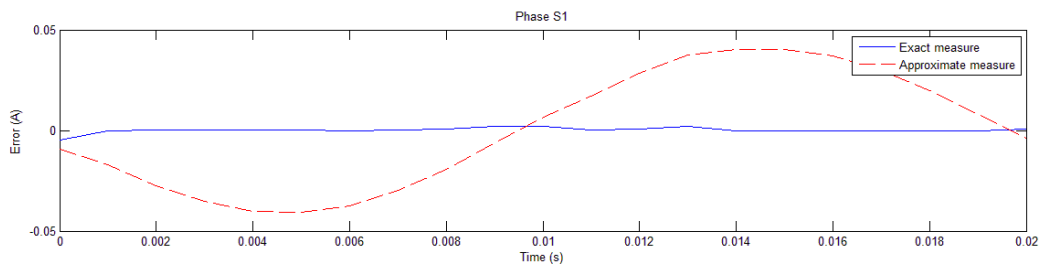
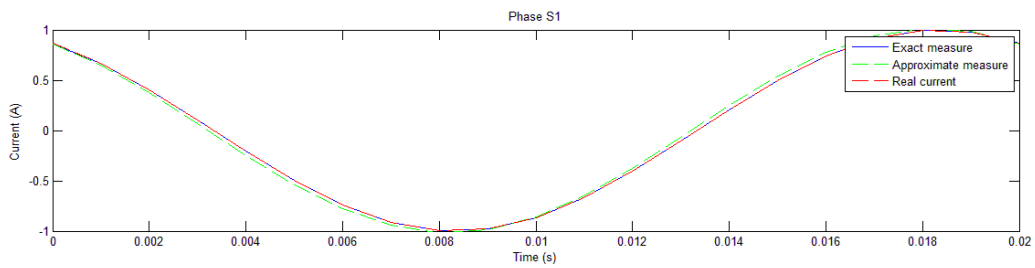
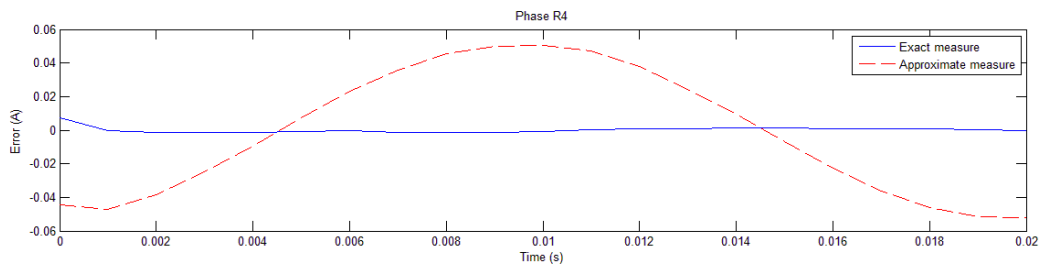
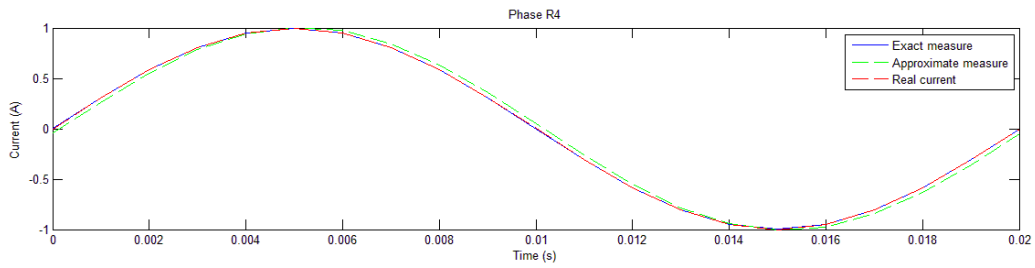
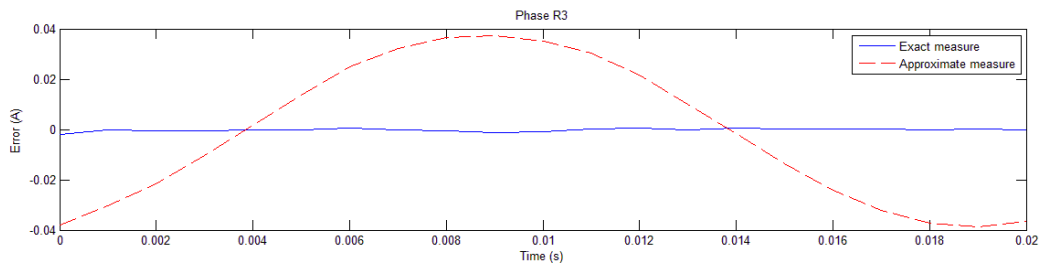
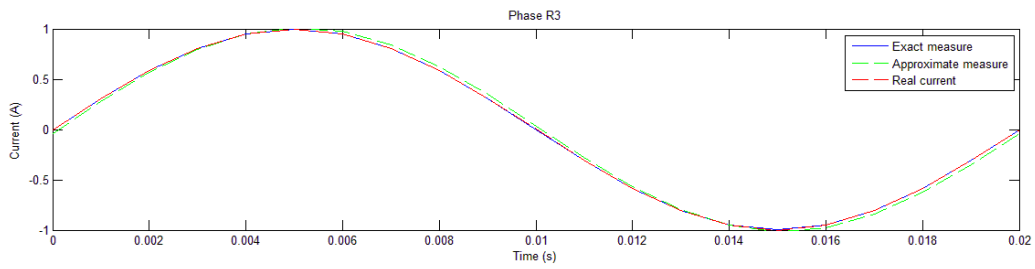
The graph referred to the bar T, presented in the 2D cut-plane, was created only for completeness because is not foreseen the installation of magnetoresistive sensors for that bar.

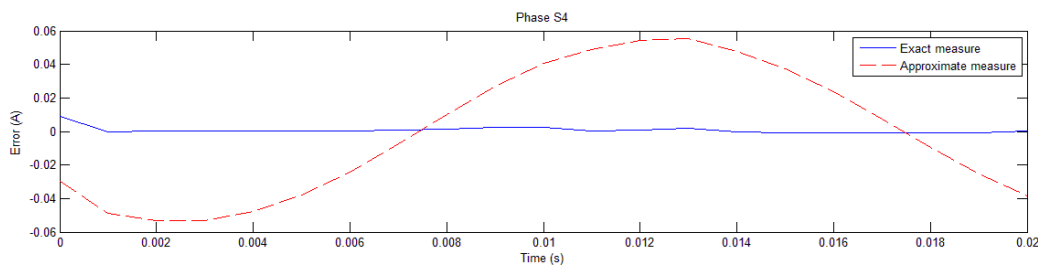
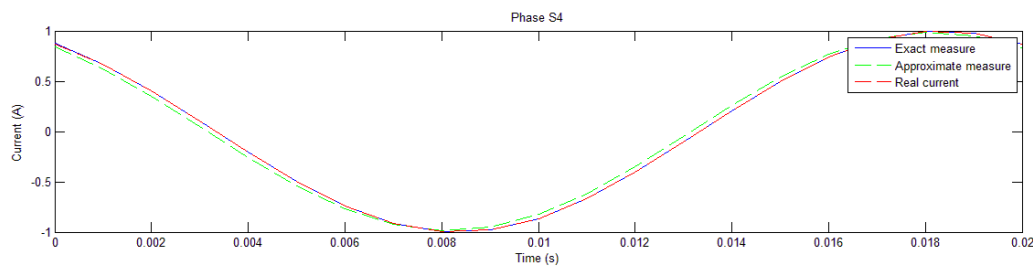
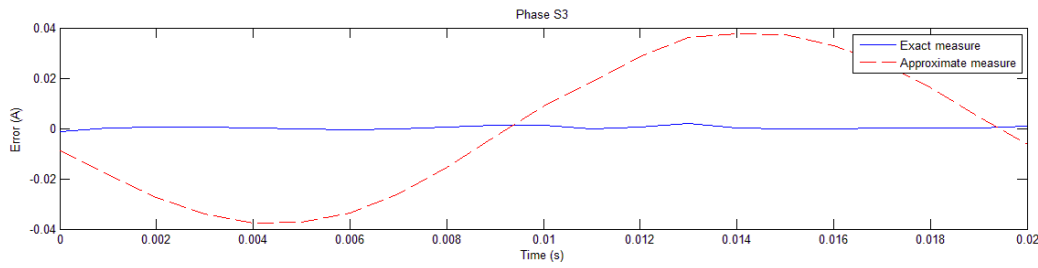
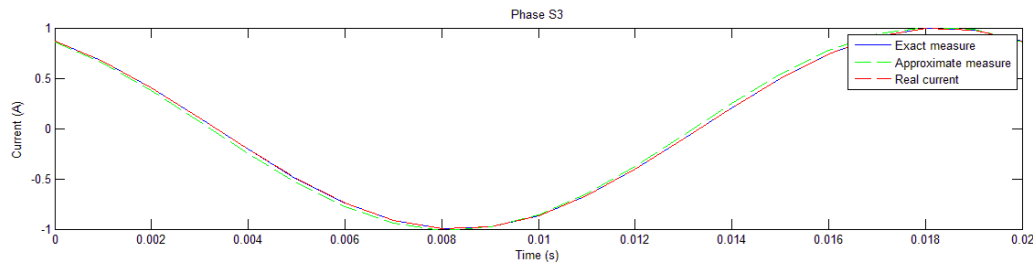
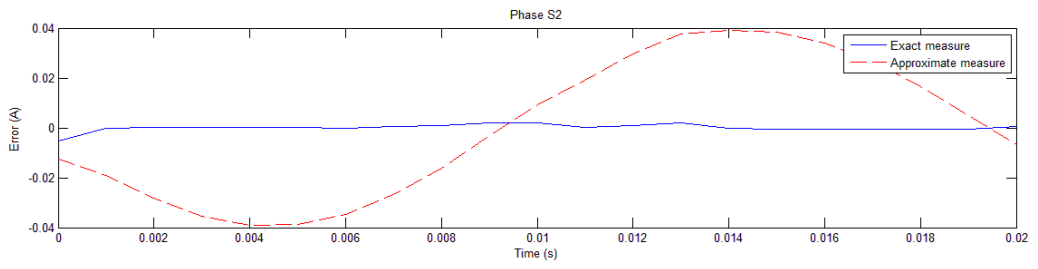
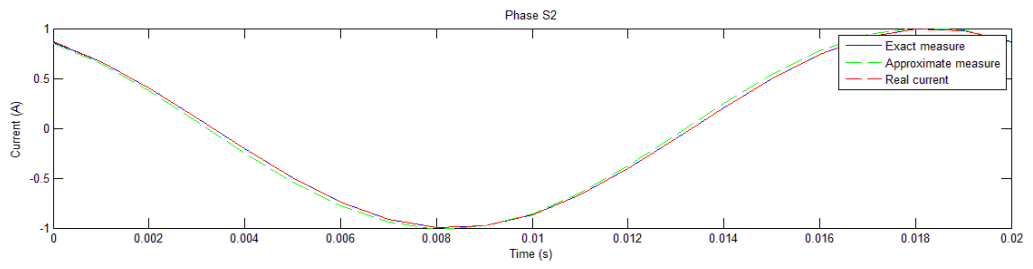
For the first groups of graphs will be take into consideration a balanced electrical system and in the *section [10.3]* will be considered a case of unbalanced electrical system.

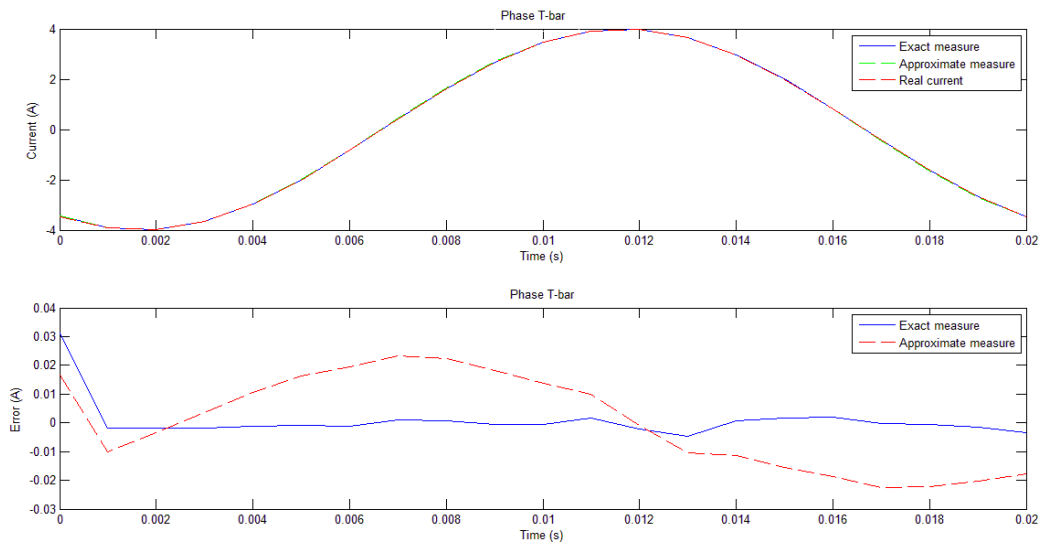
a) CASE NEGLECTING THE MUTUAL INDUCTANCE EFFECT

- PEAK VALUE = 1[A]







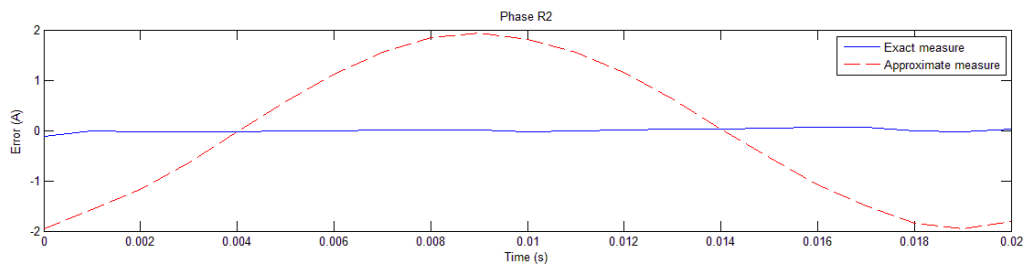
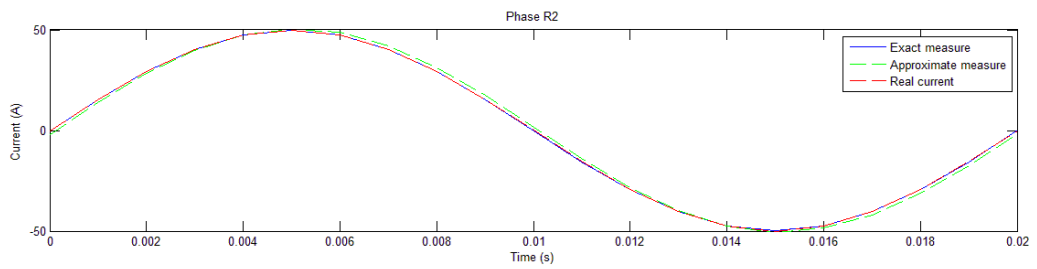
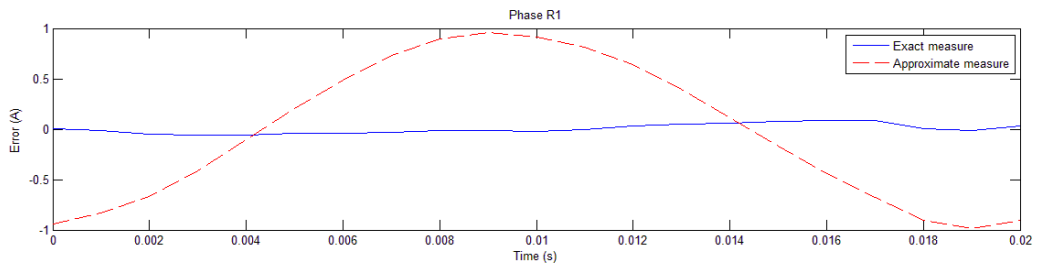
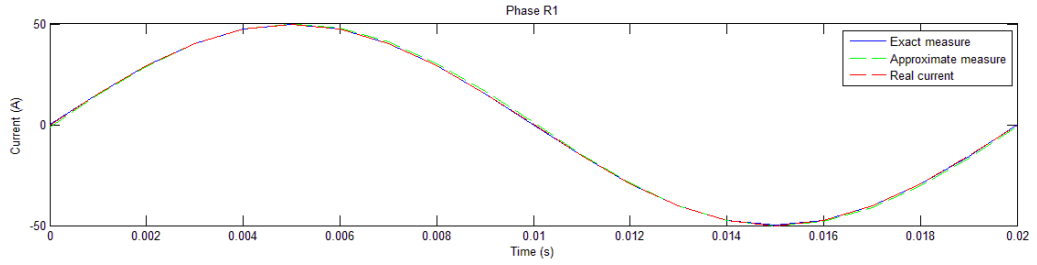


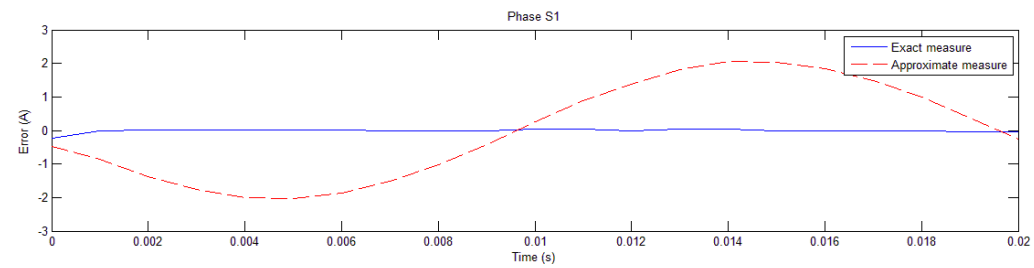
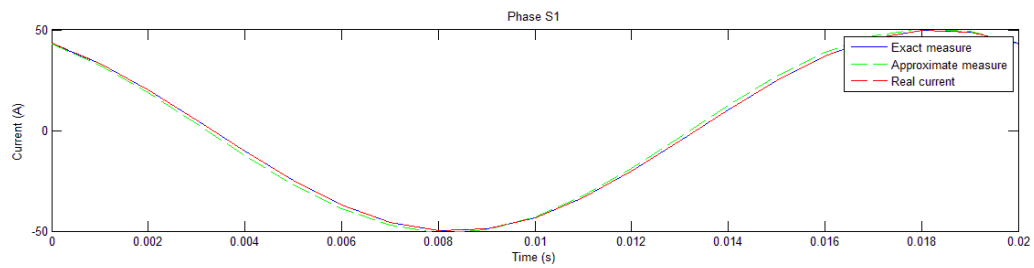
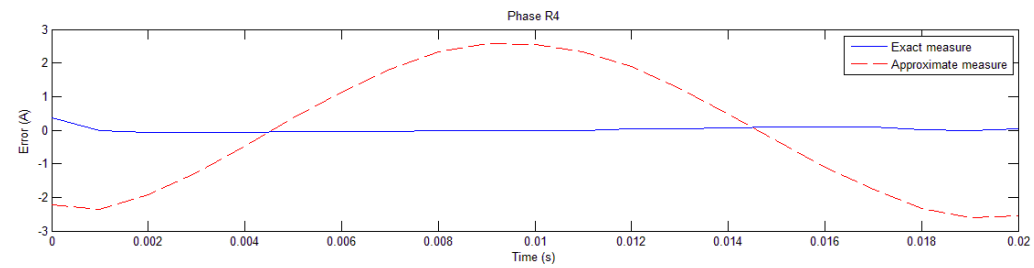
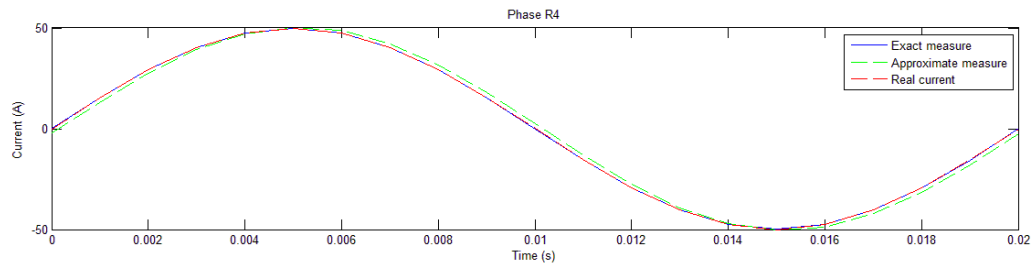
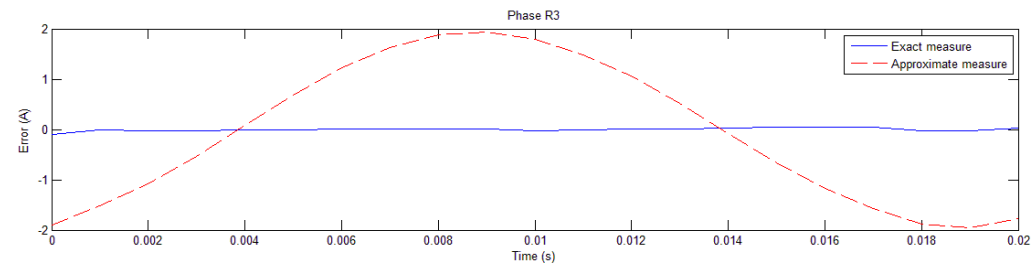
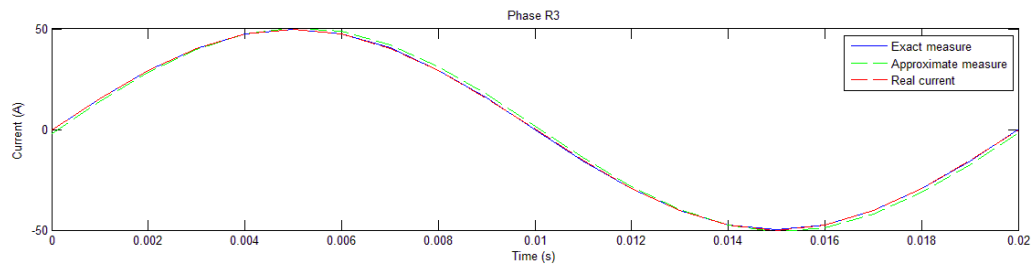
Considerations:

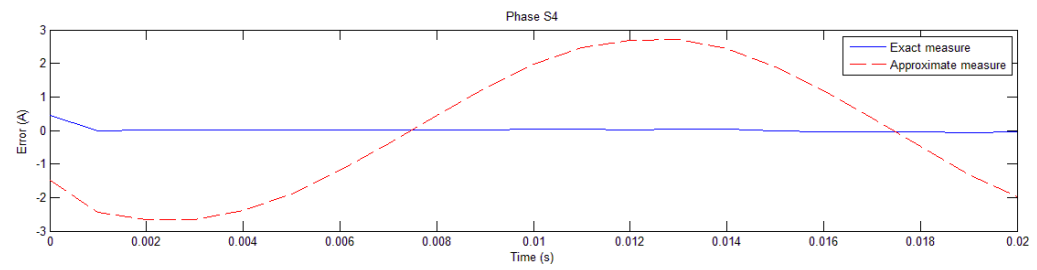
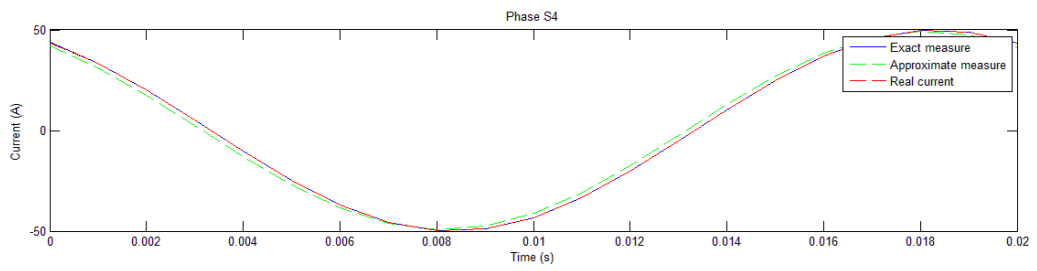
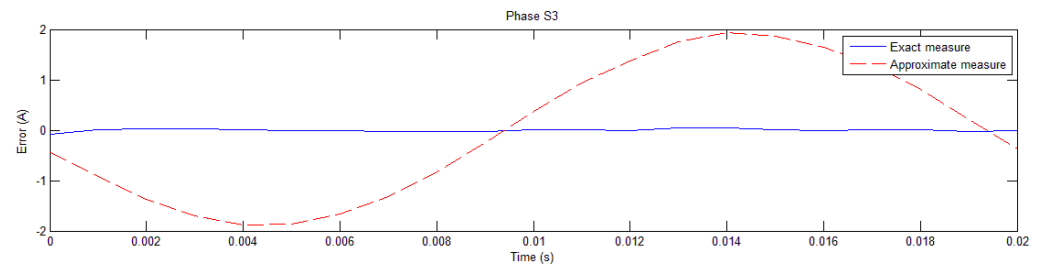
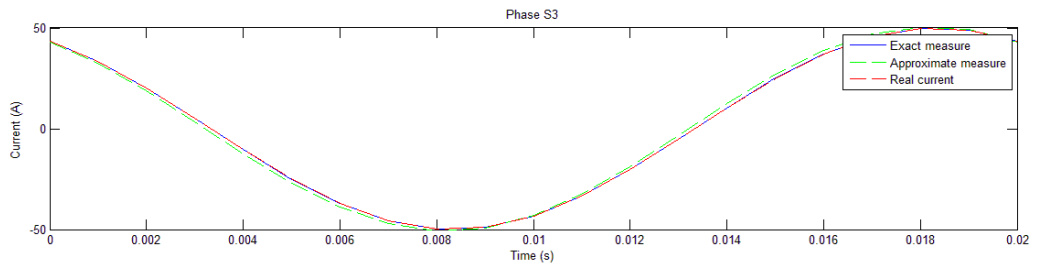
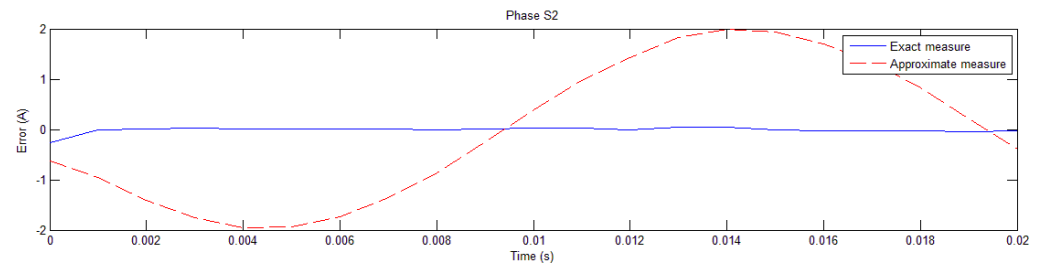
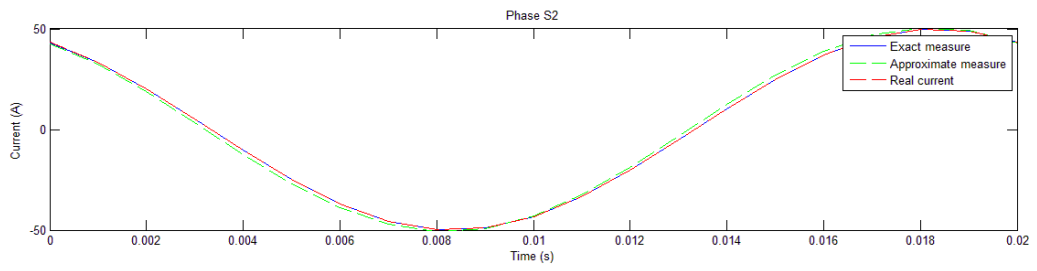
As it can be seen in the graphs, if is taken into consideration the exact measure curve, it's evident that the error is almost next to zero for every bar (highest error: $e_{max} = 1.1\%$, detected on the phase S4). This means that, neglecting the effects of the mutual inductance, the measurement system designed works perfectly.

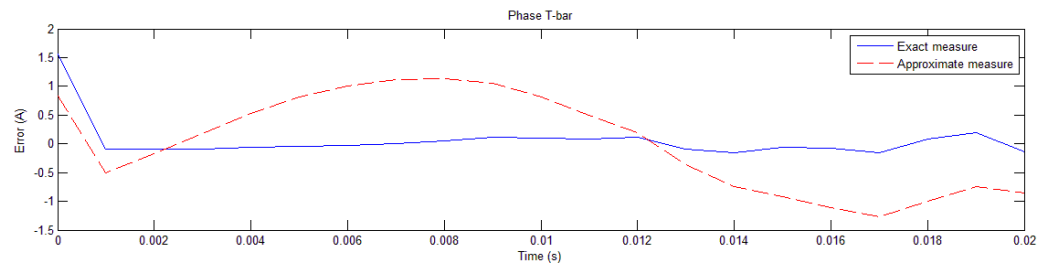
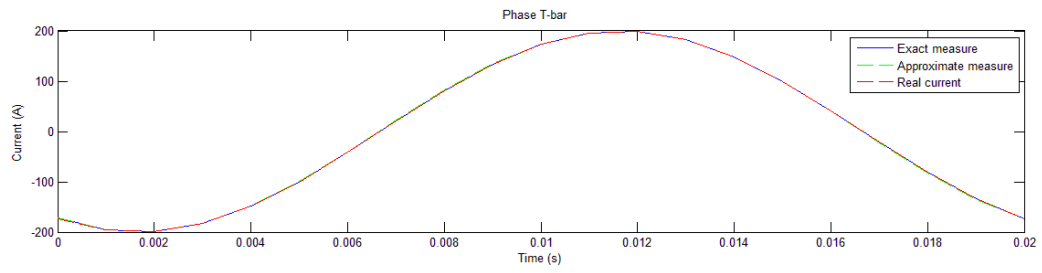
It's possible to figure out the correct functioning of the measurement system also with the graphs that show the current trends, in which it can be note the overlap of the true current curve (real current) with the measured current curve.

- PEAK VALUE = 50[A]

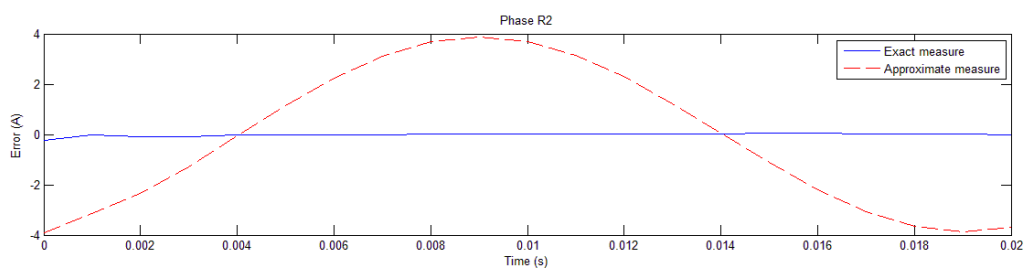
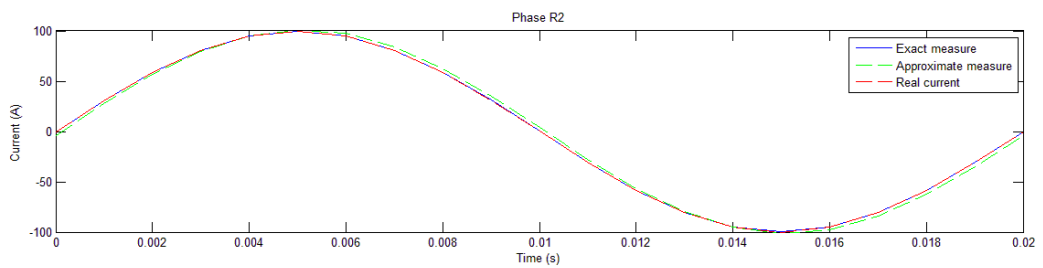
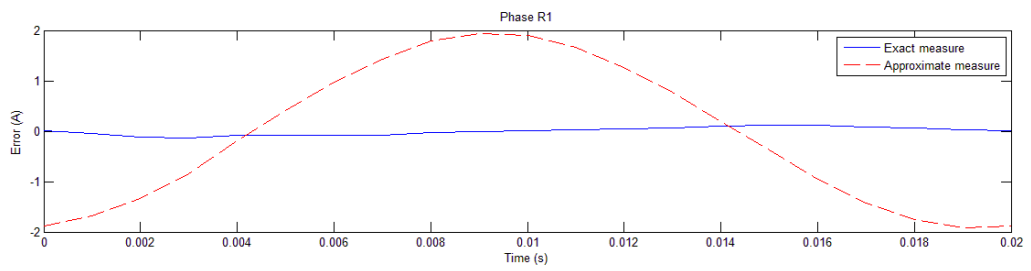
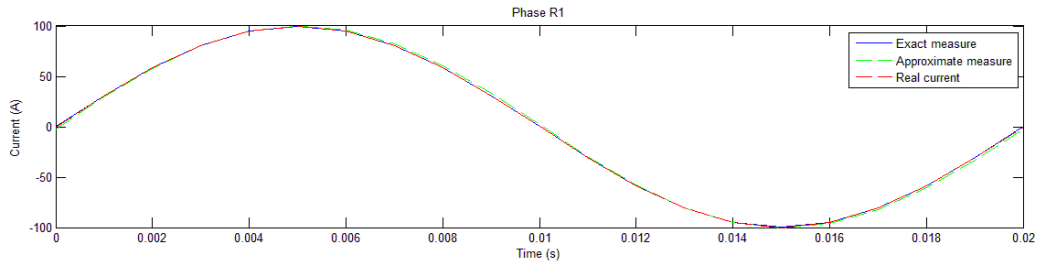


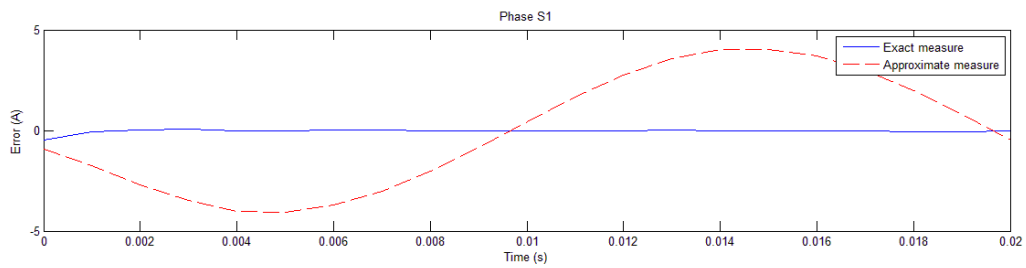
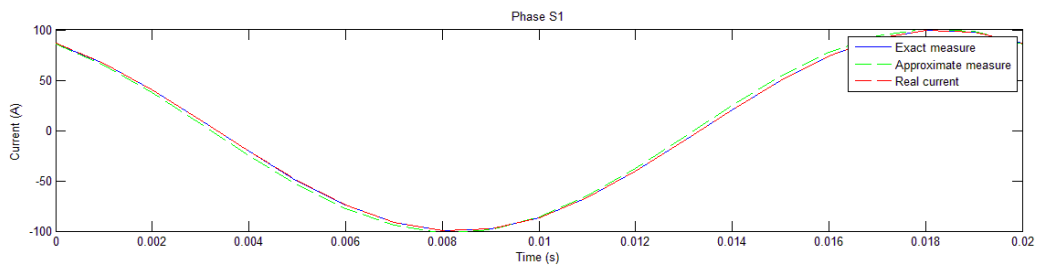
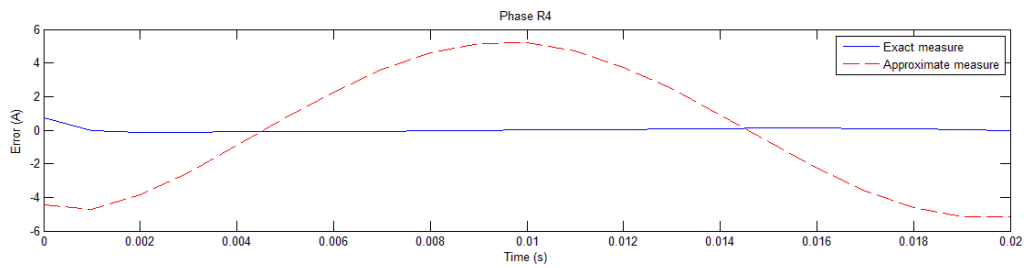
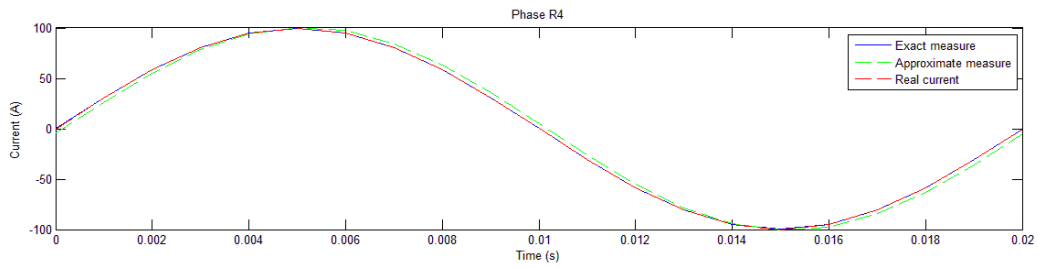
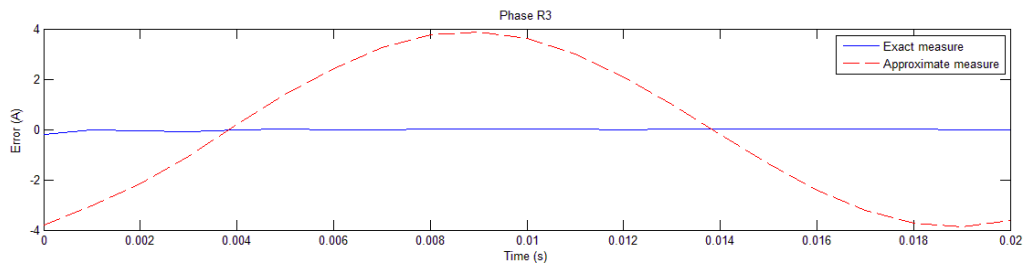
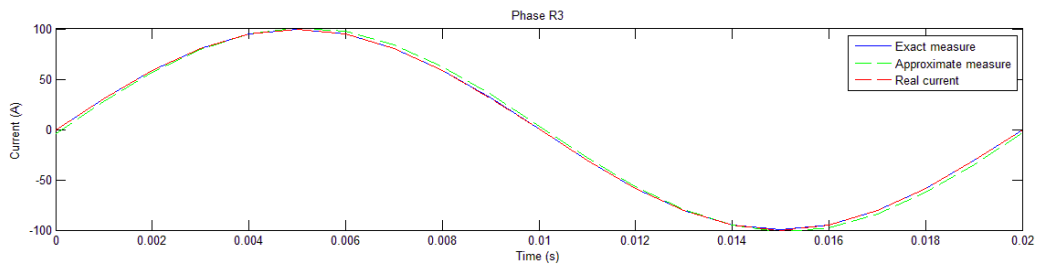


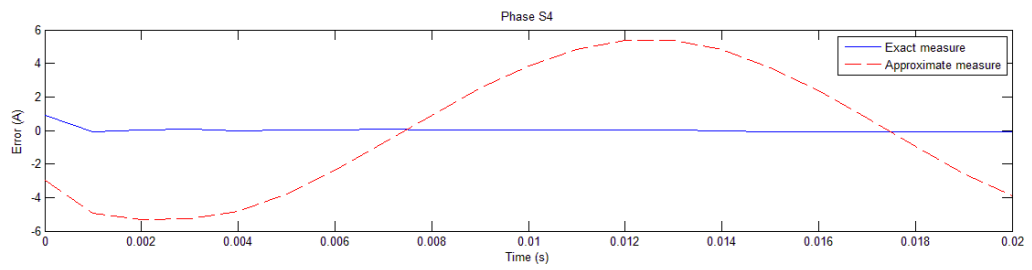
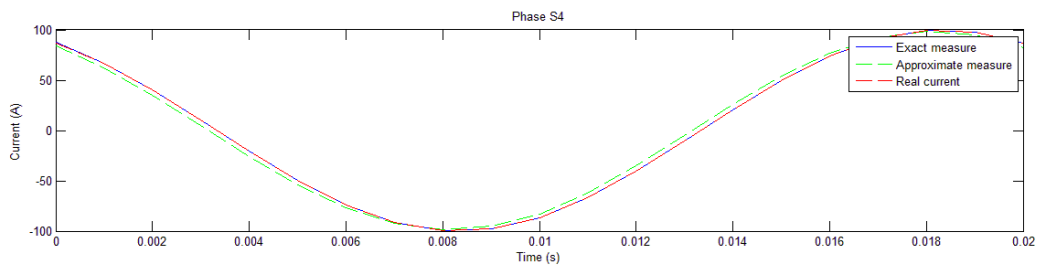
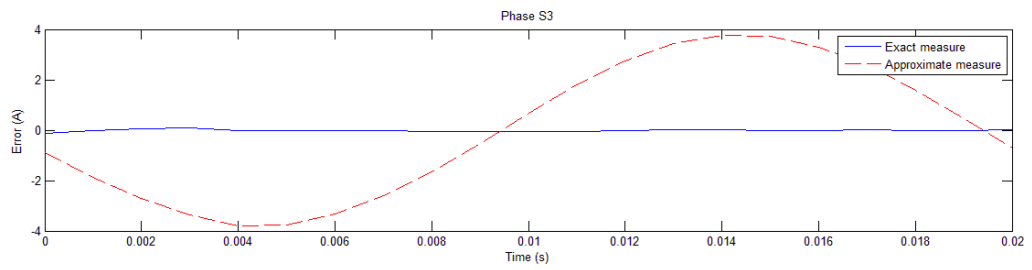
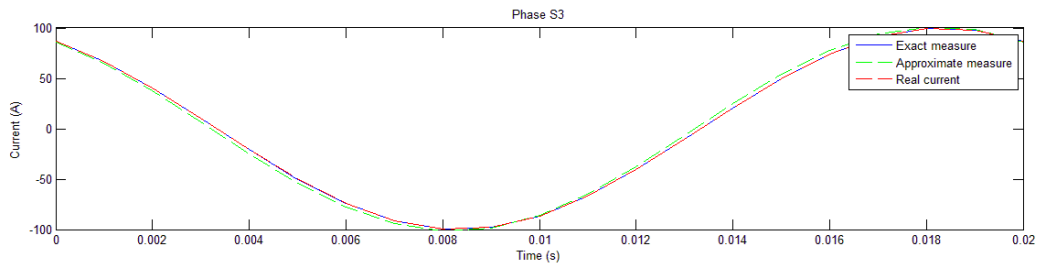
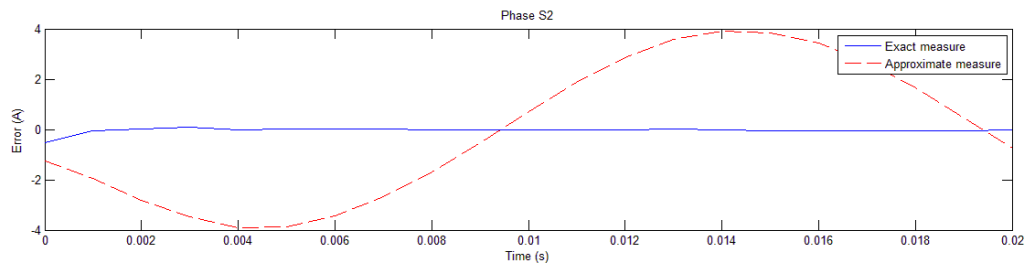
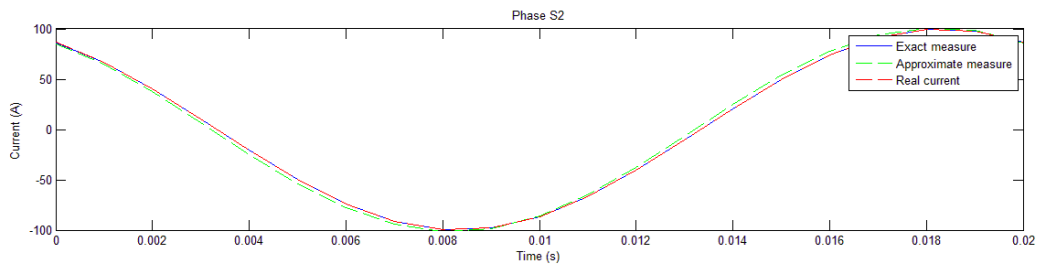


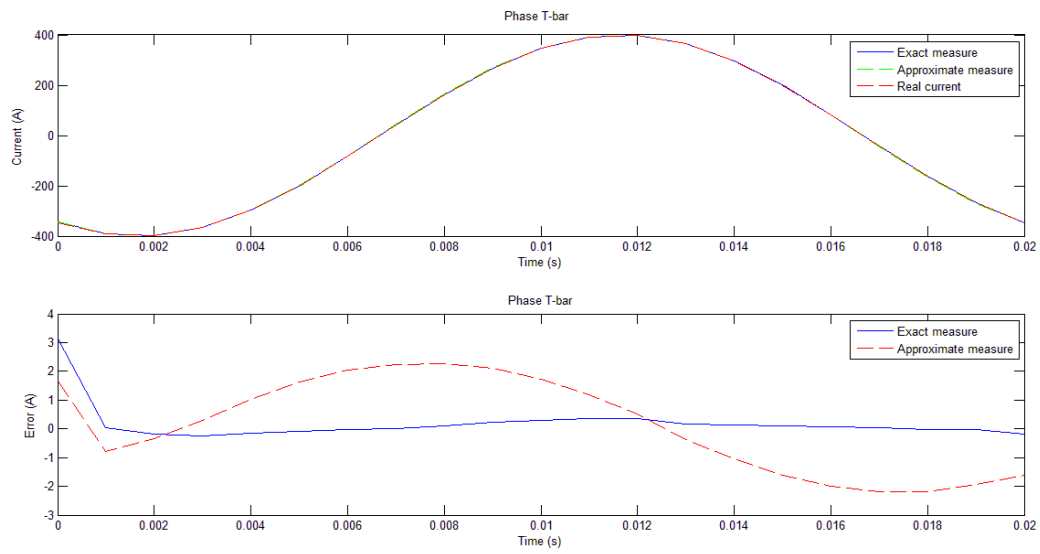


- PEAK VALUE = 100 [A]







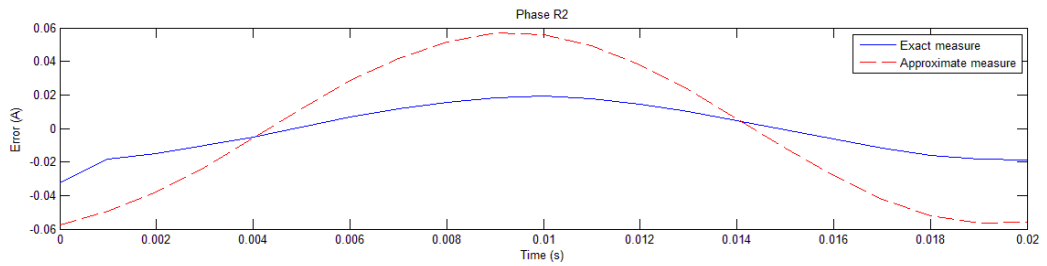
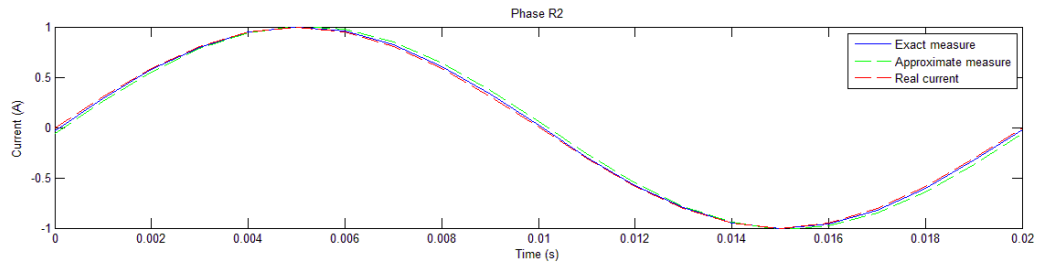
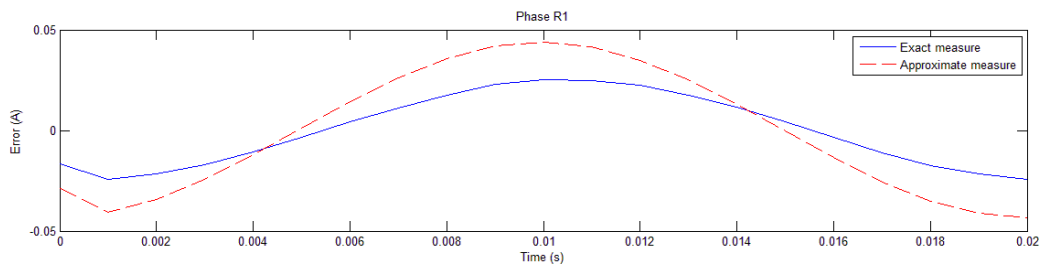
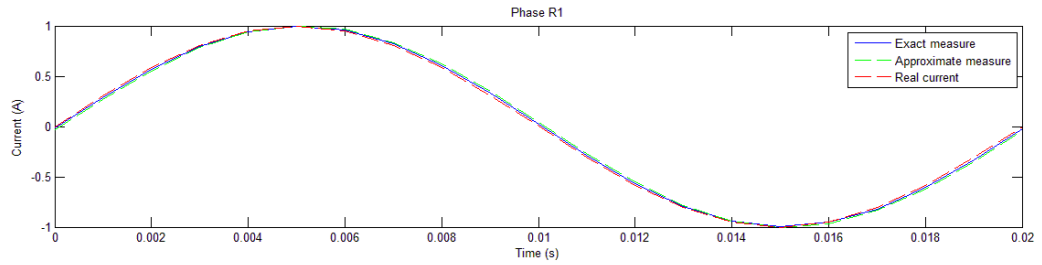


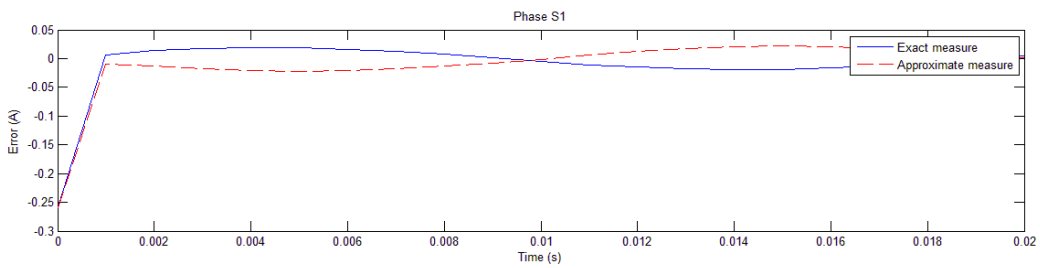
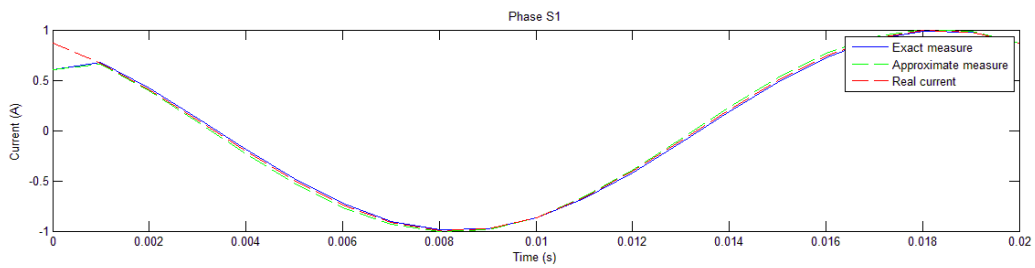
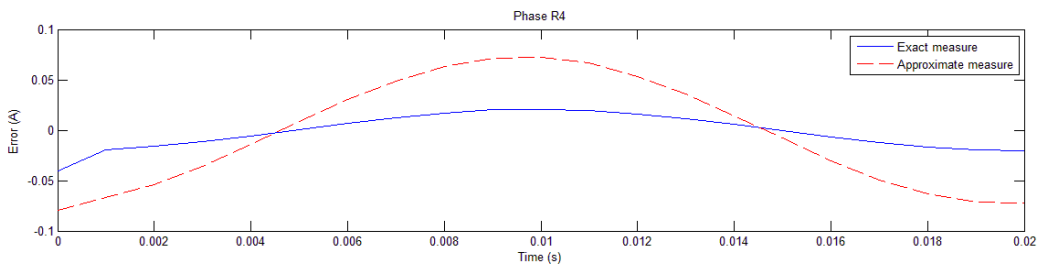
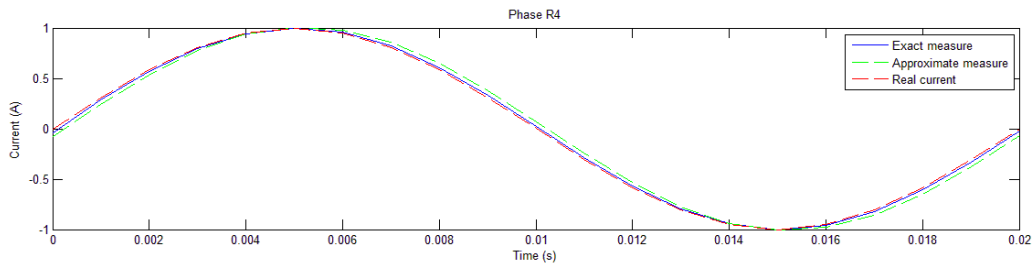
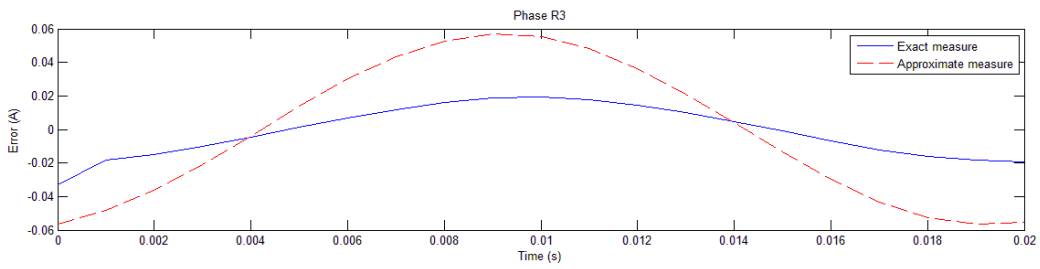
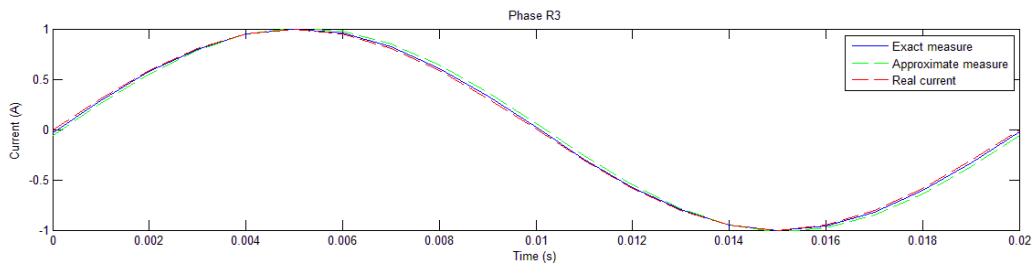
Considerations:

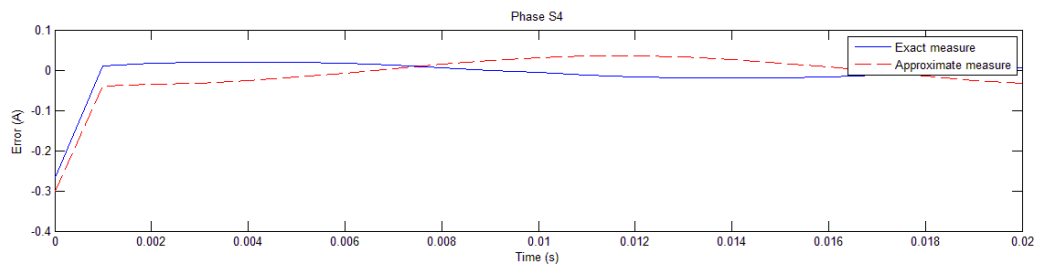
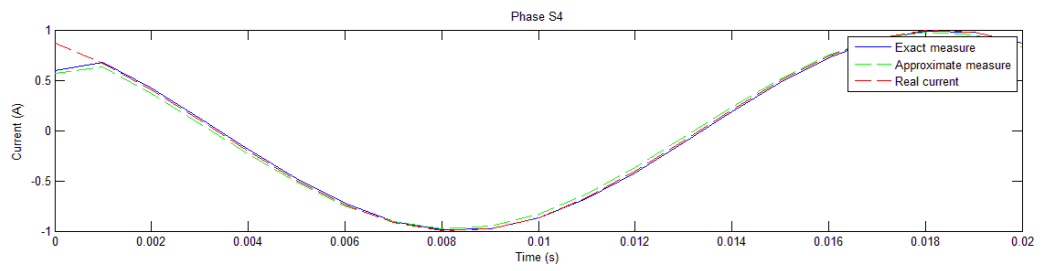
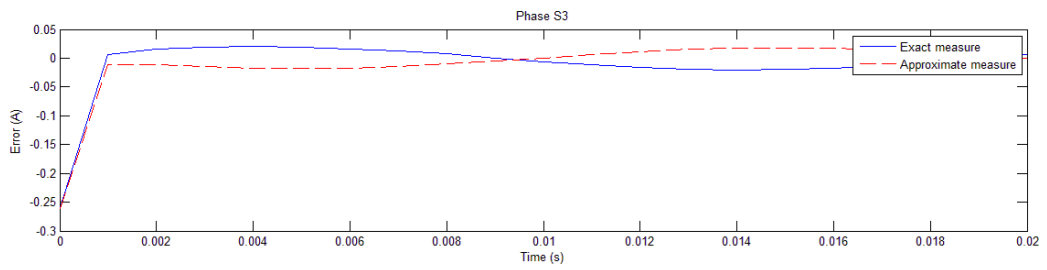
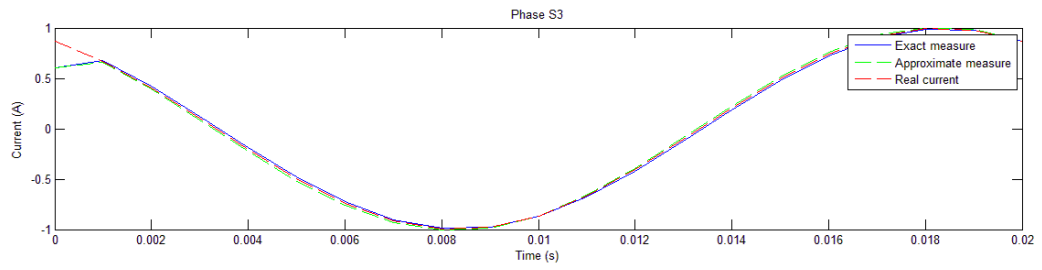
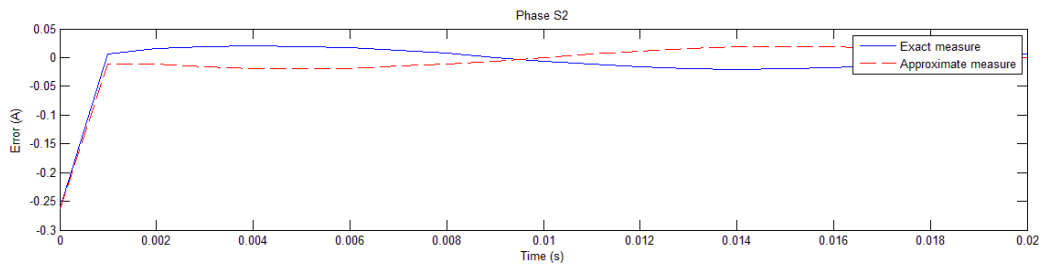
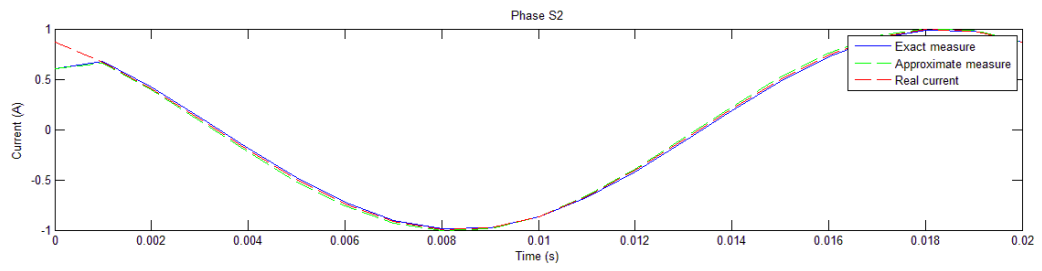
As can be seen in the graphs, the relative error is almost next to zero for every bar (highest error: $e_{max}=1.1\%$ detected on the phase S4) and its report with the input current is constant for every peak current considered.

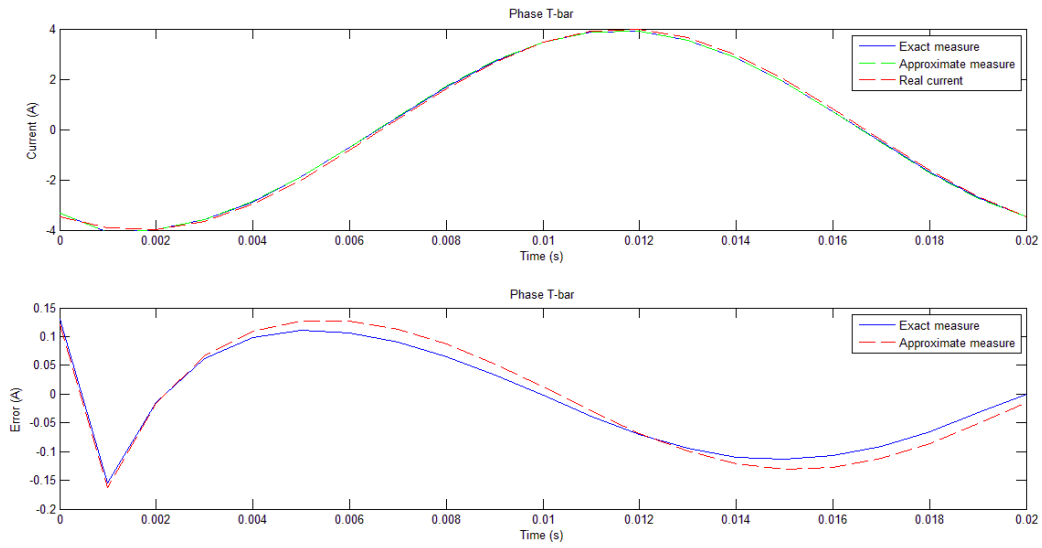
b) CASE CONSIDERING THE MUTUAL INDUCTANCE EFFECT

- PEAK VALUE = 1 [A]









Considerations:

In this case is considered the mutual inductance effect which influences the amount of current flowing through the bars. The effect of this phenomenon it can be seen in the error trends because are a little bit different to the previous case.

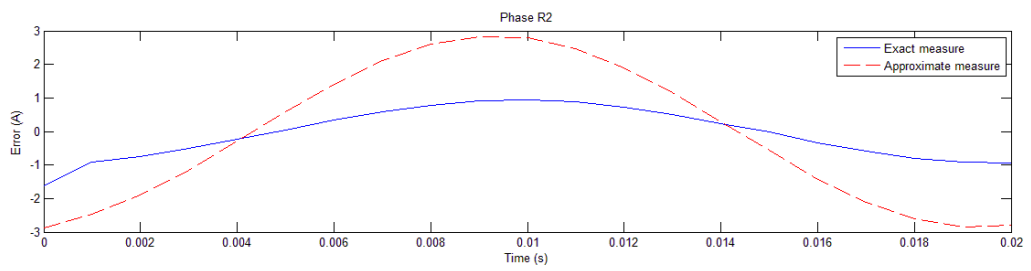
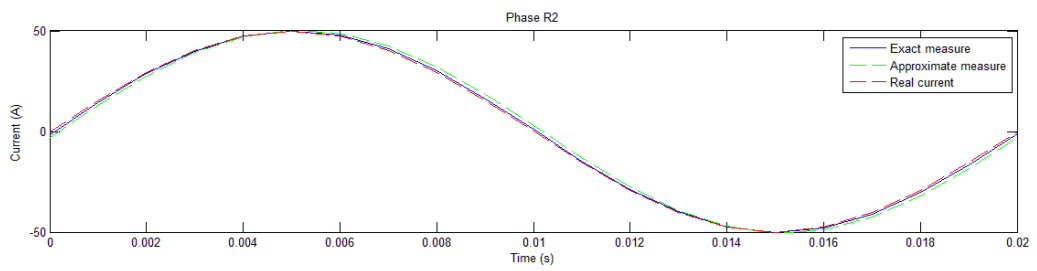
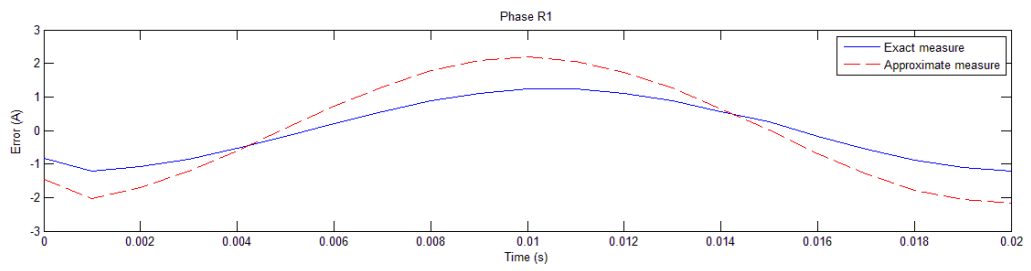
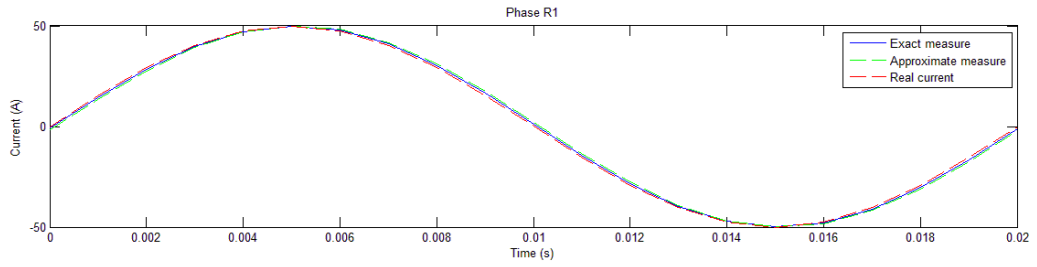
The highest error caused by this fact can be detected on the phase S_4 in the instant time $t=0$ [s]. It has an absolute value of $e_{abs} = 0.2675$.

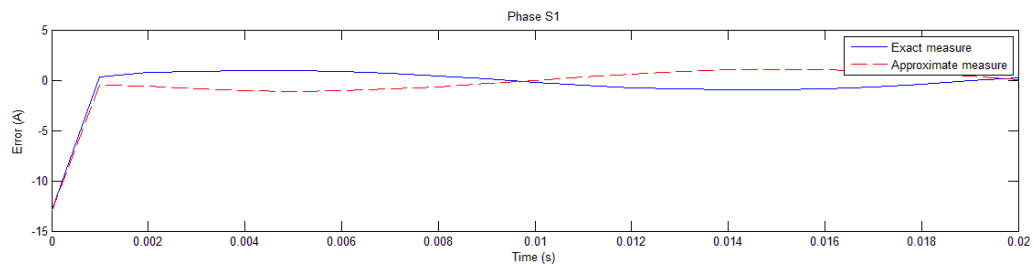
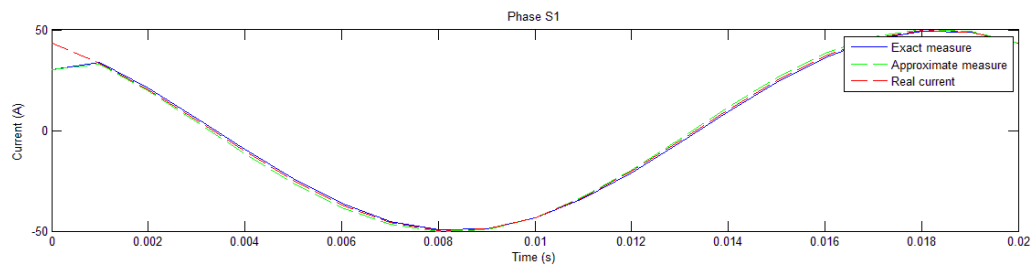
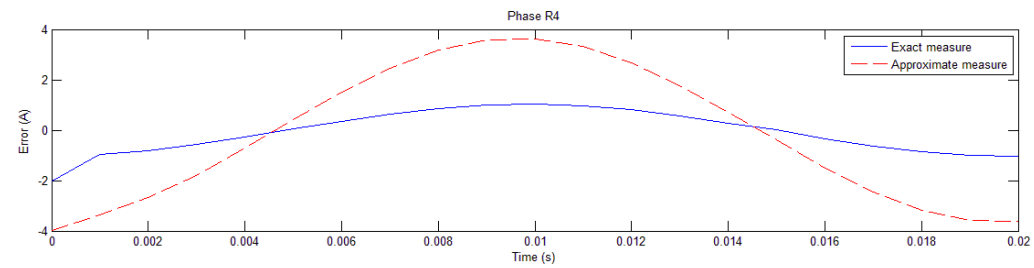
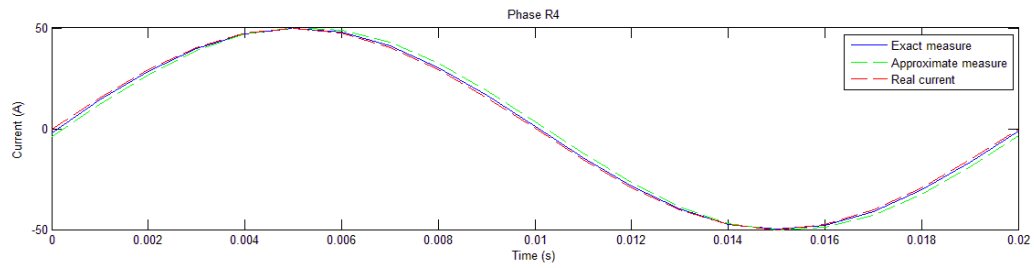
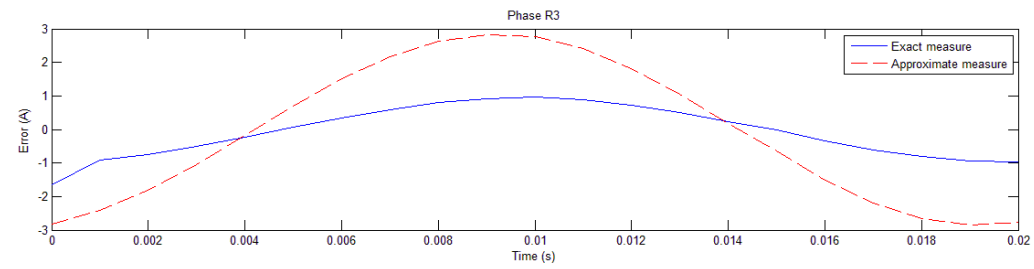
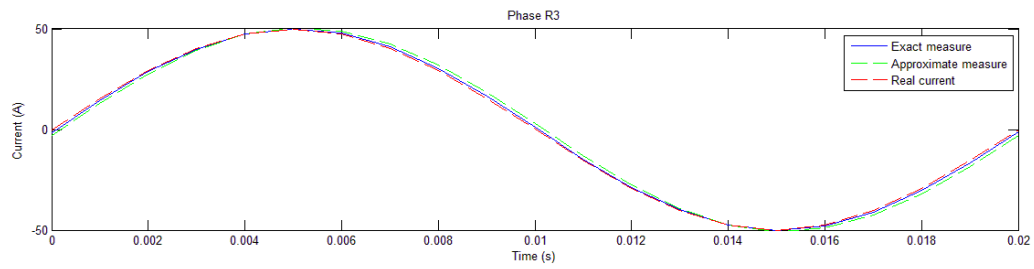
Considering that this value of absolute error is referred to a value of current of $I = 0.866$ [A] the respective relative error will be:

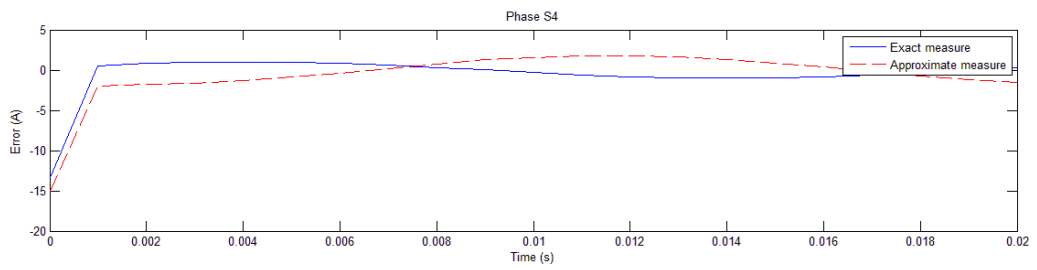
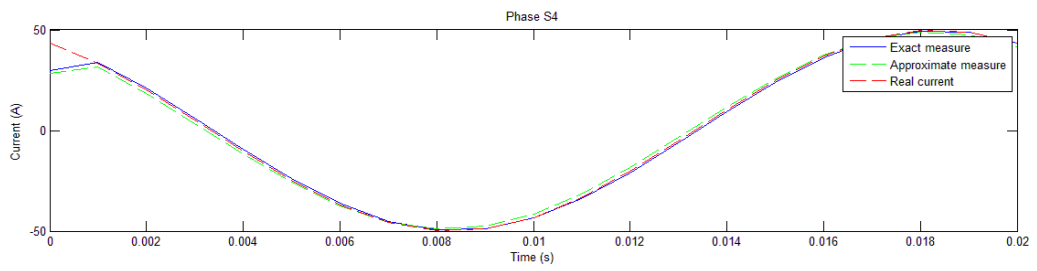
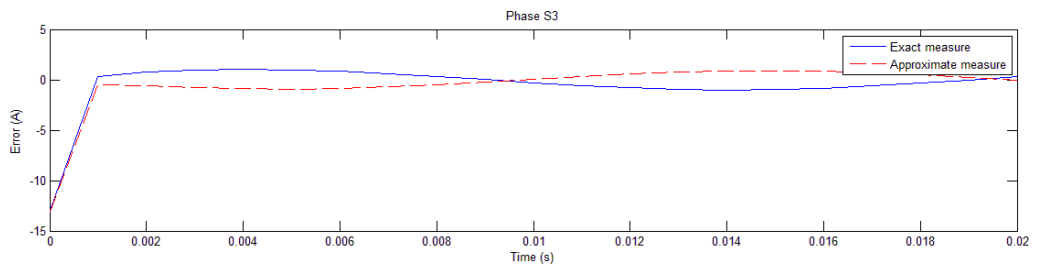
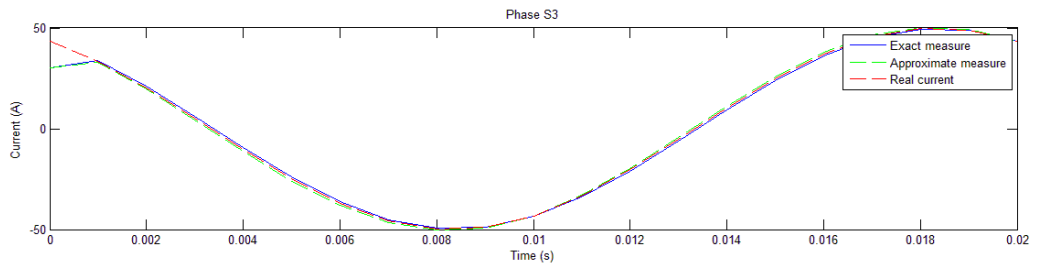
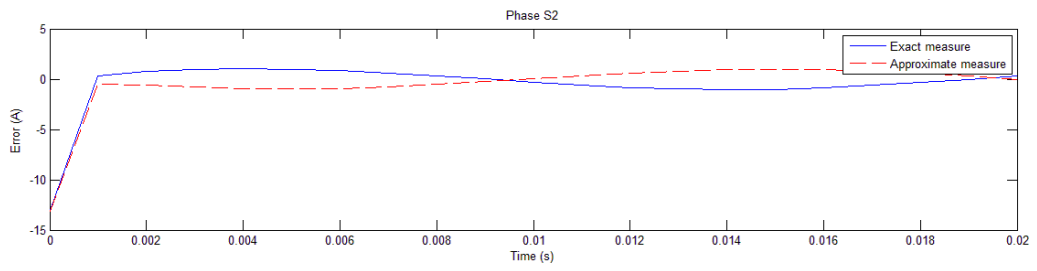
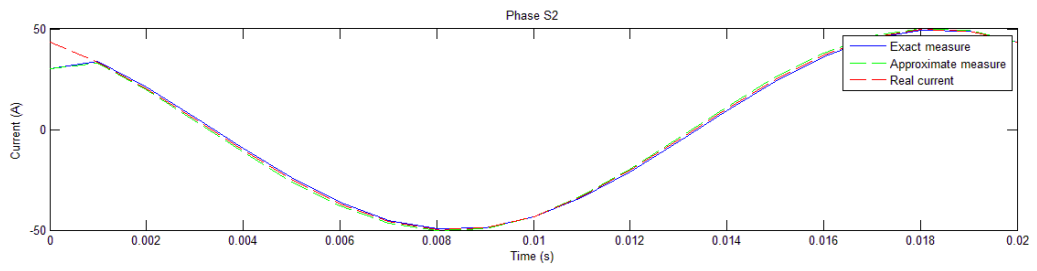
$$e_{rel} = \frac{0.2675}{0.866} 100 = 30.889\%$$

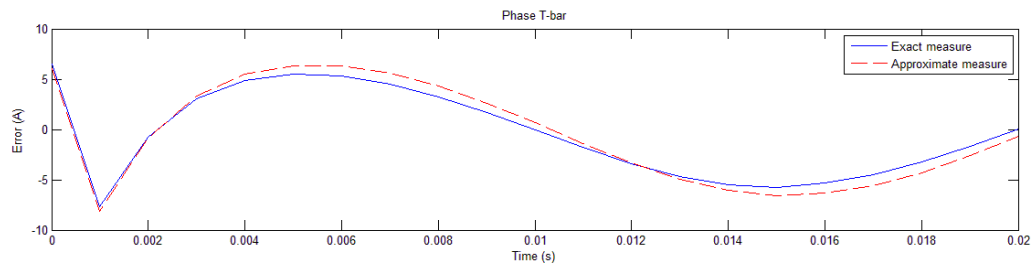
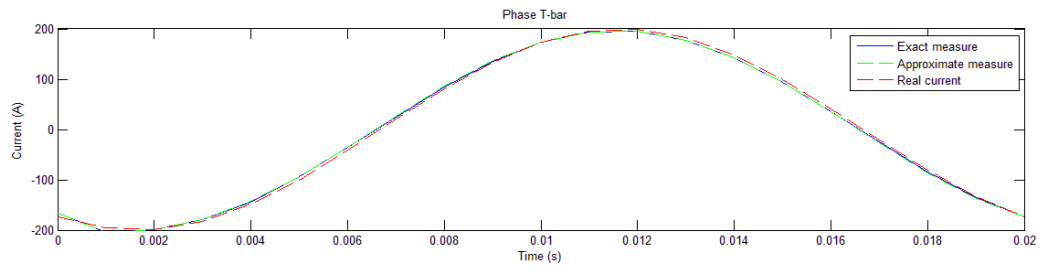
As it will be seen in the next paragraphs it will be possible to eliminate this error with a corrective coefficient applicable only if the error will be proportional to every input current.

➤ **PEAK VALUE = 50 [A]**

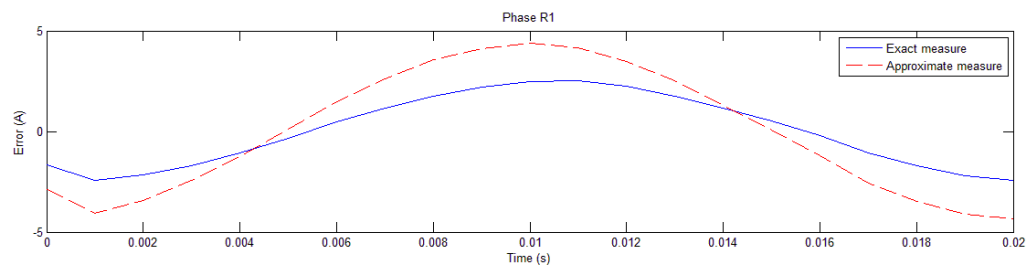
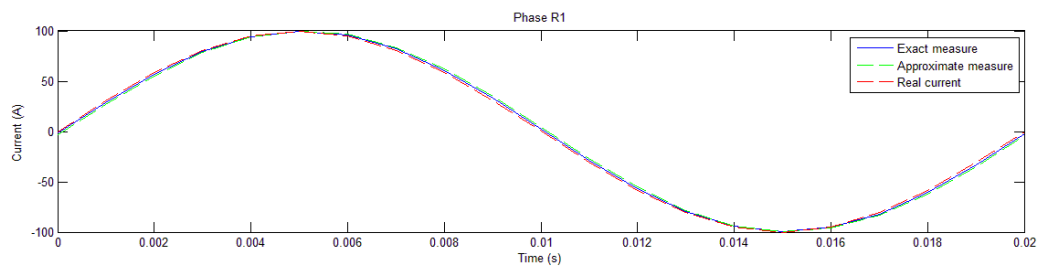


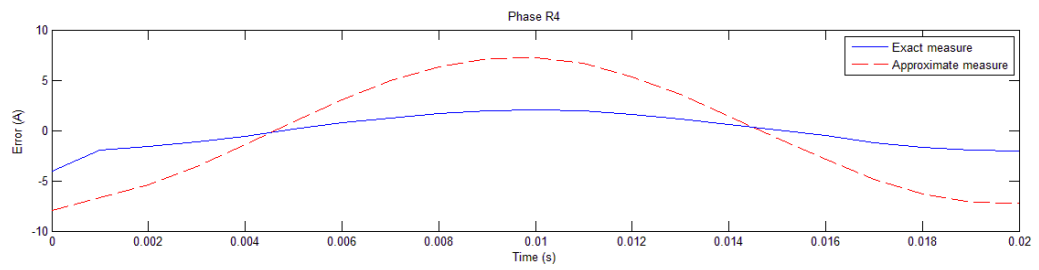
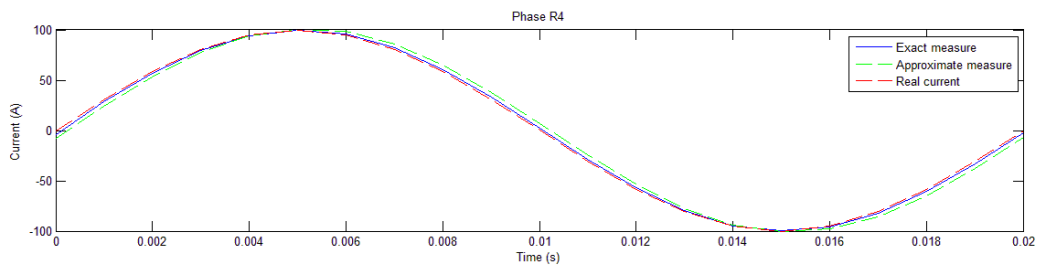
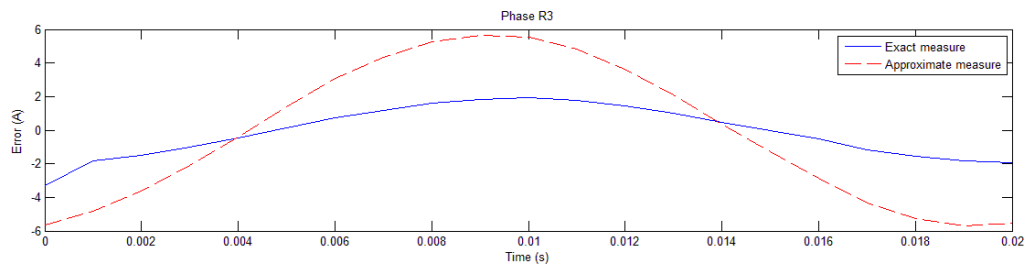
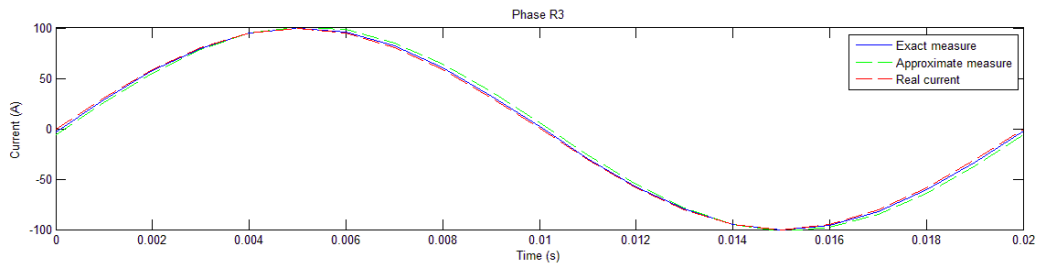
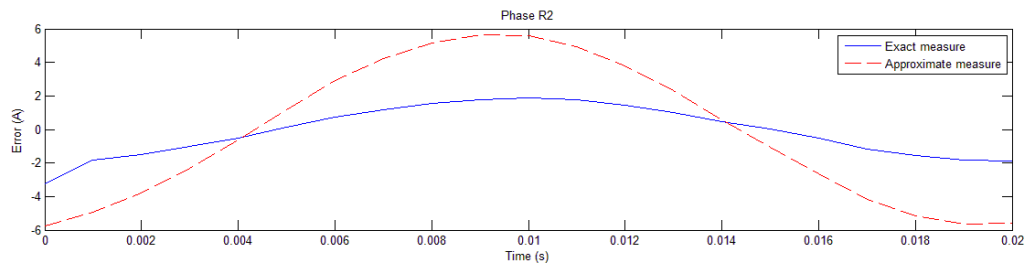
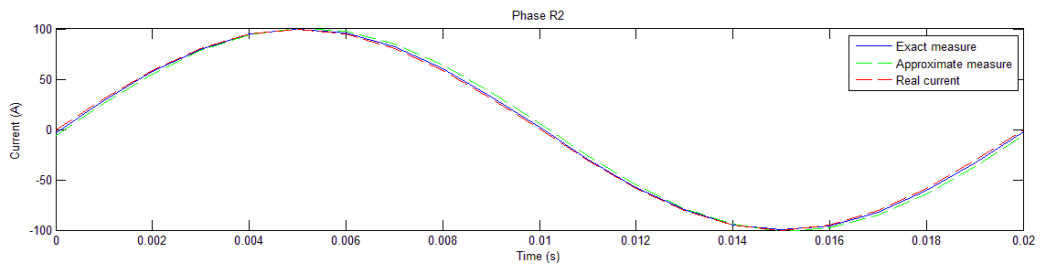


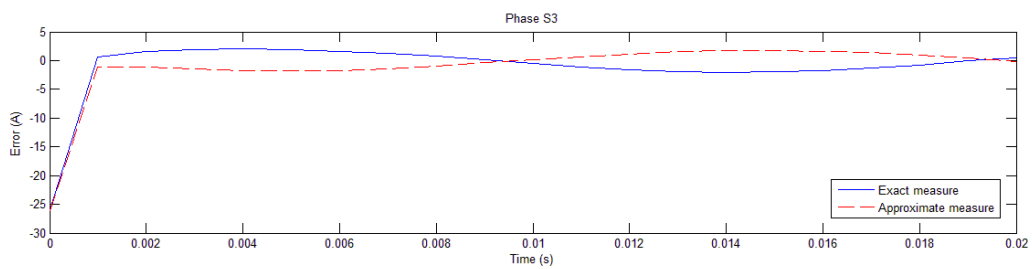
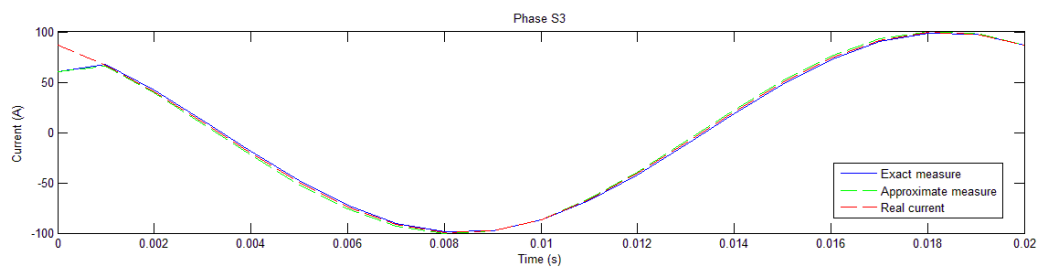
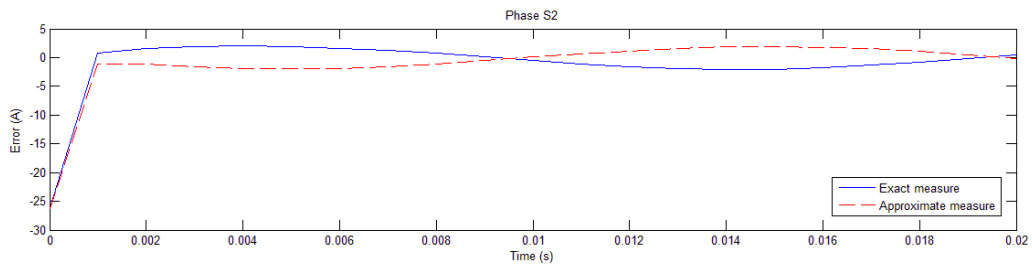
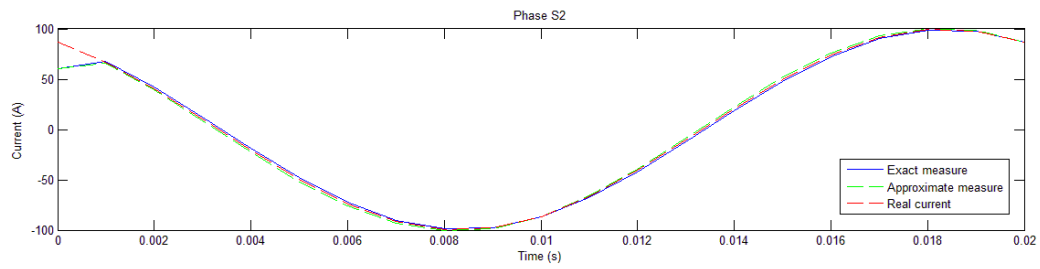
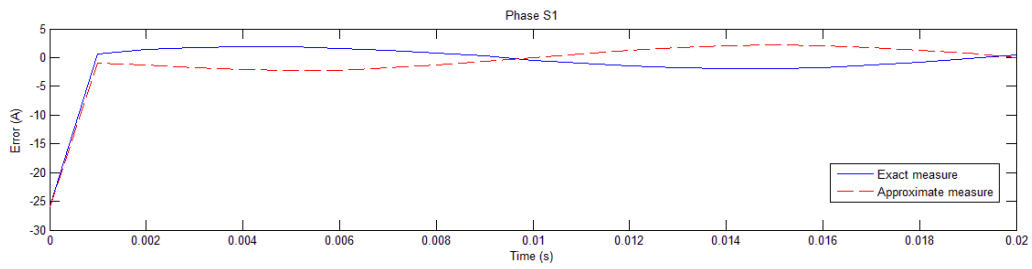
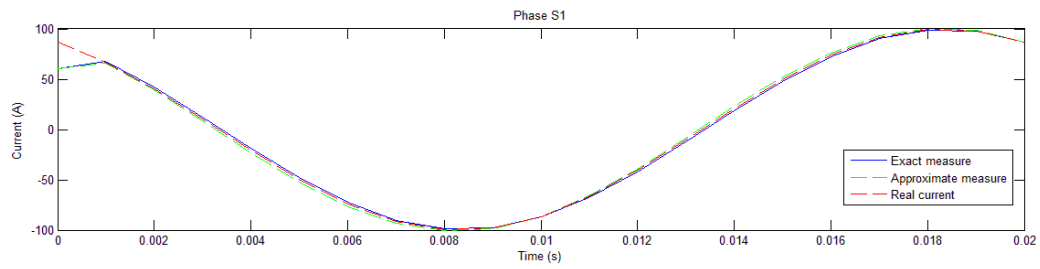


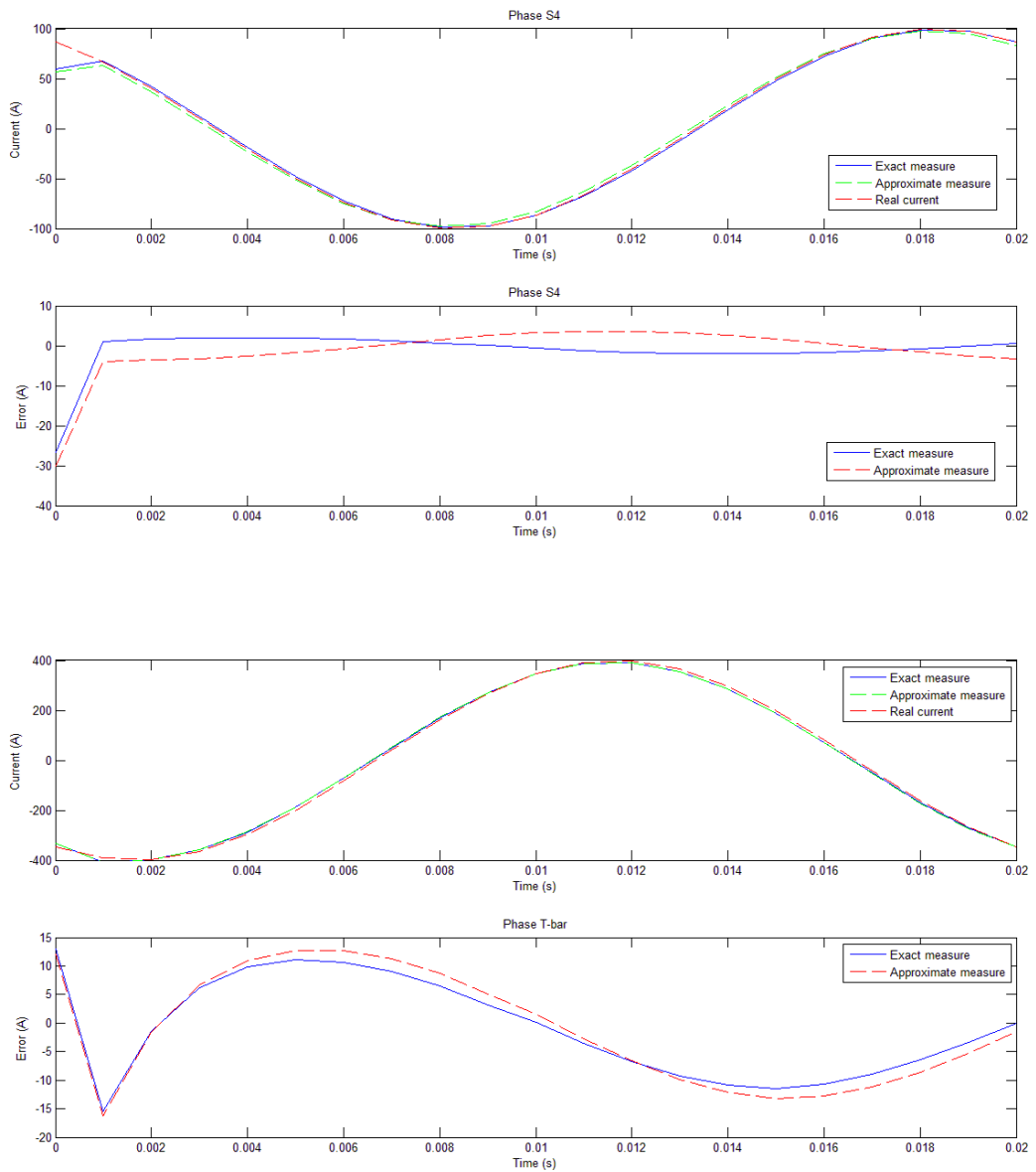


➤ **PEAK VALUE = 100 [A]**









Considerations:

As can be seen in the charts, the development of the error in the time is the same for the three different peak components used for the input current. This points to the fact that may be introduced a corrective factor in the equations in order to correct the errors in the current measurement.

In the next paragraph will be explained how to derive this corrective coefficient and how can correct the eventually measurement errors.

10.2 Corrective coefficients for the measured current

The corrective coefficients into consideration will be grouped in a matrix obtained dividing element by element two arrays of currents, as is shown in the following equation.

$$(9.11) \quad [K]_{corr} = ([I(t)]_{measured}) ./ ([I(t)]_{real})$$

where:

$[K]_{corr}$ = matrix of the corrective coefficients;

$[I(t)]_{measured}$ = array of the measured currents;

$[I(t)]_{real}$ = array of true sinusoidal currents flowing through the bars set with a peak value of 1A.

In the equation [9.11] the division element by element of the arrays has been calculated with a dedicated operator in Matlab. This operator is represented by the symbol “./” and permits to make the division between matrices despite it doesn't exist in the algebra .

Then the implementation in the computing system will be done through the following expression:

$$(9.12) \quad [I(t)]_{correct} = ([I(t)]_{measured}) ./ ([K]_{corr})$$

Where $[I(t)]_{correct}$ is the array of the measured currents corrected with the corrective coefficients matrix.

In the equation [9.12] the division is made element by element.

This will be true for every current and will be implementable in the system only if every element of the matrix $[K]_{corr}$ remains constant with the variation of the input current, initially set with a peak value of 1A to derive the matrix.

An example of corrective coefficients matrix is represented in the next page.

$ K _{corr} =$	inf	0.7029	inf	0.6994	inf	0.7007	inf	0.6911	0.9623
	0.9217	1.0084	0.9408	1.0104	0.9402	1.0101	0.9368	1.0143	1.0394
	0.9632	1.0362	0.9748	1.0397	0.9747	1.0393	0.9727	1.0427	1.0037
	0.979	1.1719	0.9872	1.1843	0.9873	1.1822	0.9859	1.1874	0.9832
	0.9887	0.9068	0.9948	0.9018	0.995	0.903	0.9941	0.9026	0.967
	0.9967	0.9623	1.0011	0.9609	1.0012	0.9614	1.0009	0.9617	0.9448
	1.0046	0.9778	1.0072	0.9774	1.0074	0.9777	1.0074	0.9781	0.8723
	1.014	0.9857	1.0143	0.986	1.0146	0.9862	1.0153	0.9866	1.216
	1.0301	0.9921	1.0267	0.9928	1.0271	0.9929	1.0287	0.9933	1.0399
	1.0736	0.9988	1.0598	0.9999	1.0606	0.9999	1.0647	1.0004	1.0126
	inf	1.0096	inf	1.0099	inf	1.0124	inf	0.6911	0.9623
	0.9193	1.0157	0.9425	1.018	0.9422	1.0178	0.9371	1.0183	0.9902
	0.9619	1.0366	0.9751	1.0404	0.975	1.0399	0.9725	1.0403	0.9823
	0.9781	1.172	0.9875	1.1857	0.9875	1.1834	0.986	1.1837	0.9743
	0.9879	0.9069	0.9949	0.9012	0.995	0.9025	0.9941	0.9031	0.963
	0.9956	0.962	1.0008	0.9604	1.0009	0.961	1.0004	0.9615	0.943
	1.0036	0.9775	1.0069	0.977	1.007	0.9773	1.0071	0.9778	0.8713
	1.0136	0.986	1.0147	0.9861	1.0149	0.9864	1.0156	0.9868	1.2159
	1.0297	0.9924	1.0272	0.9929	1.0275	0.9931	1.0291	0.9936	1.0399
	1.0706	0.9976	1.0589	0.9986	1.0595	0.9987	1.0637	0.9992	1.0123
inf	1.0059	inf	1.0084	inf	1.0095	inf	1.0103	0.9623	

10.2.1 Test of the invariance of the matrix

An important test to do before to implement, in the measuring system, the corrective coefficient is to assure that this coefficient remains constant for every current that can flow through the bars.

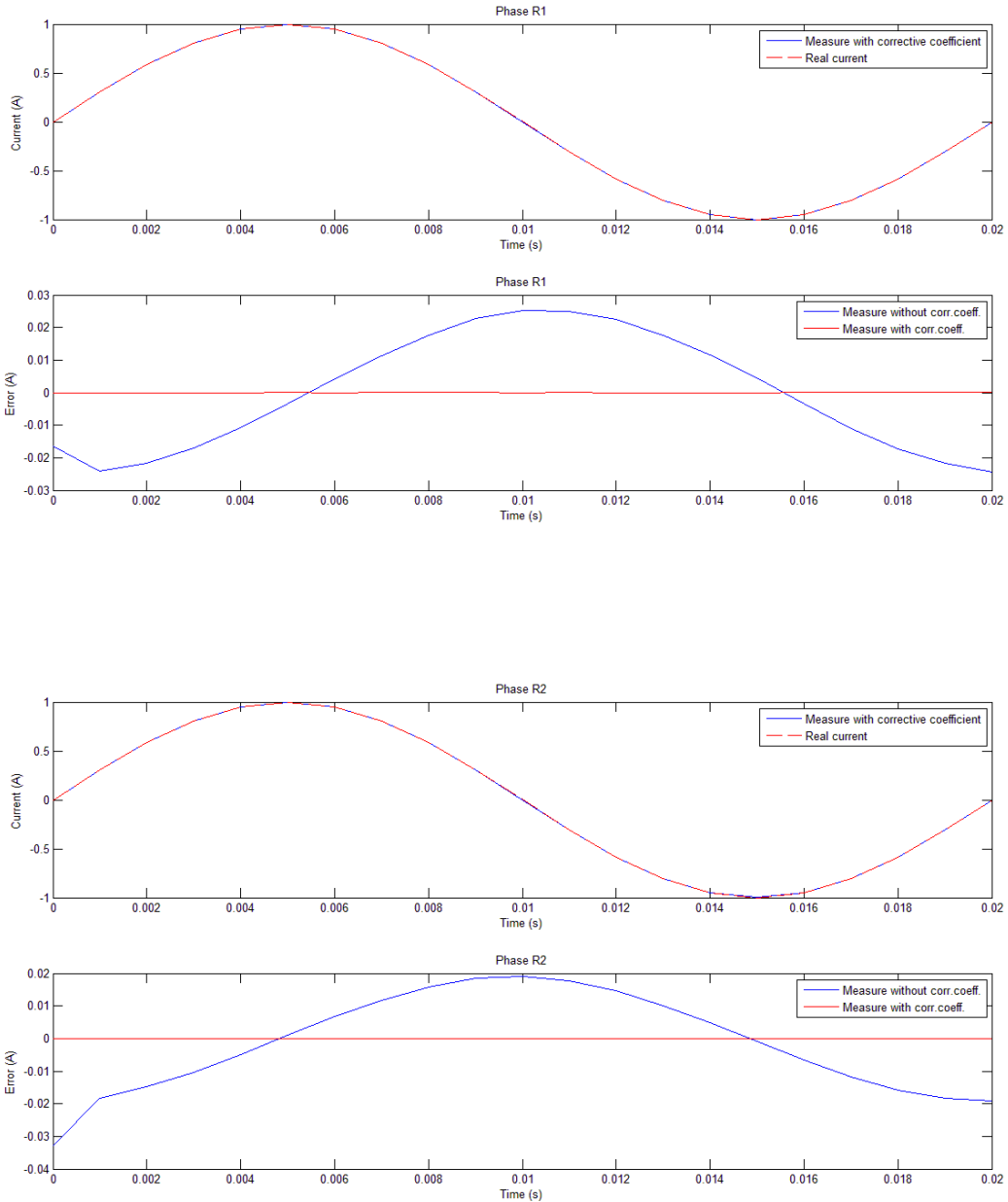
To do this test has been calculated the difference between two corrective coefficients matrices obtained with different input currents. An example of the various tests done is represented in the next matrix, in which was calculated the difference between the corrective coefficient matrix computed with an input current of 50A and the matrix with an input current of 1A:

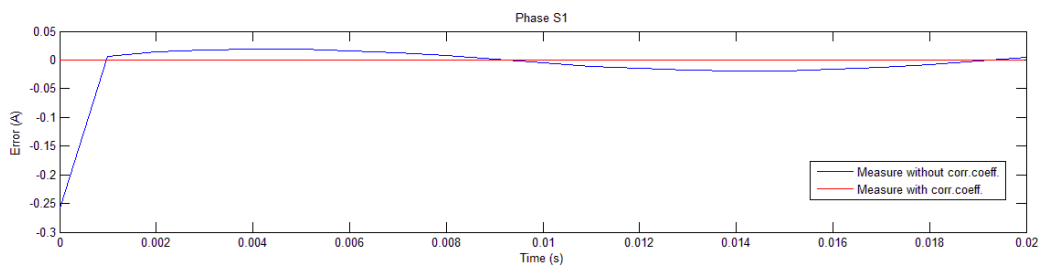
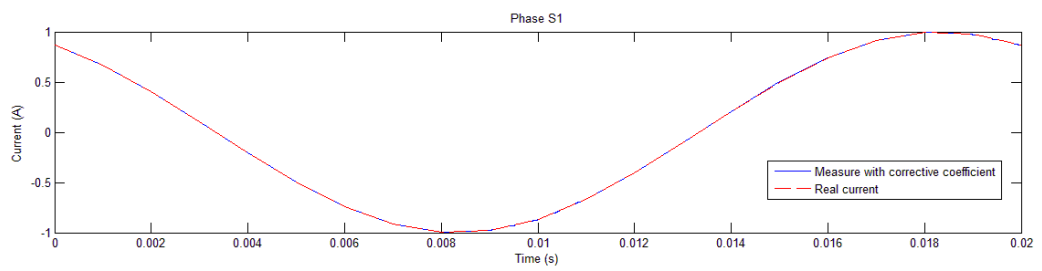
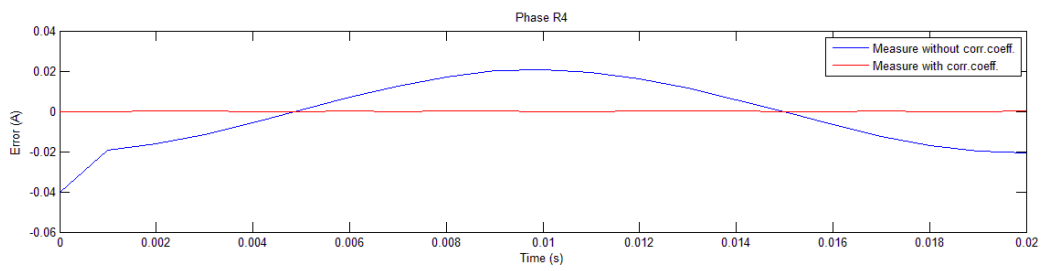
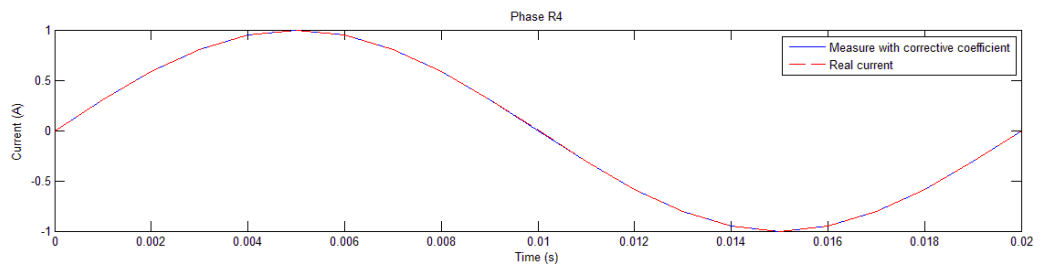
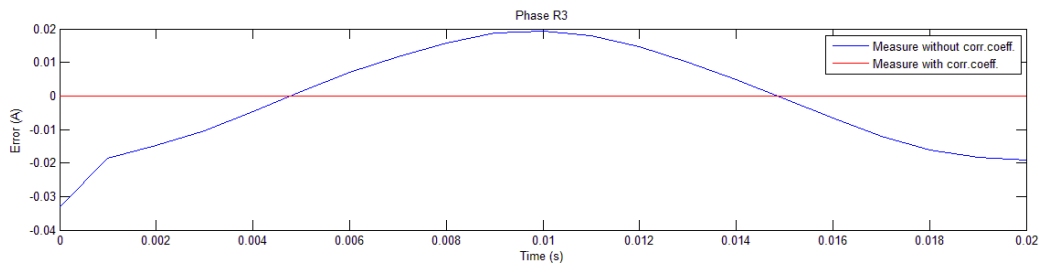
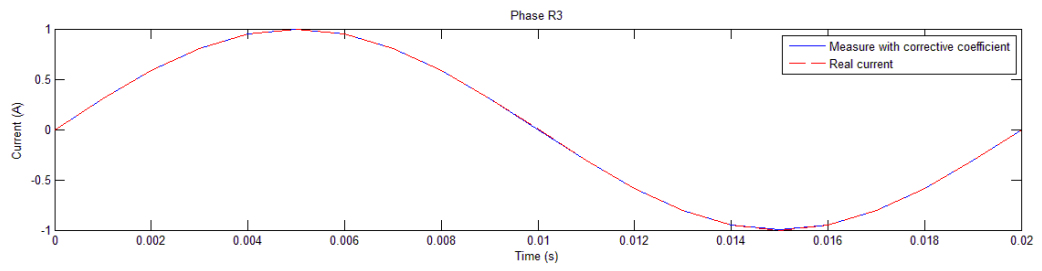
$ K_{corr} _{50A} - K_{corr} _{1A} =$	0.0000	0.0000	0.0000	0.0000	0.0000	0.0000	0.0000	0.0000	0.0000
	0.0001	0.0001	0.0001	0.0001	0.0000	0.0001	0.0000	0.0001	0.0000
	0.0000	0.0000	0.0000	0.0000	0.0000	0.0001	0.0000	0.0000	0.0001
	0.0000	0.0001	0.0000	0.0001	0.0000	0.0000	0.0000	0.0000	0.0000
	0.0001	0.0001	0.0001	0.0001	0.0000	0.0000	0.0000	0.0000	0.0000
	0.0000	0.0000	0.0000	0.0001	0.0001	0.0001	0.0000	0.0001	0.0003
	0.0003	0.0003	0.0003	0.0002	0.0002	0.0001	0.0001	0.0001	0.0002
	0.0001	0.0001	0.0001	0.0001	0.0000	0.0001	0.0001	0.0001	0.0001
	0.0003	0.0002	0.0001	0.0001	0.0002	0.0001	0.0002	0.0002	0.0001
	0.0014	0.0010	0.0010	0.0010	0.0012	0.0010	0.0010	0.0010	0.0001
	0.0000	0.0000	0.0000	0.0000	0.0000	0.0000	0.0000	0.0000	0.0000
	0.0002	0.0005	0.0001	0.0005	0.0001	0.0005	0.0001	0.0005	0.0006
	0.0002	0.0001	0.0001	0.0001	0.0001	0.0002	0.0001	0.0002	0.0005
	0.0000	0.0000	0.0001	0.0000	0.0000	0.0000	0.0001	0.0001	0.0000
	0.0002	0.0001	0.0001	0.0001	0.0001	0.0002	0.0001	0.0001	0.0002
	0.0005	0.0004	0.0006	0.0004	0.0006	0.0005	0.0005	0.0005	0.0004
	0.0004	0.0003	0.0003	0.0003	0.0004	0.0004	0.0004	0.0003	0.0005
	0.0000	0.0000	0.0000	0.0001	0.0000	0.0000	0.0000	0.0001	0.0003
	0.0003	0.0003	0.0003	0.0003	0.0003	0.0003	0.0003	0.0003	0.0001
	0.0011	0.0008	0.0010	0.0008	0.0010	0.0007	0.0009	0.0007	0.0002
0.0000	0.0000	0.0000	0.0000	0.0000	0.0000	0.0000	0.0000	0.0000	

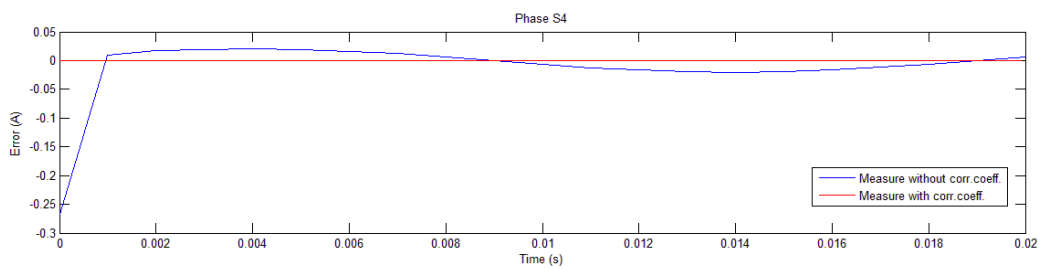
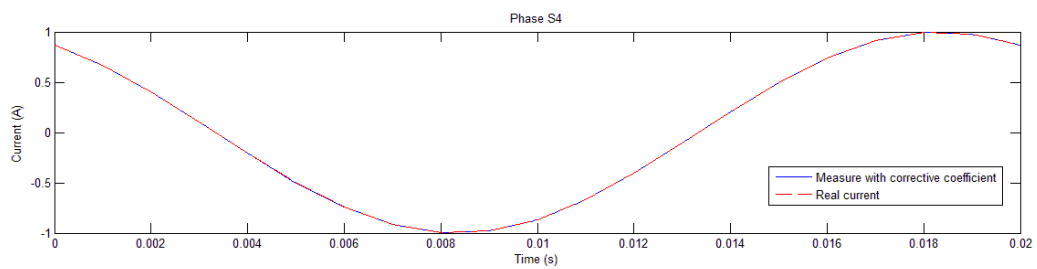
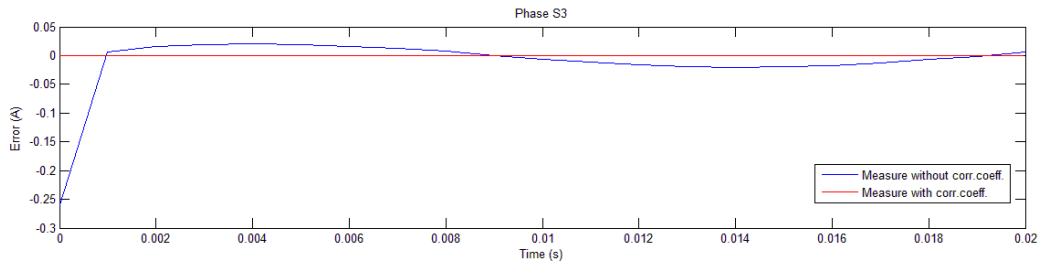
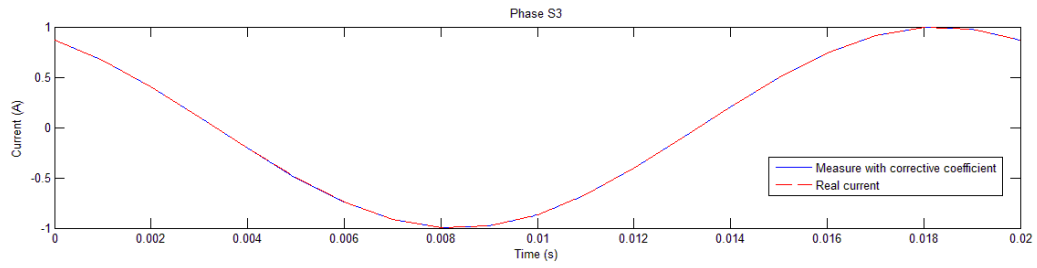
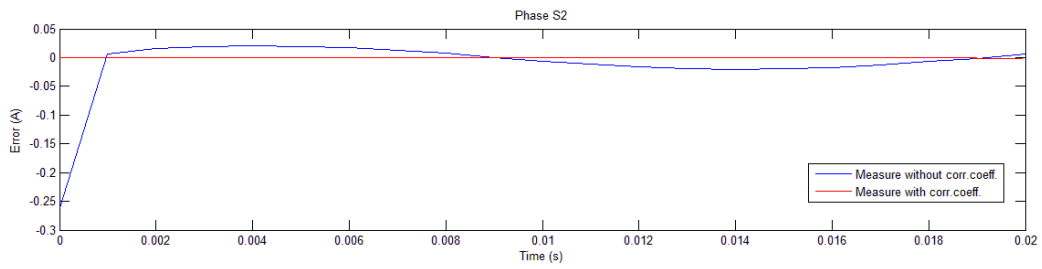
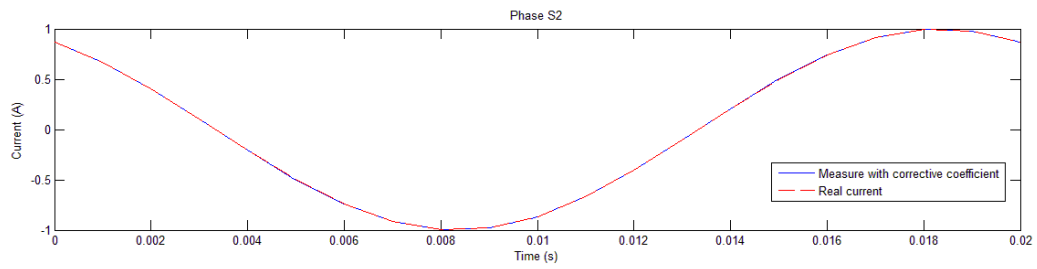
As can be seen, the difference between the two matrices obtained with different currents is next to zero and thus it means that the various corrective coefficients remain constants for different input currents.

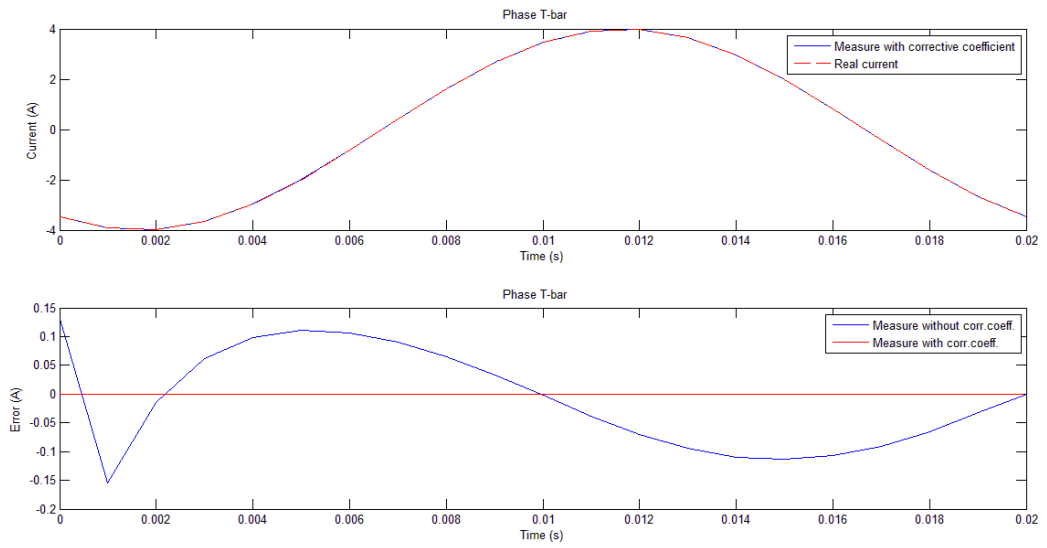
10.2.2 Results with the corrective coefficient

The following graphs show the trends of currents and errors with the implementation of the corrective coefficients matrix. These trends are compared with the trends of the true currents that flow through the bars and also with the errors trends obtained without the use of the corrective coefficients matrix.









Considerations:

In the preceding graphs it's possible to note that with the implementation of the corrective coefficients matrix the error in the measure will be zero for every phase-bar considered.

This consideration is valid also for other input currents as can be seen in the following graphical example, so in this way a perfect virtual measure system for the monitoring of the currents flowing through the bars has been obtained.

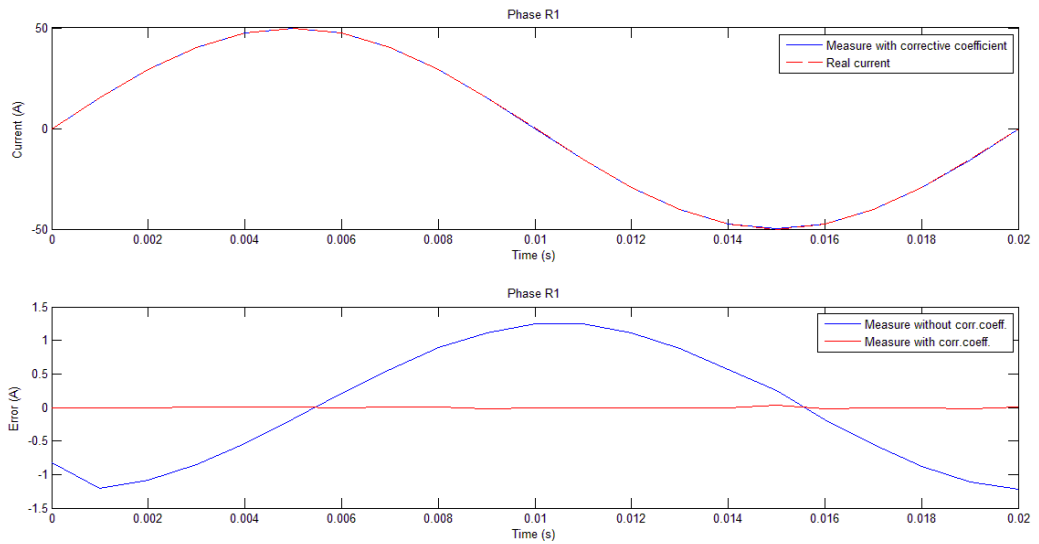


Fig. 10.1 Trends of currents and errors, case with corrective coefficient. Phase R₁, $I_{peak,input} = 50 A$.

10.3 A particular case: unbalanced electrical system

In this paragraph will be taken into consideration the same system of the previous paragraphs but subject to unbalanced input currents for the phases R, S, T of every circuit.

This implies that we have to consider also a current that flows in the neutral bar. This current will be obtained making the vector sum of all the currents flowing in all the circuits.

For this case, characterized by an unbalanced system, will be completely described only the results for the cases considering the mutual inductance effects.

The respected value of input currents set for the different circuits are:

$$\begin{array}{l|l}
 \dot{i}(t)_{R1} = I_{r1} \sin(2\pi 50 t) & I_{r1} = 10 [A] \\
 \dot{i}(t)_{R2} = I_{r2} \sin(2\pi 50 t) & I_{r2} = 30 [A] \\
 \dot{i}(t)_{R3} = I_{r3} \sin(2\pi 50 t) & I_{r3} = 40 [A] \\
 \dot{i}(t)_{R4} = I_{r4} \sin(2\pi 50 t) & I_{r4} = 50 [A] \\
 \dot{i}(t)_{S1} = I_{s1} \sin(2\pi 50 t + 2\pi / 3) & I_{s1} = 12 [A] \\
 \dot{i}(t)_{S2} = I_{s2} \sin(2\pi 50 t + 2\pi / 3) & I_{s2} = 32 [A] \\
 \dot{i}(t)_{S3} = I_{s3} \sin(2\pi 50 t + 2\pi / 3) & I_{s3} = 42 [A] \\
 \dot{i}(t)_{S4} = I_{s4} \sin(2\pi 50 t + 2\pi / 3) & I_{s4} = 51 [A]
 \end{array}$$

Where I_{r1}, \dots, I_{s4} are the peak values of the alternative currents considered.

To impose the current that flows into the neutral bar it was used the expression:

$$\mathbf{I}_N = - \left(\sum_{n=1}^4 \mathbf{I}_{Rn} + \sum_{n=1}^4 \mathbf{I}_{Sn} + \sum_{n=1}^4 \mathbf{I}_{tn} \right)$$

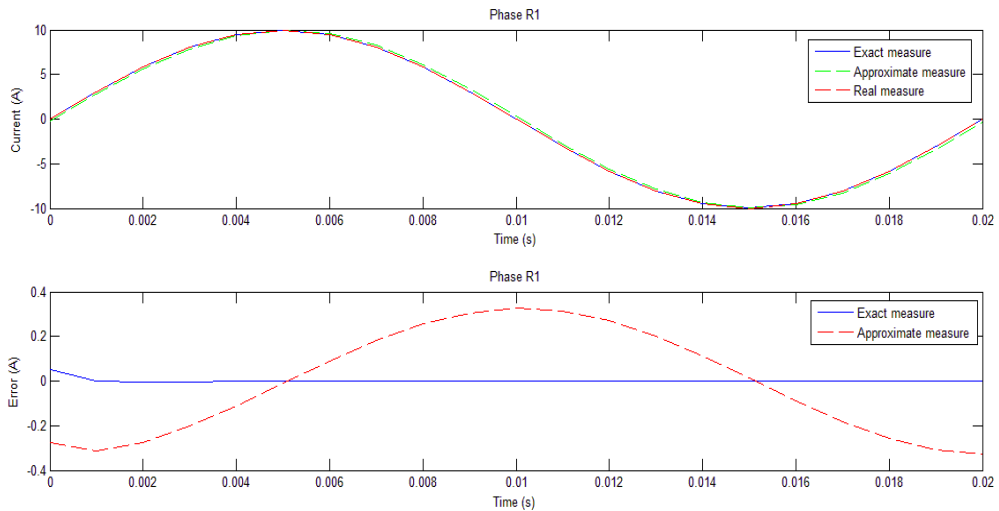
For the impossibility to consider the T bars in the present 2D study, the current flowing in the neutral bar will be considered without the \mathbf{I}_t terms. To solve the problem considering also the T sensors and the \mathbf{I}_t current will be necessary to make a 3D study.

Also for the unbalanced electrical system has been analysed the cases neglecting and considering the mutual inductance effects, as it can be seen in the next page.

a) CASE NEGLECTING THE MUTUAL INDUCTANCE EFFECT

For this particular case will not be included the graphs regarding the case neglecting the mutual inductance effect because it will not have a practical interest. Anyway, summarizing the results, it has been noted inspecting the graphs that, like in the balanced system, the error is almost next to zero for every sensor considered but is necessary the use of a corrective coefficient.

A graphical example of this case it can be the following.

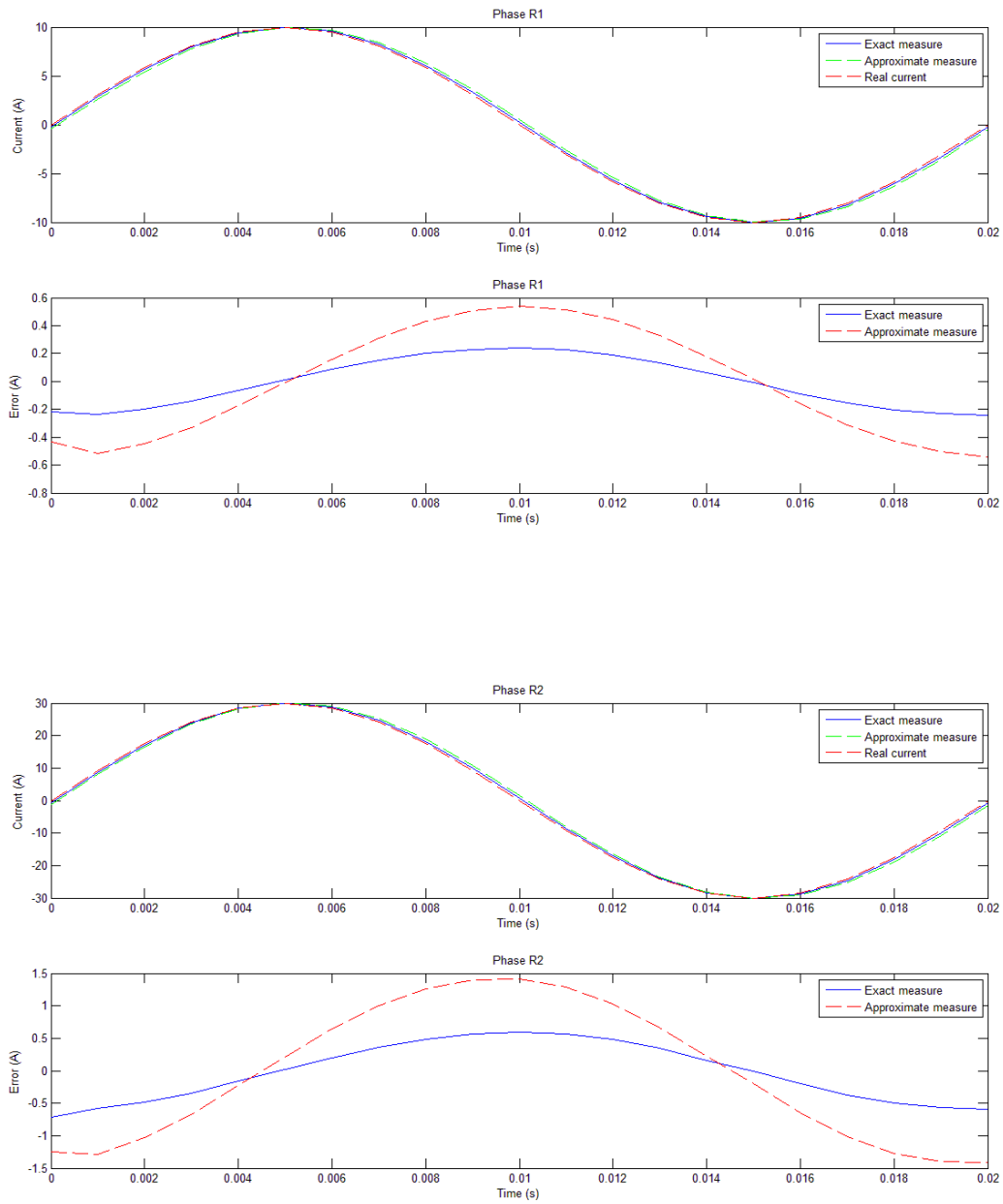


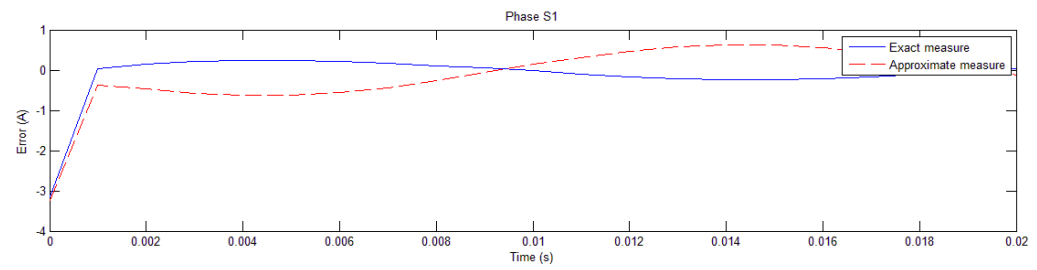
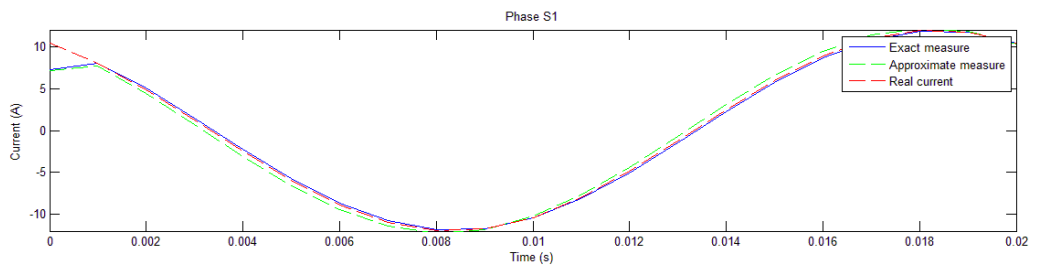
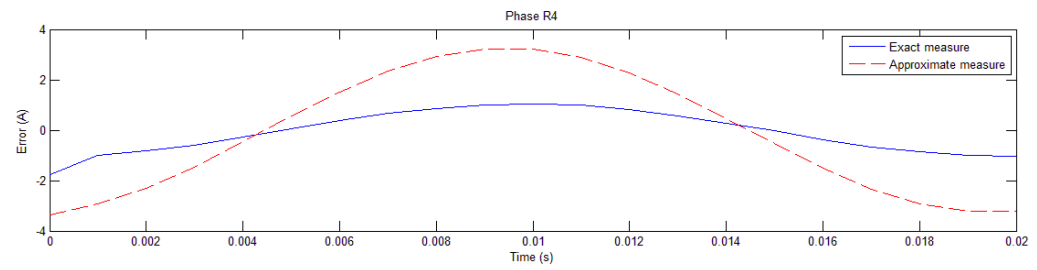
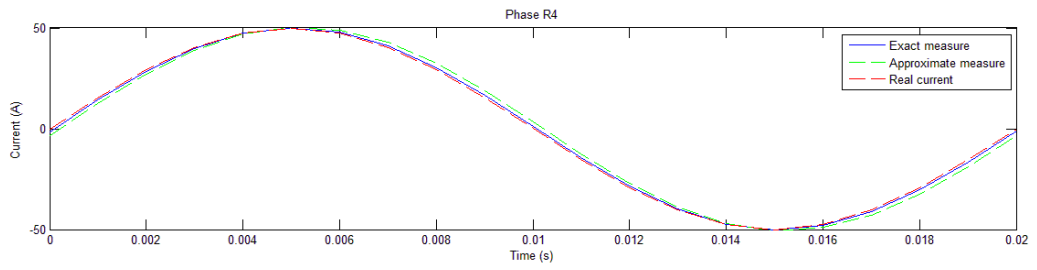
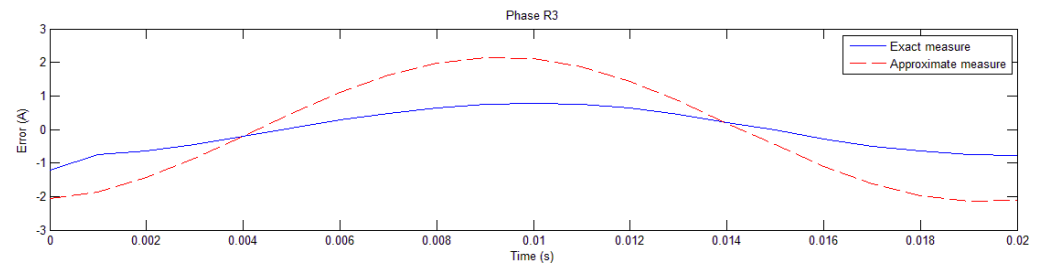
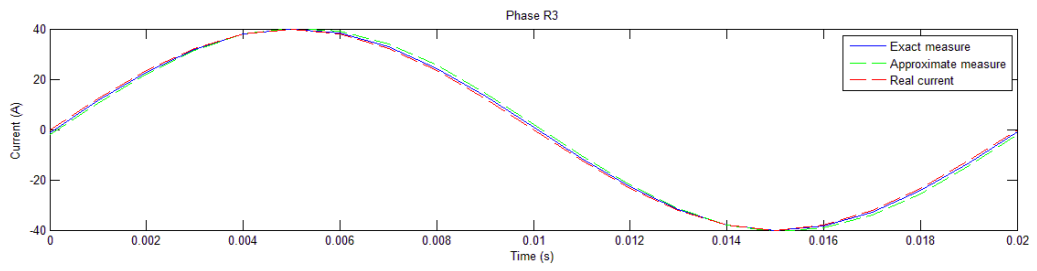
b) CASE CONSIDERING THE MUTUAL INDUCTANCE EFFECT

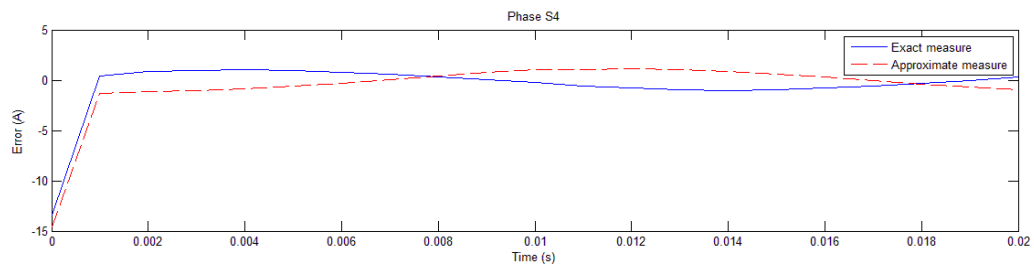
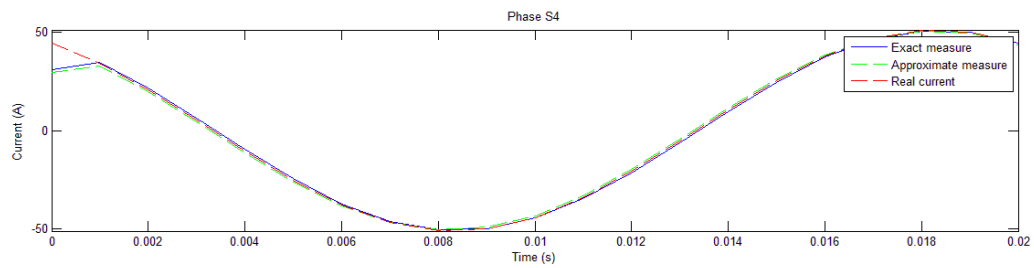
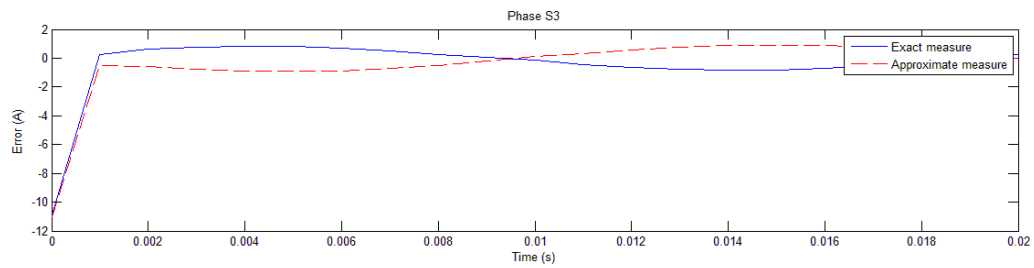
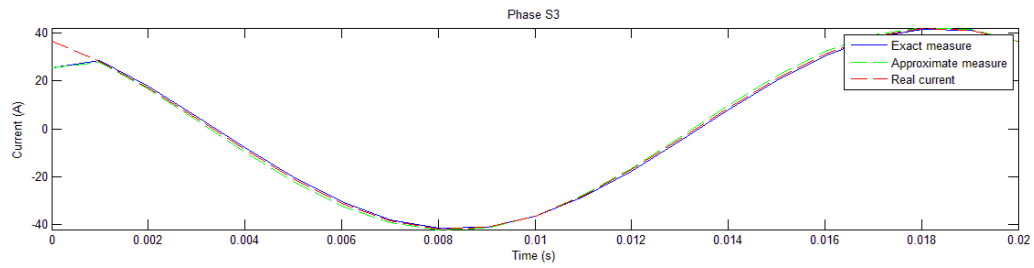
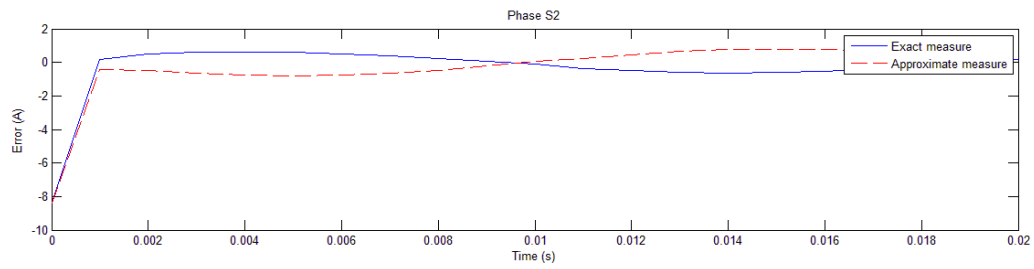
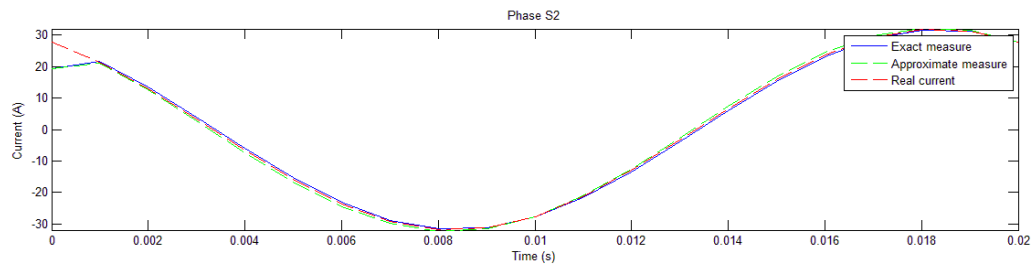
The array $[B(t)]$ used for the computing of the results was:

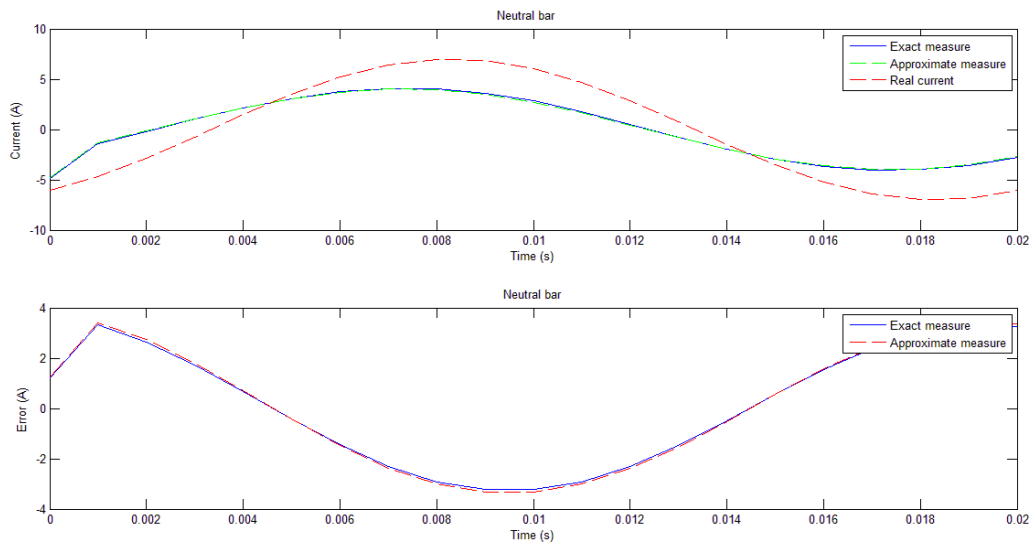
	R1	S1	R2	S2	R3	S3	R4	S4	N
$T_{ime} [s]$ 0	-14.029	232.22	-40.35	627.38	-67.211	822.61	-109.33	960.28	-59.984
0.001	83.413	248.42	259.18	681.4	340.61	894.21	407.01	1064.6	-15.872
0.002	176.19	143.16	538.68	406.68	716.19	535.28	879.35	637.27	-1.4902
0.003	251.8	22.117	765.78	87.581	1022	117.89	1265.6	140.18	13.38
0.004	302.91	-101.24	918.36	-240.5	1228.3	-311.59	1528.6	-371.2	27.037
0.005	324.16	-214.76	980.44	-545.18	1313.6	-710.76	1641	-846.43	38.41
0.006	313.69	-307.24	946.59	-796.46	1270.4	-1040.3	1592.7	-1238.7	46.382
0.007	272.54	-369.66	820.16	-969.79	1102.9	-1268.1	1388.7	-1509.8	50.133
0.008	204.65	-395.81	613.29	-1048	827.26	-1371.4	1048.5	-1632.7	49.252
0.009	116.67	-382.9	346.21	-1022.7	470.4	-1339.4	605.42	-1594.4	43.765
0.01	17.502	-332.56	45.927	-897.49	68.4	-1176.4	104.16	-1400.3	33.893
0.011	-83.489	-250.56	-259.19	-686.82	-340.74	-901.46	-407.82	-1072.9	20.751
0.012	-176.28	-143.35	-538.82	-407.07	-716.38	-535.85	-879.76	-637.62	5.5844
0.013	-251.91	-22.161	-766.01	-87.631	-1022.3	-117.98	-1266	-140.13	-10.139
0.014	-302.94	101.22	-918.39	240.49	-1228.4	311.56	-1528.7	371.25	-24.491
0.015	-323.99	214.65	-979.88	544.91	-1312.9	710.4	-1640	846.02	-36.633
0.016	-313.71	307.25	-946.63	796.48	-1270.4	1040.3	-1592.8	1238.8	-45.191
0.017	-272.57	369.69	-820.25	969.89	-1103	1268.2	-1388.9	1509.9	-49.329
0.018	-204.67	395.83	-613.34	1048	-827.31	1371.5	-1048.6	1632.8	-48.689
0.019	-116.72	383.06	-346.36	1023.1	-470.6	1339.9	-605.68	1595	-43.388
0.02	-17.5	333.15	-45.907	899.09	-68.379	1178.5	-104.15	1402.8	-33.706

10.3.1 Graphical results









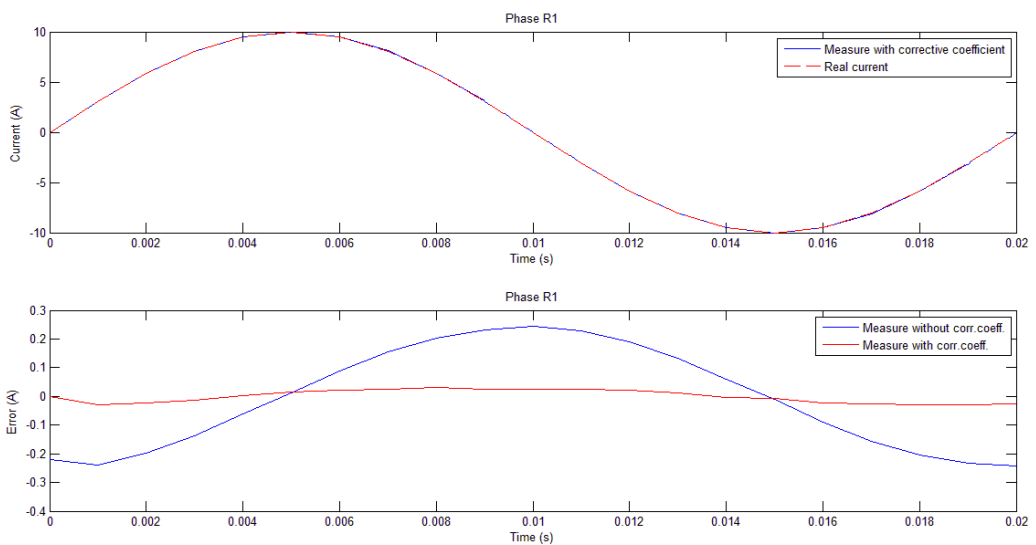
Considerations:

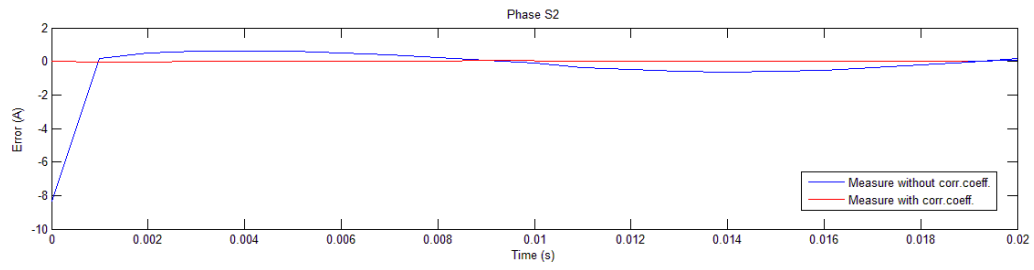
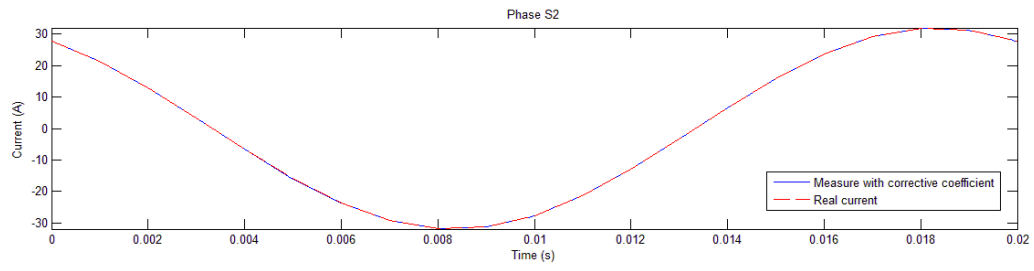
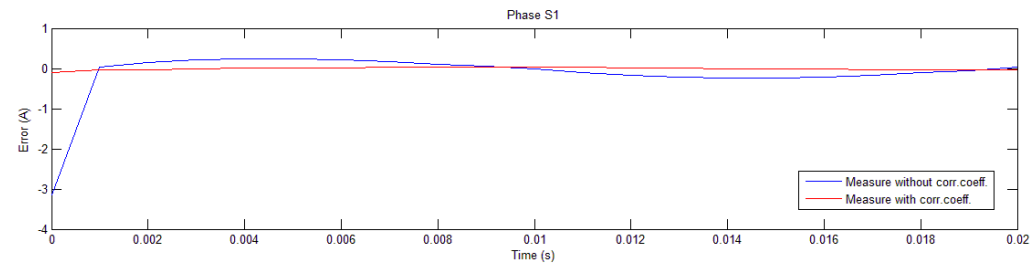
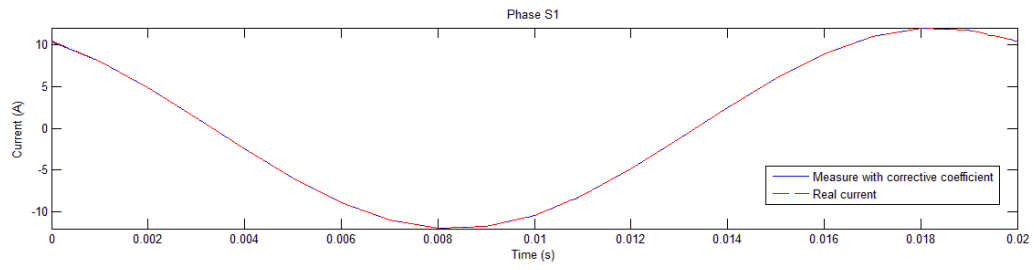
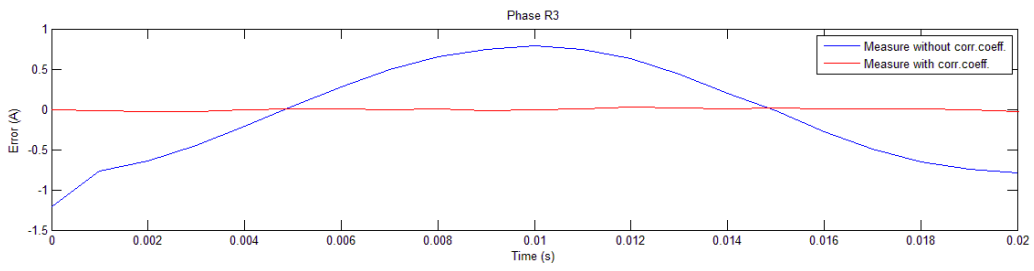
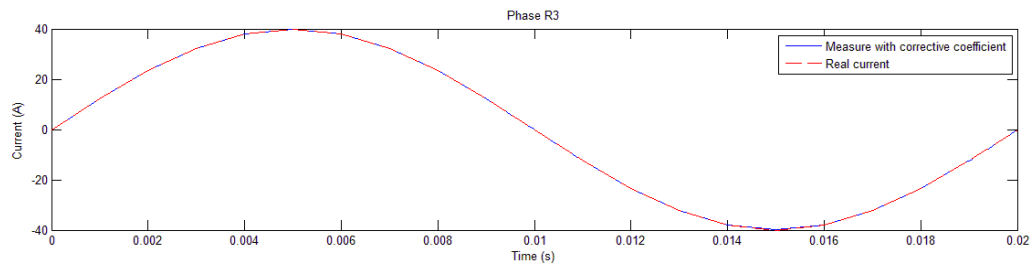
In these graphs is possible to identify a large diffusion of measurement errors, therefore, will be necessary the integration of a corrective coefficient in order to obtain an exact measure of the current, as it was explained in the paragraph [10.2].

10.3.2 Results with the implementation of a corrective coefficient

As in the previous case (paragraph 10.2.2), with the implementation of a corrective coefficient is possible to make a correction in the measurement system in order to obtain a perfect measurement of the current.

In the next graphs are reported some example of current and error trends considering the implementation of the corrective coefficients matrix.





Considerations:

In the previous graphs it's possible to ascertain that with the implementation of the corrective coefficients matrix the error in the measures will be almost zero for every bar considered.

Therefore, it has been reached, with the implementation of the corrective coefficients matrix, a good virtual monitoring system for the currents minimising the measurement errors.

10.4 Second disposition of measurement sensors

An observation to do for this plane of measure is that it will not possible the study of an eventually unbalanced system because in this cut plane is not present the neutral bar.

To not overfill the document with graphs and matrices will be take into account only the main important cases of the study, not reporting for example all the graphs obtained with the study but only a final comment about them.

It will be important, for example, focalize the document to the cases that consider the mutual inductance effect because represent more likely the real subject of study.

For this reason, the cases in which is neglected the mutual inductance effect will be not shown. For these cases, the main conclusions obtained have been:

- By comparing the two **K** matrices it was found that, such as in the paragraph [10.1.1], the two matrices are equal for the fact that in the steady-state there are not present effects of mutual inductance;
- Regarding the graphical solutions, the error is very next to zero and is not necessary the implementation of a corrective coefficient.

10.4.1 K matrix

a) CASE CONSIDERING THE MUTUAL INDUCTANCE EFFECT

With this disposition of sensors will be taken into account also the sensors for the T-bars and so the **K** matrix obtained will be a 12x12 size matrix.

All the values of the matrix elements are expressed in [μT].

		ACTIVE PHASE											
		R1	S1	T1	R2	S2	T2	R3	S3	T3	R4	S4	T4
K =	SENSOR R1	-32.43	0.065472	0.01614	-0.18569	0.022153	0.012214	-0.046374	-0.0055487	0.0052294	-0.020911	-0.0087629	0.00049702
	S1	0.065455	-32.454	0.065675	0.02217	-0.18523	0.022393	-0.0055493	-0.046053	-0.0053212	-0.0087627	-0.020623	-0.0085606
	T1	0.016144	0.065666	-32.466	0.012218	0.022395	-0.18506	0.0052298	-0.0053211	-0.045898	0.00049838	-0.0085609	-0.020486
	R2	-0.18571	0.022147	0.012217	-32.443	0.065411	0.016119	-0.18564	0.022147	0.012205	-0.046391	-0.0055453	0.0052306
	S2	0.022165	-0.18517	0.022415	0.065423	-32.456	0.065653	0.022149	-0.18527	0.022383	-0.0055409	-0.046055	-0.0053219
	T2	0.012218	0.022385	-0.18519	0.016121	0.065684	-32.453	0.012206	0.02239	-0.18508	0.0052323	-0.0053233	-0.045909
	R3	-0.046385	-0.0055564	0.0052318	-0.18565	0.022165	0.012207	-32.439	0.06543	0.01612	-0.18576	0.022159	0.012218
	S3	-0.0055481	-0.046042	-0.0053152	0.022149	-0.18539	0.022406	0.065428	-32.462	0.065666	0.022179	0.022159	0.022405
	T3	0.0052308	-0.0053184	-0.045913	0.012206	0.022401	-0.18524	0.016122	0.065667	-32.463	0.012218	0.022403	-0.18517
	R4	-0.020909	-0.0087669	0.00049828	-0.046377	-0.0055418	0.0052321	-0.18572	0.022169	0.012218	-32.443	0.065437	0.016143
	S4	-0.0087652	-0.020619	-0.008558	-0.005547	-0.046067	-0.0053147	0.022169	-0.18532	0.022414	0.065429	-32.449	0.065701
	T4	0.00049696	-0.0085567	-0.020487	0.00523	-0.0053219	-0.045917	0.012218	0.022407	-0.18519	0.01614	0.0657	-32.447

10.4.2 Array $[B(t)]$

In this case of study, the arrays $[B(t)]$ are derived with the input currents set to:

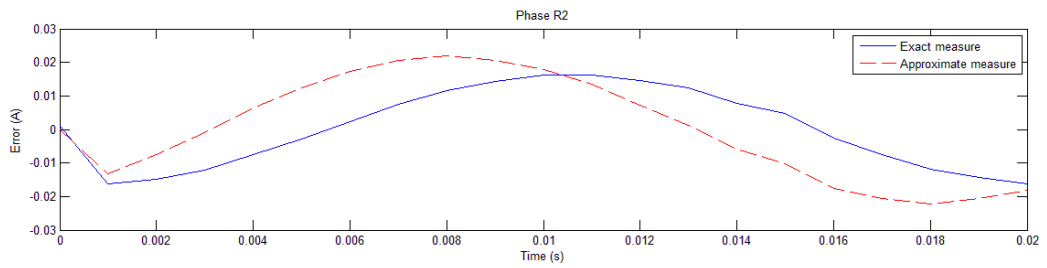
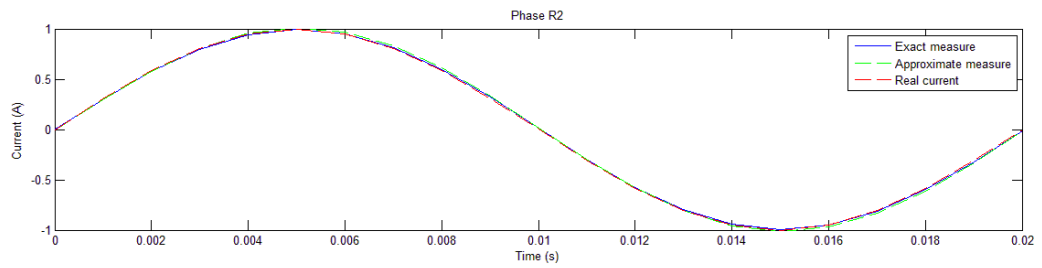
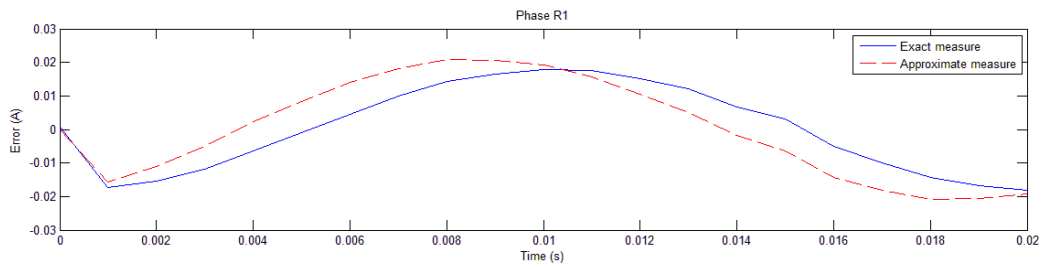
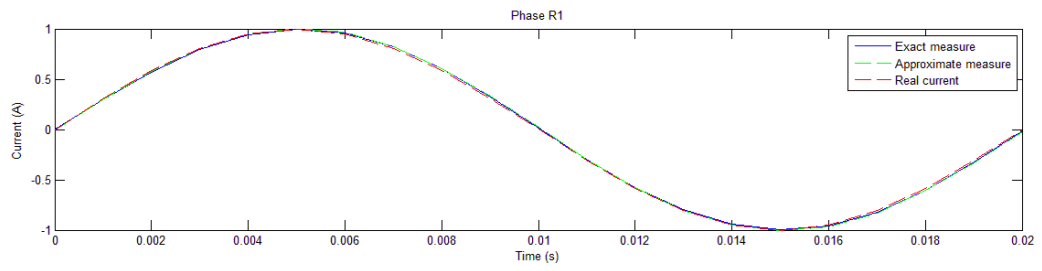
$$\begin{aligned}
 \dot{i}(t)_{R1} &= I_1 \sin(2\pi 50 t) \\
 \dot{i}(t)_{R2} &= I_2 \sin(2\pi 50 t) \\
 \dot{i}(t)_{R3} &= I_3 \sin(2\pi 50 t) \\
 \dot{i}(t)_{R4} &= I_4 \sin(2\pi 50 t) \\
 \dot{i}(t)_{S1} &= I_1 \sin(2\pi 50 t + 2\pi / 3) \\
 \dot{i}(t)_{S2} &= I_2 \sin(2\pi 50 t + 2\pi / 3) \\
 \dot{i}(t)_{S3} &= I_3 \sin(2\pi 50 t + 2\pi / 3) \\
 \dot{i}(t)_{S4} &= I_4 \sin(2\pi 50 t + 2\pi / 3) \\
 \dot{i}(t)_{T1} &= I_1 \sin(2\pi 50 t + 4\pi / 3) \\
 \dot{i}(t)_{T2} &= I_2 \sin(2\pi 50 t + 4\pi / 3) \\
 \dot{i}(t)_{T3} &= I_3 \sin(2\pi 50 t + 4\pi / 3) \\
 \dot{i}(t)_{T4} &= I_4 \sin(2\pi 50 t + 4\pi / 3)
 \end{aligned}
 \quad \left| \quad I_1 = I_2 = I_3 = I_4 = 1, 50, 100 [A]$$

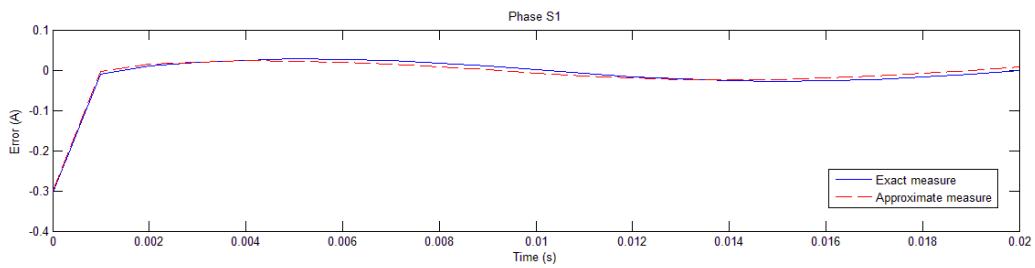
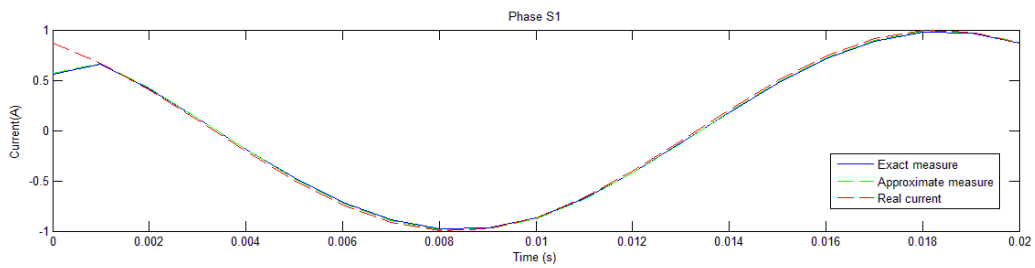
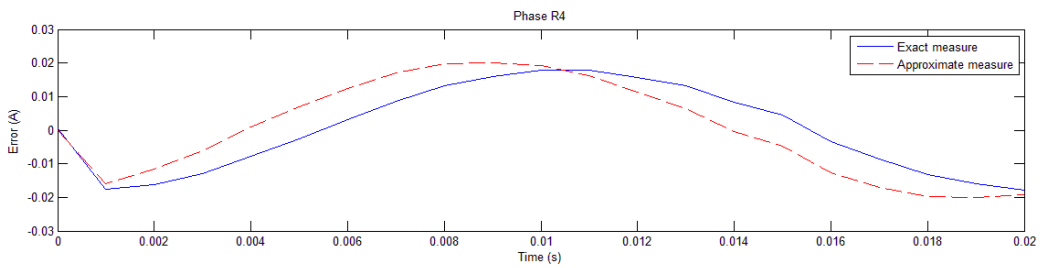
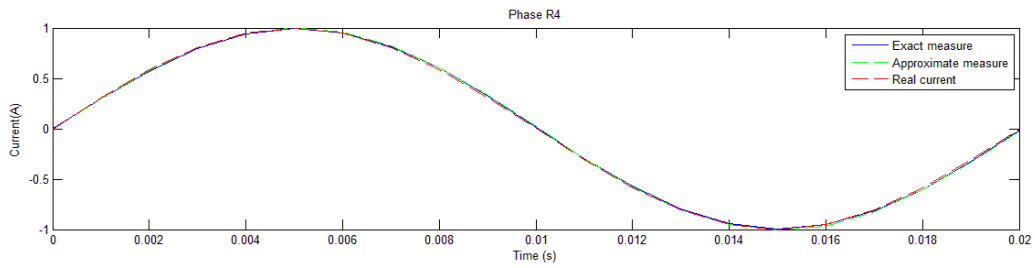
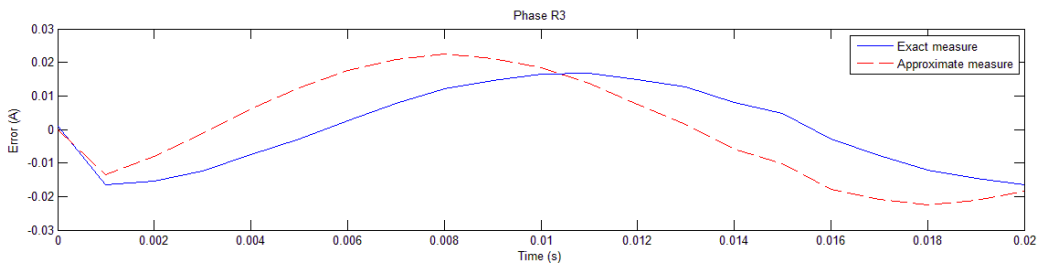
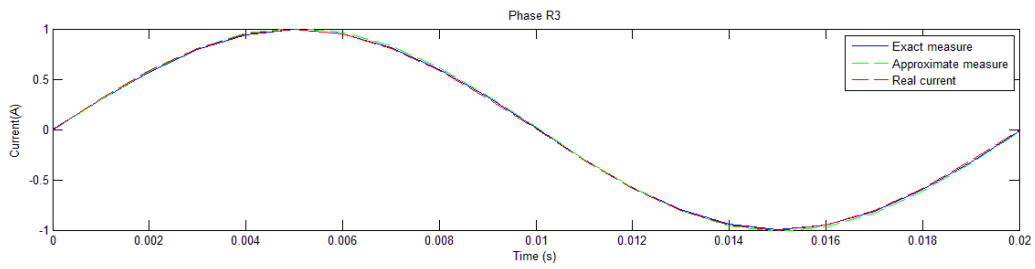
Where I_1, I_2, I_3, I_4 are the peak values of the alternative currents considered and the electrical system considered is symmetrical and balanced.

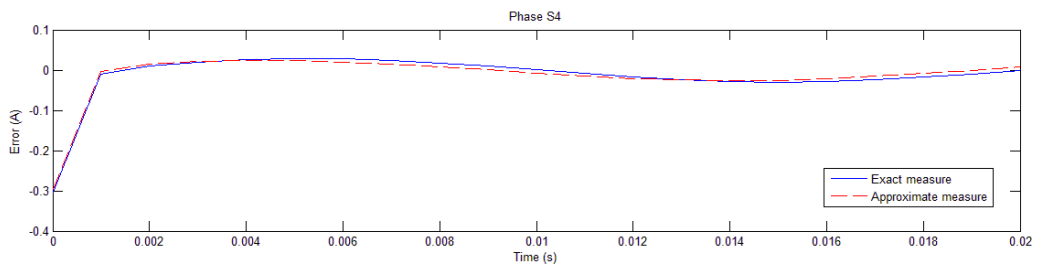
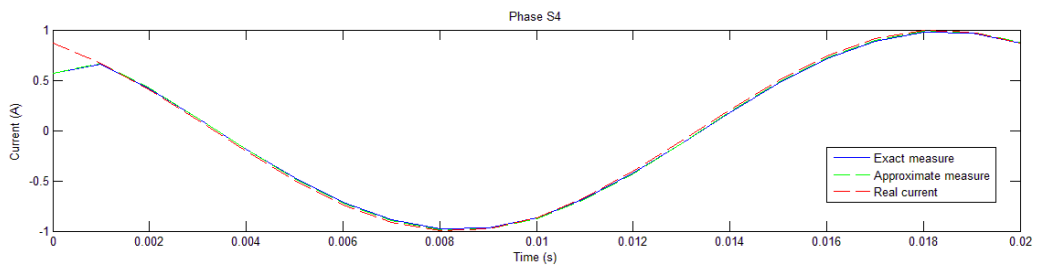
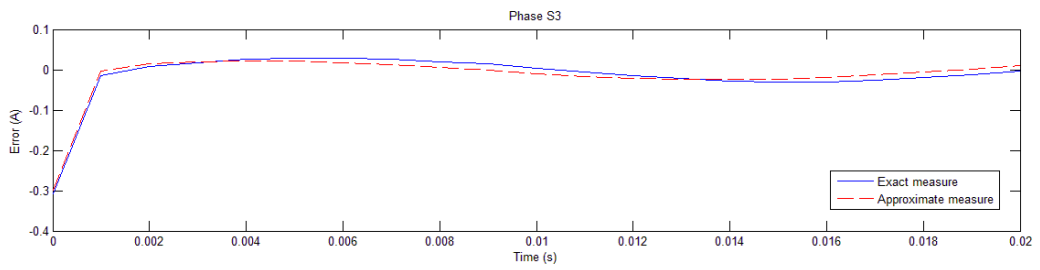
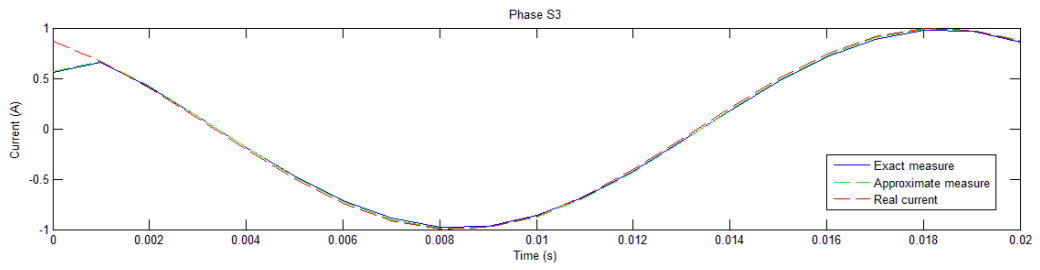
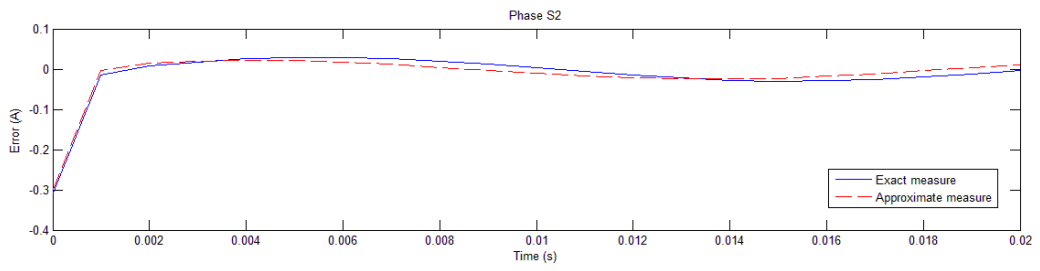
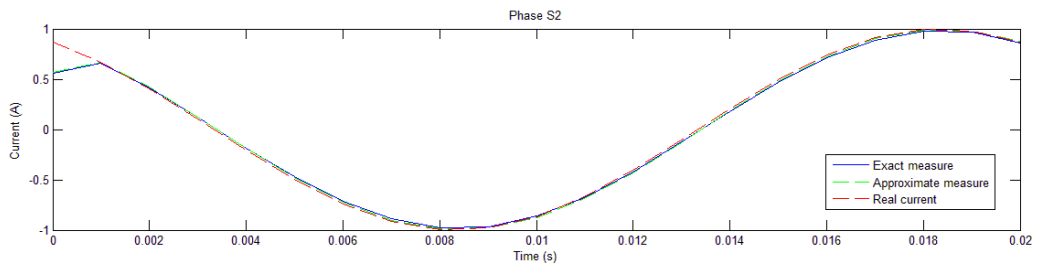
To not overfill the document, is presented below only the resulting array referred to the peak component of current set to 1[A]. All the values are in μT .

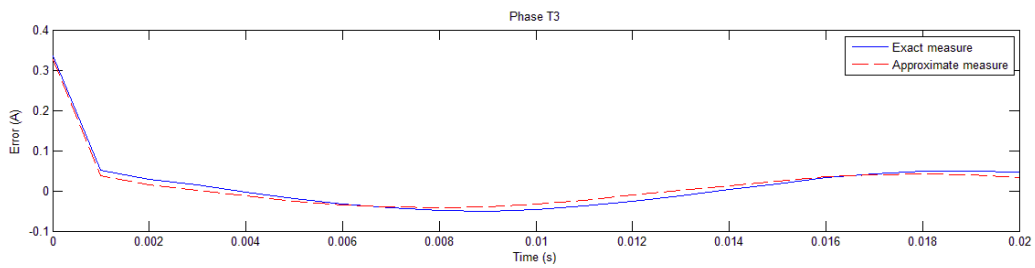
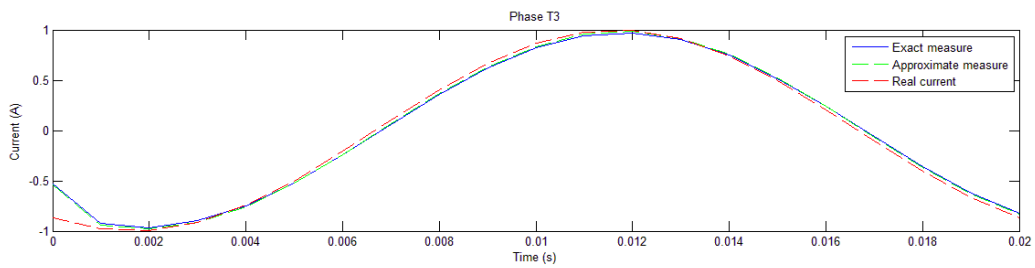
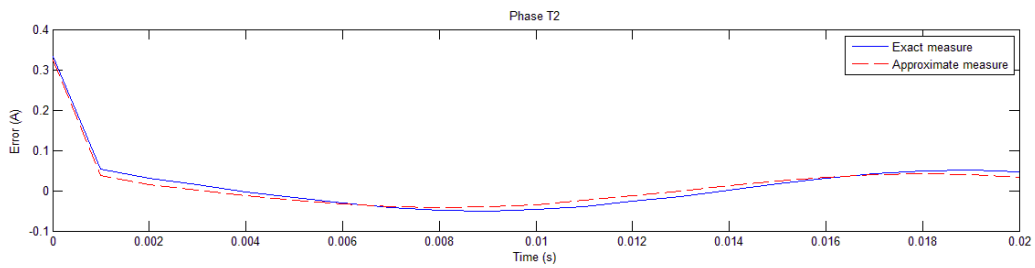
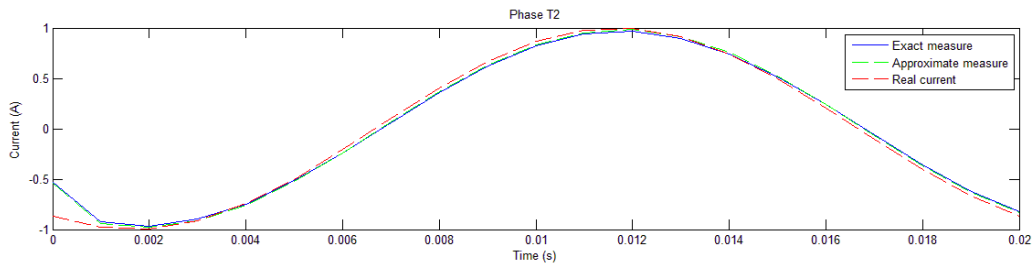
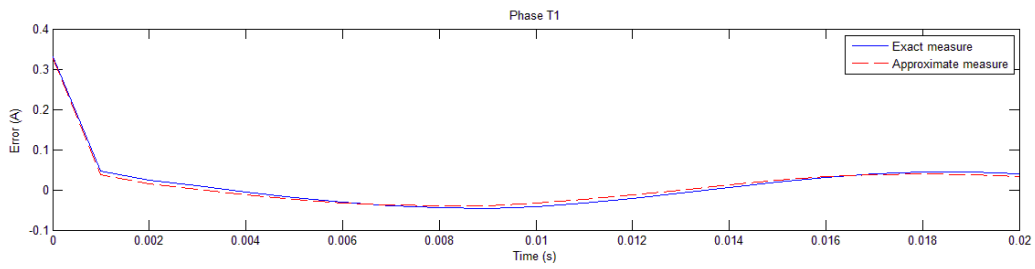
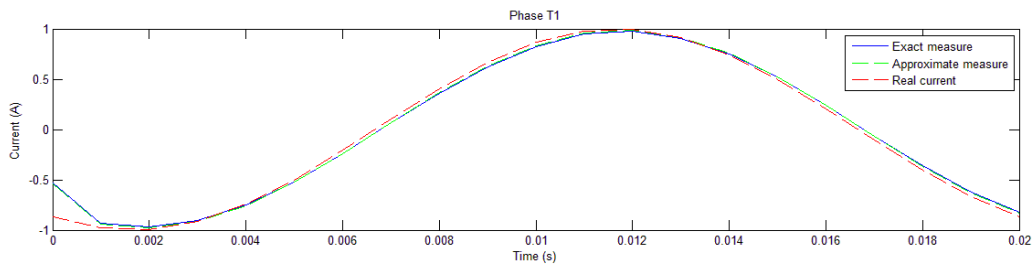
Time [s]	R1	S1	T1	R2	S2	T2	R3	S3	T3	R4	S4	T4
0	0.0050249	-18.419	17.539	0.0045087	-18.415	17.568	0.0041491	-18.425	17.536	0.0057623	-18.47	17.561
0.001	-9.5148	-21.58	30.541	-9.5976	-21.596	30.512	-9.5821	-21.589	30.547	-9.5109	-21.589	30.521
0.002	-18.706	-13.65	31.785	-18.824	-13.661	31.759	-18.809	-13.656	31.802	-18.691	-13.66	31.762
0.003	-26.074	-4.0492	29.61	-26.214	-4.0433	29.595	-26.202	-4.0424	29.638	-26.05	-4.064	29.59
0.004	-30.914	6.0007	24.529	-31.062	6.0294	24.529	-31.054	6.0269	24.567	-30.884	5.9819	24.513
0.005	-32.701	15.493	17	-32.844	15.546	17.014	-32.84	15.541	17.044	-32.668	15.472	16.99
0.006	-31.294	23.482	7.8106	-31.416	23.558	7.8378	-31.418	23.55	7.8571	-31.261	23.461	7.8059
0.007	-26.827	29.185	-2.1464	-26.918	29.278	-2.1086	-26.923	29.268	-2.1022	-26.798	29.166	-2.1452
0.008	-19.735	32.041	-11.897	-19.784	32.144	-11.852	-19.794	32.133	-11.86	-19.712	32.026	-11.891
0.009	-10.691	31.717	-20.463	-10.695	31.821	-20.416	-10.708	31.81	-20.436	-10.677	31.709	-20.452
0.01	-0.6231	28.331	-27.044	-0.58209	28.426	-26.998	-0.5961	28.416	-27.03	-0.62007	28.331	-27.029
0.011	9.5087	22.196	-31.001	9.5915	22.272	-30.962	9.5772	22.265	-31.001	9.5007	22.203	-30.985
0.012	18.722	13.854	-31.902	18.838	13.906	-31.874	18.825	13.901	-31.917	18.704	13.869	-31.886
0.013	26.069	4.1539	-29.643	26.207	4.1751	-29.627	26.196	4.1739	-29.671	26.042	4.1745	-29.629
0.014	30.9	-5.9396	-24.527	31.047	-5.9507	-24.525	31.04	-5.9482	-24.565	30.866	-5.9146	-24.516
0.015	32.636	-15.427	-16.971	32.777	-15.469	-16.983	32.774	-15.463	-17.014	32.6	-15.399	-16.964
0.016	31.306	-23.471	-7.8173	31.426	-23.541	-7.8419	31.428	-23.532	-7.8623	31.27	-23.444	-7.8159
0.017	26.829	-29.177	2.1474	26.918	-29.267	2.1126	26.924	-29.256	2.1052	26.797	-29.153	2.1431
0.018	19.739	-32.044	11.903	19.788	-32.146	11.862	19.797	-32.134	11.868	19.714	-32.024	11.893
0.019	10.693	-31.721	20.47	10.697	-31.825	20.427	10.709	-31.812	20.446	10.677	-31.708	20.456
0.02	0.62594	-28.351	27.064	0.58409	-28.446	27.024	0.59785	-28.435	27.054	0.62099	-28.345	27.047

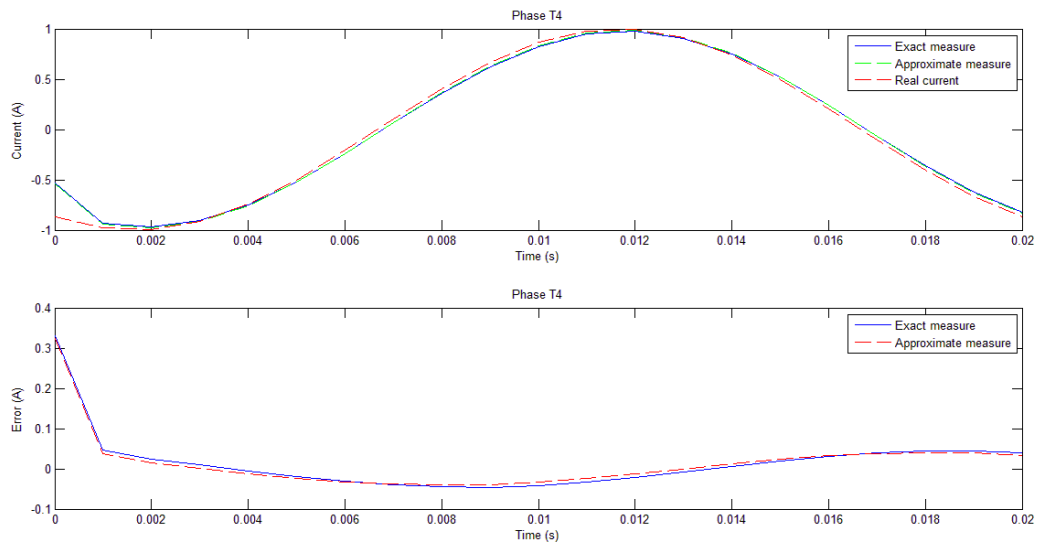
10.4.3 Graphical results











Considerations:

In these graphs can be seen a large diffusion of measurement errors, especially for the first instants of time. Thus will be necessary the integration of a corrective coefficient in order to obtain an exact measure of the current.

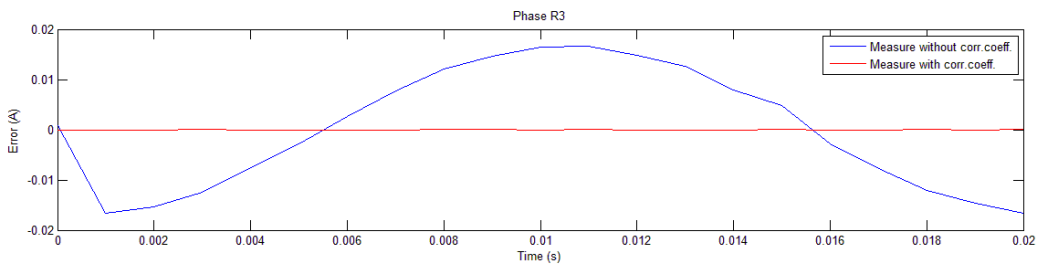
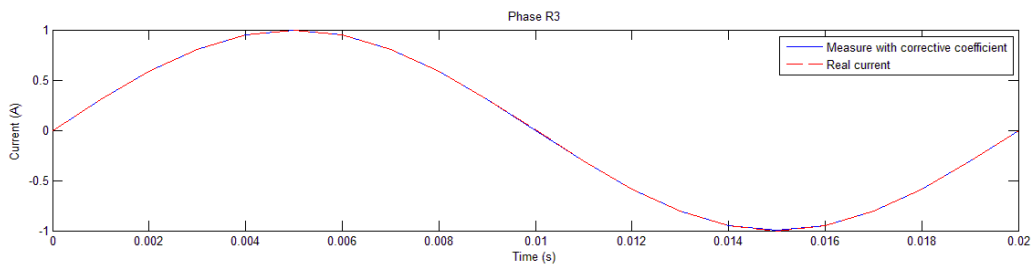
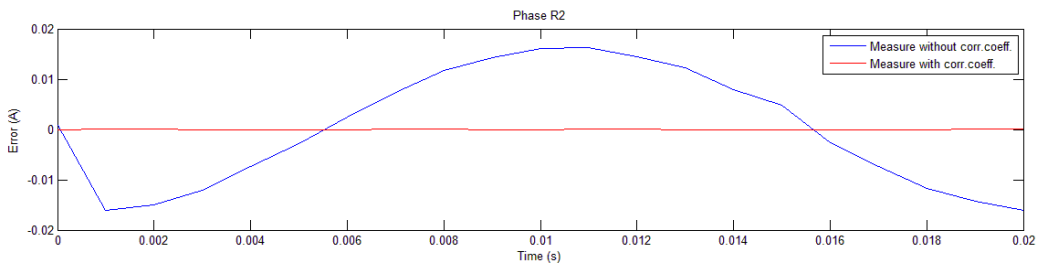
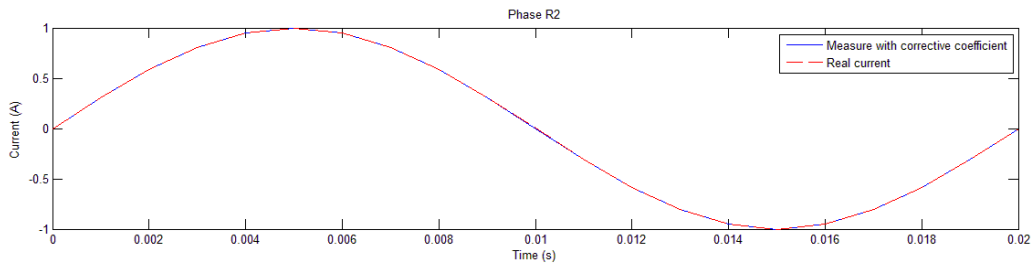
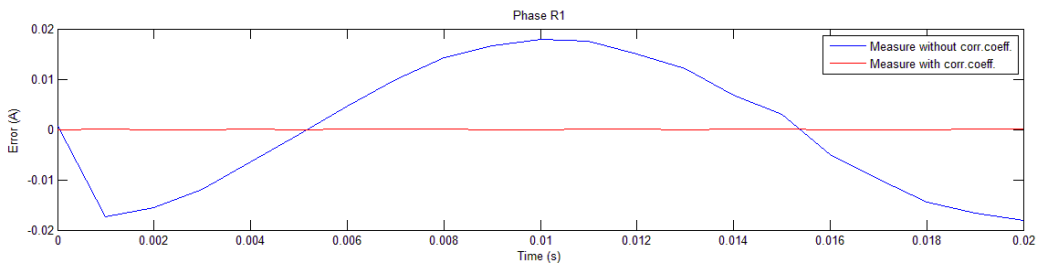
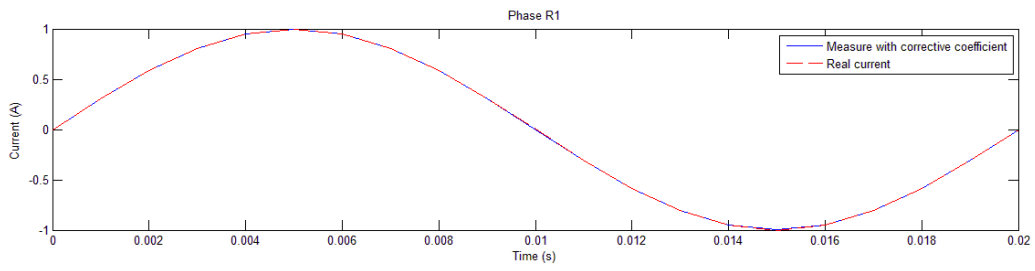
10.4.4 Implementation of a corrective coefficient

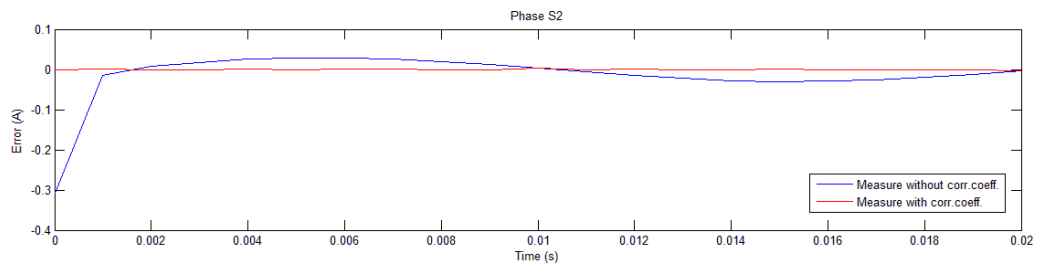
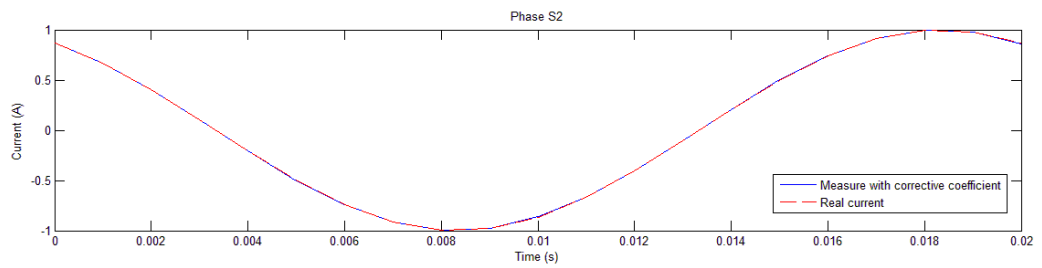
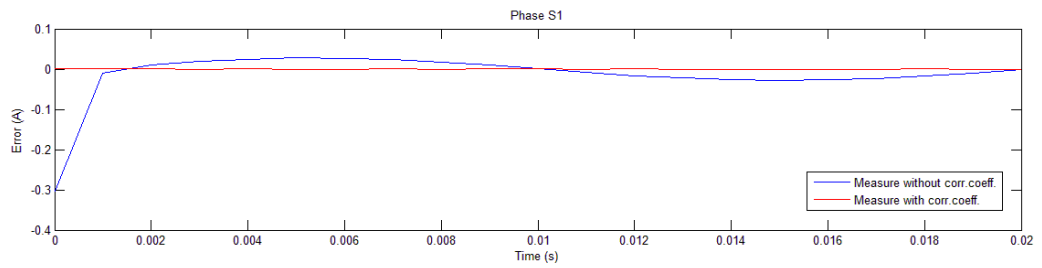
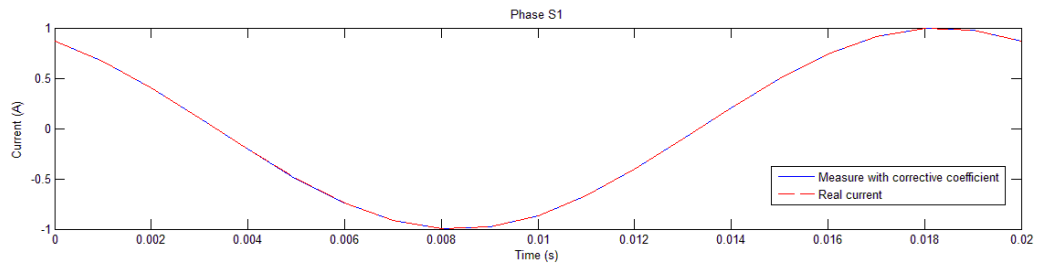
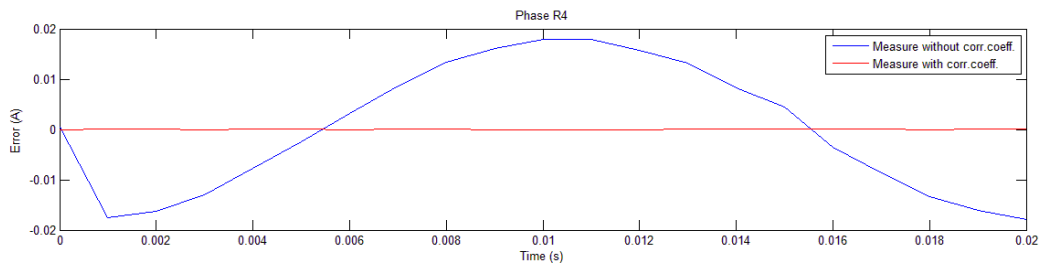
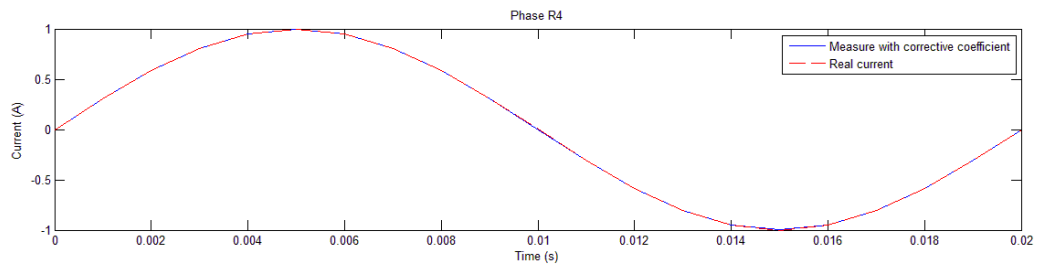
The corrective coefficients matrix used in this case is the following:

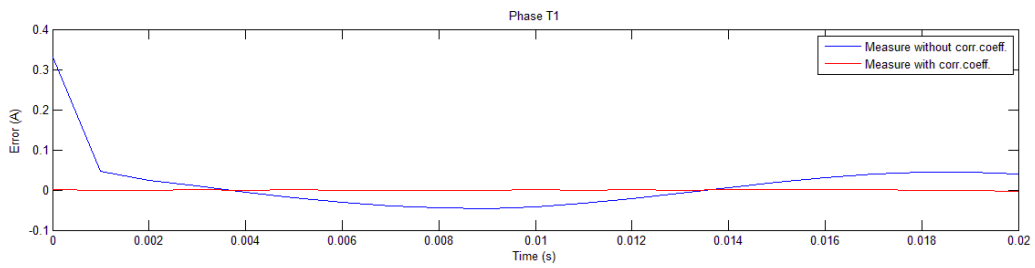
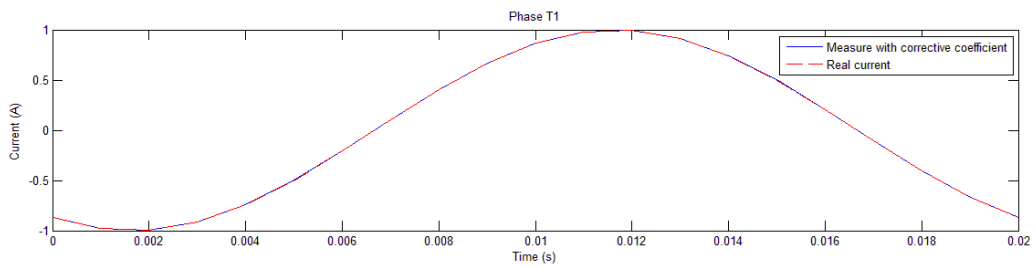
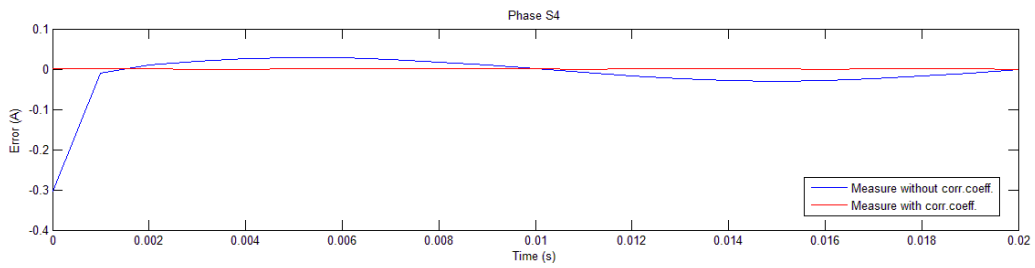
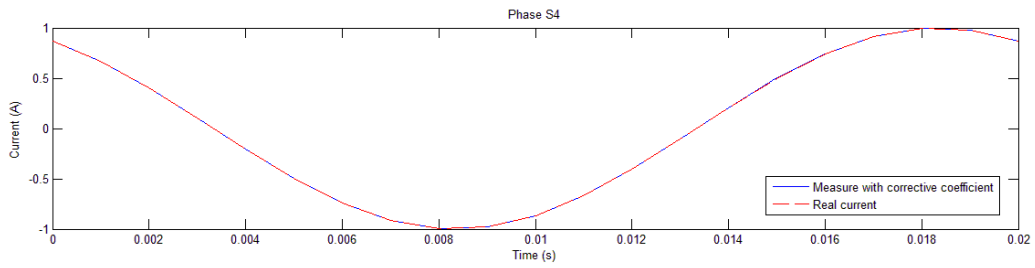
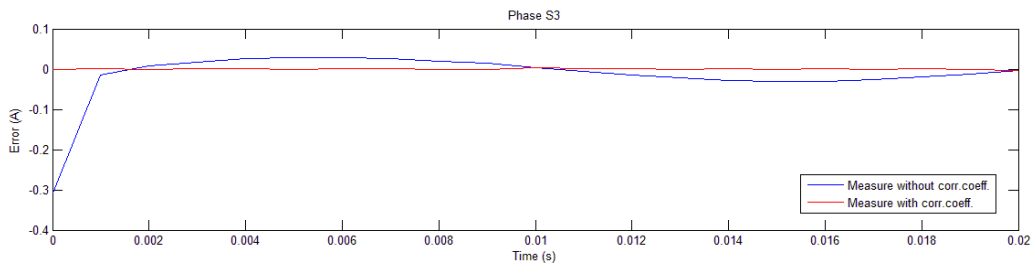
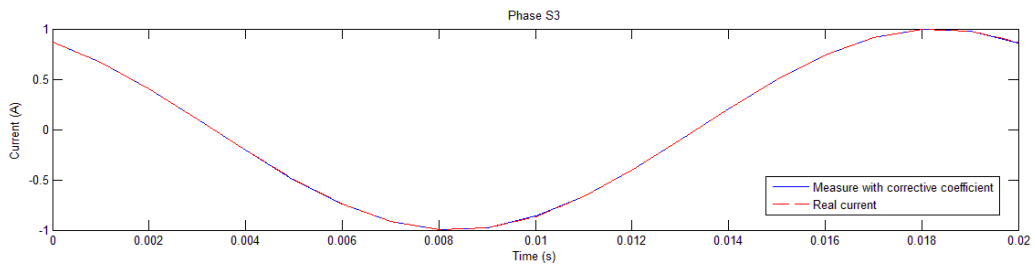
$ K _{corr} =$	<i>Inf</i>	0.6489	0.6176	<i>Inf</i>	0.6449	0.6151	<i>Inf</i>	0.6451	0.6137	<i>Inf</i>	0.6508	0.6187
	0.9437	0.9839	0.9525	0.9477	0.9787	0.9464	0.9463	0.9782	0.9472	0.9429	0.9845	0.9525
	0.9736	1.0239	0.9753	0.9745	1.0186	0.9694	0.9739	1.018	0.9704	0.9724	1.0248	0.9752
	0.9853	1.182	0.9895	0.985	1.1733	0.9839	0.9846	1.1727	0.9851	0.984	1.1865	0.9894
	0.9933	0.8805	1.0081	0.9922	0.8793	1.0032	0.9921	0.8788	1.0044	0.9919	0.8778	1.008
	0.999	0.9453	1.0393	0.9973	0.9428	1.0355	0.9973	0.9423	1.037	0.9975	0.9442	1.0393
	1.0048	0.964	1.1512	1.0025	0.9613	1.1515	1.0027	0.9608	1.154	1.0034	0.9633	1.1512
	1.0122	0.9747	0.6166	1.0091	0.9719	0.5973	1.0095	0.9714	0.5952	1.0107	0.9742	0.6166
	1.0242	0.9829	0.8902	1.0198	0.9801	0.8808	1.0205	0.9796	0.8812	1.0226	0.9826	0.8902
	1.0537	0.9893	0.932	1.0461	0.9865	0.9243	1.0475	0.986	0.9249	1.0519	0.9892	0.932
	<i>Inf</i>	1.0069	0.9502	<i>Inf</i>	1.0075	0.9501	<i>Inf</i>	1.0084	0.9503	<i>Inf</i>	1.0106	0.9501
	0.9432	1.012	0.9669	0.9473	1.0094	0.9603	0.946	1.0089	0.9613	0.942	1.0125	0.9669
	0.9745	1.0392	0.9789	0.9753	1.0369	0.9729	0.9747	1.0363	0.9739	0.9731	1.0405	0.979
	0.9851	1.2125	0.9906	0.9847	1.2116	0.985	0.9844	1.211	0.9861	0.9837	1.2188	0.9907
	0.9929	0.8715	1.008	0.9917	0.8678	1.003	0.9916	0.8672	1.0044	0.9914	0.8679	1.0082
	0.997	0.9413	1.0375	0.9952	0.9381	1.0336	0.9953	0.9376	1.0352	0.9955	0.9397	1.0377
	1.0052	0.9636	1.1522	1.0028	0.9606	1.1521	1.003	0.96	1.1548	1.0037	0.9626	1.1527
	1.0123	0.9744	0.6169	1.0091	0.9715	0.5985	1.0095	0.971	0.5961	1.0107	0.9737	0.616
	1.0244	0.983	0.8906	1.02	0.9802	0.8816	1.0207	0.9796	0.8818	1.0227	0.9825	0.8904
	1.0539	0.9894	0.9323	1.0463	0.9867	0.9248	1.0476	0.9861	0.9254	1.0519	0.9891	0.9322
<i>Inf</i>	1.0067	0.9502	<i>Inf</i>	1.0077	0.9501	<i>Inf</i>	1.0083	0.9503	<i>Inf</i>	1.0108	0.9501	

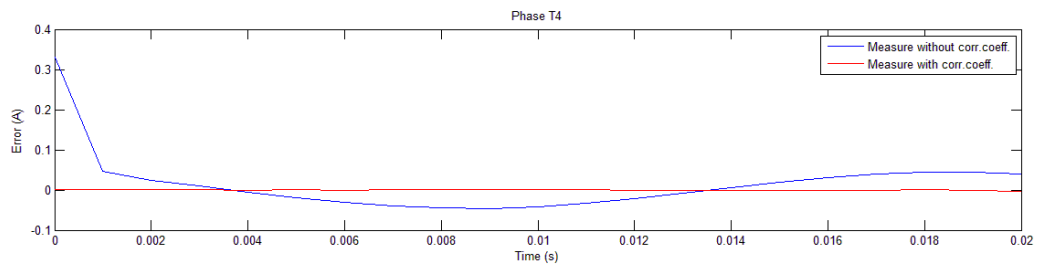
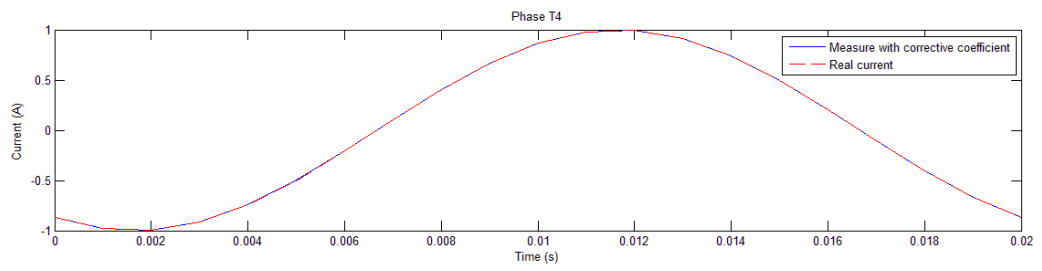
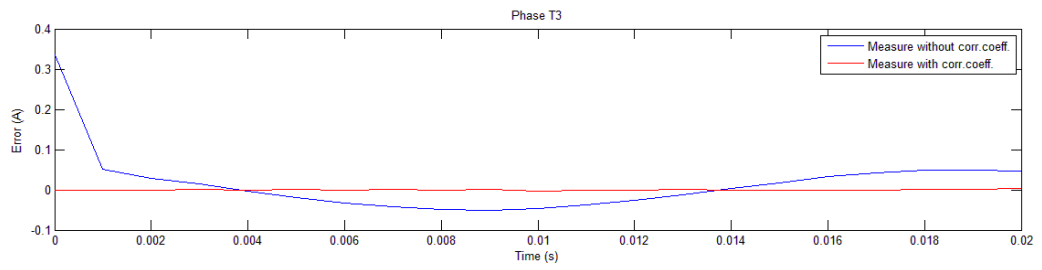
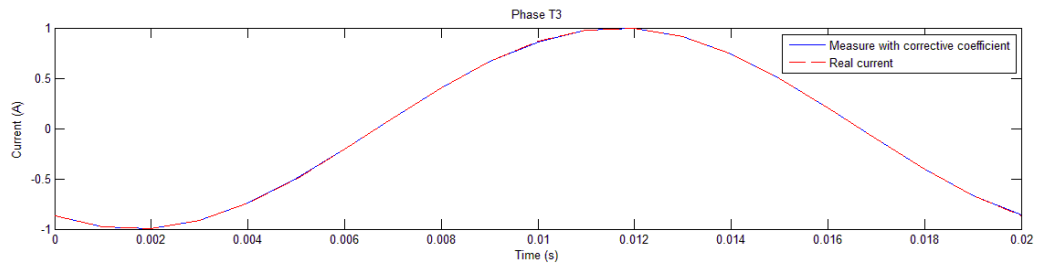
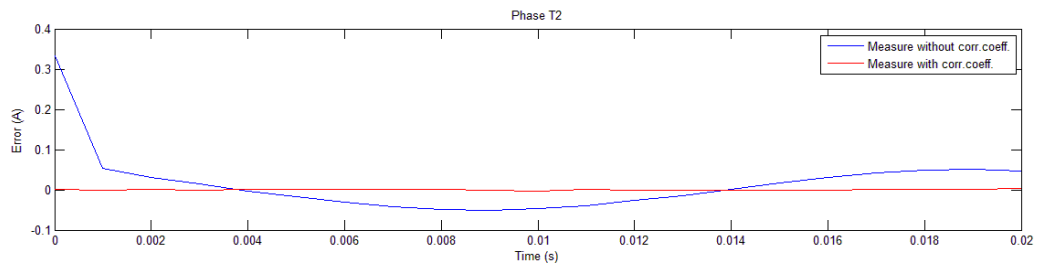
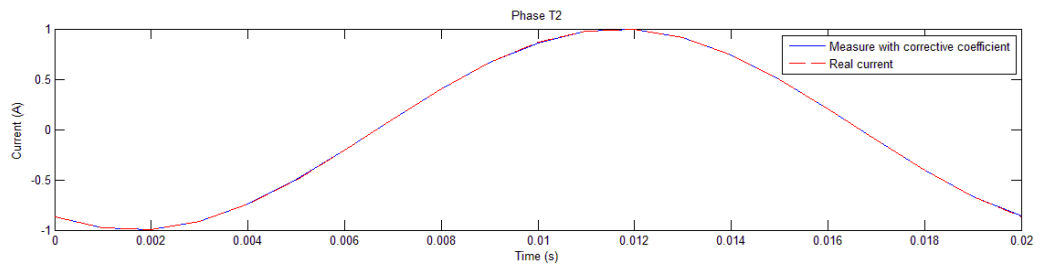
Its independence to the variation of the input current has been tested with the method used in the paragraph [10.2.1].

The charts obtained with the implementation of the corrective coefficients matrix are the following:









Considerations:

In the previous graphs it's possible to ascertain that with the implementation of the corrective coefficients matrix the error in the measures will be zero for every bar considered.

Therefore, it has been reached, with the implementation of the corrective coefficients matrix, a perfect virtual monitoring system of the currents minimising the measurement errors.

11 STUDY OF THE ERROR - 3D CASE

In this section will be reported the matrices **K** necessary for the study of the virtual measurement system in the 3D model.

With the 3D case of study there have been some technical problems using the Comsol software for the simulations. In fact, it was encountered an actual limit of the software that doesn't allow to simulate the model in the time domain with the tool "single turn coil". This fact didn't allow to simulate the model in the time domain but only in the stationary domain, for which there have been found only the matrices **K**.

A possibility to remedy the problem was to consider, instead of the "single turn coil" tool, the "multi turn coil" tool. In this case the program allowed to do the simulations in the time domain but it was found that this tool wasn't right for the present model. This because the "multi turn coil" tool is intended for the simulation of wounded coils and the results weren't reliable.

Finally, given the present impossibility to resolve the problem, it was chosen to contact the Comsol technical support and they took charge of the problem.

Anyway, when the problem will be solved, the main things to do will be to compute the array **B(t)** and, using the matrices **K** reported in this paragraph, to make the same probes made with the 2D case.

For the probes will be used the same points of measure found in the 2D case, in the two different configurations, in order to figure out the graphs of current and error trends and eventually to consider the implementation of a corrective coefficient.

The eventually matrices and coefficients obtained with this study will be implemented in the Arduino programming code.

11.1 First disposition of measurement sensors

11.1.1 K matrix

		ACTIVE PHASE												
		R1	S1	T1	R2	S2	T2	R3	S3	T3	R4	S4	T4	H
K =	SENSOR R1	-32.831	0.64935	0.064946	0.18281	0.06524	0.02508	0.047487	0.030478	0.019069	0.023636	0.021008	0.015083	-0.25363
	S1	0.63765	-32.242	0.074873	0.74573	0.14848	0.017161	0.084	0.047224	0.024651	0.032649	0.029718	0.019841	-0.017548
	T1	-0.016379	0.020836	-41.843	-0.00076916	0.0013288	0.0059477	-0.000099054	0.0012607	-0.0045018	-0.000011399	-0.00035084	-0.0043903	-0.006204
	R2	0.18092	0.62021	0.037156	-32.901	0.70329	0.10003	0.18258	0.079605	0.031798	0.047832	0.042738	0.026765	0.044387
	S2	0.08024	0.15893	0.039628	0.63347	-32.234	0.071027	0.75393	0.17375	0.036873	0.084181	0.06646	0.037603	0.038975
	T2	0.00071056	0.0029088	0.0044554	0.0052482	0.0071025	-41.487	0.0023752	0.0016328	0.0035037	0.00029369	0.00071127	-0.0079722	0.004481
	R3	0.046782	0.10408	0.053244	0.17361	0.56795	0.0606	-32.401	0.71724	0.11734	0.18495	0.099857	0.049942	0.028835
	S3	0.030835	0.072691	0.031282	0.079954	0.16647	0.036241	0.65216	-32.086	0.089938	0.71884	0.17978	0.040458	0.022486
	T3	0.00055222	0.0012622	-0.020766	0.0021416	0.0081692	-0.0079593	-0.0084621	0.038211	-40.771	0.0047122	0.0015636	-0.011191	0.0088087
	R4	0.022088	0.054103	-0.15496	0.046227	0.088622	-0.14997	0.18056	0.64904	-0.14671	-33.231	0.72189	-0.13497	0.01764
	S4	0.016361	0.033189	-0.42328	0.029421	0.051382	-0.41943	0.078297	0.14633	-0.41483	0.64543	-31.876	-0.37138	0.013975
	T4	0.00016618	-0.00068652	-0.048138	0.00038718	0.0010814	-0.048015	0.00072758	0.0022699	-0.035405	0.0024133	0.0067524	-41.816	0.0077246
	H	0.11937	0.0060035	-0.031879	-0.057347	-0.026702	-0.014737	-0.03161	-0.022529	-0.013328	-0.020274	-0.01851	-0.013876	-11.24

11.2 Second disposition of measurement sensors

11.2.1 K matrix

		ACTIVE PHASE												
		R1	S1	T1	R2	S2	T2	R3	S3	T3	R4	S4	T4	N
K =	SENSOR: R1	33.578	-0.0010866	0.0040244	0.21132	0.013566	0.0047912	0.10094	0.017959	0.0059098	0.090435	0.016529	0.0064048	-0.051197
	S1	0.059496	33.508	-0.019856	-0.014134	0.12151	-0.0029567	-0.000075164	0.019866	0.0038455	0.0053338	0.012076	0.0034113	0.0013297
	T1	-0.031699	0.10237	33.178	0.0037069	-0.026505	0.12132	-0.00036798	-0.0032312	0.017822	-0.00029669	0.0019316	0.0071699	0.0029815
	R2	0.28495	-0.002466	-0.0016212	33.222	-0.018261	-0.0024319	0.31962	-0.0027458	-0.0016343	0.20431	0.0030403	-0.00036753	-0.00037135
	S2	-0.025385	0.135	-0.00064085	-0.23951	33.901	-0.018269	-0.00837	0.15516	-0.0015241	-0.00004477	0.055951	0.0053444	0.000548
	T2	0.000037404	-0.013045	0.1396	0.057285	-0.013654	33.456	-0.0040611	-0.025739	0.12291	-0.0010839	-0.00076403	0.021897	-0.00055155
	R3	0.034221	-0.0073832	0.00026906	0.12446	-0.012447	-0.0010285	34.104	-0.029595	-0.0018831	0.17376	-0.013987	-0.0010953	-0.000054654
	S3	-0.001958	0.23899	0.0033524	-0.025502	0.35556	-0.0033847	0.046039	33.407	-0.020249	-0.015365	0.34777	-0.0033635	-0.00037954
	T3	-0.001093	0.00069895	0.050448	-0.0012501	-0.016421	0.15709	0.0021415	0.12141	33.457	0.0039958	-0.022455	0.14358	-0.0015593
	R4	0.0085104	0.0033247	0.0013407	0.016125	0.0043594	0.0006666	0.1137	-0.0011556	-0.00060904	33.127	-0.017535	-0.0014472	-0.000067175
	S4	0.0012794	0.039497	0.00032835	-0.0037214	0.047988	0.0010037	-0.027005	0.15504	-0.0056375	0.096221	33.148	-0.02276	-0.00025002
	T4	-0.00026899	0.0042918	0.22029	-0.00070784	-0.00086493	0.23127	0.00079253	-0.0097933	0.3402	0.12483	0.035878	33.593	-0.0013959
	N	-0.072972	-0.031906	-0.014629	-0.081502	-0.028286	-0.014203	-0.082411	-0.026277	-0.01368	-0.079888	-0.025117	-0.013212	-11.927

12 MONITORING OF MAGNETORESISTIVE SENSORS WITH THE IMPLEMENTATION OF AN ARDUINO® BOARD

Arduino is an open-source prototyping platform based on easy-to-use hardware and software.

The Arduino boards provide sets of digital and analog I/O pins that can interface to various expansion boards and other circuits. The boards dispose of serial communication interfaces, including Universal Serial Bus (USB) for loading programs from personal computers. For programming the microcontrollers, the Arduino project provides an integrated development environment (IDE) based on a programming language named Processing, which also supports the languages C and C++.

Arduino boards are available commercially in preassembled form, or as do-it-yourself kits. The hardware design specifications are openly available, allowing the Arduino boards to be produced by anyone. [10]

These microcontrollers permit to create devices that interact with their environment using sensors and actuators, for this reason they are particularly useful in the present project. In fact, it's also possible to connect to these boards a number of magnetoresistive sensors. This in order to obtain the correspondent values of measure and to process these data through the programming code.

Arduino boards are available commercially in preassembled form, or as do-it-yourself kits. The hardware design specifications are openly available, allowing the Arduino boards to be produced by anyone.

12.1 Arduino advantages

The mains advantages in the use of an Arduino system are:

- Arduino boards are relatively inexpensive compared to other microcontroller platforms;
- The Arduino Software (IDE) runs on Windows, Macintosh OSX, and Linux operating systems. Most microcontroller systems are limited to Windows.
- The Arduino Software (IDE) is easy-to-use for beginners, yet flexible enough for advanced users that can take advantage of as well.
- The Arduino software is published as open source tool and the language can be also expanded through C++ libraries.

In the present project, the main reason that lead to the use of an Arduino systems is principally the cost-effectiveness advantage. In fact, as it will be explained in the *paragraph* [12.7], the final total cost of the hardware components implemented in the project will be low.

12.2 Arduino model: MEGA 2560

The Arduino Mega 2560 is a microcontroller board with 54 digital input/output pins, 16 analogue inputs, 4 UARTs (hardware serial ports), a 16 MHz crystal oscillator, a USB connection, a power jack, an ICSP header, and a reset button. It's possible to connect it to a computer with a USB cable or power it with a AC-to-DC adapter or battery to get started. [11]

This microcontroller will be used in the project with the purpose to monitor all the sensors in the panel. This in order to derive the values of current and voltage and process them to figure out, for every circuit, the electrical system parameters (as active power P , reactive power Q , apparent power S , $\cos\phi$).

It has been chosen this particular model of microcontroller because provides the highest number of acquisition channels (16 analogue inputs) among all the Arduino boards. In fact, in this project, will be necessary all the 16 channels of the Arduino board, as it will be explained in the *paragraph* [12.3].

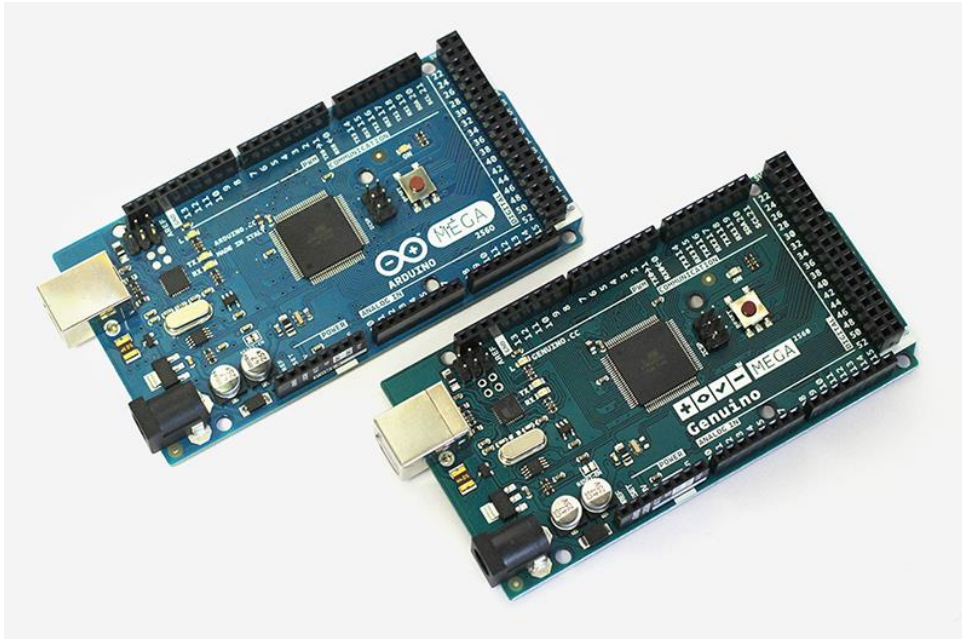


Fig. 12.1 Arduino Mega (version for USA) and Genuino Mega (version not for USA).

12.2.1 Technical specs

Microcontroller	ATmega2560 (8 bit)
Operating Voltage	5 V
Input Voltage (recommended)	7-12 V
Input Voltage (limit)	6-20 V
Digital I/O Pins	54 (of which 15 provide PWM output)
Analog Input Pins	16
DC Current per I/O Pin	20 mA
DC Current for 3.3V Pin	50 mA
Flash Memory	256 KB
SRAM	8 KB
EEPROM	4 KB
Clock Speed	16 MHz
Length	101.52 mm
Width	53.3 mm
Weight	37 g

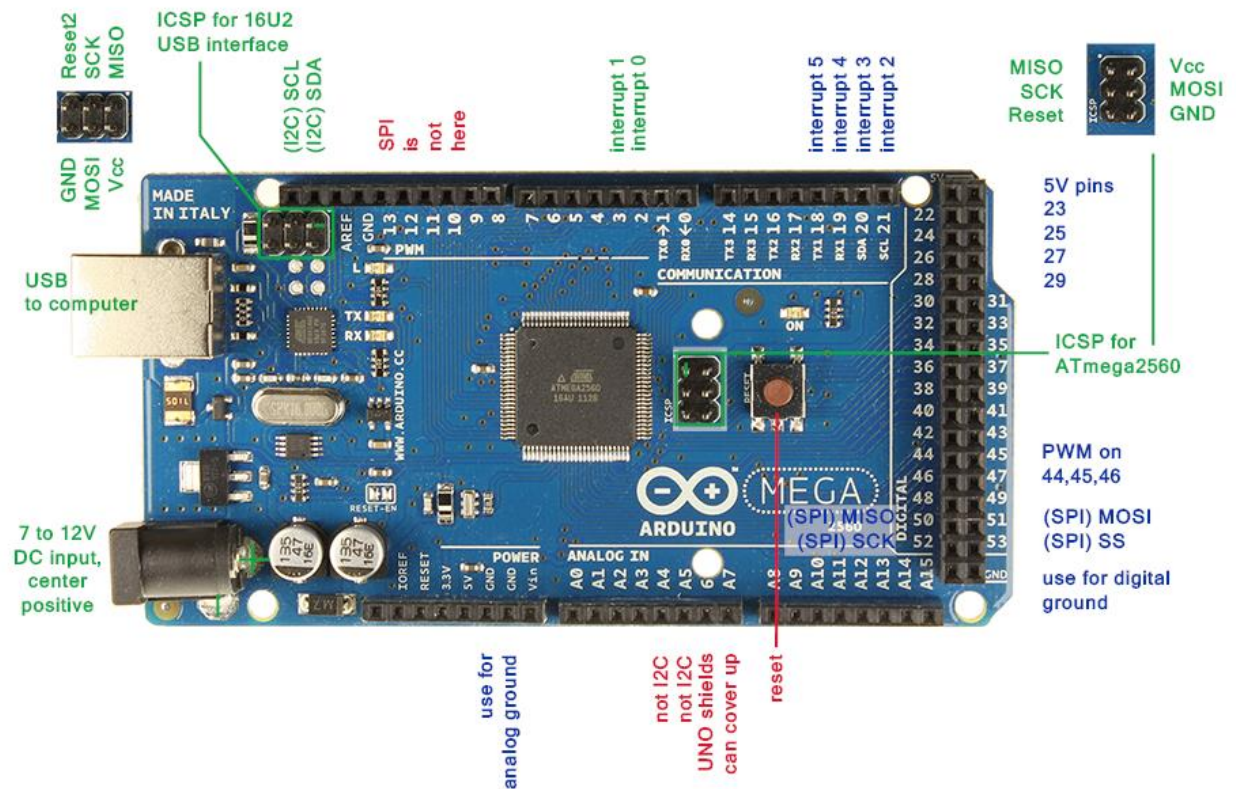


Fig. 12.2 MCU MEGA 2560.

12.3 Connection system between the sensors and the MEGA 2560 Arduino board.

About the installation of the measurement system in the electrical panel have to be done some considerations.

On the one hand is present the analogic system, formed by the sensors, and on the other hand there is the digital system, formed by the Arduino board. To connect the two systems there will be, for sure, some electronic wires and also will be necessary an analog-to-digital converter, already installed in the board.

For the connection of the sensors to the board every single sensor installed in the panel will not be connected with a respective channel. This because in this way we're going to need a lot of channels, and the board has got a maximum of 16 channels available.

For this reason, will be used another methodology for the connection that consists in add up every couple of sensors of every bar with a particular Operational Amplifier (OA): a Summing Amplifier.

Then, every OA will be connected to the input channels of the board, bringing the output value of the OA (sum of the values measured by the two sensors) to the respective input channel of the board.

Another important thing to do in the system implementation will be the realization of an adapting circuit that will have to do the following things:

- Provide the power supply to the sensors ($2.16 \div 3.6$ V) and to the OA (± 10 or 15 V);
- Adapt the output level of the OAs (a voltage signal depending on the output voltage signals of the sensors) to the admitted range of the Arduino board ($0 \div 5$ V).

As regards the last point, more precisely it will be necessary to adapt the output level of the OA introducing an offset of 2.5V. This because the sensors will work with sinusoidal values, that are positive and negative. So, in order to maintain every value in the range, it will be better to maintain the signals between the values -2.5V and +2.5V.

Regarding the input channels in the board, as anticipated before, will be used all the 16 input channels. This because will be installed 12 OAs for all the 12 bars (3 phases \times 4 circuits) more 1 OA for the neutral bar and the remaining channels will be necessary for the 3 voltages (of the phases R,S,T). These voltages will be measured probably with a voltage transformer (VT).

12.4 Limitations encountered with the implementation of the MCU

A limitation encountered, with the implementation of the Arduino board, was that it isn't possible to measure all the channels at once. This because there is only one analog-to-digital converter with a multiplexer.

This multiplexer acts as the channel selector for the reading of the selected channel. So, the multiplexer every time selects a channel and then makes the reading and performs the instructions present in the main loop. In our case we have to read 16 channels and the time to change the selection from a channel to another one is more or less fixed, but not instantaneous. Therefore, there will be always a slight delay in the switching from one channel to another.

This fact limits the initial idea to measure simultaneously all the channels, namely all the currents flowing in all the phases of the circuits. The main problem, caused by this limitation, is the correct measurement of the phase shift between current and voltage of a given circuit, and thus the measurement of the correspondent active and reactive powers. This because there will be a delay through a channel containing a value that will be translate in a current value and a channel containing a voltage value, and this delay will affect the phase shift between them.

12.5 Exceedance of the technical limitations

A solution to overcome the limitations previously presented is discussed in this paragraph.

Considering now the MCU programming part (elaborated with the Arduino software IDE), to read a channel exists a proper function named "analogRead", easy and fast to implement. The problem is that this function simplifies the program code, but doesn't optimizes the process speed.

First of all, it's necessary to take into account that will be considered the channels in pairs, confronting two channels at a time.

Then, the main idea in order to resolve the problem is, instead of using the "analogRead" function, to act directly on the ADC and its records. This can speed up the operation of switching from a channel to another.

More precisely, it will be used a timer that imposes the time in which a reading is performed in the ADC, namely the sampling speed. In this case the timer will be programmed at a sampling speed of 12.8 kHz.

At this frequency is generated a read command of the ADC, which causes what is called an "interruption". An interruption stop automatically what has been programmed to do into the principal loop and proceeds to execute what has been programmed to do into the interruption function, in this case the consecutive reading of two ADC channels. When the reading of two ADC channels has done, the running loop continues from where it was left.

Thus, the procedure is that every 78,125 μ s (12.8 kHz) is realized the consecutive sampling of two channels (voltage and current of a given phase), and the samples are stored into two vectors of 512 samples. Then, in the main loop, there will be performed the operations in order to obtain the values of interest (average values, rms values, powers and so on) and they will be sent, through the serial port, to the monitor of the Arduino GUI.

All this will be done for all the channels taken them two by two.

To increase the speed of the ADC it has been necessary to use it through its registers. The idea was that the ADC has a multiplication factor (named "prescaler") that controls the rate of conversion. This factor can speed up the operations but at the expense of the accuracy of reading.

In our case, with the settings explained before, it was found a delay of 13.9 μ s between the reading of two channels. This it means that there is only a temporal gap of 0.25° between the phases and it has not a great influence in the measuring of P and Q.

12.6 Development of the programming code

The main parts composing the programming code and the main functions utilized for its development are presented in this paragraph.

The complete programming code will be reported in the *Appendix B*.

The code was drawn up with the Arduino software IDE and the objective of the program code is to control the board in order to obtain from the sensors the respective values of voltages and currents. Processing these values can be figured out the electrical parameters of interest, such as the values of P , Q , S , $\cos\phi$ and the respective RMS values.

In general terms, concerning on what explained before, the board is programmed in order to do the following steps:

- Are sampled two channels filling two vectors of 512 samples;
- When the samples are filled, is disabled the “interruption” command for proceeding with the calculation of the parameters (P , Q , S etc.);
- The data are sent through the serial port and the function “interruption” will be re-enabled;
- In some point it has been changed the channel identifier in order to proceed to measure other two channels, and so on till to read all the 16 channels.

Regarding the Arduino codes, they are written in a modified C language and usually are composed by the following three main parts:

- Definition of constants and definition of their type (integer, long, etc.), with the possibility to include other defined libraries that can bring other useful functions;
- The development of the function “setup” where the device is initialized and the configuration of some of its functionality is performed, as the speed of sending data;
- The development of the function “loop”, where are included all the instructions that the program will do continuously in a closed loop.

The programming code used to control the MCU MEGA 2560 (reported in the *Appendix B*) is composed by the following parts:

- Definition of constants, parameters, and type of parameters;
- Initialization of the serial port for the data sending;
- Configuration of the ADC;
- Configuration of the Timer;
- Function to be executed during interruptions;
- Main loop functions;
- Several functions in order to calculate the average value, RMS, powers;
- Function to send data via serial port.

12.7 Total approximate cost for the hardware parts used in the project

The prices expressed in this paragraph will be indicative and are reported only to make an idea of the cost-effectiveness of the monitoring system developed.

The estimation includes the Arduino board that has a price of 35 €, the sensors that have a price of about 8€ (buying more than 10 sensors) and the OAs that generally have prices of about 1 €.

The totally sum will be, considering that will be necessary 26 sensors and 13 OAs, of about 250 €.

These prices are indicative because they depend on the quantities bought of every element.

It's important to consider that in this estimation are not included the cables for the wiring and the resistances, that fortunately are not expensive, and other eventually components necessary for the installation. Moreover, are not considered the prices of the three voltage transformer (VT) that probably will be used to measure the voltage of the main phases.

Should be considered also the problem of Electromagnetic Compatibility between the measuring system and the electric system into account that works with currents much bigger than the measuring system. In fact, with the use of small wires that connect the Arduino board to the sensors there will be a strong distortion of the signals passing through these wires that will affect the data. In order to eliminate this problem may be followed two different ways:

- The use of wires electronically shielded;
- The substitution of the wires with a wireless system.

For the second case will be necessary also the installation of a battery in order to power the sensors and the wireless system.

Therefore, for these reasons the total cost of the system may change but maintaining, anyway, a low cost of the system.

13 FINAL CONSIDERATIONS AND FUTURE WORKS

The main goals achieved with the present investigation are the obtaining of two different configurations for the positioning of the sensors in the panel and the obtaining, for every configuration, of a number of theoretical relationships necessary for the right measurement of the currents.

In particular, the choice between the two different configurations will depend to the geometry limitations that will be encountered at the sensors installation stage. In that moment will be chosen the configuration that permits the fastest and easiest way for the installation.

Regarding the theoretical relationships encountered in the study, as for example the various matrices and corrective coefficients, they were tested in the Comsol simulations and they will be implemented in the Arduino programming code in the future development of the project. This in order to convert the MF values measured by the sensors into current values and to obtain the electrical information required for every circuit.

Another goal achieved has been the development of a part of the Arduino programming code used to control the Arduino board. Furthermore, has been discovered a limitation in the use of the Arduino board and has been exceeded this limitation.

Regarding the objective of the work, to design a cheap monitoring system, it can be said that the system will have a good cost-effectiveness, as it can be seen in the *paragraph* [12.7].

In order to actuate the real functioning of the measurement system, the future works to do will be: first of all to compute in the 3D model the main theoretical relationships for the monitoring of the currents, as it was done in the 2D model. Then it will be necessary to develop the wiring of the circuits. This will also include the implementation of the OAs and the installation of the sensors in the panel. After that, will be necessary a further development of the Arduino programming code, with the implementation of the theoretical relationships discussed before.

An additional work to do will be to make a study of the electromagnetic compatibility between the electrical distribution system and the measurement system, this in order to find a solution about the possible electromagnetic incompatibility problems.

The last part of the work will be the realization of some measurement tests in order to verify the correct operating of the system.

Appendix A : Matlab Algorithms

Appendix A.1

```

clear all

K= [-32.43    0.0654    0.0161   -0.1857    0.0221    0.0122   -0.0463   -0.0055    0.0052   -0.0209   -0.0087    0.0004
    0.0654   -32.454    0.0656    0.0221   -0.1851    0.0223   -0.0055   -0.0460   -0.0053   -0.0087   -0.0206   -0.0085
    0.0161    0.0656   -32.4661    0.0122    0.0224   -0.1851    0.0052   -0.0053   -0.0459    0.0004   -0.0085   -0.0204
   -0.1856    0.0221    0.0122   -32.443    0.0654    0.0161   -0.1856    0.0221    0.0122   -0.0463   -0.0055    0.0052
    0.0221   -0.1852    0.0223    0.0654   -32.456    0.0656    0.0221   -0.1853   -0.0224   -0.0055   -0.0460   -0.0053
    0.0122    0.0223   -0.1850    0.0161    0.0656   -32.453    0.0122    0.0224   -0.1852    0.0052   -0.0053   -0.0459
   -0.0463   -0.0055    0.0052   -0.1856    0.0221    0.0122   -32.439    0.0654    0.0161   -0.1857    0.0221    0.0122
   -0.0055   -0.0460   -0.0053    0.0221   -0.1852    0.0223    0.0654   -32.462    0.0656    0.0221   -0.1853    0.0224
    0.0052   -0.0053   -0.0458    0.0122    0.0223   -0.1850    0.0161    0.0656   -32.463    0.0122    0.0224   -0.1851
   -0.0209   -0.0087    0.0004   -0.0463   -0.0055    0.0052   -0.1857    0.0221    0.0122   -32.443    0.0654    0.0161
   -0.0087   -0.0206   -0.0085   -0.0055   -0.0460   -0.0053    0.0221   -0.1852    0.0224    0.0654   -32.449    0.0657
    0.0004   -0.0085   -0.0204    0.0052   -0.0053   -0.0459    0.0122    0.0224   -0.1851    0.0161    0.0657   -32.447
]

% K matrix obtained with all the input currents set to 1A

B= [-32.575 %Array of measured values of B with all the circuit powered with
a current of 1A
   -32.558
   -32.609
   -32.711
   -32.663
   -32.718
   -32.707
   -32.669
   -32.728
   -32.589
   -32.553
   -32.591];

Kinv = inv(K);

I = mtimes(Kinv,B); %Array of currents calculated with the use of the matrix K.

```

Appendix A.2

```
set(0,'DefaultFigureWindowStyle','docked')
```

```
K = [ 32.448      -0.63872  -0.17978  -0.07918  -0.046106 -0.029409  -0.020951  -0.015426  -0.014192  0.26106
      -0.63766   32.441   -0.73116  -0.17971  -0.083036 -0.0461    -0.03025   -0.020949  -0.018561  0.016993
      -0.17971  -0.73139  32.447   -0.63771  -0.17963  -0.07915   -0.04609   -0.029401  -0.024522  -0.045264
      -0.079154  -0.17966  -0.63783  32.444   -0.73108  -0.17969   -0.083028  -0.046095  -0.03387  -0.039465
      -0.046097  -0.08303  -0.17971  -0.7313  32.453   -0.63794   -0.17966   -0.079151  -0.044139  -0.02936
      -0.0294    -0.04608  -0.079147  -0.17961  -0.63741  32.43    -0.73094   -0.17969  -0.033091  -0.021429
      -0.020949  -0.03025  -0.046103  -0.083045  -0.17975  -0.73166  32.46    -0.63797  0.11414  -0.016435
      -0.015421  -0.020943  -0.029397  -0.04608  -0.079129  -0.17957  -0.63729  32.446  0.29887  -0.012736
      0.014605  0.01875  0.02434  0.033251  0.045202  0.058239  0.026484  -0.3162  12.451  0.014702
      -0.10356  0.054683  0.0536  0.039178  0.028929  0.02147  0.016761  0.013215  0.014712  12.451 ];
```

```
% K matrix
```

```
B = [ -0.94151  19.699  -1.8639  19.568  -1.8395  19.598  -2.579  18.303  -41.631
       8.7127  21.372  8.4175  21.355  8.456  21.352  7.8569  20.418  -50.742
       17.964  12.798  17.834  12.808  17.89  12.824  17.334  12.028  -49.74
       25.459  2.8306  25.498  2.8657  25.567  2.8975  25.1  2.3156  -44.67
       30.462  -7.4153  30.665  -7.3578  30.74  -7.3141  30.405  -7.621  -35.646
       32.488  -16.936  32.834  -16.862  32.907  -16.81  32.738  -16.81  -23.317
       31.329  -24.798  31.783  -24.714  31.848  -24.66  31.859  -24.352  -8.7766
       27.096  -30.217  27.611  -30.132  27.662  -30.081  27.853  -29.495  6.607
       20.227  -32.691  20.752  -32.614  20.784  -32.57  21.136  -31.764  21.336
       11.391  -31.991  11.871  -31.929  11.881  -31.897  12.359  -30.949  33.983
       1.4268  -28.136  1.8161  -28.096  1.8021  -28.079  2.3603  -27.082  43.282
      -8.6819  -21.525  -8.4234  -21.51  -8.4592  -21.51  -7.8761  -20.562  48.349
      -17.939  -12.801  -17.837  -12.814  -17.891  -12.83  -17.34  -12.022  48.68
      -25.437  -2.8306  -25.504  -2.8694  -25.571  -2.9004  -25.105  -2.3128  44.265
      -30.438  7.4154  -30.667  7.354  -30.74  7.3114  -30.406  7.6213  35.5
      -32.452  16.931  -32.823  16.853  -32.895  16.803  -32.725  16.805  23.272
      -31.298  24.79  -31.774  24.702  -31.838  24.65  -31.849  24.343  8.7668
      -27.085  30.225  -27.621  30.136  -27.671  30.087  -27.861  29.502  -6.6066
      -20.218  32.701  -20.762  32.62  -20.792  32.578  -21.144  31.772  -21.336
      -11.36  31.954  -11.86  31.889  -11.868  31.858  -12.347  30.91  -33.972
      -1.4041  28.118  -1.8116  28.074  -1.7966  28.059  -2.3548  27.061  -43.315 ];
```

```
% Matrix of MF values for all the temporal instants from t=0[s] to t=0,02[s] with intervals of 0,001[s]
```

```
t =[0      %temporal intervals
    0.001
    0.002
    0.003
    0.004
    0.005
    0.006
    0.007
    0.008
    0.009
    0.01
    0.011
    0.012
    0.013
    0.014
    0.015
    0.016
    0.017
    0.018
    0.019
    0.02 ];
```

```
invK=inv(K(1:9,1:9));
IR=sin(2*pi*50*t);          %input currents set in the Comsol model
IS=sin(2*pi*50*t+2*pi/3);
IT=sin(2*pi*50*t+4*pi/3);
ITt=4*sin(2*pi*50*t+4*pi/3);
```



```
Iinput =[IR IS IR IS IR IS IR IS ITt]; % Array of input currents
```

```
%% Exact calculation
Im=zeros(21,9);
for i=1:21
Im(i,:)=(invK*B(i,:))' % calculation of currents
End
```

```
%% Approximate calculation
Iap=zeros(21,9);
for i=1:9
Iap(:,i)=inv(K(i,i))* B(:,i); % calculation of currents
End
```

```
error_exacto=(Im-Iinput); %error in the exact case
error_aprox=(Iap-Iinput); %error in the approximate case
```

```
%% Graphs for phase R
```

```
k=1;
for i=1:2:8
figure()
subplot(2,1,1)
plot(t,Im(:,i))
hold on
plot(t,Iap(:,i),'--g')
plot(t,IR,'--r')
str=sprintf('Phase R%d',k);
ylabel('Current (A)')
xlabel('Time (s)')
title(str)
legend('Exact measure','Approximate measure','Real current')
axis([0 0.02 -b b])

subplot(2,1,2)
plot(t,error_exacto(:,i))
hold on
plot(t,error_aprox(:,i),'--r')
legend('Exact measure','Approximate measure')
ylabel('Error (A)')
xlabel('Time (s)')
title(str)
k=k+1;
end
```

```
%% Graphs for phase S
```

```
k=1;
for i=2:2:8
figure()
subplot(2,1,1)
plot(t,Im(:,i))
hold on
plot(t,Iap(:,i),'--g')
```

```

plot(t,IS,'--r')
str=sprintf('Phase S%d',k);
ylabel('Current (A)')
xlabel('Time (s)')
title(str)
legend('Exact measure','Approximate measure','Real current')
axis([0 0.02 -b b])

subplot(2,1,2)
plot(t,error_exacto(:,i))
hold on
plot(t,error_aprox(:,i),'--r')
legend('Exact measure','Approximate measure')
ylabel('Error (A)')
xlabel('Time (s)')
title(str)
k=k+1;
end

```

```

%% Graphs for the phase T

```

```

k=1;
i=9;
figure()
subplot(2,1,1)
plot(t,Im(:,i))
hold on
plot(t,Iap(:,i),'-g')
plot(t,ITt,'--r')
str=sprintf('Phase T-bar');
ylabel('Current (A)')
xlabel('Time (s)')
legend('Exact measure','Approximate measure','Real current')
axis([0 0.02 -(4*b) (4*b)])

subplot(2,1,2)
plot(t,error_exacto(:,i))
hold on
plot(t,error_aprox(:,i),'--r')
legend('Exact measure','Approximate measure')
ylabel('Error (A)')
xlabel('Time (s)')
title(str)
k=k+1;

```

Appendix B: Arduino algorithm

```
#define samples 512 // Number of samples

volatile int Count = 0; // Implementation of variables
volatile int sensor1[samples]; // Vector for the storing of samples
volatile int sensor2[samples]; // Vector for the storing of samples
double S1medio = 0;
double S2medio = 0;
double S1rms = 0;
double S2rms = 0;
double pot=0;
double S=0;
double Q=0;
double fdp=0;

// Define various ADC prescaler
const unsigned char PS_16 = (1 << ADPS2);
//const unsigned char PS_32 = (1 << ADPS2) | (1 << ADPS0);
//const unsigned char PS_64 = (1 << ADPS2) | (1 << ADPS1);
//const unsigned char PS_128 = (1 << ADPS2) | (1 << ADPS1) | (1 << ADPS0);

const unsigned char CHAN0 = 0; // channel A0 / channel A8 if MUX5=1
//const unsigned char CHAN1 = (1<<MUX0); // channel A1 / channel A9 if MUX5=1
const unsigned char CHAN2 = (1<<MUX1); // channel A2 / channel A10 if MUX5=1
//const unsigned char CHAN3 = (1<<MUX1)|(1<<MUX0); // channel A3 / channel A11 if
MUX5=1
const unsigned char CHAN4 = (1<<MUX2); // channel A4 / channel A12 if MUX5=1
//const unsigned char CHAN5 = (1<<MUX2)|(1<<MUX0); // channel A5 / channel A13 if
MUX5=1
const unsigned char CHAN6 = (1<<MUX2)|(1<<MUX1); // channel A6 / channel A14 if
MUX5=1
//const unsigned char CHAN7 = (1<<MUX2)|(1<<MUX1)|(1<<MUX0); // channel A7 / channel
A15 if MUX5=1
int canal=0;
int CanalCount=0;

void setup(void)
{
  Serial.begin(115200); // transfert speed of serial port to move the data to the
monitor

  cli();//stop interrupts

  ConfigADC(CHAN0); // ADC configuration

  ConfigTimer();

  sei();//allow interrupts
}

///// ADC configuration

void ConfigADC(const unsigned char CHANNEL)
{
  DIDR0 = 0x00; //Digital input disabled on all ADC
  ADMUX = 0x00; //clearing registers.
  ADCSRA = 0x00;
  ADCSR = 0x00;

  ADCSRA |= PS_16; // prescaler = 16
```

```

if (CanalCount>6)
{
    ADCSRB |= (1<<MUX5);
}

ADMUX |= (0<<REFS1)|(1<<REFS0)|CHANNEL;

ADCSRA |= (1 << ADEN); // Enabling of the converter
}

///// Timer configuration

void ConfigTimer(void)
{

    //set timer1 interrupt at 12800Hz
    TCCR1A = 0; // set entire TCCR1A register to 0
    TCCR1B = 0; // same for TCCR1B
    TCNT1 = 0; //initialize counter value to 0
    // set compare match register for 12800hz increments
    OCR1A = 1249; // = (16*10^6) / (12800*1) - 1 (must be <65536)
    // turn on CTC mode
    TCCR1B |= (1 << WGM12);
    // Set CS10 bits for 1 prescaler
    TCCR1B |= (1 << CS10);
    // enable timer compare interrupt
    TIMSK1 |= (1 << OCIE1A);

}

///// function for every interruption

ISR(TIMER1_COMPA_vect)
{
    if(Count>=samples)
        return;

    ADCSRA|=(1<<ADSC); //start the conversion
    loop_until_bit_is_clear(ADCSRA, ADSC); // clear ADSC after the conversion
    sensor1[Count] = ADC ; // Direct Reading of the register and storage

    ADMUX +=1; //Change to the next channel

    ADCSRA|=(1<<ADSC); //start the conversion
    loop_until_bit_is_clear(ADCSRA, ADSC); // clear ADSC after the conversion
    sensor2[Count] = ADC ; // Direct Reading of the register and storage

    ADMUX -=1; // Return to the previous channel

    Count = Count + 1; // Counter for the storage
}

///// Main function

void loop(void)
{
    if(Count==samples)
    {
        cli(); // Destabilisation of interruptions in order to send the data
        Count=0; // Restart of the counter

        int t0=micros();

        Media();
        RMS();
        Potencia();
    }
}

```

```

//Resultados();
Datos();

S1medio=0;
S2medio=0;
S1rms=0;
S2rms=0;
pot=0;
S=0;
Q=0;
fdp=0;

canal=canal+2;
CanalCount=CanalCount+2;

if (CanalCount>15 | canal>6)
{
    canal=0;
}

if (CanalCount>15)
{
    CanalCount=0;
    //Serial.println("*****");
}

ConfigADC(canal);
int tf=micros()-t0;
//Serial.println(tf);

sei(); // interruptions habilitation
}
}

//// Average value computation
void Media(void)
{
    for (int i=0; i < samples; i++) // Send of the data to the serial port
    {
        S1medio+=(double)sensor1[i];
        S2medio+=(double)sensor2[i];
    }

    S1medio=S1medio/(double)samples;
    S2medio=S2medio/(double)samples;
}

//// RMS computation
void RMS(void)
{
    for (int i=0; i < samples; i++) // Send of the data to the serial port
    {
        S1rms+=sq((double)sensor1[i]);
        S2rms+=sq((double)sensor2[i]);
//        S1rms+=sq((double)sensor1[i]-S1medio);
//        S2rms+=sq((double)sensor2[i]-S2medio);
    }

    S1rms=sqrt(S1rms/(double)samples);
    S2rms=sqrt(S2rms/(double)samples);

    //in fact the definition of RMS is: sqrt(sum of (values)^2/number of values)

```

```

}

//// Power computation

void Potencia(void)
{
    for (int i=0; i < samples; i++) // Send of the data to the serial port
    {
        pot+=((double)sensor1[i])*((double)sensor2[i]);
        //pot+=((double)sensor1[i]-S1medio)*((double)sensor2[i]-S2medio);
    }

    pot=pot/(double)samples;
    S=S1rms*S2rms;
    Q=sqrt(sq(S)-sq(pot));
    fdp=pot/S;
}

//// Send of the data

void Datos(void)
{
    Serial.write('A'); // send a capital A
    Serial.println();
    delay(1);

    for (int i=0; i < samples; i++) // Send of the data to the serial port
    {
        Serial.print(sensor1[i]);
        Serial.print(",");
        Serial.println(sensor2[i]);
    }
    Serial.flush(); // Waits that all the data are sent

    delay(1);
}

//// Send of the results

void Resultados(void)
{
    //Serial.write('A'); // send a capital A
    Serial.print(" Canal ");
    Serial.println(CanalCount);
    delay(1);

    Serial.print("Valor medio sensor 1 = ");
    Serial.println(S1medio);
    Serial.print("Valor medio sensor 2 = ");
    Serial.println(S2medio);
    Serial.print("Valor RMS sensor 1 = ");
    Serial.println(S1rms);
    Serial.print("Valor RMS sensor 2 = ");
    Serial.println(S2rms);
    Serial.print("Potencia aparente = ");
    Serial.println(S);
    Serial.print("Potencia activa = ");
    Serial.println(pot);
    Serial.print("Potencia reactiva = ");
    Serial.println(Q);
    Serial.print("Factor de potencia = ");
    Serial.println(fdp);

    Serial.flush(); // Waits that all the data are sent
}

```

BIBLIOGRAPHY

- [1] Thomson, W. (18 June 1857), "*On the Electro-Dynamic Qualities of Metals: Effects of Magnetization on the Electric Conductivity of Nickel and of Iron*" (PDF)
- [2] *The Nobel Prize in Physics 2007*, Nobel Media AB, 9 Oct 2007, retrieved 25 Jun 2014
- [3] T. McGuire and R. Potter. *Anisotropic magnetoresistance in ferromagnetic 3d alloys*.
- [4] Richard Fitzpatrick (2007). "*Ampère's Circuital Law*".
- [5] Heinz E Knoepfel (2000). *Magnetic Fields: A comprehensive theoretical treatise for practical use*.
- [6] Official Comsol web site.
Link: <https://www.comsol.com/blogs/modeling-coils-in-the-acdc-module/>
- [7] Official Comsol web site.
Link: <https://www.comsol.com/blogs/exploiting-symmetry-simplify-magnetic-field-modeling/>
- [8] Official Comsol web site.
Link: <https://www.comsol.com/blogs/how-to-choose-between-boundary-conditions-for-coil-modeling/>
- [9] Official Comsol web site.
Link: <https://www.comsol.com/blogs/meshing-considerations-linear-static-problems/>
- [10] Official Arduino web site.
Link: <https://www.arduino.cc/en/Guide/Introduction>
- [11] Official Arduino web site.
Link: <https://www.arduino.cc/en/Main/ArduinoBoardMega2560>

